



National Library  
of Canada

Acquisitions and  
Bibliographic Services Branch

395 Wellington Street  
Ottawa, Ontario  
K1A 0N4

Bibliothèque nationale  
du Canada

Direction des acquisitions et  
des services bibliographiques

395, rue Wellington  
Ottawa (Ontario)  
K1A 0N4

*Your file* *Votre référence*

*Our file* *Notre référence*

## NOTICE

The quality of this microform is heavily dependent upon the quality of the original thesis submitted for microfilming. Every effort has been made to ensure the highest quality of reproduction possible.

If pages are missing, contact the university which granted the degree.

Some pages may have indistinct print especially if the original pages were typed with a poor typewriter ribbon or if the university sent us an inferior photocopy.

Reproduction in full or in part of this microform is governed by the Canadian Copyright Act, R.S.C. 1970, c. C-30, and subsequent amendments.

## AVIS

La qualité de cette microforme dépend grandement de la qualité de la thèse soumise au microfilmage. Nous avons tout fait pour assurer une qualité supérieure de reproduction.

S'il manque des pages, veuillez communiquer avec l'université qui a conféré le grade.

La qualité d'impression de certaines pages peut laisser à désirer, surtout si les pages originales ont été dactylographiées à l'aide d'un ruban usé ou si l'université nous a fait parvenir une photocopie de qualité inférieure.

La reproduction, même partielle, de cette microforme est soumise à la Loi canadienne sur le droit d'auteur, SRC 1970, c. C-30, et ses amendements subséquents.

UNIVERSITY OF ALBERTA

**Global Events and Event Stratigraphy in the Mid-Paleozoic**

By

Kun Wang



A thesis submitted to the Faculty of Graduate Studies and Research  
in partial fulfilment of the requirements for the degree of Doctor of  
Philosophy.

Department of Geology

Edmonton, Alberta

Spring, 1993



National Library  
of Canada

Acquisitions and  
Bibliographic Services Branch

395 Wellington Street  
Ottawa, Ontario  
K1A 0N4

Bibliothèque nationale  
du Canada

Direction des acquisitions et  
des services bibliographiques

395, rue Wellington  
Ottawa (Ontario)  
K1A 0N4

*Your file* *Votre référence*

*Our file* *Notre référence*

**The author has granted an irrevocable non-exclusive licence allowing the National Library of Canada to reproduce, loan, distribute or sell copies of his/her thesis by any means and in any form or format, making this thesis available to interested persons.**

**L'auteur a accordé une licence irrévocable et non exclusive permettant à la Bibliothèque nationale du Canada de reproduire, prêter, distribuer ou vendre des copies de sa thèse de quelque manière et sous quelque forme que ce soit pour mettre des exemplaires de cette thèse à la disposition des personnes intéressées.**

**The author retains ownership of the copyright in his/her thesis. Neither the thesis nor substantial extracts from it may be printed or otherwise reproduced without his/her permission.**

**L'auteur conserve la propriété du droit d'auteur qui protège sa thèse. Ni la thèse ni des extraits substantiels de celle-ci ne doivent être imprimés ou autrement reproduits sans son autorisation.**

ISBN 0-315-81970-7

**Canada**

UNIVERSITY OF ALBERTA  
RELEASE FORM

NAME OF AUTHOR: Kun Wang

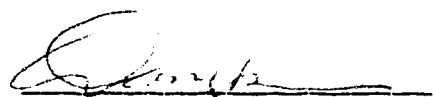
TITLE OF THESIS: **Global Events and Event Stratigraphy in the  
Mid-Paleozoic**

DEGREE: Doctor of Philosophy

YEAR OF THIS DEGREE GRANTED: 1993

Permission is hereby granted to the University of Alberta to reproduce single copies of this thesis and to lend or sell such copies for private, scholarly or scientific research purposes only.

The author reserves all other publication and other rights in association with the copyright in the thesis, and except as hereinbefore provided neither the thesis nor any substantial portion thereof may be printed or otherwise reproduced in any material from whatever without the author's prior written permission.



Kun Wang  
#2, 10636-85 Avenue  
Edmonton, Alberta  
T6E 2K7

December, 1992

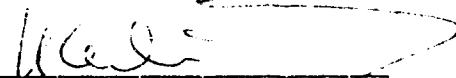
UNIVERSITY OF ALBERTA

FACULTY OF GRADUATE STUDIES AND RESEARCH

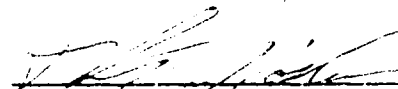
The undersigned certify that they have read, and recommend to the Faculty of Graduate Studies and Research for acceptance, a thesis entitled **Global Events and Event Stratigraphy in the Mid-Paleozoic** submitted by Kun Wang in partial fulfilment of the requirements for the degree of Doctor of Philosophy.



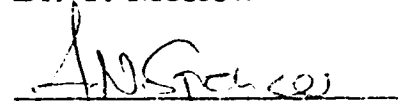
Dr. B.D.E. Chatterton  
(Supervisor)



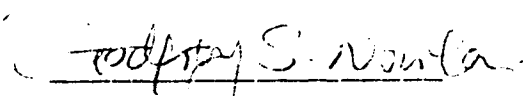
Dr. K. Muehlenbachs



Dr. T. Moslow



Dr. A. N. Spencer



Dr. G. S. Nowlan  
(External Examiner)

December, 1992

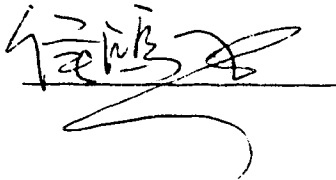
I give permission to K. Wang to use material from the following publication in his Ph.D. thesis:

Wang, K., Orth, C.J., Attrep, M. Jr., Chatterton, B.D.E., Wang, X., and Li, J., in press, *Palaeogeography, Palaeoclimatology, Palaeoecology* (accepted 07/92).

Wang, X. Wang Xiaofeng Date November, 13, 1992

I give permission to K. Wang to use material from the following publication in his Ph.D. thesis:

Wang, K., Orth, C.J., Attrep, M., Chatterton, B.D.E., Hou, H., and Geldsetzer, H. H.J., 1991, *Geology*, v. 19, p. 776-779.

Hou, H.  Date Nov. 2, 1992

I give permission to K. Wang to use material from the following publication in his Ph.D. thesis:

Wang, K., Orth, C.J., Attrep, M. Jr., Chatterton, B.D.E., Wang, X., and Li, J., in press, *Palaeogeography, Palaeoclimatology, Palaeoecology* (accepted 07/92).

Li, J. Li, J. 1992 Date 2/15/92



I give permission to K. Wang to use material from the following publications in his Ph.D. thesis:

- Wang, K., Chatterton, B.D.E., Orth, C.J., and Attrep, M., 1992, *Geology*, v. 20, p. 39-42.
- Wang, K., Orth, C.J., Attrep, M., Chatterton, B.D.E., Hou, H., and Geldsetzer, H. H.J., 1991, *Geology*, v. 19, p. 776-779.
- Wang, K., Orth, C.J., Attrep, M. Jr., Chatterton, B.D.E., Wang, X., and Li, J., in press, *Palaeogeography, Palaeoclimatology, Palaeoecology* (accepted 07/92).
- Wang, K., Chatterton, B.D.E., Attrep, M. Jr., and Orth, C.J., *Canadian Journal of Earth Sciences* (submitted 10/92).

C.J. Orth Charles J. Orth Date 10/28/92

I give permission to K. Wang to use material from the following publications in his Ph.D. thesis:

- Wang, K., Chatterton, B.D.E., Orth, C.J., and Attrep, M., 1992, *Geology*, v. 20, p. 39-42.
- Wang, K., Orth, C.J., Attrep, M., Chatterton, B.D.E., Hou, H., and Geldsetzer, H. H.J., 1991, *Geology*, v. 19, p. 776-779.
- Wang, K., Orth, C.J., Attrep, M. Jr., Chatterton, B.D.E., Wang, X., and Li, J., in press, *Palaeogeography, Palaeoclimatology, Palaeoecology* (accepted 07/92).
- Wang, K., Chatterton, B.D.E., Attrep, M. Jr., and Orth, C.J., *Canadian Journal of Earth Sciences* (submitted 10/92).

M. Attrep, Jr. Moses Attrep Date 10-28-92

I give permission to K. Wang to use material from the following publications in his Ph.D. thesis:

- Wang, K., Chatterton, B.D.E., Orth, C.J., and Attrep, M., 1992, *Geology*, v. 20, p. 39-42.
- Wang, K., Orth, C.J., Attrep, M., Chatterton, B.D.E., Hou, H., and Geldsetzer, H. H.J., 1991, *Geology*, v. 19, p. 776-779.
- Wang, K., Orth, C.J., Attrep, M. Jr., Chatterton, B.D.E., Wang, X., and Li, J., in press, *Palaeogeography, Palaeoclimatology, Palaeoecology* (accepted 07/92).
- Wang, K., Chatterton, B.D.E., Attrep, M. Jr., and Orth, C.J., *Canadian Journal of Earth Sciences* (submitted 10/92).
- Wang, K., and B.D.E. Chatterton, *Sedimentary Geology* (submitted 07/92).

B.D.E. Chatterton



Date

17/Dec/92

I give permission to K. Wang to use material from the following publication in his Ph.D. thesis:

Wang, K., Orth, C.J., Attrep, M., Chatterton, B.D.E., Hou, H., and Geldsetzer, H. H.J., 1991, *Geology*, v. 19, p. 776-779.

H.H.J. Geldsetzer H. H. J. Geldsetzer Date Nov. 27, 1992

I give permission to K. Wang to use material from the following publication in his Ph.D. thesis:

Wang, K., and Bai, S., 1989, *CSPG Memoir*, v. 14, no. 3, p. 71-79.

Bai, S. 白顺良 Date 09/12/92

**THIS THESIS IS DEDICATED TO**

**DR. DIGBY McLAREN**

**(The president of the Royal Society of Canada)**

**This study would not have started, proceeded, or finished  
without his great help, encouragement, and enthusiasm.**

## ABSTRACT

This study has examined three global (and near global) scale geologic events in the middle Paleozoic: 1) the Late Ordovician mass extinction, 2) the Frasnian-Famennian mass extinction, and 3) early Famennian meteorite-impact extinction. Stratigraphic sections spanning these events from both Canada and China have been studied, using an integrated approach which combines geochemistry (trace elements, stable isotopes of carbon and oxygen), sedimentology (microfacies), and paleontology to analyze rocks from the most important intervals of these events in each section. The study demonstrates that a global geochemical anomaly (Ir and trace elements), stratigraphically associated with the latest Ordovician mass extinction, is probably terrestrial in origin, most likely owing to a condensed horizon near the base of a global transgression. The Late Ordovician extinctions occurred at a time of dramatic changes in atmospheric and oceanic CO<sub>2</sub> levels, associated with the growth and decay of the Gondwanan ice sheets. An iridium anomaly has been found to coincide with a  $\delta^{13}\text{C}$  excursion at the Frasnian-Famennian boundary that is suggestive of a meteorite impact at the time of the Frasnian-Famennian extinction. This hypothesis has received strong support from the recent discovery of Frasnian-Famennian microtektites in Belgium. For the first time, 365-Ma-old microtektites have been found in the early Famennian, suggesting that an impact occurred at that time and, based on additional geochemical and paleontological data from South China and Western Australia, probably caused a regional extinction on eastern Gondwana. A study of different types of microspherules found in Devonian sediments from various areas indicates that the natural spherules have great significance as geologic event and sedimentary (or stratigraphic) markers.

## ACKNOWLEDGEMENTS

Throughout the past 4.3 years of my Ph.D. program, many individuals had helped me in one way or another towards the completion of my thesis. Within the University, I would like to thank Al Brandon, Margaret Campbell, Brian Chatterton, Greg Edgecombe, James Farquhar, Chris Holmden, Ian Hunter, Dave Johnston, Brian Jones, Richard Lambert, Jack Lerbekmo, Andrew Locock, Bob Luth, Tom Moslow, Karlis Muehlenbachs, Nat Rutter, James Steer, and Steve Talman for scientific input; and Yves Beaudoin, Frank Dimitrov, Garth Milvain, Don Resultay, Ron Stewart and Paul Wagner for technical support. Many people in other Canadian institutions, to mention a few, Helmut Geldsetzer, Wayne Goodfellow, Alan Hildebrand, Darrell Long, Sandy McCracken, Digby McLaren, Godfrey Nowlan, Mike Orchard, Alan Pedder, and Art Sweet, have helped me in developing ideas presented in this thesis. In particular, Brian Chatterton, my supervisor, has shown the greatest enthusiasm and supervisorship ever since I arrived in Edmonton. Much of the work for my thesis was financially supported by the NSERC operating grant to Brian for trilobite studies!

Because of the nature of my work which involves global correlations, I had a chance to benefit from international exchange and co-operation. W. Alvarez (U.S.A.), M. Attrep, Jr. (U.S.A.), T. Becker (Germany), B.F. Bohor (U.S.A.), P.J. Brenchley (U.K.), P. Claeys (U.S.A.), J.G. Casier (Belgium), Z. Chai (China), R. Feist (France), B.P. Glass (U.S.A.), A. Hallam (U.K.), W.T. Holser (U.S.A.), H. Hou (China), M. House (U.K.), K.J. Hsu (Switzerland), Q. Ji (China), M. Joachimski (Germany), G. Klapper (U.S.A.), J. Li (China), M. Magaritz (Israel), X. Mao (China), S.V. Margolis (U.S.A.), J.D. Marshall (U.K.), G. R. McGhee (U.S.A.), A. Montanari (U.S.A.), R.S. Nicoll (Australia), C.J. Orth (U.S.A.), D. Peryt (Poland), C. Sandberg (U.S.A.), E. Schindler (Germany), H.H. Tsien (Taiwan), O.H. Walliser (Germany), X. Wang (China), Y. Wang (U.S.A.), D.Y. Xu (China), Z. Yan (China), and W. Ziegler (Germany) are thanked for helpful discussions and scientific input during the development of this thesis project. W.B.N. Berry,

W.D. Goodfellow, G.A. Izett, D.G.F. Long, A.D. McCracken, G. R. McGhee, V.L. Sharpton, P. M. Sheehan, and J. Smit officially reviewed chapters 3, 4, 5, and 6 for the journals in which the papers were published.

Special thanks go to Carl Orth, Moses Attrep, Karlis Muehlenbachs, Lido Arocena and Yang Wang who made the geochemical analyses possible in their laboratories.

Finally, I am deeply indebted to Digby McLaren. This study would not have started, proceeded, or finished without his great help, encouragement, and enthusiasm. For this reason, my thesis is dedicated to him.



## TABLE OF CONTENTS

| Chapter   | Page |
|---|------|
| 1. Introduction.....  | 1    |
| Background.....   | 1    |
| Methodology.....  | 3    |
| Results.....  | 3    |
| References.....   | 5    |
| 2. Late Ordovician mass extinction event on northwestern<br>Laurentia: Geochemical, paleontological and sedimentological<br>analyses of the Ordovician-Silurian boundary interval,<br>Mackenzie Mountains, N.W.T..... | 6    |
| Introduction.....   | 6    |
| Geologic setting and stratigraphy.....  | 7    |
| Biostratigraphy and faunal turnover.....  | 9    |
| Depositional characteristics and microfacies.....   | 12   |
| Chemical analyses.....  | 13   |
| Geochemical results and interpretations.....  | 14   |
| Elemental geochemistry.....   | 14   |
| Carbon and oxygen stable isotopes.....  | 17   |
| Discussion.....   | 19   |
| Conclusions.....  | 23   |
| References.....   | 38   |
| 3. Iridium abundance maxima at the latest Ordovician mass<br>extinction horizon, Yangtze Basin, China: Terrestrial or<br>extraterrestrial?.....   | 44   |
| Introduction.....   | 44   |
| Yangtze Basin and extinctions.....  | 45   |
| Yichang and Jinxian sections.....   | 46   |
| Results and discussion.....   | 46   |
| Conclusions.....  | 49   |
| References.....   | 55   |
| 4. The Great Latest Ordovician Extinction on the South China Plate:<br>Chemostratigraphic Studies of the Ordovician-Silurian Boundary<br>Interval on the Yangtze Platform.....  | 59   |
| Introduction.....   | 59   |
| A graptolite framework.....   | 61   |

|   |     |
|---|-----|
| Tectonics and geologic setting.....   | 62  |
| The great latest Ordovician extinction.....   | 64  |
| Stratigraphic sections.....   | 66  |
| Sample preparation and chemical analysis.....   | 67  |
| Geochemical results and discussion.....   | 68  |
| Carbon isotope variations.....  | 70  |
| Discussion and interpretations.....   | 74  |
| Conclusions.....  | 77  |
| References.....   | 98  |
| 5. Geochemical evidence for a catastrophic biotic event at the<br>Frasnian/Famennian boundary in South China..... | 106 |
| Introduction.....   | 106 |
| Geologic setting and stratigraphy.....  | 107 |
| Sample preparations.....  | 109 |
| Geochemical results and discussion.....   | 110 |
| Conclusions.....  | 113 |
| References.....   | 120 |
| 6. Glassy Microspherules (Microtektites) from an Upper Devonian<br>Limestone.....                                 | 122 |
| Introduction.....   | 122 |
| Discovery of microtektites.....   | 123 |
| Description.....  | 123 |
| Chemistry.....  | 124 |
| Discussion.....   | 125 |
| Conclusions.....  | 127 |
| References.....   | 135 |
| 7. A Late Devonian impact event with a probable extinction<br>event on eastern Gondwana.....                      | 138 |
| Introduction.....   | 138 |
| Paleo-reconstruction.....   | 140 |
| Qidong Section.....   | 140 |
| Biostratigraphy.....  | 141 |
| Microtektites.....  | 142 |
| Geochemical anomalies.....  | 144 |
| Taihu impact crater.....  | 145 |
| Geochemical anomalies in Western Australia.....   | 145 |

|  |     |
|--|-----|
| Discussion and interpretations.....  | 146 |
| Conclusions.....   | 147 |
| References.....  | 153 |
| 8. Microspherules from Paleozoic marine sediments: Their<br>origins and significance as geologic event and sedimentary<br>markers..... | 157 |
| Introduction.....  | 157 |
| Methods.....   | 158 |
| Origins of microspherules.....   | 159 |
| "Conodont pearls".....   | 160 |
| Microtektites.....   | 162 |
| Suspected cosmic spherules.....  | 164 |
| Man-made spherules.....  | 165 |
| Glue balls.....  | 166 |
| Industrial slag.....   | 166 |
| Discussion.....  | 167 |
| Conclusions.....   | 172 |
| References.....  | 186 |
| 9. Conclusions.....  | 193 |
| References.....  | 194 |

## Appendices

|                  |     |
|------------------|-----|
| Appendix 1.....  | 196 |
| Appendix 2.....  | 198 |
| Appendix 3.....  | 214 |
| Appendix 4.....  | 215 |
| Appendix 5.....  | 223 |
| Appendix 6.....  | 224 |
| Appendix 7.....  | 231 |
| Appendix 8.....  | 237 |
| Appendix 9.....  | 239 |
| Appendix 10..... | 249 |
| Appendix 11..... | 251 |

## LIST OF TABLES

| Table  | Page |
|--|------|
| 4.1 Stratigraphic positions of the analyzed samples and Ir abundances in Yichang, Jinxian, Xiushan and Youyang sections.....       | 79   |
| 6.1 Major oxide composition of Qidong microspherules with comparison to microtektites.....   | 128  |
| 7.1. Major oxide composition of the Qidong microspherules.....   | 148  |
| 8.1 Chemical composition (wt. %) of "conodont pearls" by electron microprobe analysis.....   | 174  |
| 8.2 Results of X-ray microdiffraction analysis of "conodont pearls", best matching fluorapatite.....                               | 174  |
| 8.3 Oxide compositions (wt. %) of three different phases within a typical Upper Devonian Qidong microtektite from South China..... | 175  |
| 8.4 Chemical composition (wt.%) of two black, magnetic iron-spherules (suspected cosmic spherules).....                            | 175  |
| 8.5 Elemental composition (wt. %) of semi-quantitative energy dispersive analysis of the steel slag.....                           | 175  |

## LIST OF FIGURES

| Figure   | Page |
|--|------|
| 2.1 Late Ordovician-Early Silurian lithofacies and the location of the Avalanche Lake (AV) sections.....   | 25   |
| 2.2 Last occurrences of Late Ordovician and first occurrences of Early Silurian (post-extinction) trilobite and conodont taxa in Section AV4B (A) and Section AV1 (B)..... | 26   |
| 2.3 Photo of the outcrop of the Ordovician-Silurian boundary interval at Section AV4B.....   | 29   |
| 2.4 Stratigraphic column of a 5 m-thick interval in Section AV4B that has been analyzed sedimentologically and geochemically.....  | 30   |
| 2.5 Microphotos of the thin section of the rocks from around the beds A/B contact.....   | 31   |
| 2.6 Plot of the abundances and ratios for some significant elements in Section AV4B.....   | 32   |
| 2.7 Plot of the Ir abundance and Ir/Al ratio in Section AV4B.....  | 34   |
| 2.8 Plot of the values of the cerium anomaly in Section AV4B.....  | 35   |
| 2.9 Plot of the $\delta^{13}\text{C}$ and $\delta^{18}\text{O}$ in Section AV4B.....   | 36   |
| 2.10 Interplot of the Sr and Mn concentrations in Section AV4B.....  | 37   |
| 3.1 Paleogeographic map of Yangtze Basin in late Wufengian (late Ashgillian) of Late Ordovician.....   | 50   |
| 3.2 Iridium abundances and Ir/Al ratios across latest Ordovician mass extinction interval in stratigraphic sections at Yichang (A) and Jinxian (B) in Yangtze Basin.....   | 52   |
| 4.1 Correlation of the graptolite zones in the stratotype section at Dob's Linn, Scotland with those at Yichang, China.....  | 80   |
| 4.2 Latest Ordovician (Late Wufengian <i>bohemicus</i> Zone) paleogeographic and facies map of the Yangtze Platform on the South China Plate.....                          | 81   |
| 4.3 Stratigraphic ranges of 24 brachiopod genera of the <i>Hirnantia</i> fauna in the Yangtze region.....  | 83   |
| 4.4 Precise stratigraphic ranges and occurrences of "Ordovician" (pre- <i>persculptus</i> Zone) graptolites and shelly fossils in the                                      |      |

|      |  |     |
|------|--|-----|
|      | Jinxian Section, Beigong, Jinxian, Anhui Province.....   | 84  |
| 4.5  | Stratigraphic columns of the section intervals that were geochemically analyzed by NAA.....  | 86  |
| 4.6  | Abundances and ratios of some significant elements in the Jinxian Section at Beigong, Jinxian, Anhui Province.....                     | 88  |
| 4.7  | Abundances and ratios of some significant elements in the Yichang Section at Fenxiang, Yichang, Hubei Province.....                    | 90  |
| 4.8  | Abundances and ratios of some significant elements in the Xiushan Section at Datianba, Xiushan, Sichuan Province.....                  | 92  |
| 4.9  | Abundances and ratios of some significant elements in the Youyang Section at Tongguo, Youyang, Sichuan Province.....                   | 94  |
| 4.10 | Variations of carbon isotope ratios of organic material in two nearby sections at Yichang, Hubei Province.....                         | 96  |
| 5.1  | Late Devonian paleogeography and facies distribution in south China.....   | 115 |
| 5.2  | Geochemically studied section at Xiangtian, Guangxi, south China.....  | 116 |
| 5.3  | Carbon and oxygen isotopic profile of Xiangtian section.....   | 117 |
| 5.4  | Abundances and ratios of some significant elements.....  | 118 |
| 6.1  | Tectonic map of the South China Plate with locations of the Qidong microspherules and Taihu Lake impact crater.....                    | 129 |
| 6.2  | Chemostratigraphy of the Qidong Section.....   | 130 |
| 6.3  | Scanning electron micrographs of surfaces of the Qidong microspherules.....  | 131 |
| 6.4  | X-ray microdiffraction patterns of the Qidong microspherules.....  | 132 |
| 6.5  | Scanning electron micrographs in backscattered mode of polished sections of the Qidong microspherules.....                             | 133 |
| 6.6  | Oxide compositional variation diagram comparing the Qidong microspherules (cross) to microtektites from three known strewn fields..... | 134 |
| 7.1  | Tectonic units of China.....   | 149 |
| 7.2  | Stratigraphic column of Qidong section with some significant elemental abundances and stable isotope (C,O) values.....                 | 150 |
| 7.3  | Scanning electron micrographs of Qidong microtektites.....   | 152 |

|     |  |     |
|-----|--|-----|
| 8.1 | Scanning electron micrographs of Devonian "conodont pearls" recovered from (A) near the Frasnian-Famennian boundary in the Cinquefoil Mountain, Jasper, Alberta, Canada; (B) the Frasnian at the Alexandra Falls, N.W.T., Canada; and (C, D) the Eifelian at English Chief Dome, N.W.T., Canada..... | 176 |
| 8.2 | EDX spectra of "conodont pearls" (A) and fossil conodonts (B).....   | 177 |
| 8.3 | Scanning electron micrographs of surfaces of Famennian (Upper Devonian) microtektites recovered from Qidong, Hunan, China.....   | 178 |
| 8.4 | Scanning electron micrograph in the backscattered mode of the polished section of a Qidong microtektite.....   | 180 |
| 8.5 | EDX spectra of (A) Qidong microtektites, (B) suspected cosmic spherules, (C) glue balls, and (D) steel slag.....   | 181 |
| 8.6 | Scanning electron micrographs of surfaces of two black, magnetic iron-spherules (suspected cosmic spherules) recovered from the Devonian of South China.....   | 182 |
| 8.7 | Magnified surface texture of the suspected cosmic spherule in Fig. 6A, showing iron oxide (magnetite) crystals.....  | 183 |
| 8.8 | Scanning electron micrographs of small, clean and smooth-surfaced glue balls.....  | 184 |
| 8.9 | Scanning electron micrograph of a spherule interpreted as steel slag.....  | 185 |

## Chapter 1

### Introduction

*"We have two relatively rare events in Earth history:  
a mass extinction and a very large impact"*

D.M. Raup, 1986

#### Background

One of the hottest debates in science today concerns the Cretaceous/Tertiary mass extinction and proposed asteroid impact (Alvarez, et al., 1980). The evolution of Earth is not as smooth as it was thought to be at the time of publication of Lyell's Principles of Geology in the 19th century. The history of Earth comprises relatively long, stable periods alternating with brief intervals characterized by sudden, drastic changes that had a dramatic impact on the evolution of Earth and life on it. We call these latter "unusual" (occurrences) geologic events. They can be studied by examining the signatures that they left in the geologic record.

Geologic events were both biological and physical. They may include mass extinction and/or radiation of organisms, regression or transgression of sea level, sudden cooling or warming of ocean temperatures, rapid glaciation or deglaciation, massive volcanism and/or earthquake, and impact on Earth of large extraterrestrial bodies, etc. The effects of these events were often dramatic and sometimes resulted in significant changes in the course of biological and physical evolution on Earth.

Of the various events throughout geologic time, those that had global or regional effects are particularly important. These events may be intense in terms of energy release, occur in a very short time interval, and leave direct or indirect signatures of wide geographic distribution in the rock and fossil record (McLaren and Goodfellow, 1990).

Originally, most geologic boundaries were defined at times of major fossil changes recorded in strata. Geologic events are often



close to major stratigraphic boundaries. Boundary definitions and strata correlations have been mainly achieved through biostratigraphy. The establishment of a sequence of geologic events, especially of global events, in the Phanerozoic will provide an important supplement to biostratigraphy. Certain event markers, e.g. geochemical, sedimentological and/or paleontological anomalies, have an excellent potential for stratigraphic applications. The subject of event stratigraphy has emerged, and it is among the most important and active fields in today's Earth sciences. Studies of global events have drawn worldwide attention from various scientific disciplines. At this stage of event stratigraphy, studies have been focusing on the greatest (so called "first-order") global events, because they will comprise the framework of a sequence of geologic events in the Phanerozoic. The study of event stratigraphy calls for collaboration between specialists from a wide spectrum of disciplines, such as paleontology, geochemistry, stratigraphy, sedimentology, and even physics, chemistry and astronomy.

Evidence from the fossil record clearly indicates that there were numerous biological events during the evolution of organisms through time (Raup, 1986). Of these biological events, five Phanerozoic mass extinction events (first-order or largest events of Sepkoski, 1982) are of particular interest. They are end-Cretaceous, end-Triassic, end-Permian, end-Frasnian, and end-Ordovician events. These five biotic events were all characterized by a global or near-global scale mass extinction which wiped out a significant number of living organisms, an estimate of about 15%, 20%, 50%, 21%, and 22% of marine animal families becoming extinct during these events respectively (Sepkoski, 1982). A clear understanding of these drastic events is fundamental to the subject of event stratigraphy. This thesis study focuses on the end-Ordovician and end-Frasnian extinction events, but other smaller events are also dealt with.

## **Methodology**

Twelve biostratigraphically well-constrained sedimentary sections spanning the extinction horizons have been selected from

different areas around the world (e.g. Canadian Rocky Mountains in Alberta, Northwest Territories, Quebec, South China, Western Australia, and southern France), representing different geographic and tectonic settings at the time of deposition. The extinction horizons have been dated and located accurately by means of index fossils, e.g. graptolites, conodonts, brachiopods and trilobites for the Ordovician and the Silurian, and conodonts, brachiopods and corals for the Frasnian and the Famennian. Samples were collected continuously (no gaps between adjacent samples) through the extinction intervals, with a 2-3 cm thickness for each sample, because of the short duration of these events (in the order of tens of thousands of years or less). Other samples (with small gaps between adjacent samples) were collected farther away from the extinction intervals in order to form a set of "normal" or background samples whose data will be compared to those derived from the extinction intervals. The sampling thickness is normally 2-10 m for sections with clearly defined extinction intervals.

Each sample was separated into three parts in the laboratory: one small part for geochemical analyses (trace elements, stable isotopes), another part (with the orientation of bedding) for thin sectioning (microfacies), and the third part (cutoffs) for micropaleontology, microspherules and shocked quartz grain searches (after acid treatment).

## Results

Geologic events leave geochemical signatures in the rock record, if diagenesis has not altered them completely. A comparison of geochemical patterns of event horizons with those in pre- and post-event strata can provide a scientific pathway to understanding geologic events. It is important to develop global patterns of elemental abundance and stable isotope (e.g. O, C, S) variations across event boundaries by studying the geochemistry of independent sections worldwide (Corliss, 1989).

Geologic events changed life on Earth in many different ways. For any mass extinction event, what we always want to know includes: how severe it was (severity), what organisms were

affected and what were not (patterns of extinction and survivorship), how long it lasted (duration), when exactly it occurred (timing), and how widespread it was (geographic extent). These questions can be answered by studying paleontological data from published sources and/or from well-preserved stratigraphic sections around the world. The latter are more important and reliable because they enable one to examine fossil data by the same standard without contradicting information from different sources.

Geologic events resulted in major changes in various environments, which controlled the deposition of sediments. Therefore, we would expect to see these changes recorded in the sedimentary rocks deposited at the times of the events. Sedimentology and facies analysis of samples collected across the event boundaries can help document patterns of sedimentary changes through geologic events. Some anomalous deposits (e.g. boundary clays, anoxic sediments, microspherule layers, etc.) could be excellent markers for global stratigraphic correlations.

It is hoped that this study, which is an integration of global/regional geochemical, biological and sedimentological characterizations of several geologic events in the middle Paleozoic, contributes to the advancement of event stratigraphy, and to a better understanding of Earth history.

### References

- Alvarez, L.W., Alvarez, W., Asaro, F. and Michel, H.V., 1980. Extraterrestrial cause for the Cretaceous-Tertiary extinction. *Science*, 208: 1095-1108.
- Corliss, W.R., 1989. *Anomalies in Geology: physical, chemical, biological*. The Sourcebook Project, Glen Arm, MD 21057, 398 pp.
- McLaren, D.J. and Goodfellow, W.D., 1990. Geological and biological consequences of giant impacts. *Annual Review of Earth and Planetary Sciences*, 18:123-171.
- Raup, M.D., 1986. Biological extinctions in Earth history. *Science*, 231: 1528-1532.
- Sepkoski, J., Jr., 1982. Mass extinctions in the Phanerozoic oceans: A review. *Geol. Soc. Am. Spec. Paper*, 190: 283-290.

## Chapter 2

### **Late Ordovician mass extinction event on northwestern Laurentia: Geochemical, paleontological and sedimentological analyses of the Ordovician-Silurian boundary interval, Mackenzie Mountains, N.W.T.**

(A version of this chapter has been submitted for publication. Wang, K., Chatterton, B.D.E., Attrep, M. Jr., and Orth, C.J. *Canadian Journal of Earth Sciences*, 10/92)

#### **Introduction**

It is known that a major Phanerozoic mass extinction occurred near the end-Ordovician (Sepkoski, 1982). Paleontological studies in northern Canada showed that this extinction affected many faunal groups, including trilobites, conodonts, graptolites, ostracods, bryozoans, and rostroconchs (Chatterton and Ludvigsen, 1983; Chatterton and Perry, 1983; Over and Chatterton, 1987; Nowlan et al., 1988a, b; Melchin et al., 1991b; Lenz and McCracken, 1988; Copeland, 1989; Bolton and Ross, 1985; Johnston and Chatterton, 1983) on northwestern Laurentia (now northwestern and arctic Canada, Scotese and McKerrow, 1990). There is generally a faunal turnover in that region, characterized by the extinction of faunas of Ordovician aspect and the following radiation of faunas of Silurian aspect. However, the pattern and the timing of extinction and radiation for different faunal groups are not always the same. For example, the level of the most significant faunal turnover is different for ostracods, conodonts and graptolites (Copeland, 1989; Nowlan et al., 1988b; and Melchin, et al., 1991b). Several papers, dealing with the geochemical aspects of the extinction in that region, have appeared recently in the literature (Goodfellow et al., 1992; Nowlan et al., 1988a; Wang et al., 1991a; Melchin, et al., 1991a).

In this paper, we present the results of a comprehensive and detailed study of the element and stable isotope geochemistry (centimeter-scale analyses), paleontology and sedimentology of the

carbonate sequences spanning the latest Ordovician extinction and the Ordovician-Silurian transition in a slope or outer-shelf setting at the transition between the Selwyn Basin (deep basinal facies) and the Mackenzie Platform (shallow shelf facies) near Avalanche Lake in the central Mackenzie Mountains, N.W.T. Sections from such a transitional setting were selected for this study because they are complete in deposition and rich in fossils. These sections have been extensively studied biostratigraphically, and the interval of the extinction and faunal turnover was well constrained through trilobites and conodonts (Chatterton and Ludvigsen, 1983; Chatterton and Perry, 1983, 1984; Nowlan et al., 1988b; Over and Chatterton, 1987). Two Avalanche Lake sections (AV1 of Chatterton and Perry, 1983; and AV4B of Over and Chatterton, 1987) will be discussed in this paper, but all of the geochemical and microfacies data presented were obtained from Section AV4B, which is better exposed through the uppermost Ordovician and lowermost Silurian than Section AV1.

The Ordovician-Silurian boundary defined previously in these sections were based on the faunal turnover of trilobites and conodonts (Nowlan et al., 1988b; Chatterton and Ludvigsen, 1983); its exact correlation with the graptolite-defined, international Ordovician-Silurian boundary is uncertain because of the lack of information on the graptolite zonation in these sections. Although Melchin et al. (1991b) have come up with a preliminary correlation between the conodont and graptolite zonations near the Ordovician-Silurian boundary in Canadian Arctic sections, we do not attempt to locate the exact stratigraphic position for the graptolite-defined Ordovician-Silurian boundary in these sections through an indirect correlation by using Melchin et al.'s (1991b) results, because this paper mainly deals with the faunal turnover and extinction rather than the international systemic boundary. Nowlan et al. (1988a) and Goodfellow et al. (1992) proposed that the extinction event in this region is at or near the base of the graptolite *G. persculptus* Zone.

### **Geologic setting and stratigraphy**

Sections AV1 of Chatterton and Perry (1983) and AV4B of

Over and Chatterton (1987) are located near the bases of adjacent small valleys cut into the north east slope of an unnamed mountain range, and are located about 10 km east of Avalanche Lake, in the central Mackenzie Mountains, N.W.T. (Fig. 2.1). They contain strata of latest Ordovician and Silurian age (see Figure 2.2; and Nowlan et al., 1988b, Fig. 2A-D). The strata in AV4B are nicely exposed through the uppermost Ordovician and lowermost Silurian. Nearby, equivalent age strata in section AV1 are not quite as well exposed, with several covered intervals, including one near the Ordovician-Silurian boundary (see Fig. 2.2). The Upper Ordovician through Wenlock strata of these sections have been assigned to the Whittaker Formation of Douglas and Norris (1961) by Chatterton and Perry (1983, 1984), Over and Chatterton (1987), Nowlan et al. (1988b), and Chatterton et al. (1990).

Several workers have outlined the tectonic elements of the Mackenzie Mountains region during the early to middle Paleozoic (Gabrielse, 1967; Cecile, 1982; Morrow and Cook, 1987; Morrow, 1991). These elements included the Selwyn Basin, Misty Creek Embayment, Root Basin, Redstone Arch, Mackenzie Shelf, etc. (Fig. 2.1). The Avalanche Lake sections appear to have been located on the margin of the shelf or on the slope into the Selwyn Basin from a positive region known as the Redstone Arch (Fig. 2.1). These sections are located on the map produced by Gabrielse et al. (1973) at the junction between the Delorme Group carbonates and the deeper, basinal Road River Formation shales.

The Upper Ordovician and Lower Silurian sediments of these two sections are fairly typical of the Whittaker Formation of Douglas and Norris (1961). The Whittaker Formation was named for a thick sequence of limestones, dolomites and shales, with a type section on the east flank of the Whittaker Range of the Mackenzie Mountains. In the type section, the strata are 1240.5 m (4070 feet) thick and of Late Ordovician to Wenlock age. The sequence in the type section is tripartite, with a lowest interval of limestone (402 m), an intermediate interval of dolostone (262 m) and an upper interval of argillaceous limestone and siltstone (576 m). The two lower units are Upper Ordovician and the uppermost unit is Llandovery to

Wenlock in age. The Avalanche Lake sections are more distal than the Whittaker Range section, and lack dolostone, containing more argillaceous limestone and shale. They are similar enough in overall lithology and close enough to the type section to be mapped as the same formation in the geological map of the area (Gabrielse et al., 1973).

Several workers have suggested that the Selwyn Basin may have been restricted during the late Ordovician and early Silurian (Goodfellow and Jonasson, 1984, based upon sulphur isotopes; Over and Chatterton, 1987; Nowlan et al., 1988b, both based upon conodont faunas). Nowlan et al. (1988b) suggested that the absence of such distinctive, biostratigraphically important, latest Ordovician conodont genera as Amorphognathus and Gamachignathus in section AV4B was the result of these restricted conditions (oceanic barriers) which could have prevented Gamachignathus ensifer McCracken, Nowlan and Barnes, the index species of the last Ordovician conodont zone (Fauna 13), from entering this basin (Nowlan et al., 1988b).

### **Biostratigraphy and faunal turnover**

Faunas of latest Ordovician and earliest Silurian age, from the Avalanche Lake sections, have been described by a number of workers, including: trilobites (Chatterton and Perry, 1983, 1984; Chatterton and Ludvigsen, 1983; Edgecombe and Chatterton, 1987, 1990; Siveter and Chatterton, submitted), rostroconchs (Johnston and Chatterton, 1983), bryozoans (Bolton and Ross, 1985), conodonts (Over and Chatterton, 1987; Nowlan et al., 1988), and ostracodes (Copeland, 1989). Systematic work on a number of the trilobites from this critical, Upper Ordovician to Lower Silurian, interval is in progress by one of us, B.D.E.C., and several other co-workers (J.M. Adrain - aulacopleurids; M. Campbell - lichids; and R. Ludvigsen - late Ordovician fauna).

The Ordovician-Silurian boundary was placed by Nowlan et al. (1988b) at a level between two particularly prominent beds sandwiched in a shaly-looking sequence of argillaceous limestones in Section AV4B (Fig. 2.3), based upon the faunal turnover of



trilobites and conodonts. This level (AV4B 111.3 m in Fig. 2.2A) is used as a reference point in this work (see Fig. 2.4). The trilobite fauna that occurs below this horizon is very different from that occurring above it, and contains such distinctively Ordovician trilobites as Cryptolithus and Anataphrus as high as AV4B 110.65 m. These two genera plus Robergiella occur in a silicified fauna from AV4B 109.75 m (Figure 2.2A). Many other exclusively Ordovician trilobite taxa are known from slightly lower levels (the genera Ampyxina, Borealaspis, Ceraurinella, Ceraurus, Cybeloides, Dimeropyge, Holia, Isotelus, Nahannia, and Triarthrus, Chatterton and Ludvigsen, 1983; see Figure 2.2A, B). Although the trilobite faunas that occur immediately above AV4B 111.3 m are quite different from those that occur below this level, such distinctively Silurian taxa as Kettneraspis jaanussoni (Chatterton and Perry, 1983) and Acernaspis sp. do not occur until about 10-45 m above this horizon (Kettneraspis at AV4B 121 m and AV1 95.5 m; Acernaspis at AV4B 137 m and AV1 124-124.5 m, Fig. 2.2). However, when they do occur, they are found with other taxa that occur in the interval from AV4B 111.3-111.8 m (Curriella, Bumastus, Platylichas, Coniproetus). The proetid, lichid and bumastid trilobites from AV4B 111.6-111.8 m are not particularly diagnostic in age. Curriella is a genus that is more diagnostic of Llandovery strata, because all other species of Curriella found in Scotland and Illinois are of Llandovery age (Edgecombe and Chatterton, 1990; Gass et al., 1992). Harpidella appears to be the only genus that occurs in both the pre-turnover Ordovician trilobite collections and post-turnover collections with Silurian taxa, although it is represented by different species above and below the faunal turnover. Therefore, the trilobite faunas from above AV4B 111.3 m are post-turnover Silurian faunas, and the faunal turnover based on trilobites would be limited to a < 55 cm interval in Section AV4B.

Nowlan et al. (1988b) and Over and Chatterton (1987) described the distribution of conodonts in the latest Ordovician and Silurian parts of section AV1 and AV4B. They found that distinctive Ordovician conodonts occur as high as AV4B 111.0 m. A sample from AV4B 111.5 m yielded a sparse and undiagnostic conodont

assemblage, and the earliest occurrence of the conodont Ozarkodina hassi of Silurian aspect is as low as AV4B 111.6 m (Nowlan et al., 1988b). Thus, the faunal turnover based on conodonts is limited to a < 60 cm interval in Section AV4B. Nowlan et al. (1988b) noticed from the conodont distribution in the Avalanche Lake sections that of the 47 Late Ordovician conodont species, only 3 persist into the Silurian, and all the survivors are simple coniform conodonts (Goodfellow et al., 1992). This extinction pattern is essentially the same as those recorded from the Anticosti Basin, Matapedia Basin, and Richardson and Blackstone troughs (Goodfellow et al., 1992).

From discussion above, the level between the two particularly prominent beds at AV4B 111.3 m (Figs. 2.2A, 2.3, 2.4) would define a common horizon of the faunal turnover for both trilobites and conodonts in Section AV4B. This level (AV4B 111.3 m in Fig. 2.2A) of the faunal turnover is used as the trilobite and conodont defined Ordovician-Silurian boundary until the graptolite zonation becomes available in these sections. Some graptolites were indeed found from the Upper Ordovician and Lower Silurian parts of the sections, but the specimens are not particularly well preserved, and they have yet to be analyzed by a specialist. Similar to the situation encountered in the Anticosti Island Ordovician-Silurian boundary sections (Copeland, 1981), the level of the most significant faunal turnover of ostracodes in the Avalanche Lake sections is stratigraphically higher than those of trilobites and conodonts (Copeland, 1989).

Section AV1, about 1.2 km northwest of Section AV4B, has a fossil distribution similar to that of AV4B (Fig. 2.2). Trilobites are somewhat more abundant in Section AV1. Silurian trilobite genera (Acernaspis, "Deiphon", Stelckaspis, Dalaspis, and Encrinurus) that occur at AV1 124-124.5 m are in the conodont Aspelundia fluegeli Zone of middle Llandovery age (McCracken, 1991). The level of the faunal turnover and the Ordovician-Silurian boundary based on trilobites and conodonts lies between 76.5 and 77.5 m in Section AV1 (Fig. 2.2B). But a pitfall is that there is a covered interval just above the level of the faunal turnover in that section (Fig. 2.2B). Thus, a centimeter-scale geochemical study of this crucial interval in

Section AV1 is not feasible.

### **Depositional characteristics and microfacies**

The strata of the Late Ordovician and Early Silurian in the Avalanche Lake sections are predominantly micritic limestones, with varying clay contents. In some horizons, the clay content rises to the point where beds are calcareous shales. Quartzose silt and sand size fractions of terrigenous origin are inconspicuous to absent. The allochems are usually skeletal, but in some intervals peloids are very common. Chert nodules and turbiditic laminae occur at some horizons. In the interval of the faunal turnover (within 50 cm), some chain corals are found in what appears to be life position. At several horizons, trilobites have been found partly or completely articulated, implying that the sea floor was below wave base for most of this interval. In general, the levels of fragmentation and abrasion of fossils are low, also implying low energy levels for the sea floor. The litho-/bio-facies in these sections are typical of comparatively deep and quiet water environments. Most of the trilobite fossils examined for this study are silicified.

The trilobite fauna, occurring in the 20 m or so below the Ordovician-Silurian boundary in both AV4B and AV1 sections, is dominated by the distinctly Ordovician and deep water trilobites Cryptolithus, Anataphrus, and Robergiella (Chatterton and Ludvigsen, 1976; Ludvigsen, 1979). This biofacies is usually restricted to deep slope or basinal environments during the Ordovician of western North America. Occurrences in these beds of occasional to rare taxa that are common in intermediate to deeper shelf biofacies (Borealaspis, Ceraurus, Cybeloides, Holia, Nahannia, Harpidella and Sceptaspis; see Ludvigsen, 1979), would suggest that the area was located close to the outer shelf, perhaps on the slope into the Selwyn Basin.

A 5-m interval in Section AV4B (3 m above and 2 m below the Ordovician-Silurian boundary) was sampled in detail, and the thin sections of the samples were studied for microfacies changes across the boundary. The carbonate classification of Dunham (1962) and Embry and Klovan (1971) is followed here. For the convenience of

discussion, the beds involved were assigned A, B, C and D in Fig. 2.4, and the Ordovician-Silurian boundary is between the two particularly resistant beds B and C.

Beds A and D (dark, thin-bedded, laminated argillaceous limestone as observed in the field) are predominantly composed of wackestone with a few fossil fragments and non-skeletal allochems in a mud-supported matrix. At some horizons, allochems are so few that the rocks can be called a mudstone. Bed C (a light-grey coloured, thick-bedded limestone) consists of packstone in the lower and upper part, and peloidal grainstone in the middle part. This bed is almost purely composed of carbonate with very little clay component. The lower part of Bed B (a grey coloured, thick-bedded limestone) contains packstone while the rest of the Bed B is floatstone in a wackestone matrix. Comparatively bigger fossil fragments (corals, trilobites, brachiopods, etc.) are contained in the floatstone. The contact between beds A and B is sharp (Fig. 2.5), and a hard, pyritic crust can be seen at this contact. Of particular interest is that the top of Bed B and the very base of Bed A are rich in phosphatic pellets (Fig. 2.5) which are not seen elsewhere in the 5 m interval analyzed. This contact may represent a highly condensed horizon (perhaps a firmground) or a hiatus, in which a significant amount of time may have elapsed without much deposition.

The lithofacies distribution and an inferred relative water-depth curve for Section AV4B are presented in Fig. 2.4. If the relative change in water depth reflects that in sea level, the analyzed section clearly shows a regressive-transgressive cycle, with a low stand in Bed C. The inferred, relative change in water depth and sea-level from the microfacies analysis are consistent with field (paleontological and sedimentological) observations that the two particularly resistant beds B and C were deposited in relatively energetic, shallow water conditions, and beds A and D were deposited in relatively quiet, deep water conditions.

### Chemical analyses

Each of the 71 samples collected from Section AV4B were analyzed for about 40 major, minor and trace elements, and for C

and O stable isotopes. Big, block samples were collected and labelled in the field, and they were then sliced along bedding into small pieces (each about 2-3 cm thick) in the lab for chemical analyses. Samples from between 70 cm above and below the Ordovician-Silurian boundary (beds B/C contact, Fig. 2.4) are continuous, with thin (2 mm) missing sections represented by saw cuts between samples. The total thickness of the chemically analyzed interval of Section AV4B is 5 m (3 m above and 2 m below the boundary).

Except for the Ir abundance, the element abundances in the 71 samples were obtained through conventional instrumental neutron activation analysis (INAA). Radiochemical neutron activation analysis (RNAA) was then performed on 45 selected samples to acquire the Ir abundance in these samples. More details of INAA and RNAA were given in previous papers (Orth, 1989; Wang et al., in press). The detection limit for Ir through RNAA is 1 part per trillion ( $10^{-12}$ g/g).

Study of the thin sections of the isotopically analyzed samples indicates that there is little or no diagenetic recrystallization, dolomitization or alteration in the samples. We tried to use only micritic material from a sample for C and O analysis, because micrites are more likely original fabrics of deposition, and thus the results based on the micrites may be more reliable. Before the analysis, powdered samples were first soaked in liquid Javex bleach for at least 12 hours to remove organic carbon, and they were then washed with distilled water and dried at 120°C to remove moisture. The prepared samples were reacted with 100%  $H_3PO_4$  at 25.3°C for 24 hours to liberate  $CO_2$  from the carbonate. The  $CO_2$  was analyzed on a VG 602D mass-spectrometer using the University of Alberta Stable Isotope Laboratory Internal Standard (KMCC calcite) which has been calibrated to international standards (NBS 19, 20, 21). The isotopic data reported here are in per mil relative to the Peedee Belemnite (PDB).

## Geochemical results and interpretations

### *Element Geochemistry*

Abundances and ratios of some significant elements for

Section AV4B are plotted as a function of depth in Fig. 2.6. The Al abundance shows a "C" pattern, with two peak-abundance areas near the beds A/B contact and beds C/D contact, and a low-abundance area in beds B and C. The abundances of some elements (e.g., Ir, Co, Cr, etc.) simply follow the Al abundance pattern, and show correlations with Al abundance. It indicates that these elements are associated with Al-rich clay partings in the rocks analyzed. The Ir abundances in this section are too low (maximal Ir abundance = 0.051 ppb) for us to consider the possibility that the impact of a large extraterrestrial body was involved in the faunal turnover and extinction. The levels of the Ir abundances in this section are typical of those for normal marine carbonate sediments.

After normalizing elemental abundances as a ratio to the Al (we did not use a CaCO<sub>3</sub>-free normalization, as CaCO<sub>3</sub> content in most samples is near 100%, any small error in Ca abundance would result in a large CaCO<sub>3</sub>-free error), we see some interesting patterns: two peaks showing up for some elements (including Ir) as a ratio to the Al (Fig. 2.7). The stratigraphically lower Ir/Al peak area is in Bed C, and the upper Ir/Al peak is at the beds A/B contact (Fig. 2.7). The lower Ir/Al peak area actually corresponds to low Ir abundances (<0.01 ppb) and to extremely low Al abundances (≤0.1%); therefore it is probably not a real Ir-enrichment peak but rather an artifact that is caused by the extremely low numbers (from the Al abundances) for the denominator in the Ir/Al ratios. However, the upper Ir/Al peak is real, because the raw Ir abundances are coincidentally maximal (Fig. 2.7) and the "ratio artifact" is not the case here (as the Al abundances are not "extremely low"). Interestingly, this upper Ir peak area corresponds stratigraphically to a condensed horizon or a hiatus (a large period of time elapsed with little deposition) between beds A and B, which we discussed earlier (Figs. 2.4, 2.5). Condensation and slow sedimentation at the beds A/B contact would account for the Ir peak there. We also recognized previously the association of Ir abundance and Ir/Al ratio maxima with condensation in other sections spanning the interval of the latest Ordovician mass extinction (Wang et al., 1992).

Cerium anomaly ( $Ce_{anom}$ ) can be used as an effective indicator

of the paleo-redox conditions of marine environments (Wright et al., 1987). It is defined as:  $Ce_{anom} = \text{Log}[3Ce_n/(2La_n + Nd_n)]$ ; where "n" signifies the concentrations after normalization to the standard shale (Wright et al., 1987; North American Shale Composite is used here for normalization, Gromet et al., 1984). The  $Ce_{anom} = -0.1$  is the boundary between samples from reducing and oxidizing environments, based upon the chemical results of modern marine environments of varying redox conditions (Wright et al., 1987). The values of the  $Ce_{anom}$  for Section AV4B are plotted as a function of depth in Fig. 2.8. Most values of the  $Ce_{anom}$  in Bed D are  $> -0.1$ , indicating reducing conditions. A sudden shift from reducing to oxidizing conditions is seen at the beds C/D contact; while beds C and B are entirely oxidizing. A gradual return from oxidizing to reducing conditions occurs upwards in the Bed A. Apparently, a brief episode of oxygenation occurred within an otherwise dysaerobic/anoxic sequence of Section AV4B (Fig. 2.8).

As discussed earlier, the Selwyn Basin was primarily closed, restricted, stratified and reducing during late Ordovician and early Silurian time; ventilated, open ocean conditions did not appear until Wenlock time (Goodfellow and Jonasson, 1984). Dark, well laminated micritic limestone successions (with high  $Ce_{anom}$  values) of Section AV4B were the results of deposition in these reducing environments. A brief period of ventilation of the basin with oxygen as recorded by the  $Ce_{anom}$  in beds C and B of Section AV4B was probably associated with the cold climate induced by the late Ordovician glaciation which was widespread on Gondwana (Sheehan, 1988; Brenchley, 1989). This is because Bed C shows the maximum shallowing effects (low stand of sea level) in this section (Fig. 2.4), most likely coinciding with the maximum effect of a known glaciation and the resultant regression in the latest Ordovician. During this extensive glaciation, temperatures in the oceans would have dropped significantly as suggested by positive carbonate  $\delta^{18}O$  shifts recorded in brachiopod shells (Marshall and Middleton, 1990). The solubility of oxygen in the water would increase with decreasing temperature. Berry and Wilde (1978) suggested that, with successive glaciation, anoxic and stratified oceans can become

progressively ventilated, because the formation of sea ice at high latitudes would create relatively dense, well-oxygenated water which sinks and ventilates the ocean basins at mid and low latitudes. Thus, the extensive glaciation and low water temperature in the latest Ordovician can explain the brief oxygenation of the basin at the time of the deposition of beds B and C in the anoxic Selwyn Basin (Fig. 2.8).

#### *Carbon and oxygen stable isotopes*

The results of  $\delta^{13}\text{C}$  and  $\delta^{18}\text{O}$  in carbonate of Section AV4B are plotted as a function of depth in Fig. 2.9. It appears that the background  $\delta^{13}\text{C}$  values are between 0.32 and 0.88‰, as shown by the data points in the lower and upper part of the section analyzed. These "normal" background values are consistent with those reported previously for the "best preserved" late Ordovician and early Silurian carbonates (Wadleigh and Veizer, 1992; Veizer et al., 1986; Popp et al., 1986). Most fluctuations of the  $\delta^{13}\text{C}$  values take place in beds C and B, and their vicinity. From the base of the section upwards, the  $\delta^{13}\text{C}$  in the lower part of Bed D shows relatively uniform values (between 0.32-0.54‰), and then it becomes progressively positive, starting from the the upper part of Bed D, through the lower part of Bed C, until it reaches the maximum value (2.28‰) at the upper 12 cm of Bed C, where a sudden, dramatic negative  $\delta^{13}\text{C}$  shift to -0.94‰ and -1.31‰ occurs in Bed C (Fig. 2.9). Immediately following this negative shift, a return to more positive  $\delta^{13}\text{C}$  values can be seen in the upper 11 cm of Bed C and in Bed B, except for two more negative values (0.2‰ and -0.13‰) in the middle of Bed B. The  $\delta^{13}\text{C}$  values in the upper part of Bed B and the lower part of Bed A are generally high (>1‰). Upwards, the  $\delta^{13}\text{C}$  values come back to the background levels in Bed A (Fig. 2.9). For the  $\delta^{18}\text{O}$ , we do not see any significant pattern of changes with depth. Most  $\delta^{18}\text{O}$  values are more negative than those of the same age that were previously published for the "best preserved" carbonates (Wadleigh and Veizer, 1992; Veizer, et al., 1986; Popp et al., 1986), suggesting diagenetic overprint on the very sensitive oxygen isotope ratios. Several "very negative"  $\delta^{18}\text{O}$  values (< -7.5‰)



are apparently caused by the alteration of these samples as shown by the trace elements (discussion below).

As is suggested by microfacies analysis, there is little or no diagenetic recrystallization, dolomitization or alteration in the carbonate rocks that we analyzed for stable isotopes. The material used for the stable isotopic analysis is well-preserved micrite and peloids which were formed originally within the sedimentary basin. The degree of alteration can also be evaluated by using the trace element technique (Veizer, 1983; Brand and Morrison, 1987). In general, alteration leads to an increase in Mn and Fe concentrations and a decrease in Sr and Na concentrations in the final diagenetic low-Mg calcite product (Brand and Veizer, 1980; Veizer, 1983). Oxygen (and to a lesser extent carbon, which is more resistant to diagenesis) isotopic compositions tend to become lighter, as a result of alteration. We have plotted in Figure 2.10 the Sr against Mn concentrations for all of the isotopically analyzed samples. The Sr and Mn values for most samples fall within a square (Sr > 500 ppm, Mn < 100 ppm), which is close to those defined for the unaltered brachiopod-shell calcite and for the low-Mg calcite precipitated in chemical equilibrium with ambient seawater (Veizer, 1983; Brand and Morrison, 1987). Ten samples outside the square have either <500 ppm Sr or >100 ppm Mn, but none has both <500 ppm Sr and >100 ppm Mn. Plots of Sr/Mn (Fig. 2.10),  $\delta^{13}\text{C}/\delta^{18}\text{O}$ ,  $\delta^{13}\text{C}/\text{Mn}$ ,  $\delta^{18}\text{O}/\text{Mn}$ ,  $\delta^{13}\text{C}/\text{Sr}$  (not shown) do not show any apparent trend of alteration. These results conform with the thin-section observation that the degree of alteration in these samples is very low. The 10 samples with <500 ppm Sr or >100 ppm Mn have been indicated (by crosses) in Fig. 2.9, and all the "very negative"  $\delta^{18}\text{O}$  values (< -7.5‰) coincide with these samples, but the overall  $\delta^{13}\text{C}$  pattern is not affected by these "altered" samples (Fig. 2.9).

Section AV4B displays a distinctive  $\delta^{13}\text{C}$  pattern (Fig. 2.9): the  $\delta^{13}\text{C}$  gradually increases from the background value (~0.4‰) in Bed D to a maximum (2.28‰) in the upper part of Bed C, where a sudden negative excursion (>3‰ in magnitude) occurs immediately after the maximum, followed by a gradual return to more positive values and finally to the normal background values in Bed A. Although there is

no unique explanation as to the cause of the  $\delta^{13}\text{C}$  changes, the  $\delta^{13}\text{C}$  changes in Section AV4B can be best explained, particularly in light of the paleontological evidence available, as a manifestation of changes in marine biological productivity which controls the near-surface-water carbon reservoir through photosynthesis (Magaritz, 1989; Hsü and Mackenzie, 1985). Like the negative  $\delta^{13}\text{C}$  excursions associated with other major mass extinctions at the Cretaceous-Tertiary (Zachos et al., 1989), Permian-Triassic (Holser and Magaritz, 1987), Frasnian-Famennian (Wang et al., 1991b), and Precambrian-Cambrian (Magaritz, 1989) boundaries, the dramatic negative  $\delta^{13}\text{C}$  excursion in Section AV4B can be attributed to the isotopic effect of a large biomass reduction ("Strangelove Ocean" effects of Hsü and Mackenzie, 1985) associated with the extinction in the Selwyn Basin near the end-Ordovician. The following recovery of biomass is recorded by the return to more positive  $\delta^{13}\text{C}$  values after the negative  $\delta^{13}\text{C}$  excursion in the section. Coinciding with the  $\delta^{13}\text{C}$  excursion, the timing of the faunal turnover and extinction recorded by fossils in this section strongly supports this biomass-controlled- $\delta^{13}\text{C}$ -change scenario. However, the duration of these events is difficult to estimate owing to the lack of information on the sedimentation rate in this section. Other possible processes considered here include changes in rates of burial and oxidization of organic carbon, and changes in dissolved  $\text{CO}_2$  levels in the water. These processes can be related to changes in the atmospheric  $\text{CO}_2$  partial pressure which is linked to climatic conditions, such as temperature, glaciation and regression, etc. However, these processes can not be positively tested by using the evidence from this section alone (see discussion below).

### **Discussion and interpretation**

Paleontological results from trilobites and conodonts clearly show that there was a faunal turnover and extinction in the Selwyn Basin on northwestern Laurentia near the end-Ordovician. The faunal turnover is characterized by the extinction of trilobite and conodont taxa of Ordovician aspect, followed by a period of lower fossil diversity in the basin and the gradual appearance of new taxa

of Silurian aspect. The faunal turnover and extinction seems to be abrupt, and is stratigraphically constrained within a 50-60 cm interval by trilobites and conodonts at our tightest controlled AV4B Section, but the duration of the event is difficult to estimate due to the lack of information on the sedimentation rate. Isotopic evidence (i.e., sudden negative  $\delta^{13}\text{C}$  excursion in the interval of the extinction) also indicates a sudden collapse of marine primary productivity in the basin, associated with the extinction.

Centimetre-scale thin section analysis of Section AV4B across the extinction interval suggests that the faunal turnover and extinction occurred during the time of the maximum shallowing in this section, most likely coincident with a low stand of sea level, which, in turn, may have been a result of the glacio-eustatic regression induced by a known glaciation on Gondwana (Sheehan, 1988; Brenchley, 1989). Post-extinction sediments, which are dark, thin-bedded, laminated micritic limestones, were deposited in a transgressive sequence. The transgression is also probably glacio-eustatic, resulting from the melting of the Gondwanan ice sheets. The regressive-transgressive cycle recognized in the Selwyn Basin appears to be generally concordant with those documented for other parts of the world. Documented in many sedimentary basins on several continents (e.g., North America, Europe, and China), it appears to be a general pattern in the Late Ordovician that a regression was associated with the Gondwanan glaciation in the Ashgill, and a subsequent transgression coincided with the melting of the ice in the latest Hirnantian (Brenchley, 1989; Sheehan, 1988). However, more complex patterns of transgression-regression cycles may be recognized in some places, particularly in shallow shelf settings where carbonate-siliciclastic sequences allow more quantitative analyses of changes in relative water depth (e.g., Anticosti Island, Long, in press).

The Ir abundances in Section AV4B are generally low ( $< 0.051$  ppb), and therefore do not indicate that a large-body impact was involved with the faunal turnover and extinction near the end-Ordovician. The Ir abundance and Ir/Al ratio maxima appear to be associated with the condensation and low sedimentation at the beds

A/B boundary (Fig. 2.7); the mechanism of this association is explained by us elsewhere (Wang et al., 1992). The low Ir abundances and the extremely low Al abundances in Bed C indicate that the two peaks of the Ir/Al ratio in Bed C (Fig. 2.7) are not real Ir enrichment peaks but rather an artifact arising from the Al normalization.

It is noticed that the interval of the faunal turnover and extinction in Section AV4B was associated with a brief period of oxygenation in an otherwise anoxic basin. The brief ventilation of the basin with oxygen in the faunal turnover interval is indicated by the deposition of the two particularly prominent, light-coloured normal limestone beds (C and B) with abundant benthic fossils (Figs. 2.3, 2.4), and by the more negative  $C_{\text{anom}}$  values in the two beds (Fig. 2.8). Ventilation of stratified, anoxic basins can occur during a glaciation, when sea ice at high latitudes creates dense, oxygen-rich waters which sink and spread out to lower latitudes, causing anoxic basins there to be ventilated. The upwelling and overturn of the deep water in the basin can occur during ventilation through vertical advection. This process could bring toxic material from the deep water to the upper water photic zone (< 100 m) to cause the poisoning of organisms living there (Wilde et al., 1990). Wilde et al. (1990) suggested that, during cool climates with oxic deep waters (such as during a glaciation), an extinction may be caused by the upwelling of metals concentrated with depth and resulting in reduced primary productivity. The geochemical data acquired from Section AV4B are consistent with the model of Wilde et al. (1990), and suggest that an upwelling from the oxic deep-water zone during the glaciation may have greatly contributed to the faunal turnover and extinction in the Selwyn Basin.

Thin sections and the trace-element geochemistry (particularly Mn and Sr) of the isotopically analyzed carbonate samples from Section AV4B indicate that the diagenetic alteration in these samples is minimal. The selection of micrites for the isotopic analyses allows us to get more reliable isotopic data (especially for carbon) from the carbonates. Several samples, which were apparently altered, were identified by low  $\delta^{18}\text{O}$  values, low Sr

concentration, or high Mn concentration (Figs. 2.9, 2.10). Although the  $\delta^{13}\text{C}$  in Section AV4B has retained its original signal, the  $\delta^{18}\text{O}$  probably represents diagenetically overprinted values, owing to its sensitivity to alteration. A distinctive  $\delta^{13}\text{C}$  pattern across the extinction boundary in Section AV4B has been recognized, which includes a "Strangelove Ocean" perturbation in the extinction interval (Fig. 2.9). The  $\delta^{13}\text{C}$  values increase from the background values to a maximum, suddenly decrease to a minimum, then gradually increase to more positive values, and finally return to background values (Fig. 2.9). Similar isotopic patterns for both organic and carbonate carbon have been recently documented in many other sections around the world (see Wang et al., in press, for summary), including Québec and Yukon of Canada, South China, central Sweden, Latvia, and Wisconsin of U.S.A. (Wang et al., in press; Goodfellow et al., 1992; Long, in press; Marshall and Middleton, 1990; Brenchley et al., 1992; Yapp and Poths, 1992). We have suggested that the changes in carbon isotope compositions at approximately the same time in these widely separated sections around the world may be linked to changes in atmospheric and oceanic  $\text{CO}_2$  levels, associated with the growth and decay of the Gondwanan glaciation (see Wang et al., in press, for detailed discussion).

In summary, trilobite and conodont data from Avalanche Lake sections indicate a narrow interval (50-60 cm) of faunal turnover and extinction in the Selwyn Basin which was located on northwestern Laurentia in the Late Ordovician. Centimetre-scale microfacies, element geochemistry, and stable isotope analyses were performed on the samples across the extinction interval in Section AV4B with the best paleontological control. The results show that the faunal turnover and extinction occurred during the maximum shallowing (low stand of sea level), most likely associated with a regression induced by the glaciation on Gondwana. Carbon isotopes ("Strangelove Ocean" shift) clearly signal this extinction crisis. In terms of Ir concentrations, there is no clear indication of a large-body impact with the extinction in this section; higher Ir content is found to be associated with low sedimentation. Cerium anomaly

values indicate that a brief period of ventilated water conditions in the Selwyn Basin occurred during the interval of the faunal turnover. The ventilation of the basin, which was probably caused by the cold climate during the glaciation, may have triggered the upwelling of the deep, oxic water in the basin, bringing up toxic material, poisoning the upper-water photic zone and causing the faunal turnover and extinction observed in the Selwyn Basin.

### Conclusions

Avalanche Lake sections, containing a continuous Late Ordovician-Early Silurian sequence of comparatively deep-water carbonates, were deposited on the slope into the Selwyn Basin which was located on northwestern Laurentia in the Paleozoic. Paleontological analysis of trilobite and conodont faunas from these sections indicates a profound faunal turnover and extinction near the end-Ordovician. The faunal turnover and extinction, which appears to be abrupt, is constrained stratigraphically within a narrow interval (50-60 cm) in Section AV4B. Detailed analyses (centimetre-scale analyses) of microfacies, element geochemistry, and carbon and oxygen stable isotopes were performed on > 70 samples across the extinction interval in Section AV4B. The results indicate that the faunal turnover and extinction occurred during the time of the maximum shallowing (low stand of sea level) in the section, which was probably associated with a glacio-eustatic regression induced by a known glaciation on Gondwana in the latest Ordovician. The extinction crisis is clearly signalled by the change in the  $\delta^{13}\text{C}$  values in the section: a sudden "Strangelove Ocean" excursion (> 3‰ in magnitude) in the extinction interval, and a following return to the background values with the recovery of the biological productivity in the basin. Iridium abundances are low (< 0.051 ppb) across the extinction interval, and do not indicate the involvement of a large extraterrestrial impact with the faunal turnover and extinction. The highest Ir abundance in the section is found to be associated with the low sedimentation in a condensed horizon. Cerium anomalies in the section indicate a brief period of oxygenation in the otherwise anoxic Selwyn Basin. The faunal

turnover and extinction occurred during the time of the basin ventilation which was probably caused by the cold climate during the glaciation. The ventilation may have triggered upwelling through vertical advection of the deep, oxic water in the basin, bringing up toxic material, poisoning the upper-water photic zone and causing the faunal turnover and extinction in the basin.

Trace elements (particularly Sr and Mn) and thin sections of the isotopically analyzed samples suggest that the degree of alteration in the samples are very low, and that the original  $\delta^{13}\text{C}$  signals are preserved. The  $\delta^{13}\text{C}$  values display a distinctive pattern of changes across the extinction interval: an upward increase (from the background values) towards a maximum, followed by a sudden decrease to a minimum, and then a gradual increase to more positive and finally to the background values. Similar  $\delta^{13}\text{C}$  patterns have been documented in other sedimentary basins around the world (e.g., sections in Québec and Yukon of Canada, South China, central Sweden, Latvia, and Wisconsin). We have suggested that the changes in carbon isotope compositions at approximately the same time of the latest Ordovician in these widely located sections around the world may be linked to the changes in the atmospheric and oceanic  $\text{CO}_2$  levels, associated with the growth and decay of the Gondwanan ice sheets.

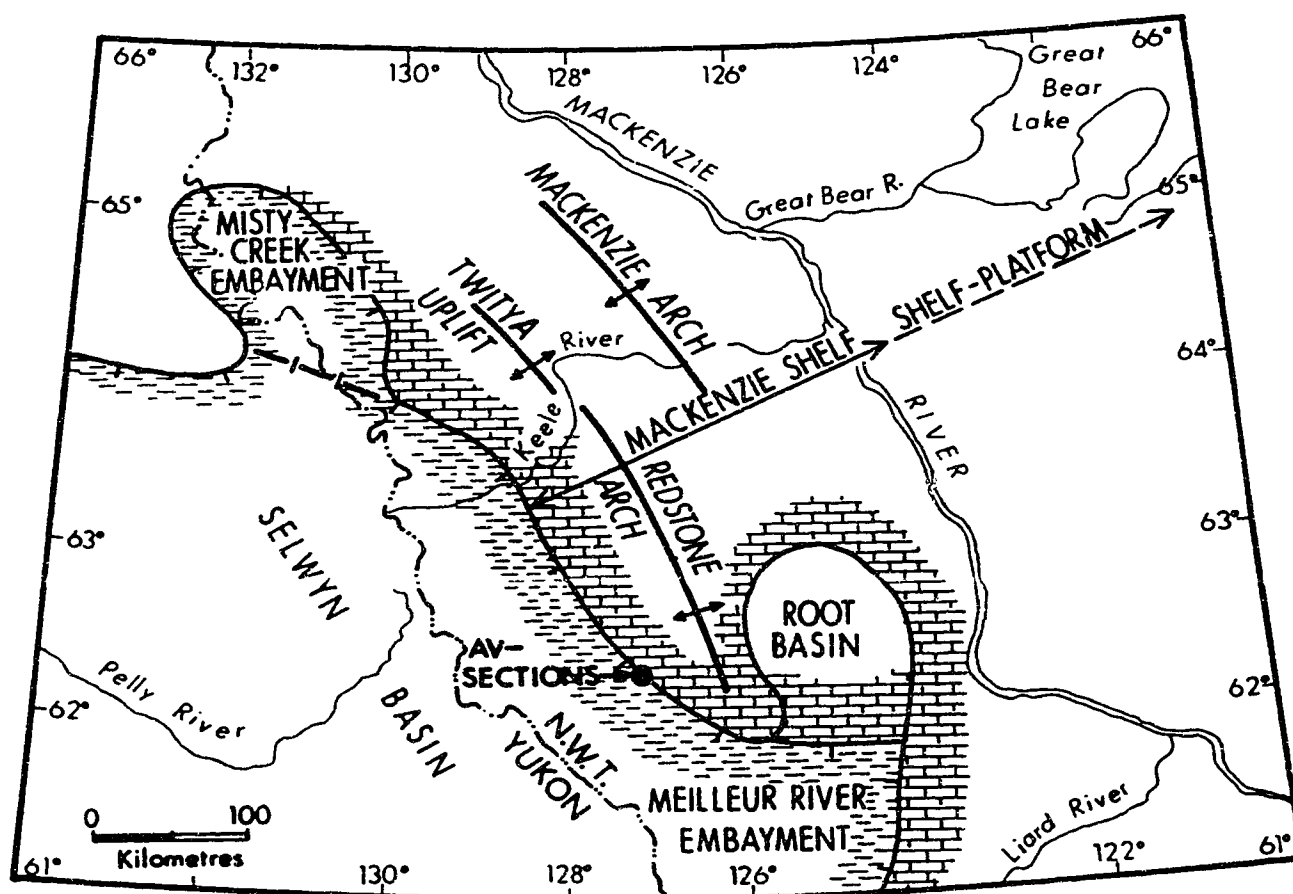
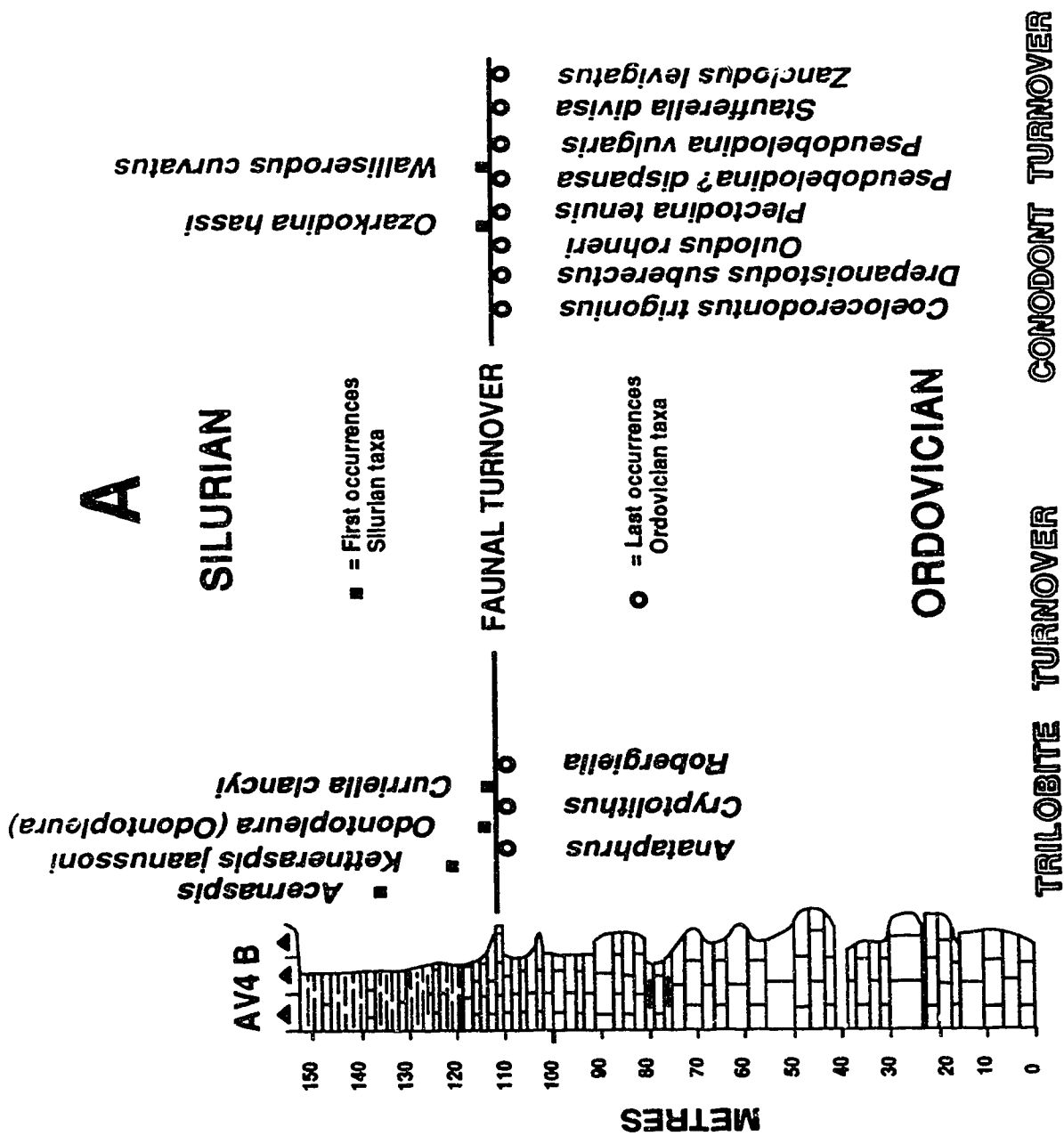
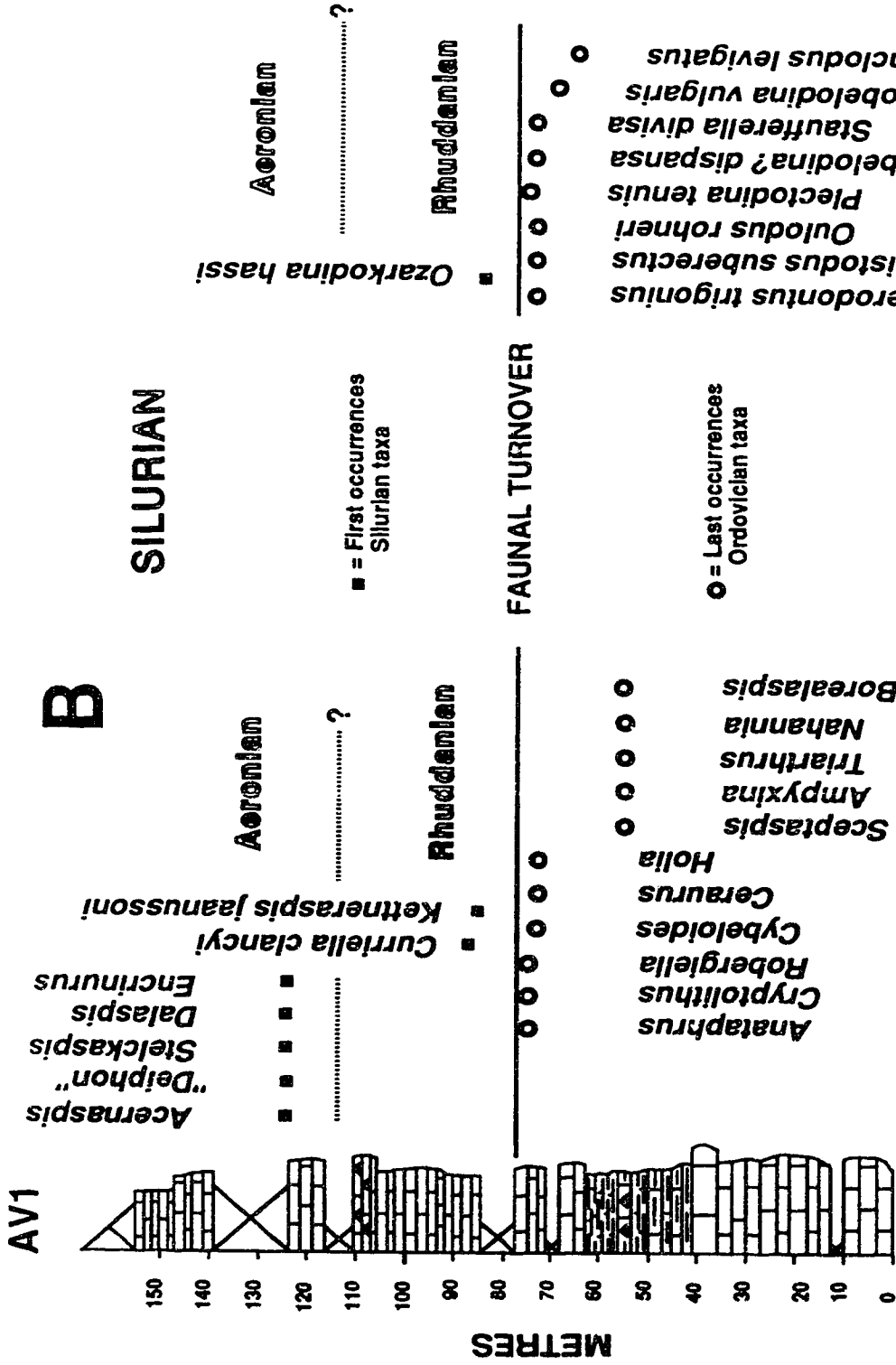


Fig. 2.1. Late Ordovician-Early Silurian lithofacies and the location of the Avalanche Lake (AV) sections.



**Fig. 2.2.** Last occurrences of Late Ordovician and first occurrences of Early Silurian (post-extinction) trilobite and conodont taxa in Section AV4B (A) and Section AV1 (B).





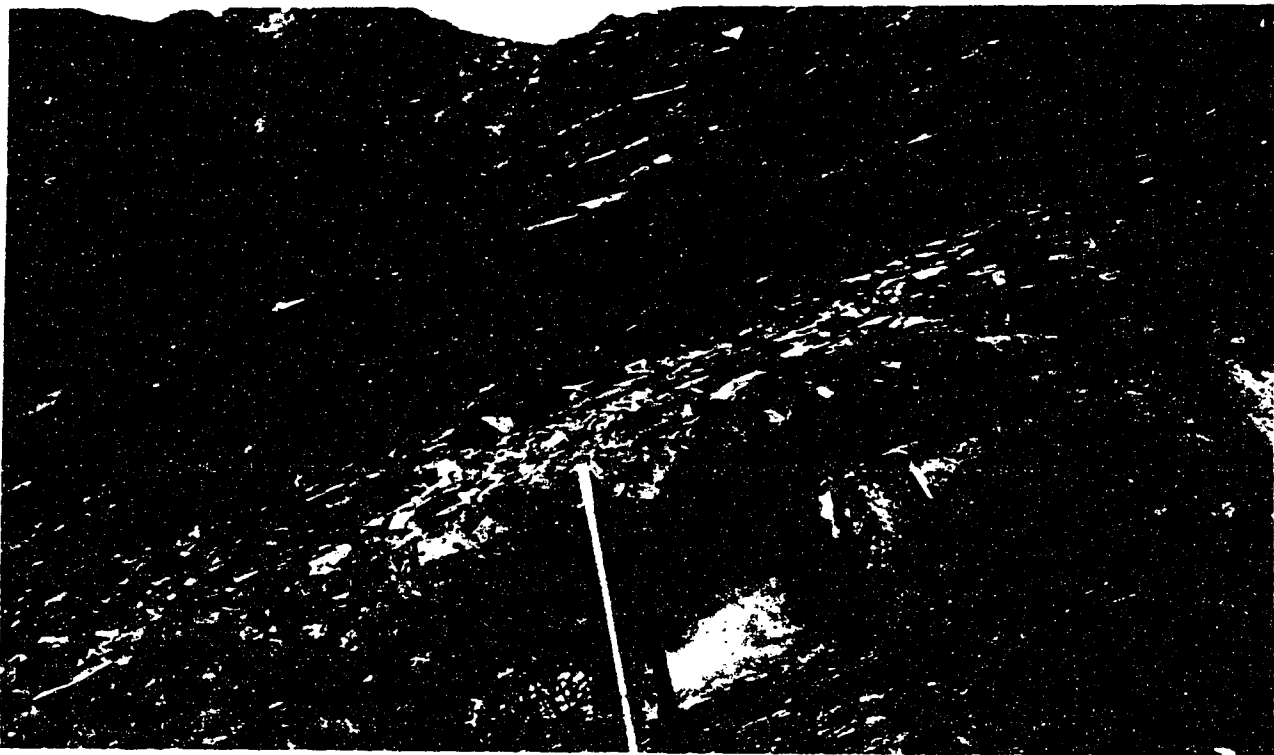
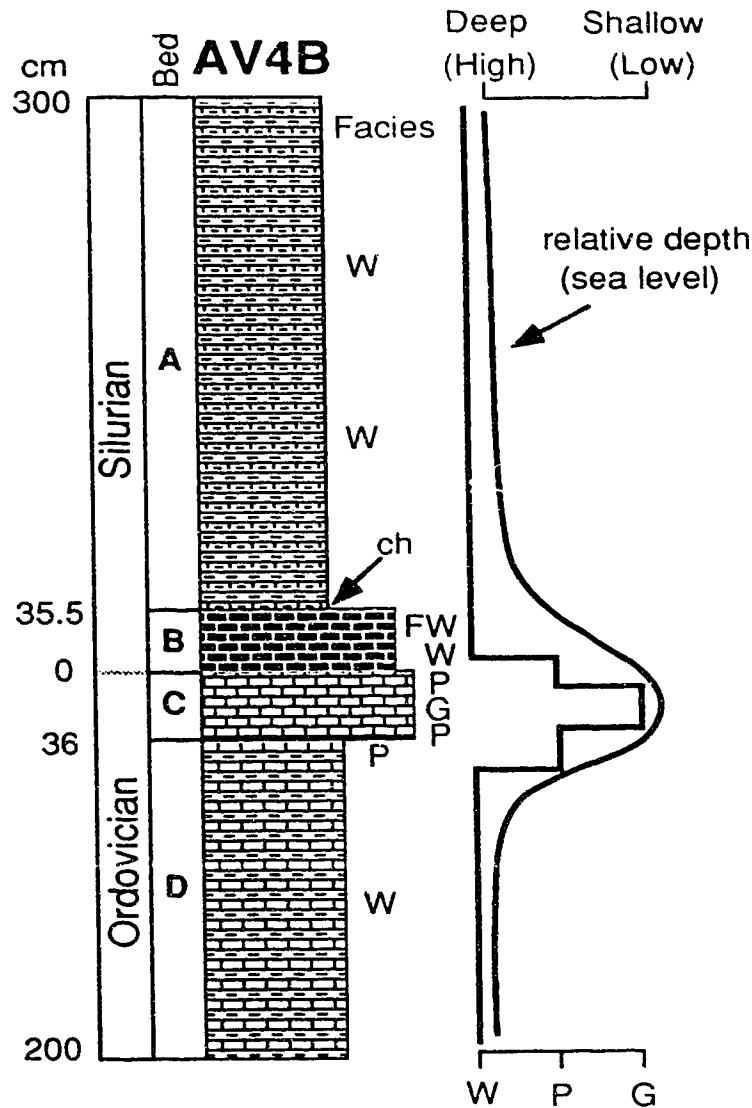


Fig. 2.3. Photo of the outcrop of the Ordovician-Silurian boundary interval at Section AV4B. Note that two particularly prominent, resistant and light-coloured limestone beds are sandwiched in a more recessive, dark-coloured, shaly-looking sequence of argillaceous limestones.



**Fig. 2.4.** Stratigraphic column of a 5 m-thick interval in Section AV4B that has been analyzed sedimentologically and geochemically. Symbols for microfacies: W, wackestone; P, packstone; G, peloidal grainstone; and FW, floatstone in wackestone matrix. A condensed horizon (ch) is recognized along the beds A and B contact. Relative water-depth curve is inferred from the microfacies in the carbonates.

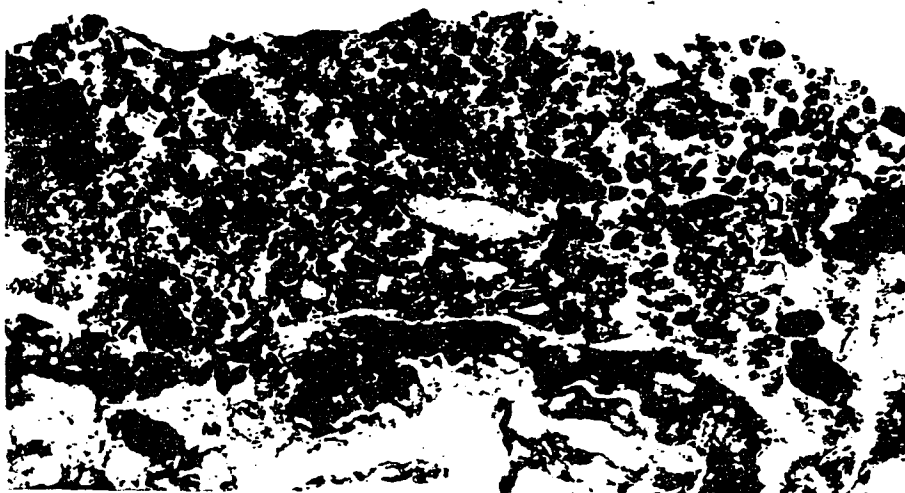
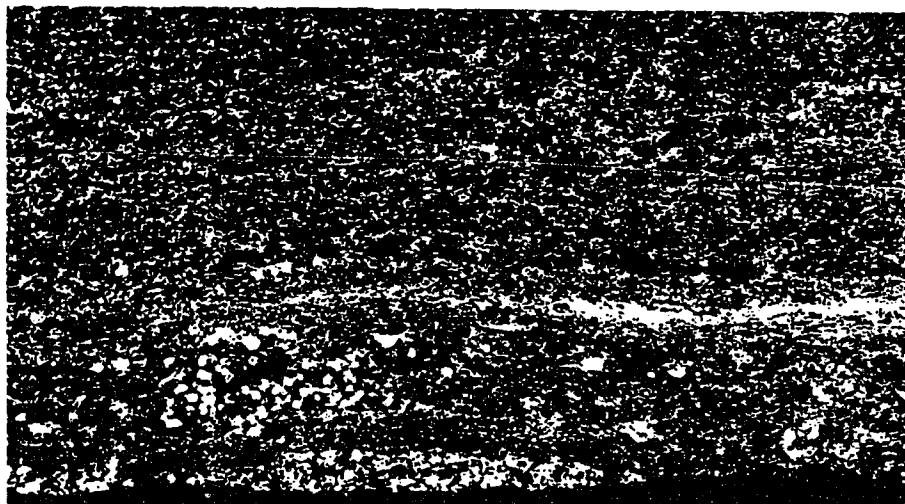
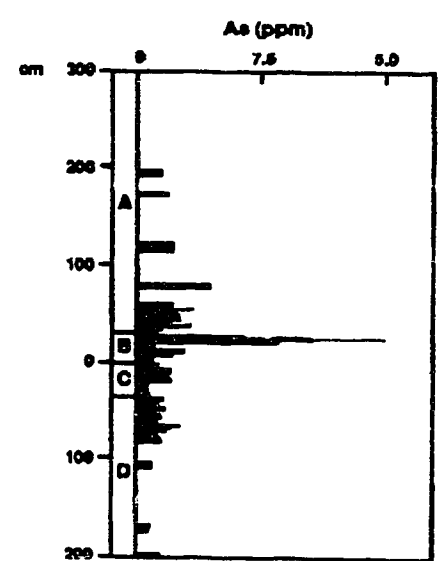
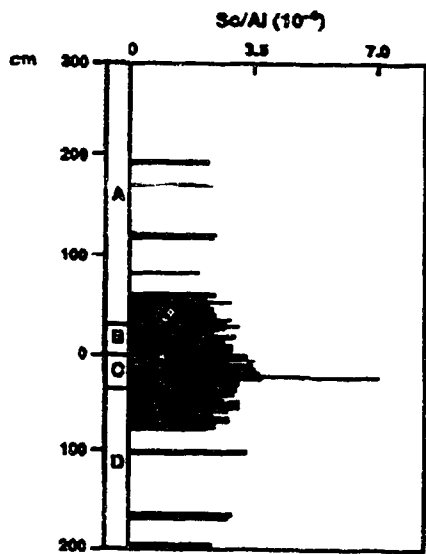
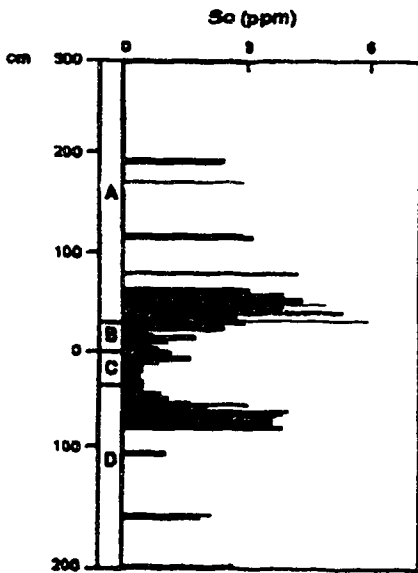
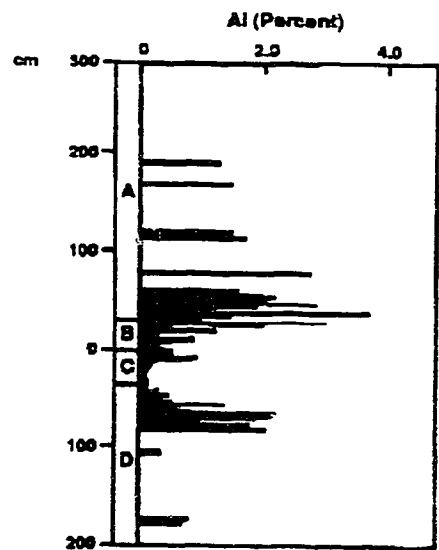
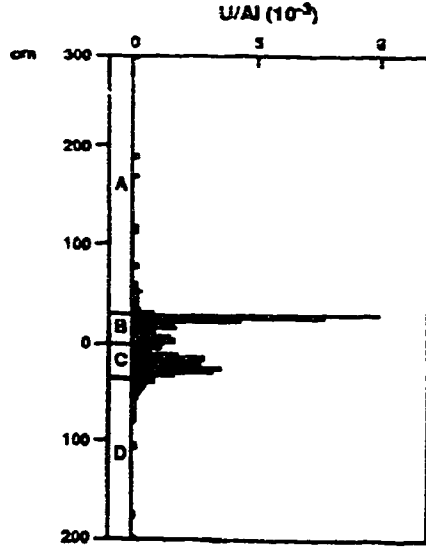
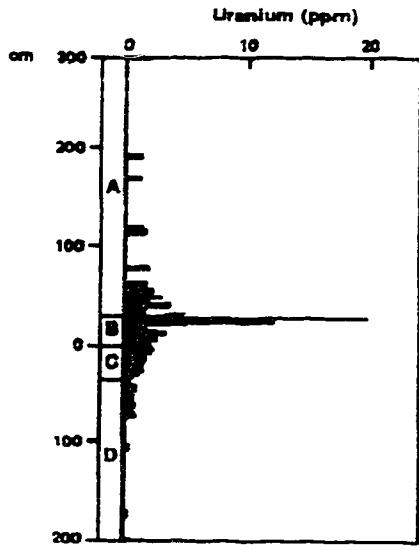
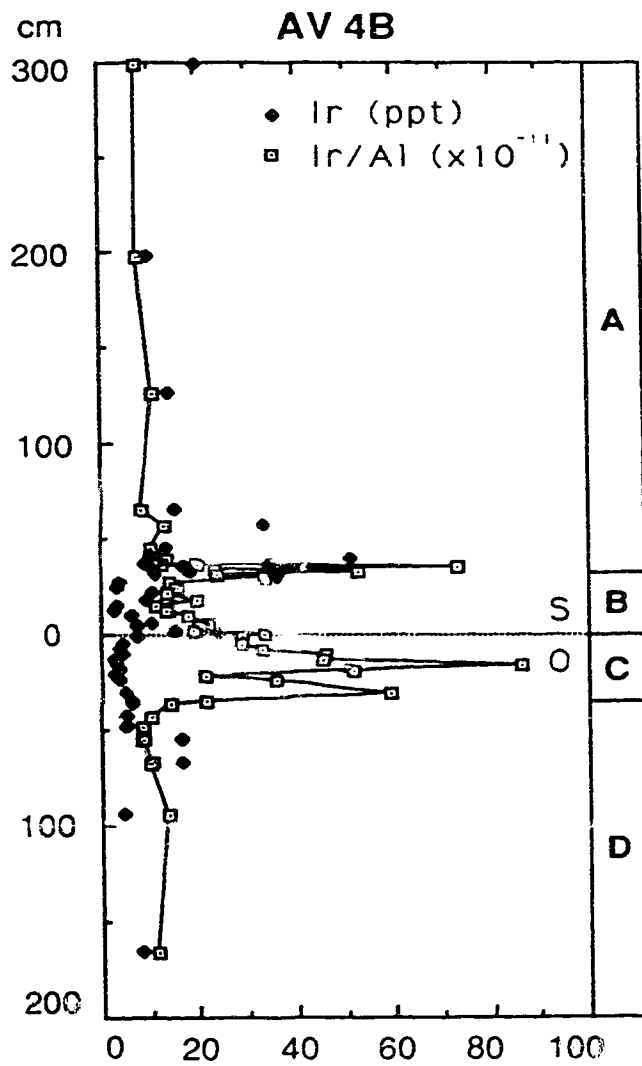


Fig. 2.5. Microphotos of the thin section of the rocks from around the beds A/B contact, representing a condensed horizon (a firmground or a hiatus). Note abundant phosphatic pellets are contained in the uppermost Bed B (B), and some are in the basal Bed A (A).

**Fig. 2.6.** Plot of the abundances and ratios for some significant elements in Section AV4B.







**Fig. 2.7.** Plot of the Ir abundance and Ir/Al ratio in Section AV4B.

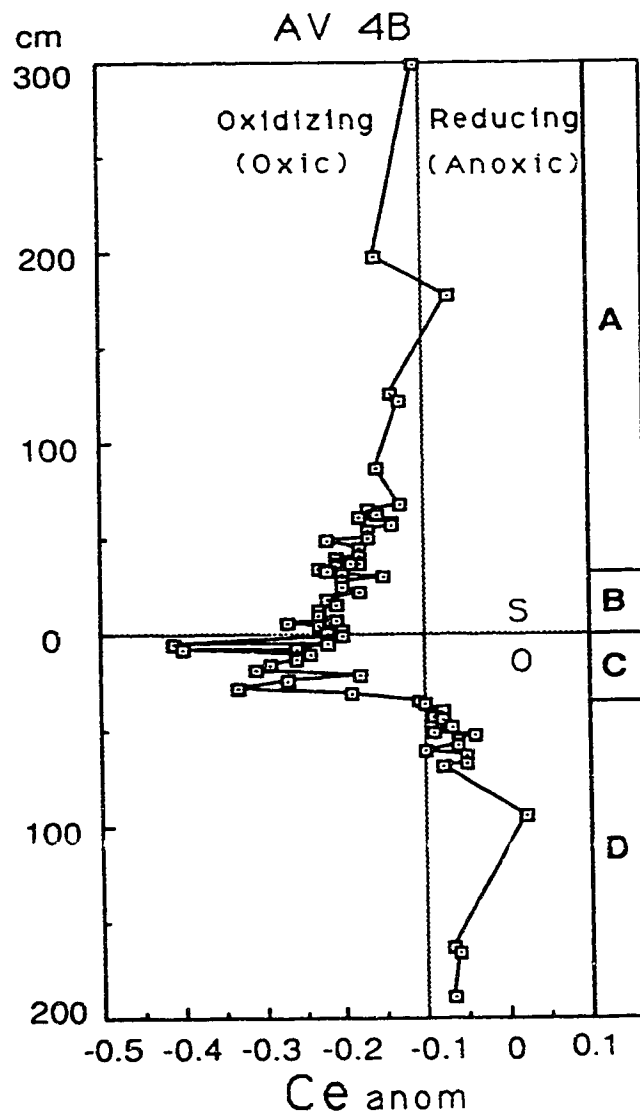


Fig. 2.8. Plot of the values of the cerium anomaly in Section AV4B.

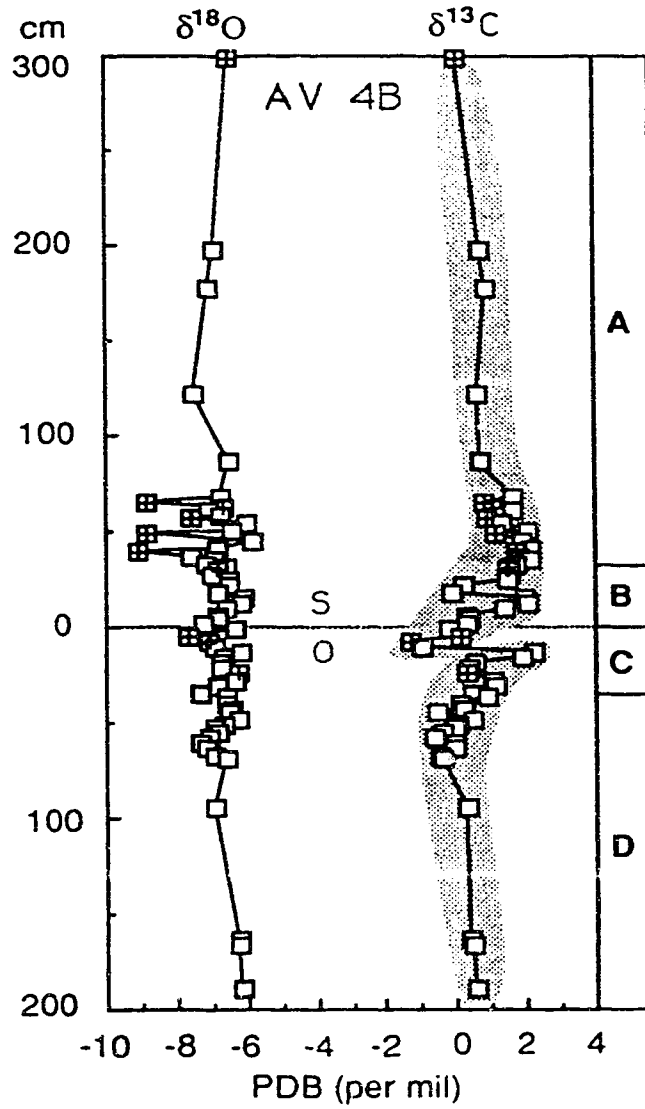


Fig. 2.9. Plot of the  $\delta^{13}\text{C}$  and  $\delta^{18}\text{O}$  in Section AV4B. Samples with  $< 500$  ppm Sr or  $> 100$  ppm Mn are indicated by crosses.

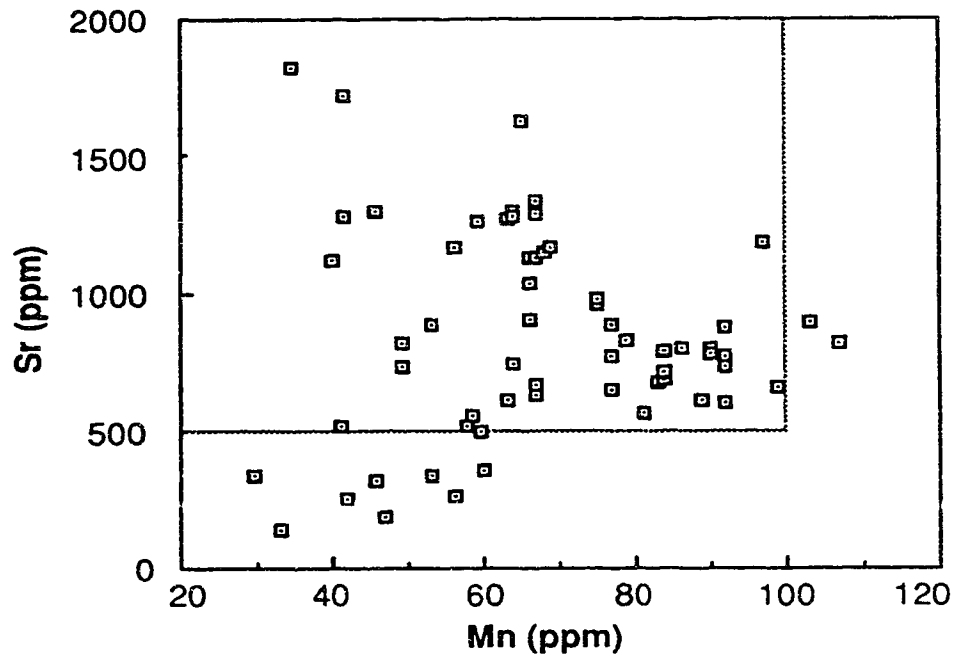


Fig. 2.10. Interplot of the Sr and Mn concentrations in Section AV4B. The square confines the "best preserved" (or least altered) samples.

## References

- Berry, W.B.N., and Wilde, P. 1978. Progressive ventilation of the oceans: An explanation for the distribution of the Lower Paleozoic black shales. *American Journal of Science*, 278: 257-275.
- Bolton, T.E., and Ross, J.R.P. 1985. The cryptostomate bryozoan *Sceptropora* (Rhabdomesina, Arthrostylidae) from Upper Ordovician rocks of southern Mackenzie Mountains, District of Mackenzie. *Geological Survey of Canada, Paper 85-1A*, pp. 29-45.
- Brand, U., and Morrison, J.O. 1987. Biogeochemistry of fossil marine invertebrates. *Geoscience Canada*, 14: 85-107.
- Brand, U., and Veizer, J. 1980. Chemical diagenesis of a Multicomponent carbonate system-1: Trace elements. *Journal of Sedimentary Petrology*, 50: 1219-1236.
- Brenchley, P.J. 1989. The late Ordovician extinction. In *Mass Extinctions: Processes and Evidence*. Edited by S.K. Donovan. Columbia University Press, New York, pp. 104-132.
- Brenchley, P.J., Marshall, J.D., Robertson, D.B.R., Hints, L., and Carden, G. 1992. Climatic-biotic interactions in the Late Ordovician mass extinction. In *Fifth International Conference on Global Bio-Events: Phanerozoic Global Bio-Events and Event-Stratigraphy*, Göttingen, Germany, February 16-19, 1992. Abstract volume, pp. 22.
- Cecile, M. 1982. The Lower Paleozoic Misty Creek embayment, Selwyn Basin, Yukon and Northwest Territories. *Geological Survey of Canada Bulletin*, 335: 1-78.
- Chatterton, B.D.E., Edgcombe, G.D., and Tuffnell, P.A., 1990. Extinction and migration in Silurian trilobites and conodonts of northwestern Canada. *Journal of The Geological Society of London*, 147: 703-715.
- Chatterton, B.D.E., and Ludvigsen, R. 1983. Trilobites from the Ordovician-Silurian boundary of the Mackenzie Mountains, Northwestern Canada. In *Papers for the Symposium on the Cambrian-Ordovician and Ordovician-Silurian Boundaries*.

- Nanjing, China, October, 1983. Nanjing Institute of Geology and Palaeontology, Academia Sinica, pp. 146-147.
- Chatterton, B.D.E., and Ludvigsen, R. 1976. Silicified Middle Ordovician trilobites from the southern Nahanni River area, District of Mackenzie, Canada. *Palaeontographica Abt A*, 154: 1-106.
- Chatterton, B.D.E., and Perry, D.G. 1983. Silicified Silurian odontopleurid trilobites from the Mackenzie Mountains. *Palaeontographica Canadiana*, 1: 1-127.
- Chatterton, B.D.E., and Perry, D.G. 1984. Silurian cheirurid trilobites from the Mackenzie Mountains, northwestern Canada. *Palaeontographica Abt A*, 184: 1-78.
- Copeland, M.J. 1981. Latest Ordovician and Silurian ostracode faunas from Anticosti Island, Québec. In Volume II: Stratigraphy and paleontology: IUGS Subcommision on Silurian Stratigraphy, Ordovician-Silurian Boundary Working Group, Field Meeting, Anticosti-Gaspé, Québec, 1981. Edited by P.J. Lespérance. University of Montreal, Montreal, pp. 185-195.
- Copeland, M.J. 1989. Silicified Upper Ordovician-Lower Silurian ostracodes from the Avalanche Lake area, southwestern District of Mackenzie. *Geological Survey of Canada Bulletin*, 341: 1-100.
- Douglas, M.J., and Norris, D.K. 1961. Camsell Bend and Root River map-area. *Geological Survey of Canada, Paper 61-13*, pp. 1-36.
- Dunham, R.J. 1962. Classification of carbonate rocks according to depositional texture. In *Classification of carbonate rocks*. Edited by W.E. Ham. American Association of Petroleum Geologists, *Memoir 1*, pp. 108-121.
- Edgecombe, G.D., and Chatterton, B.D.E. 1987. Heterochrony in the Silurian radiation of encrinurine trilobites. *Lethaia*, 20: 337-351.
- Edgecombe, G.D., and Chatterton, B.D.E. 1990. Systematics of Encrinuroides and Curriella, with a new Early Silurian encrinurine from the Mackenzie Mountains. *Canadian Journal of Earth Sciences*, 27: 820-833.
- Embry, A.F., and Klovan, J.E. 1971. A late Devonian reef tract on northeastern Banks Island, Northwest Territories. *Bulletin of Canadian Petroleum Geology*, 19: 730-781.

- Gabrielse, H. 1967. Tectonic evolution of the northern Canadian Cordillera. *Canadian Journal of Earth Sciences*, 4: 271-298.
- Gabrielse, H., Blusson, S.L., and Roddick, J.A. 1973. Flat River, Glacier Lake, and Wrigley Lake map areas (95E, L, M), District of Mackenzie and Yukon Territory. *Geological Survey of Canada Memoir*, 366: 1-200.
- Gass, K.C., Edgecombe, G.D., Ramsköld, L., Mikulic, D.G., and Watkins, R. 1992. Silurian Encrinurinae (Trilobita) from the central United States. *Journal of Paleontology*, 66: 75-89.
- Goodfellow, W.D., and Jonasson, I.R. 1984. Ocean stagnation and ventilation defined by  $\delta^{34}\text{S}$  secular trends in pyrite and barite, Selwyn Basin, Yukon. *Geology*, 12: 583-586.
- Goodfellow, W.D., Nowlan, G.S., McCracken, A.D., Lenz, A.C., and Grégoire, D.C., 1992. Geochemical anomalies near the Ordovician-Silurian boundary, northern Yukon Territory, Canada. *Historical Biology*, 6: 1-23.
- Gromet, L.P., Dymek, R.F., Haskin, L.A., and Korotev, R.L. 1984. The "North American shale composite": Its compilation, major and trace characteristics. *Geochimica et Cosmochimica Acta*, 48: 2469-2482.
- Holser, W.T., and Magaritz, M. 1987. Events near the Permian-Triassic boundary. *Modern Geology*, 11: 155-180.
- Hsü, K.J., and Mackenzie, J.A. 1985. A "Strangelove" ocean in earliest Tertiary. In *The carbon cycle and atmospheric CO<sub>2</sub>: Natural variations, Archean to present*. Edited by E.T. Sunquist and W. Broecker. American Geophysical Union, *Geophysics Monograph* 32, pp. 487-492.
- Johnston, D.I., and Chatterton, B.D.E. 1983. Some silicified Middle Silurian rostroconchs (Mollusca) from the Mackenzie Mountains, N.W.T., Canada. *Canadian Journal of Earth Sciences*, 20: 844-858.
- Lenz, A.C., and McCracken, A.D. 1988. Ordovician-Silurian boundary, northern Yukon. *Bulletin of the British Museum (Natural History) Geology Series*, 43: 265-271.
- Long, D.G.F., in press. Oxygen and carbon isotopes and event stratigraphy near the Ordovician-Silurian boundary, Anticosti Island, Québec. *Palaeogeography, Palaeoclimatology,*

## Palaeoecology.

- Ludvigsen, R. 1979. Middle Ordovician trilobite biofacies, southern Mackenzie Mountains. In *Western and Arctic Canada biostratigraphy*. Edited by C.R. Stelck and B.D.E. Chatterton. Geological Association of Canada, Special Paper 18, pp. 1-33.
- Magaritz, M. 1989.  $^{13}\text{C}$  minima follow extinction events: A clue to faunal radiation. *Geology*, 17: 337-340.
- Marshall, J.D., and Middleton, P.D. 1990. Changes in marine isotopic composition and the late Ordovician glaciation. *Journal of the Geological Society of London*, 147: 1-4.
- McCracken, A.D. 1991. Silurian conodont biostratigraphy of the Canadian Cordillera with a description of new Llandovery species. *Geological Survey of Canada Bulletin*, 417: 97-127.
- Melchin, M.J., McCracken, A.D., and Goodfellow, W.D. 1991a. Bioevents and geochemical anomalies near the Ordovician-Silurian boundary on Cornwallis and Truro islands, Arctic Canada. In *Event Makers in Earth History. Program and Abstracts of the Joint Meeting of the IGCP Projects 216, 293 and 303, August 28-30, Calgary, Alberta, Canada*, pp. 54.
- Melchin, M.J., McCracken, A.D., and Oliff, F.D. 1991b. The Ordovician-Silurian boundary on Cornwallis and Truro islands, Arctic Canada: preliminary data. *Canadian Journal of Earth Sciences*, 28: 1854-1862.
- Morrow, D.W. 1991. The Silurian-Devonian sequence in the northern part of the Mackenzie Shelf, Northwest Territories. *Geological Survey of Canada Bulletin*, 413: 1-121.
- Morrow, D.W., and Cook, D.G. 1987. The Prairie Creek Embayment and Lower Paleozoic strata of the southern Mackenzie Mountains. *Geological Survey of Canada Memoir*, 412: 1-123.
- Nowlan, G.S., Goodfellow, W.D., McCracken, A.D., and Lenz, A.C. 1988a. Geochemical evidence for sudden biomass reduction and anoxic basins near the Ordovician-Silurian boundary in northwestern Canada. In *Abstracts of the 5th International Symposium of the Ordovician System, August, 1988, Memorial University of Newfoundland, St. John's, Canada*, pp. 66.
- Nowlan, G.S., McCracken, A.D., and Chatterton, B.D.E. 1988b.



- Conodonts from Ordovician-Silurian boundary strata, Whittaker Formation, Mackenzie Mountains, Northwest Territories. Geological Survey of Canada Bulletin, 373: 1-99.
- Orth, C.J. 1989. Geochemistry of the bio-event horizons. In Mass Extinctions: Processes and Evidence. Edited by S.K. Donovan. Columbia University Press, New York, pp. 37-72.
- Over, D.J., and Chatterton, B.D.E. 1987. Silurian conodonts from the south Mackenzie Mountains, Northwest Territories, Canada. *Geologica et Palaeontologica*, 21: 1-49.
- Popp, B.N., Anderson, T.F., and Sandberg, P.A. 1986. Brachiopods as indicators of original isotopic compositions in some Paleozoic limestones. *Geological Society of America Bulletin*, 97: 1262-1269.
- Scotese, C.R., and McKerrow, W.S. 1990. Revised world maps and introduction. In *Paleozoic Palaeogeography and Biogeography*. Edited by W.S. McKerrow and C.R. Scotese. Geological Society of London Memoir, 12: 1-21.
- Sepkoski, J.J., Jr. 1982. Mass extinctions in the Phanerozoic oceans: A review. *Geological Society of America, Special Paper 190*, pp. 293-289.
- Sheehan, P.M. 1988. Late Ordovician events and the terminal Ordovician extinction. *New Mexico Bureau of Mines and Mineral Resources, Memoir 44*, pp.405-415.
- Siveter, D.J., and Chatterton, B.D.E. submitted. Silicified calymenid trilobites from the Silurian of the Mackenzie Mountains, northwest Canada. *Canadian Journal of Earth Sciences*.
- Veizer, J. 1983. Trace elements and isotopes in sedimentary carbonates. *Reviews in Mineralogy*, 11: 265-300.
- Veizer, J., Fritz, P., and Jones, B. 1986. Geochemistry of brachiopods: Oxygen and carbon isotopic records of Paleozoic oceans. *Geochimica et Cosmochimica Acta*, 50: 1679-1696.
- Wadleigh, M.A., and Veizer, J. 1992.  $^{18}\text{O}/^{16}\text{O}$  and  $^{13}\text{C}/^{12}\text{C}$  in lower Paleozoic articulate brachiopods: Implications for the isotopic composition of seawater. *Geochimica et Cosmochimica Acta*, 56: 431-443.
- Wang, K., Chatterton, B.D.E., Attrep, M., and Orth, C.J. 1992. Iridium

- abundance maxima at the latest Ordovician mass extinction horizon, Yangtze Basin, China: Terrestrial or extraterrestrial? *Geology*, 20: 39-42.
- Wang, K., Chatterton, B.D.E., Orth, C.J., and Attrep, M. 1991a. Geochemical, paleontological and sedimentological studies of the end-Ordovician mass extinction, Mackenzie Mountains, N.W.T., Canada. *Geological Society of America Abstracts with Programs*, 23: A181.
- Wang, K., Orth, C.J., Attrep, M., Jr., Chatterton, B.D.E., Hou, H., and Geldsetzer, H.H.J. 1991b. Geochemical evidence for a catastrophic biotic event at the Frasnian/Famennian boundary in South China. *Geology*, 19: 776-779.
- Wang, K., Orth, C.J., Attrep, M., Jr., Chatterton, B.D.E., Wang, X., and Li, J. in press. The great latest Ordovician extinction on the South China Plate: Chemostratigraphic studies of the Ordovician-Silurian boundary interval on the Yangtze Platform. *Palaeogeography, Palaeoclimatology, Palaeoecology*.
- Wilde, P., Quinby-Hunt, M.S., and Berry, W.B.N. 1990. Vertical advection from oxic or anoxic water from the main pycnocline as a cause of rapid extinction or rapid radiations. In *Extinction events in Earth history*. Edited by E.G. Kauffman and O.H. Walliser. Springer-Verlag, Berlin, pp. 85-98.
- Wright, J., Schrader, H., and Holser, W.T. 1987. Paleoredox variations in ancient oceans recorded by rare earth elements in fossil apatite. *Geochimica et Cosmochimica Acta*, 51: 631-644.
- Yapp, C.J., and Poths, H. 1992. Ancient atmospheric CO<sub>2</sub> pressures inferred from natural goethites. *Nature*, 355: 342-344.
- Zachos, J.C., Arthur, M.A., and Dean, W.E. 1989. Geochemical evidence for suppression of pelagic marine productivity at the Cretaceous/Tertiary boundary. *Nature*, 337: 61-64.

## Chapter 3

### Iridium abundance maxima at the latest Ordovician mass extinction horizon, Yangtze Basin, China: Terrestrial or extraterrestrial?

(A version of this chapter has been published. Wang, K., Chatterton, B.D.E., Attrep, M. Jr., and Orth, C.J., 1992. *Geology*, 20: 39-42.)

#### Introduction

One of the largest global extinction events in Earth history occurred near the end of the Ordovician. This extinction was the second most severe biological crisis in the Phanerozoic, with an estimated 22% loss of diversity at the family level (Sepkoski, 1982). It has been demonstrated that the late Ordovician extinction occurred in two major steps (Brenchley, 1989; Owen et al., 1991). An earlier phase of graptolite extinctions was at the end of the Rawtheyan (end-*pacificus* event, Koren, 1991; Melchin and Mitchell, 1991), and a second phase of both shelly and pelagic fauna extinctions was in the late Hirnantian (end-*bohemicus* event, Rong and Chen, 1986; Rong and Harper, 1988; Sheehan, 1988; Li et al., 1984; Cocks and Rickards, 1988), which coincided with a rapid transgression (Brenchley, 1989; Sheehan, 1988). Evidence has been obtained from around the globe that this last step of the late Ordovician extinction occurred very close to the traditional O/S boundary at the base of the graptolite *Glyptograptus persculptus* biozone (Cocks and Rickards, 1988; McLaren and Goodfellow, 1990). This horizon is one biozone below the recently defined international O/S systemic boundary at the base of the *Parakidograptus acuminatus* zone (Bassett, 1985). Thus, the extinction is now placed within the latest Ordovician and is no longer a boundary event. However, concerns and criticisms have followed this decision, and a reconsideration of this boundary is likely (Lespérance et al., 1987; Berry, 1987). Chinese paleontologists have long adopted the traditional O/S boundary and are still using it (Mu, 1988) because the mass extinction is so evident at this horizon that it can be

recognized in most of the sections throughout the Yangtze region (Rong and Chen, 1986; Li et al., 1984).

Wang and Chai (1989) reported an Ir anomaly of 0.64 ppb at the base of the *G. persculptus* zone at Yichang in the Yangtze Basin and hypothesized that the latest Ordovician extinction was related to extraterrestrial causes. However, only six samples in this section were analyzed for Ir. Two previous chemostratigraphic studies of the O/S boundary sections found no impact-related Ir anomaly in sections on Anticosti Island, Quebec (Orth et al., 1986) and at Dob's Linn, Scotland (Wilde et al., 1986). Because this biotic event coincided with an extensive glaciation in the African and South American parts of Gondwana and with the associated glacio-eustatic regression elsewhere (Sheehan, 1988; Brenchley, 1988), there are few sequences in the world with continuous sedimentation across the O/S boundary. The fact that the absence of an impact-related Ir anomaly could be due to local preservation factors, such as erosion or nondeposition, led Wilde et al. (1986) and Berry (1987) to hope that a geochemical study of the sections in the Yangtze Basin, where the most complete fossil and rock record of the extinction is present, might shed light on the cause of the extinction. To test the hypothesis that all major extinctions might have been caused by extraterrestrial impacts (McLaren and Goodfellow, 1990), we measured the Ir and other elemental abundances across the latest Ordovician extinction horizon (end-*bohemicus* event) in two stratigraphic sections in the Yangtze Basin. One of the analyzed sections (Yichang section) also contains the horizon of the end-Rawtheyan extinction (end-*pacificus* event). The full story with about 40 elemental abundance patterns for each section will be published elsewhere.

### Yangtze Basin and extinction

The Yangtze Basin (Yangtze Platform) was a primary sedimentary basin from Sinian to Triassic time in China. It encompassed a broad continental shelf sea (Yangtze Sea) on the South China plate in the Paleozoic. The basin, partially enclosed by the old lands in the Late Ordovician, comprised a largely enclosed

western Upper Yangtze and an eastern Lower Yangtze that was open to the Pearl River Sea to the southeast (Fig. 3.1). It is believed that the water depth was less than 150 m in the Late Ordovician and that the Ashgillian regression did not drain the basin (Chen, 1984; Rong and Chen, 1986).

More than 30 continuous O/S boundary sections from this region have been studied during the past decade (Mu, 1988). Although the end-Rawtheyan extinction can be recognized in some sections, the most prominent and severe extinction of both pelagic and benthic faunas occurred at the base of the *persculptus* zone, with the disappearance of the brachiopod *Hirnantia* fauna and a 79% loss of graptolite diversity, at the generic level (Rong and Chen, 1986; Rong and Harper, 1988; Wang and Chai, 1989; Li et al., 1984). This extinction boundary in China was dated at  $439 \pm 18$  Ma by the Rb/Sr whole-rock method (Wang and Chai, 1989).

### Yichang and Jinxian sections

Two analyzed sections, located at Fenxiang, Yichang, Hubei Province, and Beigong, Jinxian, Anhui Province, were deposited some 700 km apart in the Upper and Lower Yangtze basins, respectively (Fig. 3.1). The Yichang section is the type section for the O/S boundary in China and was one of the three candidates for the international O/S boundary stratotype. Thus, it has been the subject of the most extensive biostratigraphic studies (Mu, 1988; Wang et al., 1983). The latest Ordovician extinction is most clearly displayed at the Jinxian locality (Li, et al., 1984). In the field, one can actually see the sudden disappearance of a large number of species, including graptolites, brachiopods, trilobites, nautiloids, ostracods and bivalves, right at the base of the *G. persculptus* zone.

### Results and discussion

Continuous samples were collected across the latest Ordovician extinction horizon in both of the sections, and neutron activation analysis (Orth, 1989) was performed on more than 60 samples. The Ir abundances and Ir/Al ratios in these sections are plotted in Figure 3.2.

Both sections are composed of graptolitic shales or mudstones, and they contain very little carbonate (less than 0.6%). Therefore, it is not necessary to normalize the Ir values on a carbonate-free basis to substantiate the Ir variation patterns. Ir concentrations range from 0.035 to 0.23 ppb, averaging about 0.08 ppb, in the Yichang section, and they range from 0.026 to 0.092 ppb, averaging about 0.06 ppb, in the Jinxian section. The latter may be compared to the Ir range of from 0.02 to 0.12 ppb, averaging about 0.05 ppb, in Paleozoic marine shales and mudstones (Wilde et al., 1986). The Ir abundances reach their maxima at the base of the *G. persculptus* zone (the latest Ordovician extinction horizon) in both sections, 0.23 and 0.092 ppb at Yichang and Jinxian, respectively. Because Ir is usually associated with clay minerals and the Al abundance is a relative measure of the clay content, we plotted the Ir/Al ratios to avoid variations caused by varying clay content. The Ir/Al ratios still show the maxima at the base of the *G. persculptus* zone in both sections (Fig. 3.2).

Wang and Chai (1989) analyzed six samples for Ir in the Yichang section and reported a stronger Ir anomaly of 0.64 ppb in two samples at and immediately above the base of the *G. persculptus* zone. They speculated that the Ir anomaly was due to an impact associated with the latest Ordovician extinction. We analyzed all 30 samples in this section and observed a 0.23 ppb Ir abundance maximum only in the sample at the base of the *G. persculptus* zone.

Assuming a constant influx of cosmic Ir, the abundances of Ir in deep-sea sediments should correlate negatively with the rate of sedimentation,  $\text{Ir (ppb)} = (0.07 + 0.094 [1/\text{rate of sedimentation in mm/ka}])$  for modern red clays (Barker and Anders, 1968). The Yichang section is extremely condensed, as it was deposited in the restricted Upper Yangtze Basin, in which, due to the blocking by the old lands of open sea circulation, the water was very quiet and anoxic (indicated by finely laminated black shales) (Chen et al., 1987; Rong and Chen, 1987). Under such a condition, the sedimentation rate was very slow. The calculated rate of sedimentation for the analyzed part of this section averages a

minuscule 0.35 mm/ka (Geng, 1984). On the other hand, the Jinxian section was deposited under near-normal marine conditions in the open Lower Yangtze Basin, and its rate of sedimentation was much faster (indicated by strata of equivalent age that are ten times as thick, see Fig. 3.2). The difference in sedimentation rates between these two sections is well reflected by the difference in the overall Ir concentrations in these sections. The lower rate of sedimentation may account for the overall higher Ir values in the Yichang section.

A rapid sea-level rise could lead to marine sediment starvation due to sediment entrapment in flooded river valleys and resultant decrease in sediment supply (Wignall, 1991; Vail et al., 1977). The basal part of a transgressive sequence is commonly the most condensed. The base of the *G. persculptus* zone marks the beginning of a very rapid transgression in the Yangtze area (Chen, 1984; Wang et al., 1983; Rong and Chen, 1986; Rong and Harper, 1988; Mu et al., 1981), possibly as a result of glacial retreat, and thus the sedimentary sequence in the lower *G. persculptus* zone is more condensed than the rest of these sections. The slower sedimentation rates at the base of the *G. persculptus* zone in both sections may account for the maxima of the Ir concentrations and Ir/Al ratios at the Chinese O/S boundary. Therefore, the Ir maxima do not indicate a sudden influx of excess cosmic material, such as an impact, at this extinction level. Wallace et al. (1991) also observed Ir abundance maxima associated with the beginning of rapid transgressions in the Early Cambrian and Oligocene.

The maximum Ir concentration in the Yichang section (0.23 ppb) is almost as high as the late Eocene impact Ir anomaly (Keller et al., 1987; Alvarez et al., 1982) but lower than that found at the K/T boundary. Using the equation of Ir and sedimentation rate relation, we would expect an average of 0.338 ppb Ir from normal cosmic influx in the Yichang section (rate of sedimentation = 0.35 mm/ka). Therefore, with such a low sedimentation rate, normal cosmic influx alone can account for the Ir peak at the boundary in this section.

The ratios of Ir to other siderophile elements are often used to evaluate the origin of Ir anomalies. We compared the Co/Ir ratio in

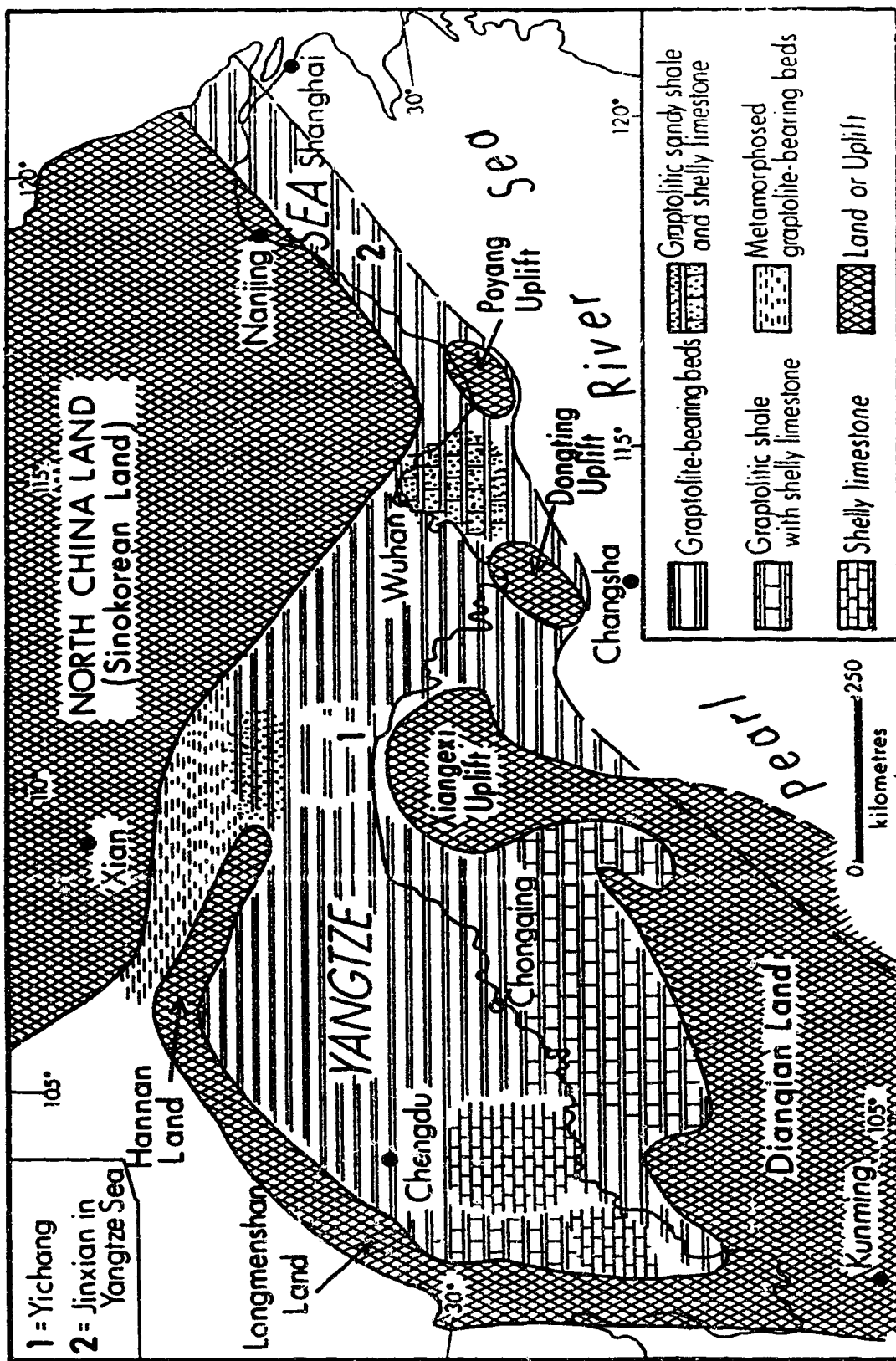
the boundary sediments at Yichang ( $7.3 \times 10^4$ ) and Jinxian ( $2.6 \times 10^4$ ) with that in the K/T boundary clay ( $2 \times 10^3$ ) (Schmitz et al., 1988) and in meteorites ( $2.8 \times 10^3$ ) (Wasson, 1974). They are obviously not comparable. Furthermore, at Jinxian, As, Mo, Sb, and U (not shown) are enriched as much as the Ir, suggesting that reducing conditions might have been associated with the Ir at the time of deposition of the boundary. From the discussion above, it is our conclusion that the latest Ordovician extinction in the Yangtze Basin does not appear to be linked with an extraterrestrial impact, although merely on the basis of Ir we cannot preclude impact by a comet with very low Pt-group element abundances.

### Conclusions

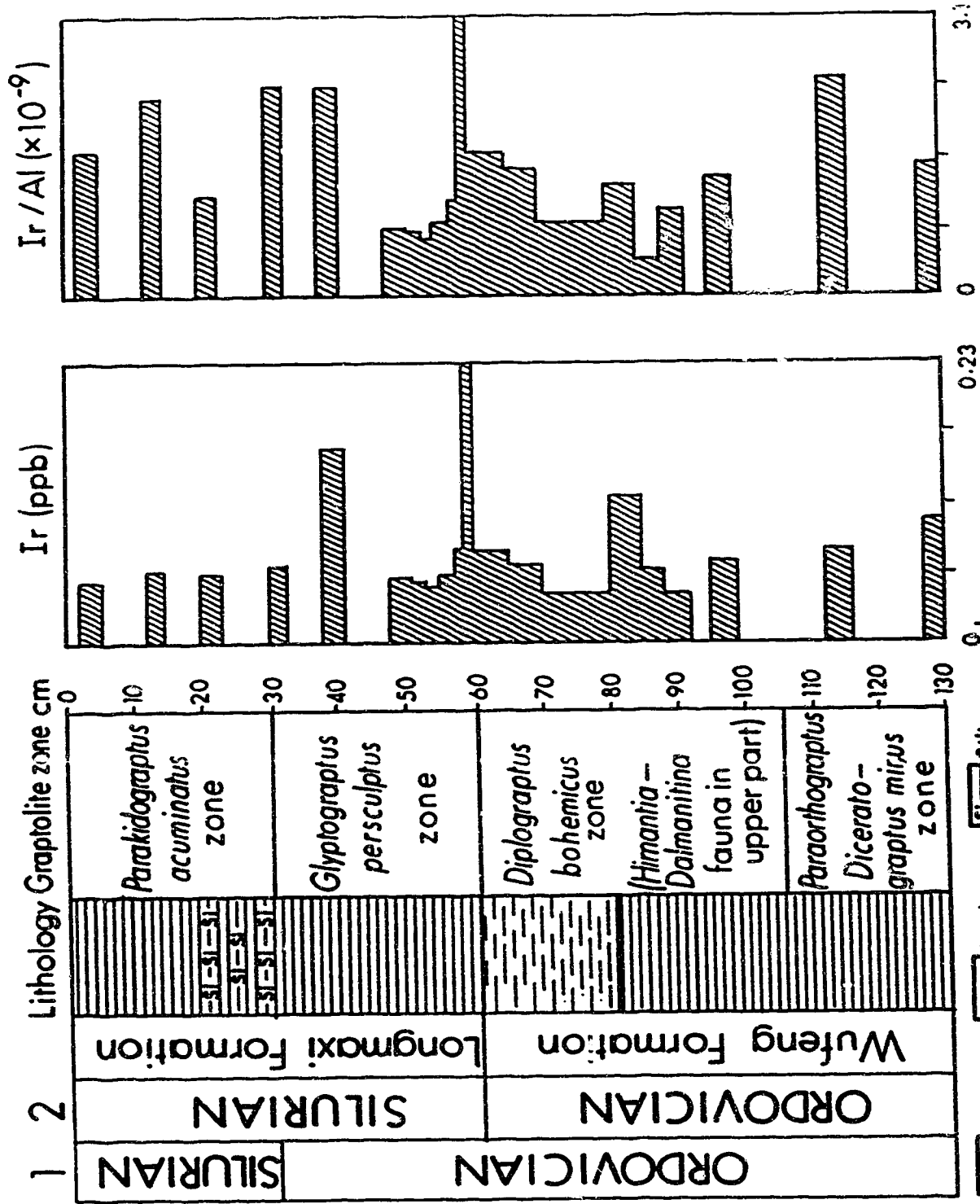
Neutron activation analysis of the Chinese Ordovician/Silurian (O/S) boundary sections at two distant localities in the Yangtze Basin, spanning the horizon of a major latest Ordovician global extinction event, shows the maxima of iridium abundances coincident with the extinction horizon at the base of the graptolite *Glyptograptus persculptus* zone. The 0.23 ppb Ir maximum in the Yichang type section is almost as large as the late Eocene impact Ir anomaly. However, we have observed that the Ir abundances in the Chinese sections are closely correlated with the sedimentation rates, and we therefore have concluded that the Ir maxima do not indicate a cataclysmic extraterrestrial impact at this extinction level.



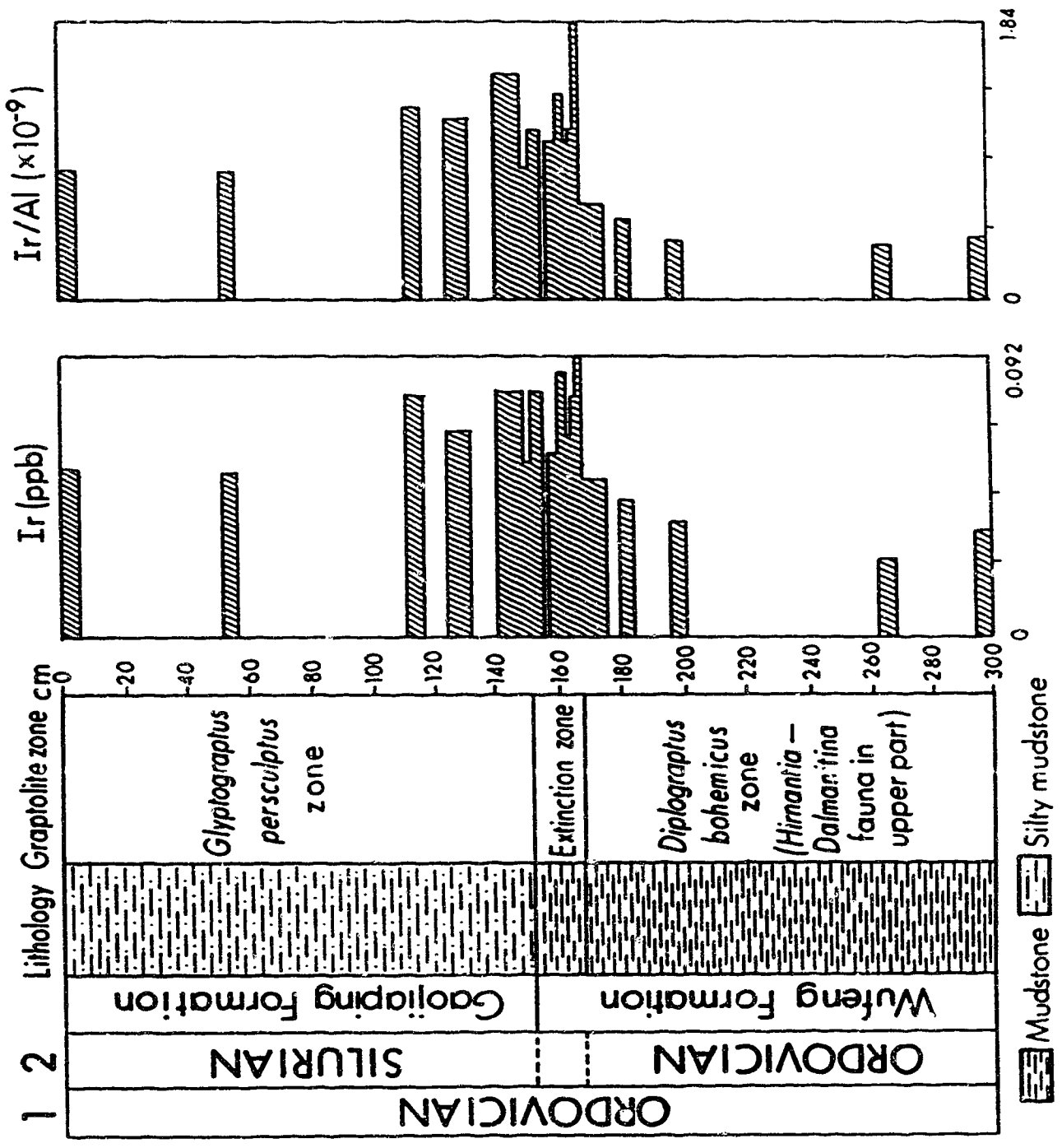
**Fig. 3.1. Paleogeographic map of Yangtze Basin in late Wufengian (late Ashgillian) of Late Ordovician.**



**Fig. 3.2.** Iridium abundances and Ir/Al ratios across latest Ordovician mass extinction interval in stratigraphic sections at Yichang (A) and Jinxian (B) in Yangtze Basin. 1-- International stratigraphic division; 2--Chinese stratigraphic division. *G. gracilis* zone in Jinxian section is equivalent to *G. persculptus* zone (Li et al., 1984). Latest Ordovician extinction coincides with Chinese (traditional) O/S boundary at base of graptolite *G. persculptus* zone. O/S systemic boundary is defined at base of *A. acuminatus* zone at Dob's Linn, Scotland. This is a shift up one zone from traditional boundary at base of *G. persculptus* zone.



A



**B**

## References

- Alvarez, W., Asaro, F., Michel, H.V., and Alvarez, L.W., 1982. Iridium anomaly approximately synchronous with terminal Eocene extinctions. *Science*, 216: 886-888.
- Barker, J.L., and Anders, E., 1968. Accretion rate of cosmic matter from iridium and osmium contents of deep-sea sediments. *Geochimica et Cosmochimica Acta*, 32: 627-645.
- Bassett, M.G., 1985. Towards a 'Common Language' in stratigraphy. *Episodes*, 8: 87-92.
- Berry, W.B.N., 1987. The Ordovician-Silurian boundary: New data, new concerns. *Lethaia*, 20: 209-216.
- Brenchley, P.J. 1988. Environmental changes close to the Ordovician-Silurian boundary. In: L.R.M. Cocks and R.B. Rickards (Editors), A global analysis of the Ordovician-Silurian boundary. *British Museum (Natural History) Bulletin, Geology Series 43*: 377-385.
- 1989. The late Ordovician extinction. In: S.K. Donovan (Editor), *Mass extinctions: Processes and evidence*. Columbia University Press, New York, pp. 104-132.
- Chen, X., 1984. Influence of the Late Ordovician glaciation on basin configuration of the Yangtze Platform in China. *Lethaia*, 17: 51-60.
- Chen, X., Xiao, C., and Chen, H., 1987. Graptolite diversity and anoxic environments in the Wufengian in South China. *Acta Palaeontologica Sinica*, 26: 326-344.
- Cocks, L.R.M., and Rickards, R.B., 1988. A global analysis of the Ordovician-Silurian boundary. *British Museum (Natural History) Bulletin, Geology Series 43*, 394 pp.
- Geng, L., 1984. Late Ashgillian glaciation-- Effects of eustatic fluctuations on the Upper Yangtze Sea. In: E. Mu (Editor), *Stratigraphy and palaeontology of systemic boundaries in China: Ordovician-Silurian boundary*: Anhui Science and Technology Publishing House, Hefei, pp. 269-286.
- Keller, G., D'Hondt, S.L., Orth, C.J., Gilmore, J.S., Oliver, P.O., Shoemaker, E.M., and Molina, E., 1987. Late Eocene impact

- microtektites: Stratigraphy, age and geochemistry. *Meteoritics*, 22: 25-60.
- Koren, T.N., 1991. Evolutionary crisis of the Ashgill graptolites. In: C.R. Barnes and S.H. Williams (Editors), *Advances in Ordovician geology*. Geological Survey of Canada Paper 90-9: 157-164.
- Lespérance, P.J., Barnes, C.R., Berry, W.B.N., Boucot, A. J., and Mu, E., 1987. The Ordovician-Silurian boundary stratotype: consequences of its approval by the IUGS. *Lethaia*, 20: 217-222.
- Li, J., Qian, Y., and Zhang, J., 1984. Ordovician-Silurian boundary section from Jinxian, South China. In: E. Mu (Editor), *Stratigraphy and palaeontology of systemic boundaries in China: Ordovician-Silurian boundary*: Anhui Science and Technology Publishing House, Hefei, pp. 287-308.
- McLaren, D.J., and Goodfellow, W.D., 1990. Geological and biological consequences of giant impacts. *Annual Reviews of Earth and Planetary Sciences*, 18: 123-171.
- Melchin, M.J., and Mitchell, C.E., 1991. Late Ordovician extinction in the Graptoloidea. In: C.R. Barnes and S.H. Williams (Editors), *Advances in Ordovician geology*. Geological Survey of Canada Paper 90-9: 143-156.
- Mu, E., 1988. The Ordovician-Silurian boundary in China. In: L.R.M. Cocks and R.B. Rickards (Editors), *A global analysis of the Ordovician-Silurian boundary*. British Museum (Natural History) Bulletin, Geology Series 43: 117-132.
- Mu, E., Li, J., Ge, M., Chen, X., Ni, Y., and Lin, Y., 1981. Late Ordovician paleogeography of South China. *Acta Stratigraphia Sinica*, 5: 165-170.
- Orth, C.J., 1989. Geochemistry of the bio-event horizons. In: S.K. Donovan (Editor), *Mass extinctions: Processes and evidence*. Columbia University Press, New York, pp. 37-72.
- Orth, C.J., Gilmore, L.R., Quintana, L.R., and Sheehan, P.M., 1986. Terminal Ordovician extinction: Geochemical analysis of the Ordovician/Silurian boundary, Anticosti Island, Quebec. *Geology*, 14: 433-436.
- Owen, A.W., Harper, D.A.T., and Rong, J., 1991. Hirnantian trilobites and brachiopods in space and time. In: C.R. Barnes and S.H.

- Williams (Editors), *Advances in Ordovician geology*. Geological Survey of Canada Paper 90-9: 179-190.
- Rong, J., and Chen., 1986. A big event of the latest Ordovician in China. In: O. Walliser (Editor), *Global bio-events*. Springer-Verlag, Berlin, pp. 127-131.
- 1987. Faunal diversity, biofacies and lithofacies of the Late Ordovician in South China. *Acta Palaeontologica Sinica*, 26: 507-535.
- Rong, J., and Harper, D.A.T., 1988. A global synthesis of the latest Ordovician Hirnantian brachiopod faunas. *Royal Society of Edinburgh Transactions, Earth Sciences* 79: 383-402.
- Schmitz, B., Andersson, P., and Dahl, J., 1988. Iridium, sulfur isotopes and rare earth elements in the Cretaceous-Tertiary boundary clay at Stevns Klint, Denmark. *Geochimica et Cosmochimica Acta*, 52: 229-236.
- Sepkoski, J.J., Jr., 1982. Mass extinctions in the Phanerozoic oceans: A review. In: L.T. Silver and P.H. Schultz (Editors), *Geological implications of impacts of large asteroids and comets on the Earth*. Geological Society of America Special Paper 190: 293-289.
- Sheehan, P.M., 1988. Late Ordovician events and the terminal Ordovician extinction. *New Mexico Bureau of Mines and Mineral Resources, Memoir* 44: 405-415.
- Vail, P.R., Mitchum, R.M., Jr., and Thompson, S., 1977. Relative changes of sea level from coastal onlap. In: C.E. Payton (Editor), *Seismic stratigraphy---Applications to hydrocarbon exploration*. American Association of Petroleum Geologists, *Memoir* 26: 63-82.
- Wallace, M.W., Keays, R.R., and Gostin, V.A., 1991. Stromatolitic iron oxides: Evidence that sea-level changes can cause sedimentary iridium anomalies. *Geology*, 19: 551-554.
- Wang, X., and Chai, Z., 1989. Terminal Ordovician mass extinction and its relationship to iridium and carbon isotope anomalies. *Acta Geologica Sinica*, 63: 255-264.
- Wang, X., Zeng, Q., Zhou, T., Ni, S., Xu, G., Sun, Q., Li, Z., Xiang, L., and Lai, C., 1983. Latest Ordovician and earliest Silurian faunas from the eastern Yangtze Gorges, China, with comments on



- Ordovician-Silurian boundary. Yichang Institute of Geology and Mineral Resources Bulletin, 6: 57-163.
- Wasson, J.T., 1974. Meteorites. Springer-Verlag, New York, 316 pp.
- Wignall, P.B., 1991. Model for transgressive black shales. *Geology*, 19: 167-170.
- Wilde, P., Berry, W.B.N., Quinby-Hunt, M.S., Orth, C.J., Quintana, L.R., and Gilmore, J.S., 1986. Iridium abundances across the Ordovician-Silurian stratotype. *Science*, 233: 339-341.

## Chapter 4

# The Great Latest Ordovician Extinction on the South China Plate: Chemostratigraphic Studies of the Ordovician-Silurian Boundary Interval on the Yangtze Platform

(A version of this chapter has been accepted for publication. Wang, K., Orth, C.J., Attrep, M. Jr., Chatterton, B.D.E., Wang, X. and Li, J., in press. *Palaeogeography, Palaeoclimatology, Palaeoecology*, accepted 07/92)

### Introduction

Raup and Sepkoski's (1982) chart of marine animal diversity through the Phanerozoic shows that about 22% of all families became extinct in the Late Ordovician, making this one of the five greatest episodes of mass extinction in the Phanerozoic. Evidence from Europe, North America, Asia, North Africa and South America indicates that the Late Ordovician extinctions eliminated a large number of unrelated groups of organisms on a global scale. The extinctions severely affected trilobites, brachiopods, echinoderms, corals, bryozoans, ostracodes, bivalves, cephalopods, graptolites, conodonts, chitinozoans, and acritarchs. Extensive summaries of the Late Ordovician extinctions can be found in Barnes (1986), Brenchley (1984, 1989), Chen and Rong (1991), Colbath (1986), Eckert (1988), Fortey (1989), McLaren and Goodfellow (1990), Owen et al. (1991), Rong and Harper (1988a), Sheehan (1988), and Tuckey and Anstey (1992).

Although the main phase of extinctions was in the Late Ashgill (Hirnantian), the Late Ordovician extinctions occurred in two main steps with some possible minor ones between them (Brenchley, 1984, 1989; Chen and Rong, 1991; Owen et al., 1991; Tuckey and Anstey, 1992). The earlier episode of extinctions coincided with the start of a regression (glaciation) at the beginning of the Hirnantian, and is characterized by a major graptolite extinction at the end of the graptolite *pacificus* Zone (end-*pacificus* event, Koren, 1991; Melchin and Mitchell, 1991). The later and final phase of extinctions

coincided with the start of a rapid transgression (deglaciation) in the Late (or at the end, depending on definition of the Hirnantian) Hirnantian, and is marked by an extinction of both benthic and pelagic faunas at the base of the graptolite *persculptus* Zone (base-*persculptus* event, Brenchley, 1984, 1989; Rong and Chen, 1986; McLaren and Goodfellow, 1990; Rong and Harper, 1988a, 1988b; Sheehan, 1988; Li et al., 1984; Wang and Chai, 1989). This latest Ordovician extinction is especially well represented on the South China Plate, and has been referred to as the *end-bohemicus* event (Wang et al., 1992). This paper focuses primarily on this latest Ordovician extinction on the South China Plate, because it is the most drastic biological crisis, reflected by the fossil record, in the Late Ordovician in that region.

It is interesting that the two main episodes of Late Ordovician extinctions were coincident with the start and the end of a glaciation on Gondwana, and with the resultant eustatic sea level drop and rise, respectively (Brenchley, 1988, 1989; Sheehan, 1988). It seems that the driving force behind the extinctions was the climate change which resulted in the growth and decay of the Gondwana ice caps (Berry and Boucot, 1973; Sheehan, 1973, 1975; Brenchley and Newall, 1984; Barnes, 1986). Numerous hypotheses have been proposed to explain the extinctions, including changes in sea level (Berry and Boucot, 1973), in temperature (Stanley, 1984), and in paleoceanography (Wilde and Berry, 1984), reduction in habitats (Sheehan, 1988), bolide impact (Goodfellow et al., 1992), and any of the above combinations.

The possibility that bolide impact is a general cause of extinctions in the geologic past has been raised by Raup (1990), who used a Monte Carlo simulation, based on known impact rates and a kill curve, to produce patterns of extinction remarkably close to those observed in the Phanerozoic record of fossil genera. McLaren and Goodfellow (1990) suggested, on the basis of available geological information, that all major mass extinctions (including the latest Ordovician extinction) might have been caused by giant impacts. Geochemical analyses of the crucial intervals of extinctions are important to test an impact hypothesis. Several of these kinds of

studies have been reported previously, representing the most important Ordovician-Silurian boundary sections on Anticosti Island, Quebec (Orth et al., 1986), at Yichang, Hubei and Jinxian, Anhui (Wang et al., 1992, 1990), at Dob's Linn, Scotland (Wilde et al., 1986), at Yichang, Hubei (Wang and Chai, 1989), and in northwestern Canada (Goodfellow et al., 1992; Wang et al., 1991; Melchin et al., 1991a). Although all of the above studies have observed a weak geochemical anomaly (including Ir) at their alleged extinction horizon, no convincing evidence indicating an impact, such as that documented for the Cretaceous-Tertiary boundary (Alvarez and Asaro, 1990), was found to be associated with the Late Ordovician extinctions. However, one can not rule out the possibility that the original geochemical signature of an impact, even if there was indeed one, might have been altered after such a long time of complex and subtle geologic processes, e.g., diagenesis, weathering and mixing. Nor can we exclude the possibility of erosion destroying crucial intervals, leaving hiatuses due to a widespread glacio-eustatic regression in the Late Ordovician. In this paper, we present the results of chemostratigraphic analyses of four continuous Ordovician-Silurian boundary sections with a complete graptolite sequence from the Yangtze Platform on the South China Plate.

### **A graptolite framework**

Until 1985, the Ordovician-Silurian boundary had been recognized at the base of the graptolite *persculptus* Zone, which corresponds to a time of rapid sea-level rise and hence a change from shallow marine sediments with shelly faunas to deeper-water sediments with graptolites (Brenchley, 1984, 1988, 1989). The Hirnantian, as originally envisaged, included shallow marine rocks with a distinctive *Hirnantia* brachiopod fauna (Temple, 1965; Rong, 1979, 1984a). Its upper boundary was marked by a change to graptolitic shales with *persculptus* Zone graptolites. There are a number of records of a *persculptus* occurring with a *Hirnantia* fauna, but most of these have been disputed (Rong and Harper, 1988a, 1988b; Mu, 1988; Li, 1984). The redefinition of the Ordovician-Silurian boundary (Cocks, 1985) has entailed

repositioning the base of the Silurian upwards to the base of the graptolite *acuminatus* Zone (Fig. 4.1). Therefore, by definition, the Hirnantian now includes both the traditional Hirnantian containing shelly fossils and the overlying graptolitic shales of the *persculptus* Zone.

As part of the decision made by the Ordovician-Silurian Boundary Working Group in 1985, the international stratotype section chosen for the Ordovician-Silurian boundary is located at Dob's Linn, Scotland (Cocks, 1985); a section that contains one of the best studied graptolite sequences (Williams, 1983, 1986). Although there might be some hiatuses in this section (Berry, 1987), the graptolite zonation at Dob's Linn can be approximately correlated with that at Yichang, Hubei (Fig. 4.1), a standard area for the Ordovician-Silurian boundary in China, where two schemes of the graptolite zonation for the Upper Ordovician and Lower Silurian are currently in use (Fig. 4.1), one used by Mu (1988) and the other by Wang et al. (1983). The Ordovician-Silurian boundary defined at the base of the *acuminatus* Zone at Dob's Linn, Scotland does not correspond to the base of the *acuminatus* Zone in China, but is within the *persculptus* Zone (Fig. 4.1) (Melchin et al., 1991b; Melchin and Mitchell, 1991; Rong and Harper, 1988a), which makes it difficult to apply the international Ordovician-Silurian boundary in China. The base of the *persculptus* Zone, which had been the traditional level for the Ordovician-Silurian boundary, is used by most workers in China because of the occurrence of a major faunal turnover at this level and its ease of recognition in the field. In this paper, we have indicated in the analyzed Chinese sections both the Ordovician-Silurian boundary, which is arbitrarily drawn within the *persculptus* Zone, and the local level for the systemic boundary which is at the base of the *persculptus* Zone (Fig. 4.1) corresponding to the latest Ordovician extinction in China.

### Tectonics and geologic setting

It has been recognized that the region which is now China consisted of several major separate plates during the Ordovician: North China (Sino-Korea), South China, Tarim and part of Indochina

plates (Scotese and McKerrow, 1990; Wang, 1989). A major Paleozoic unconformity is widely present in North China and Tarim, where most of the strata from the Upper Ordovician to the Lower Carboniferous are missing (Wang, 1985). The lack of record of this stratigraphic interval makes a study of the Late Ordovician extinctions impossible in these regions. But the geologic history of South China is quite different. Continuous, stable sedimentation from the Sinian through the Paleozoic to the Late Triassic was widespread on the South China Plate (Wang, 1985).

One of the most important Late Ordovician paleogeographic features on the South China Plate was a so-called Yangtze Platform (the Yangtze Basin under the Yangtze Sea), covered by a broad epeiric sea and bordering to the southeast, the deep Pearl River Sea (or Southeast China Sea Trough, Wang, 1985) (Fig. 4.2). The Yangtze Sea was divided by the Jiujiang Strait into a western Upper Yangtze Sea and an eastern Lower Yangtze Sea (Mu et al., 1981; Chen, 1984). As old lands and uplifts expanded and coalesced, the Yangtze Sea, especially the Upper Yangtze Sea, became largely enclosed during the Wufengian (Ashgill). An environment like today's Dead Sea was formed in the Upper Yangtze Basin, characterized by restricted, quiet, low-energy and extremely reducing bottom water conditions, and slow sedimentation (Mu et al., 1981; Chen et al., 1987). In this environment, graptolites flourished in the upper water column, but shelly faunas could not live in the anoxic bottom waters. The reducing bottom water conditions could have enhanced the preservation of graptolites. It is believed that the water depth in the Yangtze Sea was less than 150 m during the Late Ordovician and the Ashgill regression did not drain the basin (Chen, 1984; Rong and Chen, 1986).

Because of the excellent preservation of graptolite sequences in the Yangtze Basin, more than three dozen fossiliferous sections with continuous deposition through the Late Ordovician faunal turnover have been studied in this region during the past two decades (Mu, 1988). The most profound changes in both benthic and pelagic faunas occurred at the base of the *persculptus* Zone, the level for the local systemic boundary in China (the Chinese

"Ordovician-Silurian" boundary) (Rong and Chen, 1986; Rong, 1984b; Wang and Chai, 1989; Li et al., 1984; Li, 1984; Rong and Harper, 1988a, 1988b). This extinction boundary has been dated at  $439 \pm 18$  Ma by the Rb/Sr whole-rock method (Wang and Chai, 1989).

### The great latest Ordovician extinction on the South China Plate

It has been revealed by many biostratigraphic studies that there was a major faunal turnover at the base of the *persculptus* Zone, involving virtually all groups of living organisms at the time (Mu et al., 1984; Wang et al., 1983; Li et al., 1984; Rong, 1984b). Graptolites and brachiopods are most commonly found in the boundary interval, but trilobites, nautiloids, ostracodes, bivalves, gastropods, chitinozoans, conodonts, and acritarchs are also present in many sections in this region (e.g., Li et al., 1984; Wang et al., 1983). The largest loss in biomass and diversity occurred between the *bohemicus* and *persculptus* zones.

According to Wang and Chai (1989), of 88 species of 19 genera of graptolites living in the Wufengian (Ashgill) at Yichang, only 4 species of 3 genera survived into the Early "Silurian". Of more than 100 species belonging to 25 genera of graptolites living in the Wufengian in the Yangtze Basin, only 8 species of 4 genera made their appearance in the Early "Silurian" (Wang and Chai, 1989; Mu et al., 1984). It has been recorded and discussed by many workers (Rong and Chen, 1986; Li et al., 1984; Wang et al., 1983) that the graptolite faunal changeover, i.e., the final extinction of the Ordovician dicellograptid fauna and the subsequent radiation of the Early "Silurian" monograptid fauna, occurred at the base of the *persculptus* Zone. Although the dicellograptid fauna had been in decline for some time since the early Ashgill, the most severe phylogenetic crisis in the history of the Ordovician dicellograptid fauna occurred in China at the base of the *persculptus* Zone (Rong and Chen, 1986).

Rong (1979, 1984a, b) and Rong and Harper (1988a, b) extensively reviewed the *Hirnantia* fauna of China and the rest of the world. The *Hirnantia* fauna included a very diverse and

abundant brachiopod fauna, living in the Late Ashgill. Its occurrence is best known in the Yangtze region, where it first appeared in the *mirus* Zone, spread rapidly, and became suddenly extinct as a whole at the base of the *persculptus* Zone (Fig. 4.3). Wang et al. (1983) reported a diverse *Hirnantia-Dalmanitina* fauna in the Late Wufengian at Yichang, consisting of at least 35 brachiopod species of 25 genera and 8 trilobite species of 4 genera. The whole fauna suddenly disappeared at the base of the *persculptus* Zone. Although there were some reports of a *Hirnantia* fauna in the *persculptus* Zone in other parts of the world, most of them have been disputed due to the mis-identification of either graptolites or brachiopods (Rong and Harper, 1988a, 1988b; Mu, 1988; Li, 1984). Rong and Harper (1988a, b) and Rong and Chen (1986) concluded that "...to date there is no unequivocal evidence for the coeval occurrence of a typical *Hirnantia* fauna and the *persculptus* Zone anywhere in the world...". It appears that the *Hirnantia* fauna was devastated before the *persculptus* Zone, in spite of the questionable occurrences of some sparse species reported from the *persculptus* Zone.

One of the best examples of the end-*bohemicus* Zone (or base-*persculptus* Zone) extinction in South China can be found in a section at Jinxian, Anhui Province (Fig. 4.2, Fig. 4.4), where extremely diverse faunas are present throughout the section (Li et al., 1984; Li, 1984). In this section, a sudden extinction of Ordovician graptolites and other organisms (trilobites, brachiopods, nautiloids, ostracodes, bivalves, gastropods, and acritarchs) occurred in a 17-cm-thick mudstone ("extinction layer") which marks the local systemic boundary (Fig. 4.4). The mudstone is underlain by the *bohemicus* Zone and overlain by the *gracilis* Zone (= *persculptus* Zone, Li et al., 1984). According to Li (1984, p. 317), of 31 graptolite species in the latest Ordovician *bohemicus* Zone, only 4 or 5 species made their way through the "extinction layer" into the *persculptus* Zone. Most of them disappeared at the base of the *persculptus* Zone (Fig. 4.4). Not a single species of the latest Ordovician shelly faunas (represented by more than 20 genera of trilobites, brachiopods, nautiloids, ostracodes, bivalves, and gastropods) survived into the *persculptus* Zone at this locality (Li et al., 1984). The following



graptolite radiation appears to be rapid; five species appeared immediately after the deposition of the boundary mudstone (Li et al., 1984). In the field, one can clearly see that the latest Ordovician graptolites and shelly fossils range up to the boundary mudstone, and *persculptus* Zone graptolites appear immediately above the mudstone. Thus, the rapid faunal turnover and extinctions are evidently recorded in the Jinxian Section (Fig. 4.4).

### Stratigraphic sections

Biostratigraphically well-constrained sections from four different localities in the Yangtze Basin were chosen for chemostratigraphic studies. They are the Yichang Section at Fenxiang, Yichang, Hubei Province, the Jinxian Section at Beigong, Jinxian, Anhui Province, the Xiushan Section at Datianba, Xiushan, Sichuan Province, and the Youyang Section at Tongguo, Youyang, Sichuan Province. The Jinxian Section was deposited in the Lower Yangtze Basin, and the other three in the Upper Yangtze Basin (Fig. 4.2)

Figure 4.5 shows the biostratigraphic correlations between these sections, using the fossil zonation of Wang et al. (1983) (Fig. 4.1). The Yichang Section is the type section for the Ordovician-Silurian boundary in China, and thus has received the most attention in the past (Wang et al., 1983; Mu et al., 1984). The Xiushan and Youyang sections are very similar in sequence to the Yichang Section, as they were all deposited in the restricted Upper Yangtze Basin. The fossils in these three sections are mainly graptolites, except in the uppermost part of the *bohemicus* Zone (of Mu, 1988, Fig. 4.1) where the benthic *Hirnantia-Dalmanitina* fauna occurs. The Jinxian Section was deposited in the open Lower Yangtze Basin, where the sedimentation rate was faster as indicated by a greater thickness of time-equivalent strata. The benthic fauna here in the uppermost *bohemicus* Zone is more diverse than that in the Upper Yangtze Basin (Li et al., 1984), possibly due to more ventilated bottom water conditions in the Lower Yangtze Basin.

Distinct boundary sediments, such as the thin clay layer at the Cretaceous-Tertiary boundary, deserve special attention. At Jinxian,

there is a 17 cm thick mudstone layer separating the *persculptus* Zone (= *gracilis* Zone) above from the *bohemicus* Zone below (Fig. 4.5). This mudstone, containing only fragments of the underlying Ordovician shelly fossils, was thought to be the "extinction layer" (Li et al., 1984). At both Xiushan and Youyang sections, X. Wang found a thin boundary clay layer (1 cm) right at the local systemic boundary at the base of the *persculptus* Zone (Fig. 4.5). At Yichang, there is no abnormal boundary layer. But in the original stratigraphic columns of Wang et al. (1983), there is a thin tuff layer in the uppermost *bohemicus* Zone (of Mu, 1988, Fig. 4.1) (Fig. 4.5).

### Sample preparation and chemical analysis

The sampling for this work was centered around the interval between the *bohemicus* and *persculptus* zones to ensure that the latest Ordovician extinction horizon was sampled in each section. As shown in Figure 4.1 the span of the sampled interval in each section varies, but samples from near the base of the *persculptus* Zone were collected in greater detail. A total of 82 geochemical samples (31 from Jinxian, 30 from Yichang, 14 from Xiushan and 7 from Youyang) were collected and analyzed for elemental abundances by means of neutron activation analysis (NAA). Continuous samples were collected across the extinction interval at Jinxian and Yichang sections, but Xiushan and Youyang sections were sampled in less detail. Stratigraphic positions for analyzed geochemical samples relative to the local systemic boundary in these sections can be found in Table 4.1.

The chemical analyses were performed on 1-2 g crushed samples by neutron activation analysis for about 40 common and trace elements and iridium (Orth, 1989). Instrumental neutron activation analysis (INAA), performed by the Los Alamos Research Reactor Group using their automated system as described by Minor et al. (1982), provided the abundances of about 40 elements except Ir. Powdered samples were irradiated in the reactor (thermal flux =  $5 \times 10^{12}$  neutrons/cm<sup>2</sup>/second) for 20 seconds. The samples were removed from the reactor and were counted for delayed neutrons for uranium determination. Following 20 minutes after irradiation,

the samples were gamma ray counted by a germanium detector for short lived nuclides. The samples were then irradiated again for 500 seconds and gamma ray counted 5 days and 2 or 3 weeks after irradiation for intermediate and long lived nuclides.

Iridium abundances in selected samples were determined by radiochemical neutron activation analysis (RNAA). Samples for Ir analysis were first irradiated for 7 hours in a thermal neutron flux ( $5.7 - 9.7 \times 10^{12}$  n/cm<sup>2</sup>/sec.) to produce 74-day <sup>192</sup>Ir from the (n,  $\gamma$ ) reaction on stable <sup>191</sup>Ir. Following at least a one week period for radioactive decay of shorter lived nuclides, the samples were dissolved in strong mineral acids and the <sup>192</sup>Ir was radiochemically isolated. The prepared samples were then counted in a high resolution gamma-ray detector to measure the 316.5 keV photopeak of the 74-day <sup>192</sup>Ir. Approximately 1 ppT ( $10^{-12}$  g/g) of Ir can be determined using this method.

### Geochemical results and discussion

Geochemical data for four sections containing the latest Ordovician mass extinction horizon in the Yangtze Basin are presented here (Figs. 4.6, 4.7, 4.8, 4.9). Since the carbonate content in these samples is usually less than 1%, the Ir and other elements are expressed as a ratio to Al relative to the local systemic boundary at the base of the *persculptus* Zone as indicated in each figure.

The Ir abundance varies from 24 to 230 ppT in the Yichang Section, 26 to 92 ppT in the Jinxian Section, 15 to 75 ppT in the Xiushan Section, and 6.6 to 88 ppT in the Youyang Section (Table 4.1). The Ir data for Yichang and Jinxian sections have been reported in Wang et al. (1992). The Ir reaches its maximum abundance in the extinction horizon at the base of the *persculptus* Zone in Yichang (230 ppT), Jinxian (92 ppT), and Youyang (88 ppT) sections, but not in the Xiushan Section (50 ppT at the extinction boundary) where the 75 ppT Ir maximum occurs about 1.15 m lower in the *mirus* Zone (Table 4.1). Wang et al. (1992) observed a close correlation between the Ir abundances and the sedimentation rates for Yichang and Jinxian sections, and suggested that the Ir abundance maxima at the base of the *persculptus* Zone were probably a result of reduced

sedimentation at the beginning of a rapid transgression induced by rapid melting of the Late Ordovician ice caps on Gondwana. The maximum Ir abundance at Jinxian, Xiushan and Youyang is slightly higher than that in a clay on top of the oncolite bed of the Member 7 of the Ellis Bay Formation on Anticosti Island, Quebec (58 ppT, Orth et al., 1986). This clay probably lies between the *bohemicus* and *persculptus* zones (Melchin et al., 1991b). The maximum Ir abundance at Yichang can be compared to that in the *persculptus* Zone of the stratotype section at Dob's Linn, Scotland (250 ppT, Wilde et al., 1986).

Reducing environmental conditions might have played a role in the enhancement of the Ir and other elements at the local systemic boundary in these Chinese sections. In Figure 4.6, Al abundance and 11 other elements expressed as ratios to Al have been plotted on an approximate 5 m span of the Jinxian Section. The As, Mo and Sb (not figured) show distinctive maxima in the "extinction layer" marking the local systemic boundary. To a lesser extent, Ir, U, Cr, Co and Mn also indicate maxima in the "extinction layer". The V/Al increases at the boundary and then the elevated value is maintained in the subsequent samples analyzed in the strata above the boundary. However, Ba, Sc, Th and Ti (not figured) do not exhibit any significant change across the boundary. These data may indicate that the "extinction layer" (mudstone) at the local systemic boundary in the Jinxian Section might have been deposited under strong reducing water conditions.

In Figure 4.7 selected elements, expressed as ratios to Al, have been plotted on an approximate 5 m span of the Yichang Section. The pattern of elemental abundances of this section is similar to that of the Jinxian Section discussed above. The abundances of the Ir, As, Mo (not figured) and Sb (not figured) show elevated values at the local systemic boundary. Lithophile elements, such as Mg and Sc, do not exhibit any significant change across the boundary. The Ce/La ratios in the Yichang Section are consistently high (approximately 2) and are typical of that observed from terrigenous deposition. These values would be lower if the Ce and La were precipitated from sea water alone.

Figure 4.8 illustrates the geochemical results of 14 selected samples that were analyzed at the Xiushan Section. In the Youyang Section, results from seven samples are given in Figure 4.9. Because both the latter sections were sampled in less detail, the results cannot be directly compared in the same detail as is given for the previous two sections. However, there is general agreement of the elemental abundance patterns.

Although reports at other Ordovician-Silurian boundary sections (Anticosti Island, Quebec and Dob's Linn, Scotland) indicate weak geochemical anomalies including Ir near the extinction horizon, there had been no clear conclusion as to the origin. Wang et al. (1992) have suggested that a reducing environment might have provided the conditions to show the enhancement of these elements in the Chinese sections. In addition it was noted that the Ir enrichment pattern observed in these sites can be explained on the basis of changes in the sedimentation rates. A comparison of the Ir concentrations at the four sections in the Yangtze Basin shows considerable variability in the strength of the Ir signal. The strongest, 230 ppT, is at Yichang. The Jinxian and Youyang sections have comparable Ir concentrations at 92 and 88 ppT, respectively. The weakest is at Xiushan with 50 ppT. The values of the Ir/Al ratio are approximately  $2 \times 10^{-9}$  and are similar to that observed in crustal rocks. Furthermore, the Co/Ir ratio for samples in Yichang and Jinxian sections is not consistent with high Ir meteoritic origins (Wang et al., 1992). Thus, indications from the elemental abundance patterns (Ir, in particular) are not supportive of an impact for the observed Ir at the local systemic boundary in China but are supportive of changing sedimentation rates and reducing conditions. However, merely on the basis of the Ir abundances, we cannot preclude impact by a comet with low platinum group element (PGE) abundances.

**Carbon isotope variations across the latest Ordovician extinction: indications for changes in atmospheric and marine pCO<sub>2</sub>**

Due to extremely low carbonate content in the graptolitic shale samples in the Yichang Section (carbonate content < 0.5%), it was only possible to determine carbon isotope ratios in organic components of the samples. Figure 4.10 shows the organic  $\delta^{13}\text{C}$  values in two other nearby sections at Yichang (Xu et al., 1989, 1991), both of which have a virtually identical stratigraphic sequence to the Yichang Section that we analyzed by NAA. It has been shown that changes in organic carbon isotopic composition during diagenesis are very small (Deines, 1980); thus  $\delta^{13}\text{C}$  of the organic matter in marine sediments can provide a more reliable proxy to the original isotopic composition.

As can be seen in Figure 4.10, there are several  $\delta^{13}\text{C}$  peaks in the two sections. The most striking feature is that, starting in the *mirus* Zone (beginning of the Hirnantian, see Fig. 4.3), the  $\delta^{13}\text{C}$  becomes consistently more positive toward the base of the *persculptus* Zone, and reaches maximum values in the *Hirnantia-Kinnella* Zone, just before a drastic drop at the local systemic boundary at the base of the *persculptus* Zone.

Variations of carbon isotopic composition in organic matter of marine sediments have been noted as a function of the surface water temperature (Sackett et al., 1965), biological productivity (Hollander and McKenzie, 1991; Welte et al., 1975), influx of terrestrial organic matter (Deines, 1980), and concentration of the dissolved  $\text{CO}_2$  ( $\text{CO}_2(\text{aq})$ ) in the ocean (Arthur et al., 1985; Rau et al., 1989), which is controlled by, together with temperature, atmospheric  $\text{CO}_2$  partial pressures ( $\text{pCO}_2$ ) in balance with oceanic  $\text{pCO}_2$  (Henry's Law,  $\text{CO}_2(\text{aq}) = \alpha \times \text{pCO}_2$ ). The pattern of the increasing  $\delta^{13}\text{C}$  values from the *mirus* Zone to the local systemic boundary would suggest any of the following trends: 1. decrease in  $\text{pCO}_2$ ; 2. increase in biological productivity; 3. increase in surface water temperature; or 4. increase in influx of terrestrial organic matter (especially isotopically heavier  $\text{C}_4$  plants). The latter two are considered to be unlikely because a glaciation was developing in the Hirnantian and terrestrial plants were not present at this time. An increase in marine productivity in the Yangtze Sea towards the end of the Hirnantian appears to be consistent with the fossil record,

which suggests an increase in brachiopod diversity of the *Hirnantia* fauna (Fig. 4.3, Fig. 4.4). However, it is inconsistent with the trend documented by Brenchley (1984) that a decreasing plankton productivity was associated with the glaciation during the latest Ordovician. Nevertheless, one thing is clear that this isotopic trend is associated with the development of a glaciation, and probably with a lowering in the atmospheric and marine  $p\text{CO}_2$ , because a  $p\text{CO}_2$  decrease (no increase in temperature) would reduce  $\text{CO}_2(\text{aq})$  concentration and the carbon isotopic fractionation between the dissolved  $\text{CO}_2$  and the organic carbon of photosynthetic origin resulting in a positive  $\delta^{13}\text{C}$  shift. This carbon isotope variation pattern, i.e., general increasing of heavier carbon  $^{13}\text{C}$  toward a  $\delta^{13}\text{C}$  maximum in the latest Ordovician, was also observed in the Siljan area, central Sweden (Marshall and Middleton, 1990), in the Mackenzie Mountains, northwestern Canada (Wang et al., in preparation), on Anticosti Island, Quebec (Long, this volume), in a core section from Latvia (Brenchley et al., 1992), and in Wisconsin, U.S.A. (Yapp and Poths, 1992). These latest Ordovician positive  $\delta^{13}\text{C}$  shifts are approximately 5‰ in the Siljan area (data based on both brachiopod shells and marine cements), 2‰ in the Mackenzie Mountains (bulk-carbonate), 4‰ in Anticosti Island sections (bulk-carbonate), 3‰ in Wisconsin (goethites) and 5‰ in the Yichang sections (organic carbon). Marshall and Middleton (1990) suggested that an increase in the deposition of organic carbon was the cause of the carbon isotope shift in the Siljan area. The additional isotopic data from Yichang, the Mackenzie Mountains, Latvia, and Wisconsin appear to indicate that this positive carbon isotope shift in the latest Ordovician is of global significance, and possibly has a common cause which might be a lowering of  $p\text{CO}_2$  in the ocean and atmosphere, together with a higher organic carbon burial rate associated with a period of the enhanced glaciation and the resultant glacio-eustatic regression in the Hirnantian. Marshall and Middleton (1990) also pointed out that the enhanced deposition of organic carbon would have decreased  $p\text{CO}_2$  leading to rapid global cooling in the latest Ordovician. Their oxygen isotope data from the unaltered brachiopod

shells appear to indicate this cooling trend (Marshall and Middleton, 1990).

Once across the extinction horizon at the base of the *persculptus* Zone, the  $\delta^{13}\text{C}$  values drop dramatically, a sudden negative excursion of about ‰ at Wangjiawan and 6‰ at Huanghuachang, respectively (Fig. 4.10). A similar  $\delta^{13}\text{C}$  drop at this extinction level was also recorded in the Mackenzie Mountains (Wang et al., submitted), where we found a 3‰ sudden isotopic shift towards the lighter carbon immediately after the pre-extinction  $\delta^{13}\text{C}$  maximum discussed above. No isotopic data for this stratigraphic interval are available from the Siljan area, Latvia and Wisconsin. A sudden decrease in carbonate  $\delta^{13}\text{C}$  of about 1‰ was reported to be associated with the Ir maximum in the Anticosti Island Section (Orth et al., 1986). A decrease in carbonate  $\delta^{13}\text{C}$  at the systemic boundary was also observed in sections from Yukon Territory, Canada (Goodfellow et al., 1992). There seems to be a sudden, strong negative  $\delta^{13}\text{C}$  shift in carbonate at the Becscie/Ellis Bay contact in Anticosti Island sections (Long, in press). It appears that these negative carbon isotope excursions occurred too suddenly to be explained as a result of any gradual processes, such as oxidation of organic carbon. In fact, it is best interpreted as the oceanic chemical response (excess  $^{12}\text{C}$  in the upper water column) to a sudden marine biomass reduction at the end of the Hirnantian. This explanation is in good accordance to the paleontological evidence indicating the occurrence of a mass extinction at the isotopic excursion level in both China and Canada. It is also consistent with a general trend of the association of mass extinctions with carbon isotope excursions ("strangelove ocean" excursions) documented at the Cretaceous-Tertiary (Zachos et al., 1989), Permian-Triassic (Holser et al., 1989), Frasnian-Famennian (Wang et al., 1991; Yan et al., in press), and Precambrian-Cambrian (Hsü et al., 1985) boundaries. However, according to the "strangelove"-respiring ocean model of Hsü and McKenzie (1990), a "strangelove" perturbation (normally about 2‰) alone can not account for this very large carbon isotope excursion at the latest Ordovician extinction in South China. A sudden, large increase in the atmospheric and marine  $\text{pCO}_2$ , together with the



"strangelove ocean" effect, is suggested here to account for the large carbon isotope excursions at Yichang. This is because increasing CO<sub>2</sub> availability in the ocean would result in a decrease in organic  $\delta^{13}\text{C}$  and an increase in the fractionation between the  $\delta^{13}\text{C}$  of organic matter and that of the dissolved CO<sub>2</sub> (Rau et al., 1989). The consequences of such a sudden, large increase in atmospheric and marine pCO<sub>2</sub> would be a greenhouse effect, global warming, rapid deglaciation of the Gondwana ice caps, and possibly (causing?) the final extinction of the cold-water inhabitant *Hirnantia* fauna (Sheehan, 1973, 1975, 1988). These were all observed as prominent latest Ordovician events at the base of the *persculptus* Zone.

In summary, carbon isotope data from South China, northwestern Canada, central Sweden, Latvia, Quebec, and Wisconsin indicate that a period of decreasing atmospheric and marine pCO<sub>2</sub> and increased organic carbon burial was associated with the Hirnantian glaciation in the latest Ordovician. This trend was suddenly terminated by a large increase in the atmospheric and marine pCO<sub>2</sub> and a mass extinction at the base of the *persculptus* Zone, which may have resulted in a rapid deglaciation of the Gondwana ice caps and possibly a (surface water) <sup>12</sup>C-enriched "strangelove ocean" in the earliest *persculptus* Zone, respectively, shortly before another biological bloom that occurred later in the *persculptus* Zone. The ultimate cause of the sudden pCO<sub>2</sub> increase at the base of the *persculptus* Zone is uncertain, although volcanism, tectonics, and/or extra-terrestrial impact could have been responsible.

### Discussion and interpretations

Paleontological data from South China, in accordance with the data from other parts of the world, indicate that a latest Ordovician extinction of many unrelated groups of organisms occurred at the base of the graptolite *persculptus* Zone, which marks the local systemic boundary in China. This extinction event in China is best displayed in the Yangtze Basin, which, unlike many other areas, was not drained by the Late Ordovician glacio-eustatic regression that may have lowered the sea level by as much as 100 m (Brenchley

and Newall, 1980; Sheehan, 1975). The preservation of the fossil record of the extinction in many well-exposed stratigraphic sections in the Yangtze Basin provides a good opportunity for exploring and understanding the causative factors of the extinction. Four selected stratigraphic sections for chemostratigraphic studies from the Yangtze Basin were found to have distinctive strata in the extinction interval: a mudstone "extinction layer" in the Jinxian Section, a boundary clay in both Xiushan and Youyang sections, and a tuff bed in the Yichang Section.

Geochemical analyses of the four stratigraphic sections from the Yangtze Basin indicate iridium abundance maxima at the extinction boundary in three of the four sections: Yichang, Jinxian and Youyang. Other elements that show enrichment at the boundary include some siderophiles and chalcophiles, e. g., Co, Cr, As, Mo, Sb, and V. Although there is no unique explanation for the origin of the elemental enrichment, similar geochemical anomalies were also found in the latest Ordovician extinction interval in other parts of the world. In a section on Anticosti Island, Quebec, Orth et al. (1986) observed an Ir abundance maximum in a clay, which is about 30 cm below a short "transitional zone" of mixed Ordovician and Silurian conodont species (McCracken and Barnes, 1981). According to Melchin et al. (1991b, p. 1861), this clay, sitting on top of the oncolite bed of the basal Member 7 of the Ellis Bay Formation, is probably between the *bohemicus* and *persculptus* zones. In the stratotype section at Dob's Linn, Scotland, Ir abundances show maxima in the *persculptus* and *extraordinarius* graptolite zones (Wilde et al., 1986); the contact of the two zones corresponds to the local systemic boundary in China (Fig. 4.1). In three sections spanning the latest Ordovician extinction in Yukon Territory, Canada, Goodfellow et al. (1992) found geochemical anomalies marked by an increase in organic carbon, and siderophile (Ni, V) and chalcophile (Zn, Cd, Hg, As, Sb, Se, Mo) elements at a level that is no older than the base of the *persculptus* Zone. In the Mackenzie Mountains of the Northwest Territories, Canada, we have observed that Ir, Co, and Cr as ratios to Al show distinctive maxima in the latest Ordovician extinction interval (Wang et al., submitted) as defined by trilobites

and conodonts (Chatterton and Ludvigsen, 1983; Nowlan et al., 1988). In sections from Arctic Canada, Melchin et al. (1991a) reported anomalously high chalcophile (As, Se, Sb) element and high organic carbon concentrations at the base of the *persculptus* Zone. Wang and Chai (1989) also analyzed samples from the Yichang Section and found a marked increase in Ir, Au, Ni, Cr, As and Sb at the base of the *persculptus* Zone.

It seems clear that the latest Ordovician extinction at or near the base of the *persculptus* Zone is associated with geochemical anomalies of siderophile and chalcophile elements (including Ir) on a global basis (South China, northwestern Canada, Quebec, and Scotland). McLaren and Goodfellow (1990) and Goodfellow et al. (1992) interpreted the geochemical data as possible effects of a giant impact. "The magnitude and apparent global synchronicity for most faunal groups in a large range of sedimentary environments suggest that it (the latest Ordovician extinction) must have been sudden and of catastrophic effect" (Goodfellow et al., 1992, p. 20). It is also clear that the shallow water biota was already under stress as a result of the loss of epicontinental habitats through the Hirnantian glaciation (Sheehan, 1988). A giant impact could have provided a knockout punch to devastate an already stressed biota on a global basis. The problem with an impact scenario is that there has been no evidence of shocked quartz, chondritic PGE anomalies, tektites, or tsunami deposits such as those documented at the Cretaceous-Tertiary boundary (Alvarez and Asaro, 1990). Goodfellow et al. (1992) addressed the question that the Ir of extraterrestrial origin could have been redistributed and separated from other siderophile elements by sedimentary reworking and diagenetic remobilization. Wang et al. (1992) suggested, on the basis of existing geochemical data and geological observation, that the geochemical anomalies may be a result of reduced sedimentation and reducing water conditions at the local systemic boundary between the "Ordovician" and "Silurian" in South China. However, merely on the geochemical data, we cannot preclude impact by a comet with low PGE abundances.

Organic carbon isotope data in two sections at Yichang, Hubei, in accordance with isotopic data from central Sweden, northwestern Canada, Latvia, Quebec, and Wisconsin may indicate a general decreasing  $p\text{CO}_2$  in the ocean and atmosphere associated with the expansion of the Gondwana glaciation in the Hirnantian of the Late Ordovician. A sudden, large  $p\text{CO}_2$  increase (up to 32% as inferred from the organic carbon isotope data of the Wangjiawan Section at Yichang, Fig. 4.10) in the atmosphere and ocean may have occurred coincident with the extinction at the base of the *persculptus* Zone, and probably caused the rapid melting of the Gondwana ice caps and the resultant sea level rise at the latest Ordovician. What impact such a sudden, large  $p\text{CO}_2$  increase would have on the biota is uncertain, but a greenhouse effect may have persisted as a result. The ultimate cause of the  $p\text{CO}_2$  increase is unknown, although a rapid  $\text{CO}_2$  degassing caused by volcanism, tectonics, and/or extraterrestrial impact could have been responsible.

## Conclusions

Continuous samples from four Ordovician-Silurian boundary sections of graptolitic shales and mudstones in the Yangtze Basin (Yangtze Platform) on the South China Plate, spanning the latest Ordovician mass extinction of many unrelated groups of organisms, were chemically analyzed for the abundances of about 40 common and trace elements and iridium. It is observed that the abundances of Ir and other siderophile and chalcophile elements (e.g., Co, Cr, As, Mo, Sb, and V) show elevated values in the extinction horizon at the base of the graptolite *persculptus* Zone, which corresponds to the stratigraphic level for the local systemic boundary in China between the "Ordovician" and "Silurian". Iridium abundances show maxima at this extinction level in three of the four sections analyzed with varying strength, 230 ppT at Yichang, 92 ppT at Jinxian, and 88 ppT at Youyang (but 50 ppT at Xiushan). These geochemical patterns appear to be of global significance, since similar geochemical anomalies (including weak Ir anomaly) were also recorded at about the same stratigraphic level in many other sections previously studied in Quebec, Yukon, Arctic and Northwest Territories, Canada,

and Scotland. Although impact by a comet with low platinum group element abundances could have been responsible for the geochemical anomalies, we find it is most plausible to attribute the geochemical signal to the effects of a lower sedimentation rate and reducing water conditions at this horizon, the beginning of a rapid transgression induced by rapid melting of the ice caps on Gondwana. Carbon isotope excursions in organic material at Yichang, together with other carbon isotope data from central Sweden, northwestern Canada, Latvia, Quebec, and Wisconsin, suggest that, after a period of decreasing atmospheric and marine  $p\text{CO}_2$  in the latest Ordovician (the Hirnantian), a sudden, large  $p\text{CO}_2$  increase in the ocean and atmosphere may have occurred at the extinction horizon at the base of the *persculptus* Zone. A greenhouse effect might have existed for a short time. What triggered such a sudden  $p\text{CO}_2$  increase is uncertain, but a rapid  $\text{CO}_2$  degassing caused by volcanism, tectonics, and/or extraterrestrial impact could have been responsible.

Table 4.1 . Stratigraphic positions of the analyzed samples and Ir abundances in Yichang, Jinxian, Xiushan and Youyang sections.

| Yichang Section              |                |           | Jinxian Section               |               |         | Xiushan Section              |               |         |
|------------------------------|----------------|-----------|-------------------------------|---------------|---------|------------------------------|---------------|---------|
| Sample                       | cm from "O/S"  | Ir (ppT)* | Sample                        | cm from "O/S" | Ir(ppT) | Sample                       | cm from "O/S" | Ir(ppT) |
| FOW-29                       | 107            | 38        | S-8                           | 280           | 41      | DTBL-5                       | 65            | 44      |
| FOW-28                       | 57             | 48        | S-7                           | 220           | 85      | DTBL-4                       | 45            | 49      |
| FOW-27                       | 47             | 61        | S-6                           | 170           | 55      | DTBL-3                       | 25            | 29      |
| FOW-26                       | 40             | 56        | S-5                           | 100           | 54      | DTBL-2                       | 10            | 46      |
| FOW-25                       | 30             | 63        | S-4                           | 35--40        | 80      | DTBL-1                       | 0             | 50      |
| FOW-24                       | 22             | 170       | S-3                           | 19--27        | 67      | <i>perscriptus/bohemicus</i> | Contact       |         |
| FOW-23                       | 9--12          | 51        | S-2                           | 2--9          | 81      | DTBW-21                      | 2             | 15      |
| FOW-22                       | 7--9           | 47        | S-1                           | 0--2          | 58      | DTBW-20                      | 30            | 15      |
| FOW-21                       | 5--7           | 45        | <i>perscriptus</i> Zone above |               |         | DTBW-19                      | 80            | 51      |
| FOW-20                       | 3--5           | 55        | EXTIN-9                       | 0--5          | 81      | DTBW-18                      | 85            | 55      |
| FOW-19                       | 1--3           | 77        | EXTIN-8                       | 5--10         | 60      | DTBW-17                      | 100           | 59      |
| FOW-18                       | 0--1           | 230       | EXTIN-6                       | 10--14        | 87      | DTBW-16                      | 105           | 50      |
| <i>perscriptus/bohemicus</i> | Contact("O/S") |           | EXTIN-5                       | 10--12        | 65      | DTBW-15                      | 110           | 60      |
| FOW-17                       | 0--5           | 74        | EXTIN-4                       | 12--14        | nd      | DTBW-14                      | 115           | 75      |
| FOW-16                       | 5--10          | 63        | EXTIN-3                       | 14--17        | 67      | DTBW-13                      | 210           | 54      |
| FOW-15                       | 10--20         | 40        | EXTIN-2                       | 14.6--17      | 79      |                              |               |         |
| FOW-14                       | 20--25         | 120       | EXTIN-1                       | 15.3--17      | 92      |                              |               |         |
| FOW-13                       | 25--28         | 59        | EXTIN-0                       | 17            | 58      |                              |               |         |
| FOW-12                       | 28--32         | 43        | <i>bohemicus</i> Zone below   |               |         |                              |               |         |
| FOW-11                       | 32--35         | nd**      | O-1                           | 0--7          | 52      | TGL-3                        | 29            | 50      |
| FOW-10                       | 35--39         | 67        | O-2                           | 7--12         | nd      | TGL-2                        | 24            | 48      |
| FOW-9                        | 39--45         | nd        | O-3                           | 12--17        | 45      | TGL-1                        | 20            | 53      |
| FOW-8                        | 57             | 73        | O-4                           | 17--24        | nd      | TGL-0                        | 0             | 88      |
| FOW-7                        | 70             | 100       | O-5                           | 24--30        | nd      | <i>perscriptus/bohemicus</i> | Contact       |         |
| FOW-6                        | 82             | nd        | O-6                           | 30--33        | 38      | TGG-3                        | 5             | 6.6     |
| FOW-5                        | 115            | nd        | O-7                           | 33--37        | nd      | TGG-2                        | 25            | 21      |
| FOW-4                        | 210            | 30        | O-8                           | 100           | 26      | TGW-1                        | 30            | 66      |
| FOW-3                        | 260            | 24        | O-9                           | 121           | nd      |                              |               |         |
| FOW-2                        | 360            | nd        | O-10                          | 131           | 35      |                              |               |         |
| FOW-1                        | 430            | 150       | O-11                          | 151           | nd      |                              |               |         |
|                              |                |           | O-12                          | 200           | nd      |                              |               |         |
|                              |                |           | O-13                          | 226           | 38      |                              |               |         |

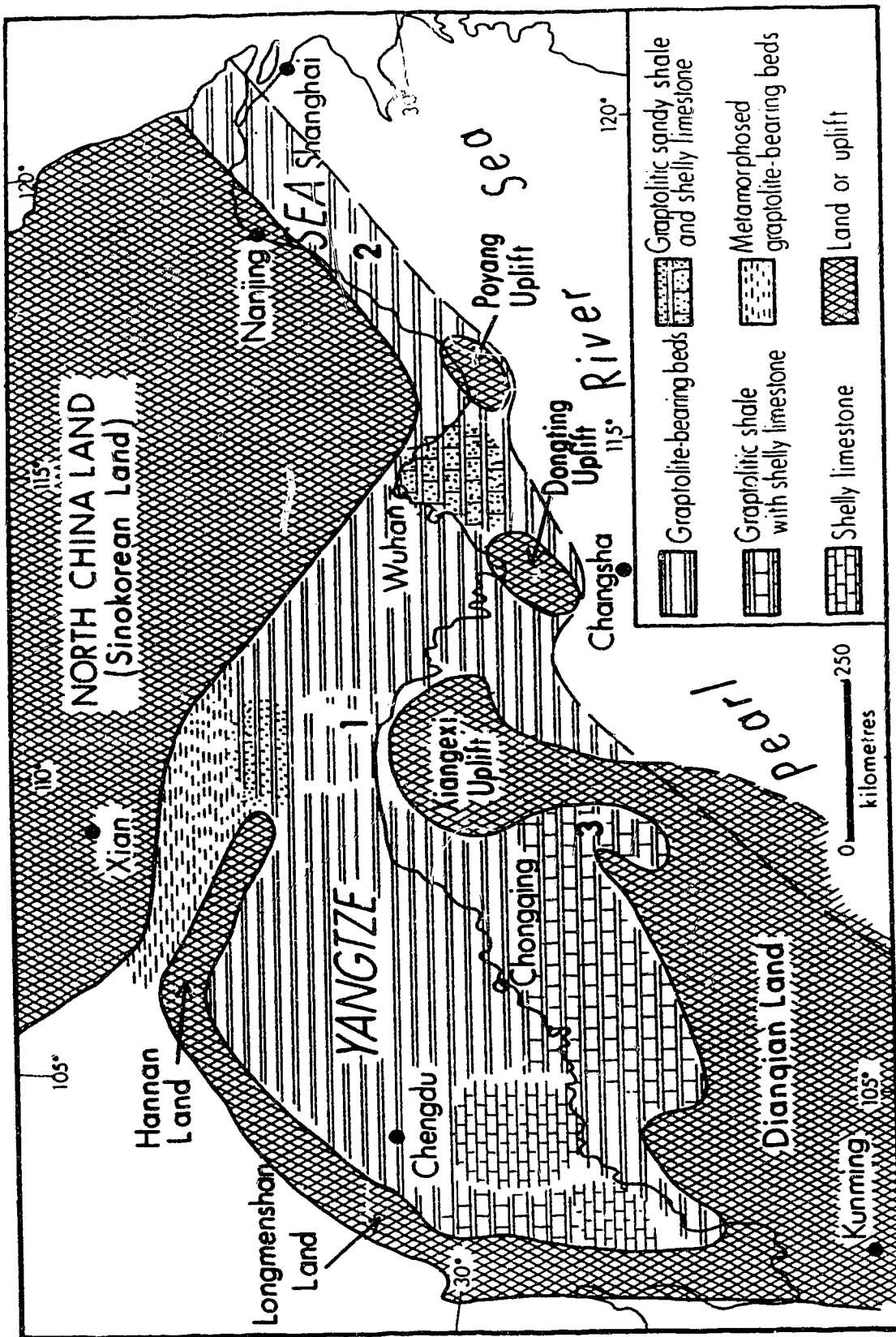
\* ppT: part per trillion; \*\* nd: not detected or not determined

| SILURIAN                | Dob's Linn<br>Scotland<br>(Williams, 1983) |                     | Yichang, China       |   | "SILURIAN"                  |
|-------------------------|--|---------------------|----------------------|---|-----------------------------|
|                         |  |                     | (Mu, 1988)           | (Wang et al., 1983)                           |                             |
|                         | <i>acuminatus</i>                          |                     | <i>acuminatus</i>    | <i>acuminatus</i>                             | "SILURIAN"                  |
|                         | <i>persculptus</i>                         |                     | <i>persculptus</i>   | <i>persculptus</i>                            |                             |
|                         | <i>extraordinarius</i>                     |                     | <i>bohemicus</i>     | <i>Hirnantia-Kinnella</i><br><i>bohemicus</i> |                             |
| ORDOVICIAN<br>(ASHGILL) | anceps                                     | <i>pacificus</i>    | <i>uniformis</i>     | <i>mirus</i>                                  | "ORDOVICIAN"<br>(WUFENGIAN) |
|                         |  |                     | <i>mirus</i>         |   |                             |
|                         |  |                     | <i>typicus</i>       | <i>typicus</i>                                |                             |
|                         |  | <i>complexus</i>    | <i>szechuanensis</i> |   |                             |
|                         | <i>complanatus</i>                         | <i>yangtzeensis</i> | <i>szechuanensis</i> |   |                             |

Fig. 4.1. Correlation of the graptolite zones in the stratotype section at Dob's Linn, Scotland with those at Yichang, China. The Ordovician-Silurian boundary is at the base of the *acuminatus* Zone at Dob's Linn, Scotland. It does not correspond to the base of the *acuminatus* Zone in China, but is within the *persculptus* Zone. The local systemic boundary that is used by most workers in China corresponds to the traditional Ordovician-Silurian boundary used before 1985 at the base of the *persculptus* Zone. Periods/systems recognized in China are shown in quotation marks. (Correlation after Mu et al., 1984; Rong and Harper 1988a; Koren, 1991; Melchin et al., 1991b; and Melchin and Mitchell, 1991).

**Fig. 4.2.** Latest Ordovician (Late Wufengian *bohemicus* Zone) paleogeographic and facies map of the Yangtze Platform on the South China Plate. Stratigraphic section localities: 1. Yichang, Hubei Province; 2. Jinxian, Anhui Province; 3. Xiushan, Sichuan Province and Youyang, Sichuan Province.





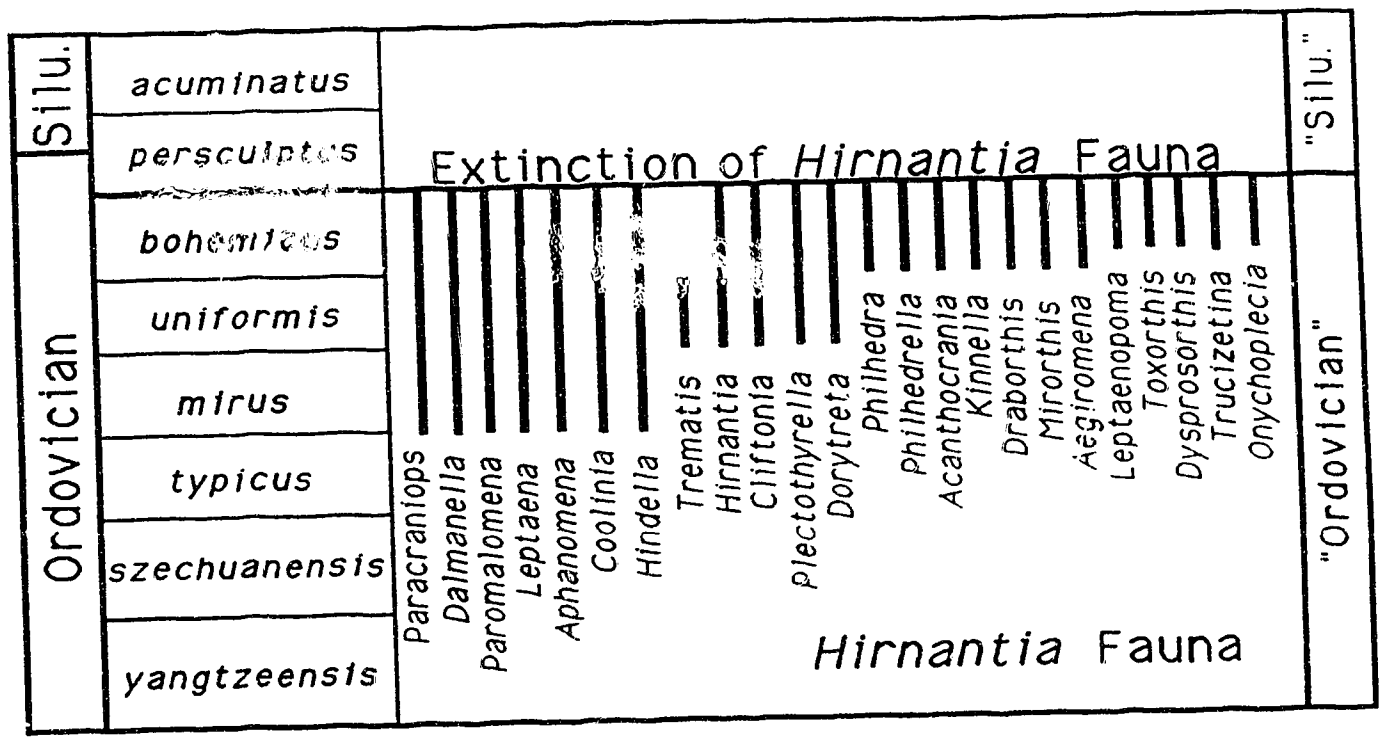


Fig. 4.3. Stratigraphic ranges of 24 brachiopod genera of the *Hirnantia* fauna in the Yangtze region. The *Hirnantia* fauna became extinct at the base of the *persculptus* Zone. Periods/systems recognized in China are shown in quotation marks. (After Rong, 1979, 1984b).

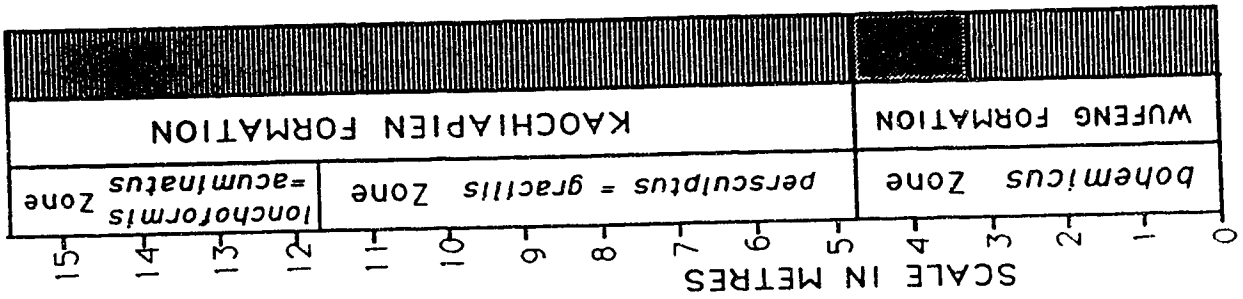
**Fig. 4.4.** Precise stratigraphic ranges and occurrences of "Ordovician" (*pre-persculptus* Zone) graptolites and shelly fossils in the Jinxian Section, Beigong, Jinxian, Anhui Province. An extinction of both graptolites and shelly fossils occurred in a 17 cm mudstone (see Fig. 5) at the base of the *persculptus* Zone (= *gracilis* Zone, Li et al., 1984). Only 4 or 5 "Ordovician" graptolite species (not shown) survived into the *persculptus* Zone. See Li et al. (1984) and Li (1984) for details.

Shelly Fossils

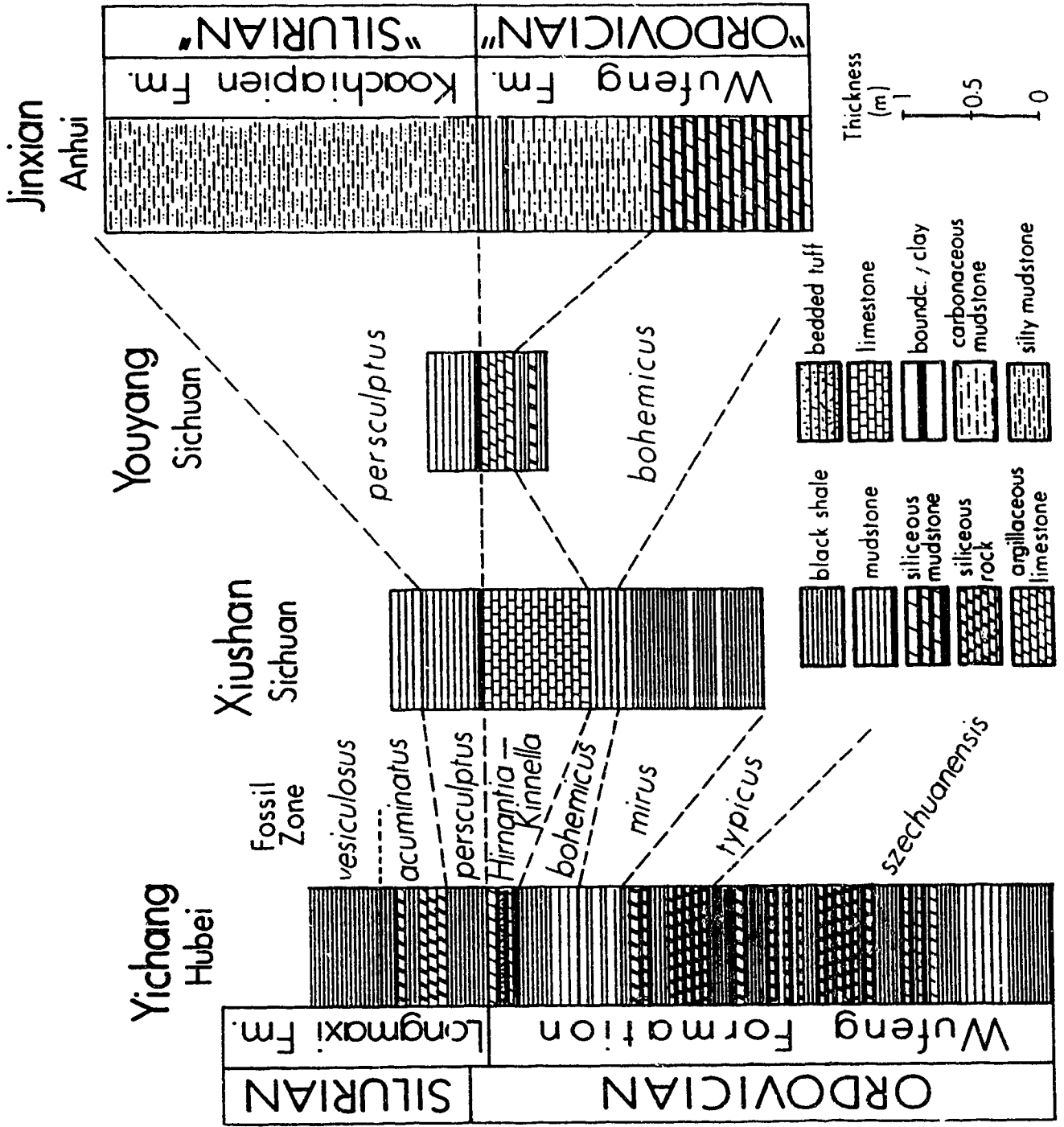
- Dalmantina jingxiensis Qian
- D. anhuiensis Qian
- Platyacoryphe beigongensis Qian
- P. shancongensis Qian
- Paramalomena cf. polonica (Temple)
- Aegirymena cf. ultima Marek & Havlicek
- Oxoplecta ? inconsta Rong
- Coolinia ? sp.
- Pleurothoceras beigongense Zou
- P. shancongense Zou
- P. jingxiense Zou
- Ctenobolbina sp. & Primitiella sp.

Graptolites

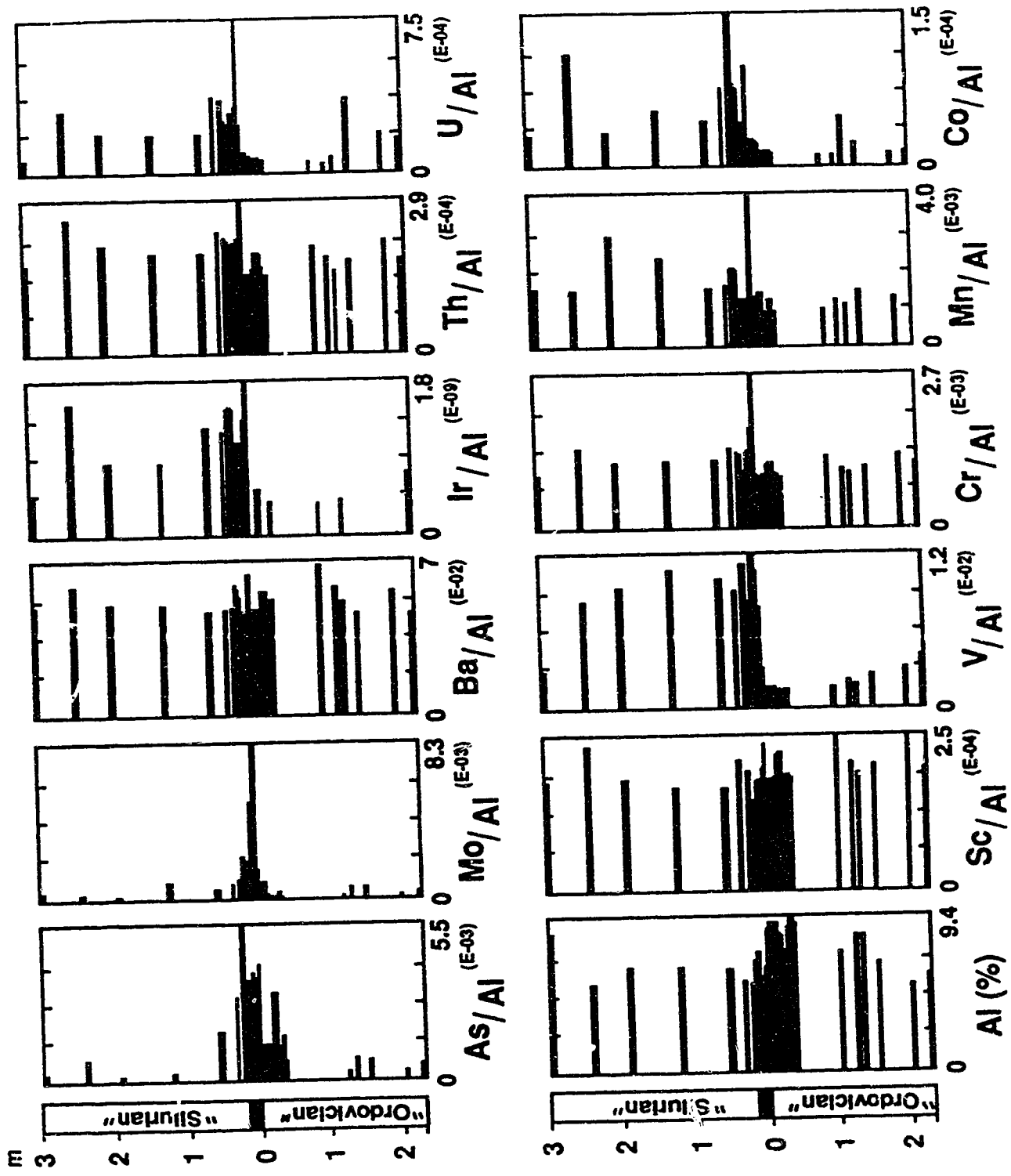
- Glyptograptus daedalus Mu & Ni
- G. elegantulus Mu & Ni
- G. praetamariscus Li
- G. nanus Mu & Ni
- A. cf. extraordinarius (Sobalavskaya)
- Amphioxograptus cf. orientalis (Mu et al.)
- Diplograptus chairs Mu & Ni
- D. bohemicus (Koren & Mikaylova)
- D. beigongensis Li
- D. maturatus Mu & Ni
- D. ojsuensis (Koren & Mikaylova)
- D. viriosus Mu & Ni
- Climacograptus shancongensis Li



**Fig. 4.5.** Stratigraphic columns of the section intervals that were geochemically analyzed by NAA. Fossil zones are those of Wang et al. (1983) (see Fig. 1 for correlation). Periods/systems recognized in China are shown on far right in quotation marks.



**Fig. 4.6.** Abundances and ratios of some significant elements in the Jinxian Section at Beigong, Jinxian, Anhui Province. The datum in this figure is the base of the 17 cm mudstone "extinction layer". Periods/systems recognized in China are shown in quotation marks.





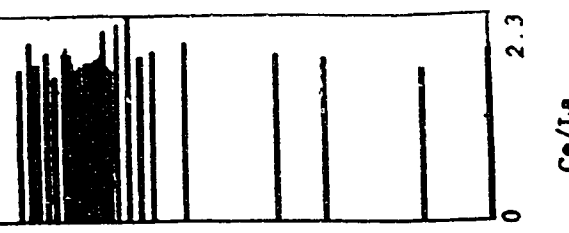
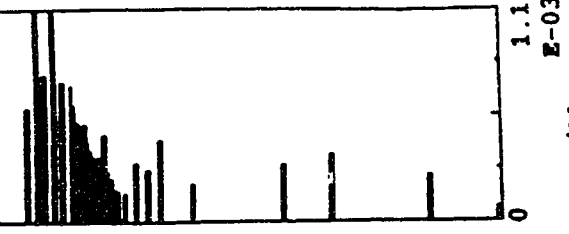
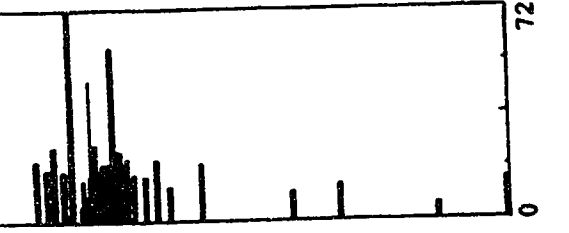
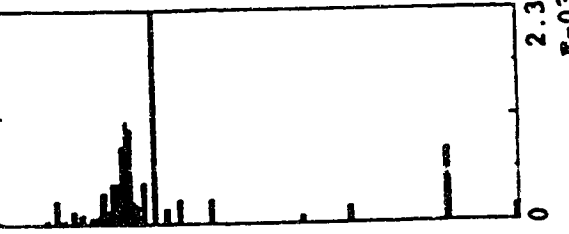
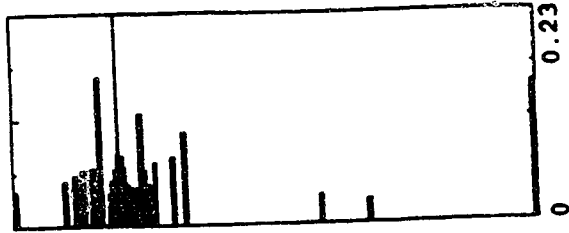
**Fig. 4.7.** Abundances and ratios of some significant elements in the Yichang Section at Fenxiang, Yichang, Hubei Province. The datum is the local systemic boundary recognized in China. Periods/systems recognized in China are shown in quotation marks.

Distance from "O/S" Boundary (cm)

100 0 100 200 300 400

"Ordovician"

"Stl."

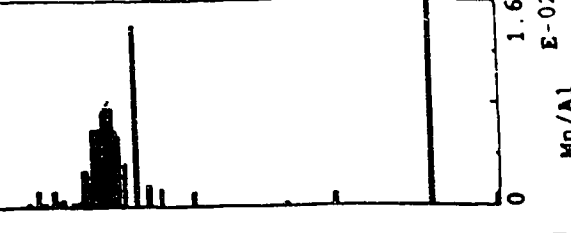
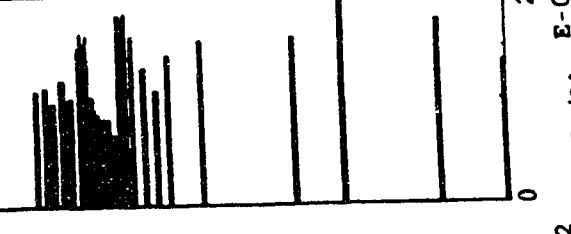
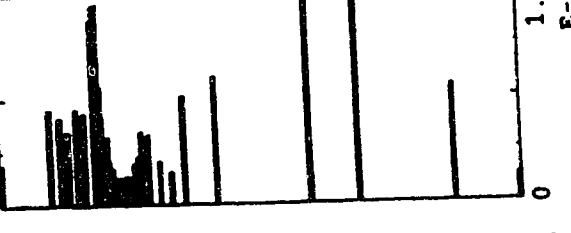
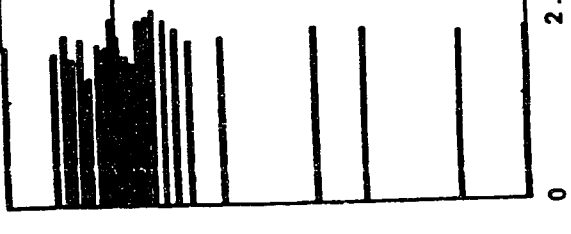
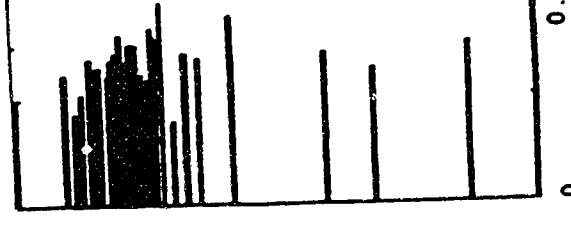
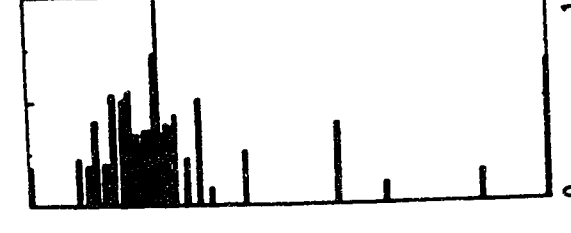


Distance from "O/S" Boundary (cm)

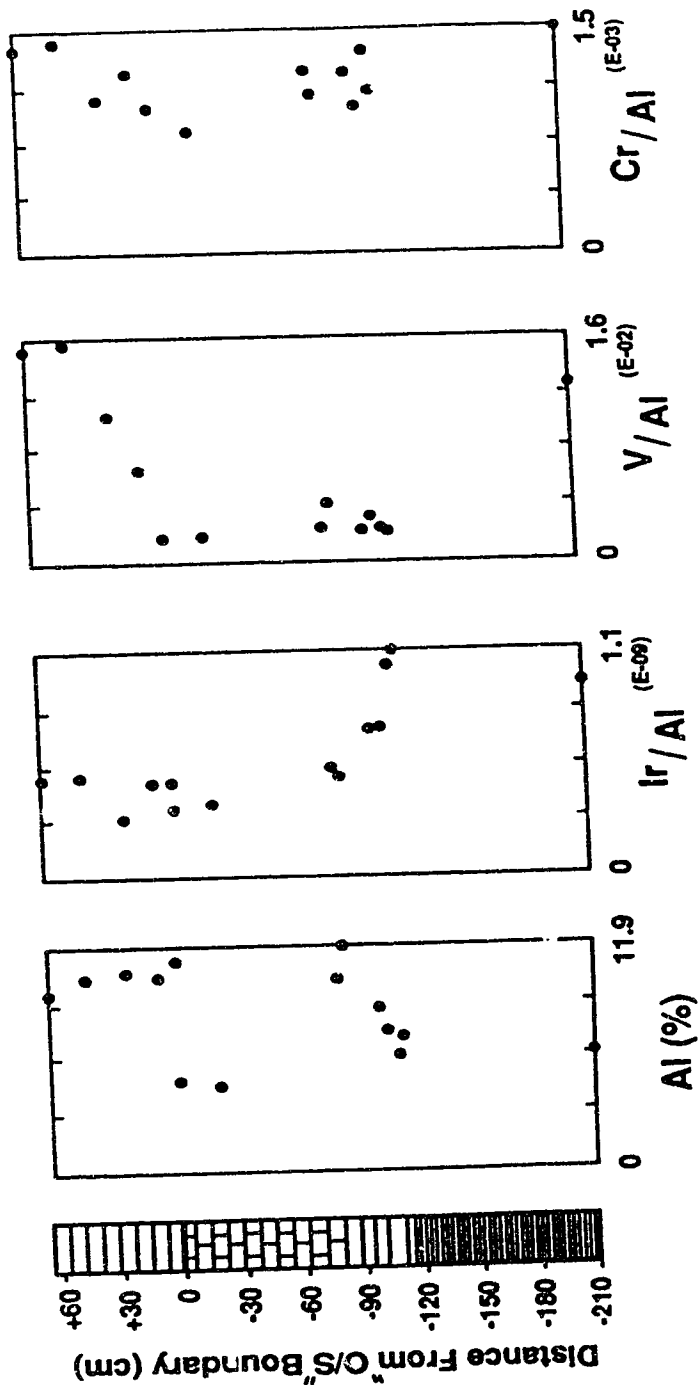
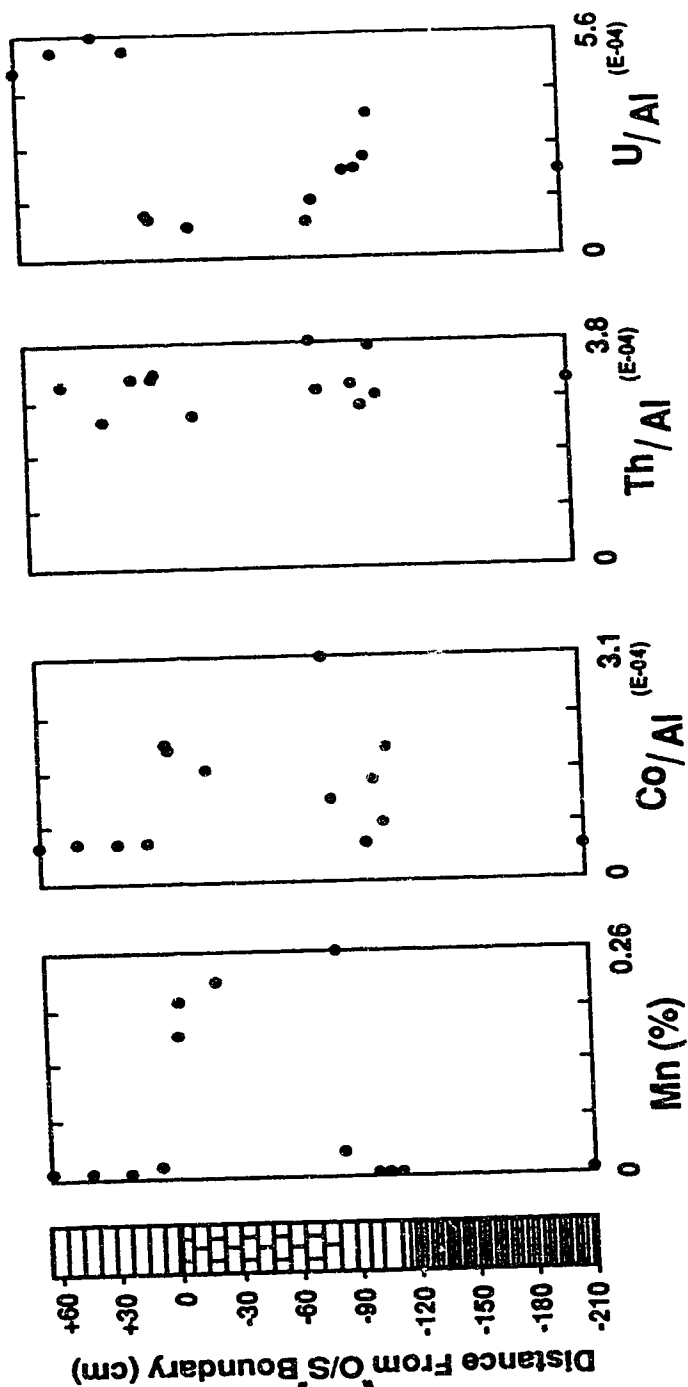
100 0 100 200 300 400

"Ordovician"

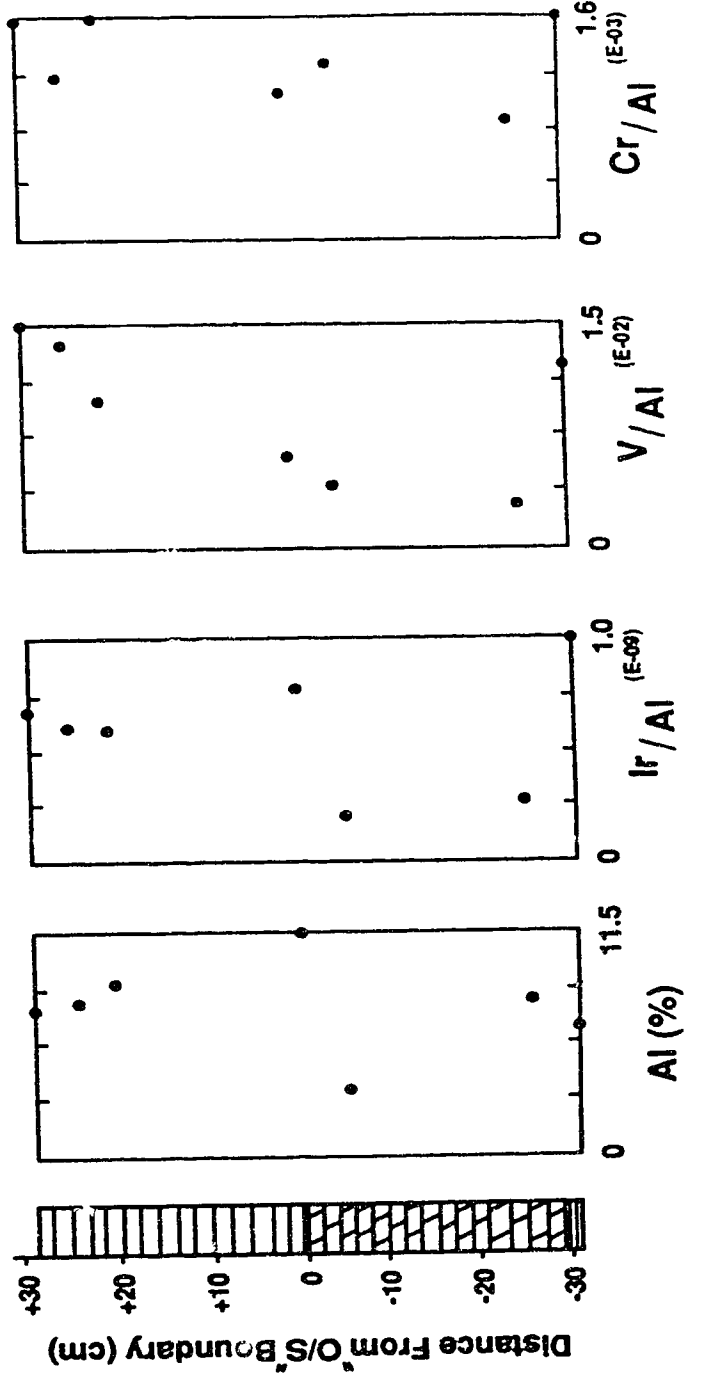
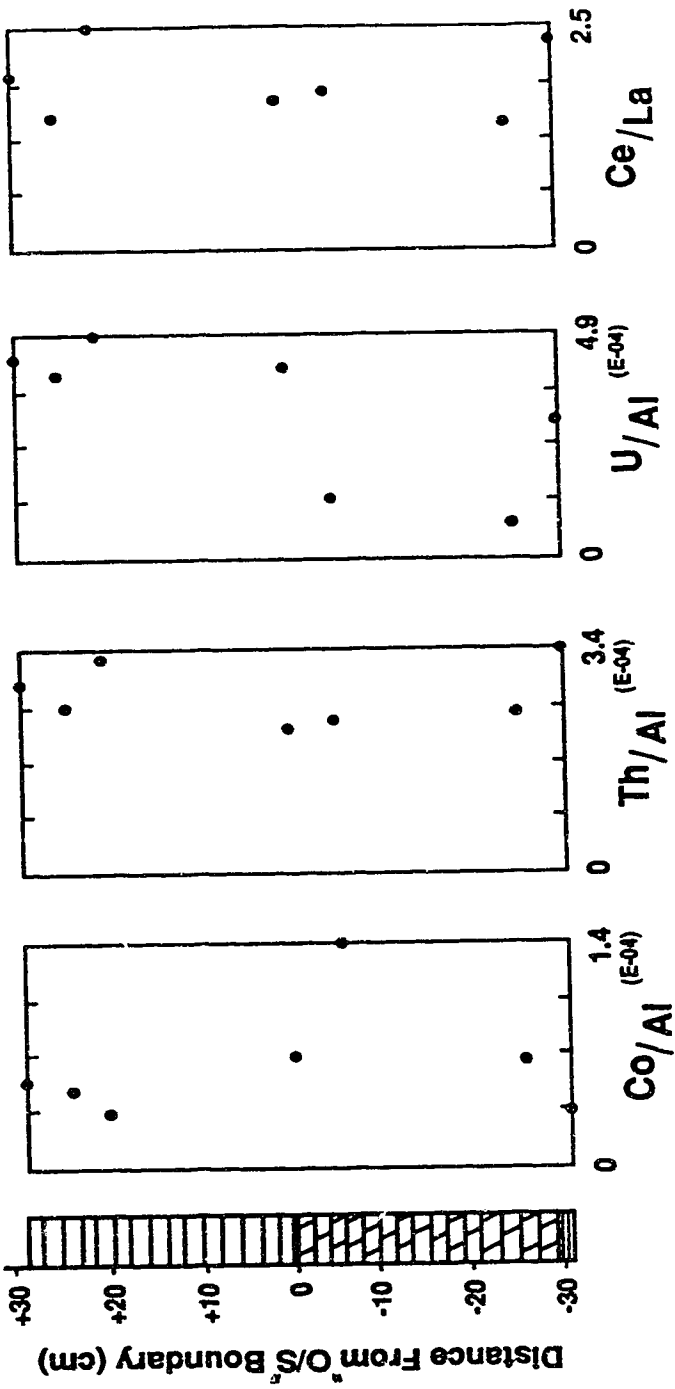
"Stl."



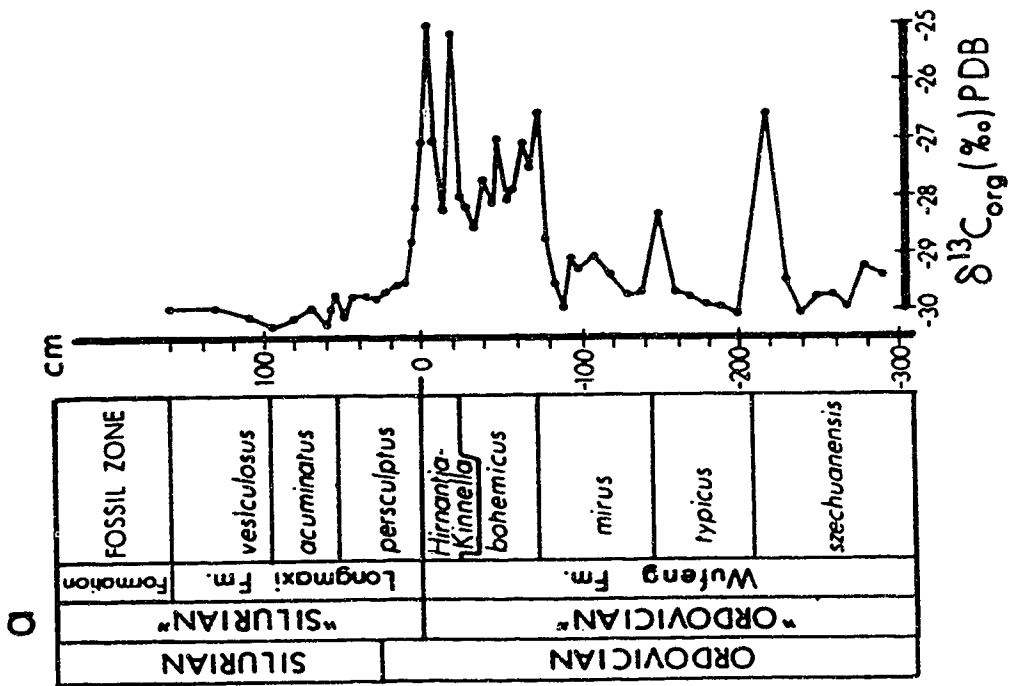
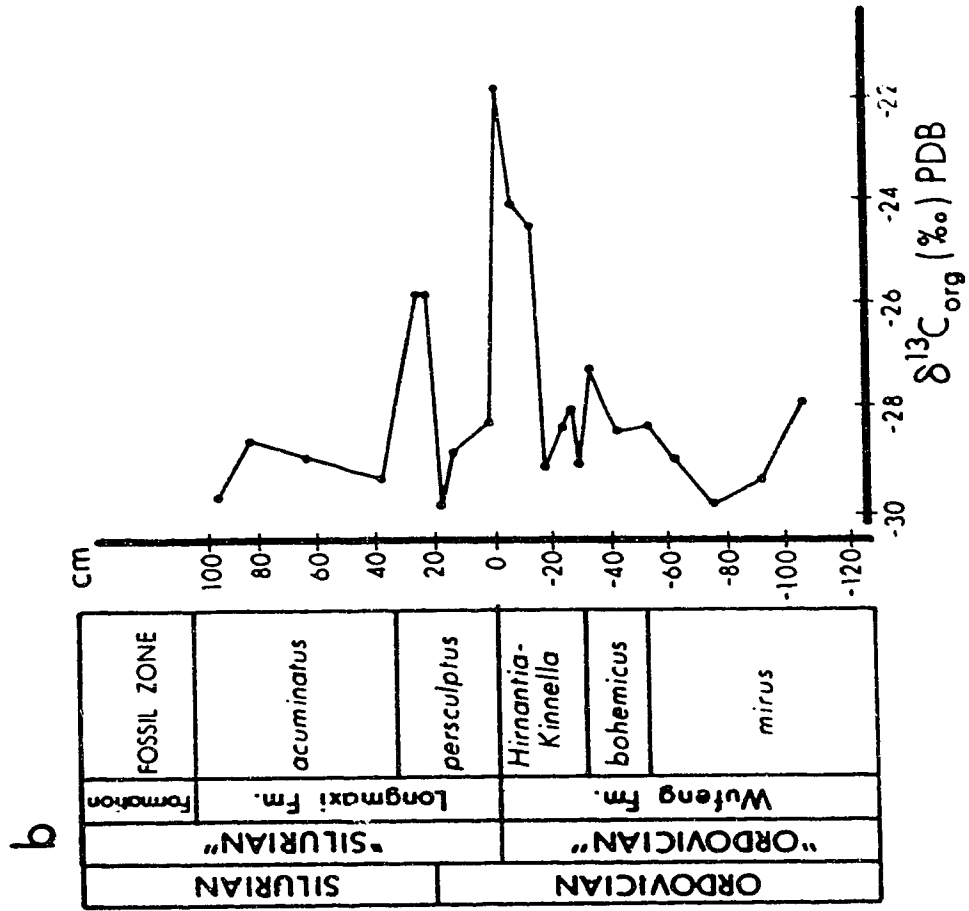
**Fig. 4.8.** Abundances and ratios of some significant elements in the Xiushan Section at Datianba, Xiushan, Sichuan Province. The datum is the local systemic boundary recognized in China. Periods/systems recognized in China are shown in quotation marks.



**Fig. 4.9.** Abundances and ratios of some significant elements in the Youyang Section at Tongguo, Youyang, Sichuan Province. The datum is the local systemic boundary recognized in China. Periods/systems recognized in China are shown in quotation marks.



**Fig. 4.10.** Variations of carbon isotope ratios of organic material in two nearby sections at Yichang, Hubei Province. a---Wangjiawan Section; b---Huanghuachang Section. Periods/systems recognized in China are shown in quotation marks. (After Xu et al., 1989, 1991).





## References

- Alvarez, W. and Asaro F., 1990. An extraterrestrial impact. *Scientific American*, 10: 78-84.
- Arthur, M.A., Dean, W.E. and Claypool, G.E., 1985. Anomalous C-13 enrichment in modern marine organic carbon. *Nature*, 315: 216-218.
- Barnes, C.R., 1986. The faunal extinction event near the Ordovician-Silurian boundary: A climatically induced crisis. In: O. Walliser (Editor), *Global Bio-Events*. Springer-Verlag, Berlin, pp. 121-126.
- Berry, W.B.N., 1987. The Ordovician-Silurian boundary: New data, new concerns. *Lethaia*, 20: 209-216.
- Berry, W.B.N. and Boucot, A.J., 1973. Glacio-eustatic control of Late Ordovician-Early Silurian platform sedimentation and faunal changes. *Geological Society of America Bulletin*, 84: 275-284.
- Brenchley, P.J., 1984. Late Ordovician extinctions and their relationship to the Gondwana glaciation. In: P.J. Brenchley (Editor), *Fossils and Climate*. Wiley and Sons, Chichester, pp. 291-315.
- 1988. Environmental changes close to the Ordovician-Silurian boundary. In: L.R.M. Cocks, and R.B. Rickards (Editors), *A Global Analysis of the Ordovician-Silurian Boundary*. British Museum (Natural History) *Bulletin Geology Series*, 43: 377-385.
- 1989. The late Ordovician extinction. In: S.K. Donovan (Editor), *Mass Extinctions: Processes and Evidence*. Columbia Univ. Press, New York, pp. 104-132.
- Brenchley, P.J., Marshall, J.D., Robertson, D.B.R., Hints, L. and Carden, G., 1992. Climatic-biotic interactions in the Late Ordovician mass extinction. *Fifth International Conference on Global Bio-Events: Phanerozoic Global Bio-Events and Event-Stratigraphy*, Gottingen, Germany, Feb. 16-19. Abstract Volume, p. 22.
- Brenchley, P.J. and Newall, G., 1980. A facies analysis of Upper Ordovician regressive sequences in the Oslo region, Norway: A record of glacio-eustatic changes. *Palaeogeography, Palaeoclimatology, Palaeoecology*, 31: 1-38.

- 1984. Late Ordovician environmental changes and their effect on faunas. In: D.L. Bruton (Editor), *Aspects of the Ordovician System. Paleontological Contributions from the University of Oslo*, 295: 65-79.
- Chatterton, B.D.E. and Lu Jansen, R., 1983. Trilobites from the Ordovician-Silurian boundary of the Mackenzie Mountains, Northwestern Canada. In: *Papers for the Symposium on the Cambrian-Ordovician and Ordovician-Silurian Boundaries*, Nanjing, China, October, 1983. Nanjing Institute of Geology and Palaeontology, Academia Sinica, pp. 146-147.
- Chen, X., 1984. Influence of the Late Ordovician glaciation on basin configuration of the Yangtze Platform in China. *Lethaia*, 17: 51-60.
- Chen, X. and Rong, J., 1991. Concepts and analysis of mass extinction with the Late Ordovician events as an example. *Historical Biology*, 5: 107-121.
- Chen, X., Xiao, C. and Chen, H., 1987. Graptolite diversity and anoxic environments in the Wufengian in South China (in Chinese, with English abstract). *Acta Palaeontologica Sinica*, 26: 326-344.
- Cocks, L.R.M., 1985. The Ordovician-Silurian boundary. *Episodes*, 8: 98-100.
- Colbath, G.K., 1986. Abrupt terminal Ordovician extinction in phytoplankton associations, southern Appalachians. *Geology*, 14: 943-946.
- Deines, P., 1980. The isotopic composition of reduced organic carbon. In: P. Fritz and J.Ch. Fontes (Editors), *Handbook of Environmental Isotope Geochemistry*, v. 1, *The Terrestrial Environment*. Elsevier, Amsterdam, pp. 329-406.
- Eckert, J.D., 1988. Late Ordovician extinction of North American and British crinoids. *Lethaia*, 21: 147-167.
- Fortey, R.A., 1989. There are extinctions and extinctions: examples from the Lower Palaeozoic. *Phil. Trans. R. Soc. Lond.*, B325: 327-355.
- Goodfellow, W.D., Nowlan, G.S., McCracken, A.D., Lenz, A.C. and Grégoire, D.C., 1992. Geochemical anomalies near the Ordovician-

- Silurian boundary, northern Yukon Territory, Canada. *Historical Biology*, 6: 1-23.
- Hollander, D.J. and Mckenzie, J.A., 1991. CO<sub>2</sub> control on carbon-isotope fractionation during aqueous photosynthesis: A paleo-pCO<sub>2</sub> barometer. *Geology*, 19: 929-932.
- Holser, T.H. and 14 others, 1989. A unique geochemical record at the Permian/Triassic boundary. *Nature*, 337: 39-44.
- Hsü, K.J. and Mckenzie, J.A., 1990. Carbon-isotope anomalies at era boundaries: Global catastrophes and their ultimate cause. *Geological Society of America Special Paper*, 247: 61-70.
- Hsü, K.J., Oberhansli, H., Gao, J.Y., Shu, S., Haihong, C. and Krahenbul, U., 1985. "strangelove ocean" before the Cambrian explosion. *Nature*, 316: 809-811.
- Koren, T.N., 1991. Evolutionary crisis of the Ashgill graptolites. In: C.R. Barnes and S.H. Williams (Editors), *Advances in Ordovician Geology*. Geological Survey of Canada Paper 90-9: 157-164.
- Li, J., 1984. Graptolites across the Ordovician-Silurian boundary from Jinxian, Anhui. In: E. Mu (Editor), *Stratigraphy and Palaeontology of Systemic Boundaries in China: Ordovician-Silurian Boundary*. Anhui Science and Technology Publishing House, Hefei, pp. 309-388.
- Li, J., Qian, Y. and Zhang, J., 1984. Ordovician-Silurian boundary section from Jinxian, South China. In: E. Mu (Editor), *Stratigraphy and Palaeontology of Systemic Boundaries in China: Ordovician-Silurian Boundary*. Anhui Science and Technology Publishing House, Hefei, pp. 287-308.
- Long, D.G.F., in press. Oxygen and carbon isotopes and event stratigraphy near the Ordovician-Silurian boundary, Anticosti Island, Quebec. *Palaeogeography, Palaeoclimatology, Palaeoecology*
- Marshall, J.D. and Middleton, P.D., 1990. Changes in marine isotopic composition and the late Ordovician glaciation. *Journal of the Geological Society of London*, 147: 1-4.
- McCracken, A.D. and Barnes, C.R., 1981. Conodont biostratigraphy and paleontology of the Ellis Bay Formation, Anticosti Island, Quebec, with special reference to Late Ordovician-Early Silurian

- . chronostratigraphy and the systemic boundary. Geological Survey of Canada Bulletin 329: 51-134.
- McLaren, D.J. and Goodfellow, W.D., 1990. Geological and biological consequences of giant impacts. *Annual Reviews of Earth and Planetary Sciences*, 18: 123-171.
- Melchin, M.J., McCracken, A.D. and Goodfellow, W.D., 1991a. Bioevents and geochemical anomalies near the Ordovician-Silurian boundary on Cornwallis and Truro islands, Arctic Canada. In: *Event Makers in Earth History. Program and Abstracts of the Joint Meeting of the IGCP Projects 216, 293 and 303*, Calgary, Alberta, Canada, p. 54.
- Melchin, M.J., McCracken, A.D. and Oliff, F.D., 1991b. The Ordovician-Silurian boundary on Cornwallis and Truro islands, Arctic Canada: preliminary data. *Can. J. Earth Sci.*, 28: 1854-1862.
- Melchin, M.J. and Mitchell, C.E., 1991. Late Ordovician extinction in the Graptoloidea. In: C.R. Barnes and S.H. Williams (Editors), *Advances in Ordovician Geology*. Geological Survey of Canada Paper 90-9: 143-156.
- Minor, M.M., Hensley, W.K., Denton, M.M. and Garcia, S.R., 1982. An automated activation analysis system. *Journal of Radioanalytical Chemistry*, 70: 459-471.
- Mu, E., 1988. The Ordovician-Silurian boundary in China. In: L.R.M. Cocks and R.B. Rickards (Editors), *A Global Analysis of the Ordovician-Silurian Boundary*. British Museum (Natural History) Bulletin Geology Series, 43: 117-132.
- Mu, E., Li, J., Ge, M., Chen, X., Ni, Y. and Lin, Y., 1981. Late Ordovician paleogeography of South China (in Chinese). *Acta Stratigraphica Sinica*, 5: 165-170.
- Mu, E., Zhu, Z., Lin, Y. and Wu, H., 1984. The Ordovician-Silurian boundary in Yichang, Hubei. In: E. Mu (Editor), *Stratigraphy and Palaeontology of Systemic Boundaries in China: Ordovician-Silurian Boundary*. Anhui Science and Technology Publishing House, Hefei, pp.15-41.
- Nowlan, G.S., McCracken, A.D. and Chatterton, B.D.E., 1988. Conodonts from Ordovician-Silurian boundary strata, Whittaker Formation,

- Mackenzie Mountains, Northwest Territories. Geological Survey of Canada Bulletin 373: 1-99.
- Orth, C.J., 1989. Geochemistry of the bio-event horizons. In: S.K. Donovan (Editor), *Mass Extinctions: Processes and Evidence*. Columbia University Press, New York, pp. 37-72.
- Orth, C.J., Gilmore, L.R., Quintana, L.R. and Sheehan, P.M., 1986. Terminal Ordovician extinction: Geochemical analysis of the Ordovician/Silurian boundary, Anticosti Island, Quebec. *Geology*, 14: 433-436.
- Owen, A.W., Harper, D.A.T. and Rong, J., 1991. Hirnantian trilobites and brachiopods in space and time. In: C.R. Barnes and S.H. Williams (Editors), *Advances in Ordovician Geology*. Geological Survey of Canada Paper 90-9: 179-190.
- Rau, G.H., Takahashi, T. and Des Marais, D.J., 1989. Latitudinal variations in plankton  $\delta^{13}\text{C}$ : implications for  $\text{CO}_2$  and productivity in past oceans. *Nature*, 341: 516-518.
- Raup, M.R., 1990. Impact as a general cause of extinction: A feasibility test. *Geological Society of America Special Paper* 247: 27-32.
- Raup, M.R. and Sepkoski, J.J., Jr, 1982. Mass extinctions in the marine fossil record. *Science*, 215: 1501-1503.
- Rong, J., 1979. The *Hirnantia* fauna of China with comments on the Ordovician-Silurian boundary (in Chinese). *Acta Stratigraphica Sinica*, 3: 1-8.
- 1984a. Distribution of the *Hirnantia* fauna and its meaning. In: D.L. Bruton (Editor), *Aspects of the Ordovician System*. Paleontological Contributions from the University of Oslo, 295: 101-112.
- 1984b. Brachiopods of the latest Ordovician in the Yichang District, West Hubei, Central China. In: E. Mu (Editor), *Stratigraphy and Palaeontology of Systemic Boundaries in China: Ordovician-Silurian Boundary*. Anhui Science and Technology Publishing House, Hefei, pp. 111-176.
- Rong, J. and Chen, X., 1986. A big event of the latest Ordovician in China. In: O. Walliser (Editor), *Global Bio-Events*. Springer-Verlag, Berlin, pp. 127-131.

- Rong, J. and Harper, D.A.T., 1988a. A global synthesis of the latest Ordovician Hirnantian brachiopod faunas. Royal Society of Edinburgh Transactions Earth Sciences, 79: 383-402.
- 1988b. The Ordovician-Silurian boundary and the *Hirnantia* fauna. Lethaia, 21: 168.
- Sackett, W.M., Eckelmann, W.R., Bender, M.L. and Bé, A.W.H., 1965. Temperature dependence of carbon isotope composition in marine plankton and sediments. Science, 148: 235-237.
- Scotese, C.R. and McKerrow, W.S., 1990. Revised world maps and introduction. In: W.S. McKerrow and C.R. Scotese (Editors), Paleozoic Palaeogeography and Biogeography. Geological Society of London Memoir, 12: 1-21.
- Sheehan, P.M., 1973. The relationship of late Ordovician glaciation to the Ordovician-Silurian changeover in North American brachiopod faunas. Lethaia, 6: 147-154.
- 1975. Brachiopod synecology in a time of crisis (late Ordovician-early Silurian). Paleobiology, 1: 205-212.
- 1988. Late Ordovician events and the terminal Ordovician extinction. New Mexico Bureau of Mines and Mineral Resources Memoir 44: 405-415.
- Stanley, S.M., 1984. Temperature and biotic crises in the marine realm. Geology, 12: 205-208.
- Temple, J.T., 1965. Upper Ordovician brachiopods from Poland and Britain. Acta Paleontologica Polonica, 10: 379-450.
- Tuckey, M.E. and Anstey, R.L., 1992. Late Ordovician extinctions of bryozoans. Lethaia, 25: 111-117.
- Wang, H., 1985. Atlas of the Palaeogeography of China. Cartographic Publishing House, Beijing, 143 pp.
- Wang, K., Chatterton, B.D.E., Attrep, M. and Orth, C.J., 1992. Iridium abundance maxima at the latest Ordovician mass extinction horizon, Yangtze Basin, China: Terrestrial or extraterrestrial? Geology, 20: 39-42.
- 1991. Geochemical, paleontological and sedimentological studies of the end-Ordovician mass extinction, Mackenzie Mountains, N.W.T., Canada. Geological Society of America Abstracts with Programs, 23 (5): A181.

- submitted. Late Ordovician mass extinction event on northwestern Laurentia: Geochemical, paleontological and sedimentological analyses of the Ordovician-Silurian boundary interval, Mackenzie Mountains, N.W.T. Canadian Journal of Earth Sciences.
- Wang, K., Chatterton, B.D.E., Orth, C.J., Attrep, M. and Li, J., 1990. Geochemical analyses through the Ordovician/Silurian mass extinction boundary, Anhui Province, South China. Geological Society of America Abstracts with Programs, 22 (7): A365.
- Wang, K., Orth, C.J., Attrep, M., Jr., Chatterton, B.D.E., Hou, H. and Geldsetzer, H.H.J., 1991. Geochemical evidence for a catastrophic biotic event at the Frasnian/Famennian boundary in south China. *Geology*, 19: 776-779.
- Wang, X., 1989. Palaeogeographic reconstruction of Ordovician in China and characteristics of its sedimentary environment and biofacies (in Chinese, with English abstract). *Acta Palaeontologica Sinica*, 28: 234-248.
- Wang, X. and Chai, Z., 1989. Terminal Ordovician mass extinction and its relationship to iridium and carbon isotope anomalies (in Chinese, with English abstract). *Acta Geologica Sinica*, 63: 255-264.
- Wang, X., Zeng, Q., Zhou, T., Ni, S., Xu, G., Sun, Q., Li, Z., Xiang, L. and Lai, C., 1983. Latest Ordovician and earliest Silurian faunas from the eastern Yangtze Gorges, China, with comments on Ordovician-Silurian boundary (in both Chinese and English). *Yichang Institute of Geology and Mineral Resources Bulletin*, 6: 57-163.
- Welte, D.H., Kalkreuth, W. and Hoefs, J., 1975. Age-trend in carbon isotopic composition in Paleozoic sediments. *Naturwissenschaften*, 62: 482-483.
- Wilde, P. and Berry, W.B.N., 1984. Destabilisation of the oceanic density structure and its significance to marine extinction events. *Palaeogeography, Palaeoclimatology, Palaeoecology*, 48: 143-162.

- Wilde, P., Berry, W.B.N., Quinby-Hunt, M.S., Orth, C.J., Quintana, L.R. and Gilmore, J.S., 1986. Iridium abundances across the Ordovician-Silurian stratotype. *Science*, 233: 339-341.
- Williams, S.H., 1983. The Ordovician-Silurian boundary graptolite fauna of Dob's Linn, southern Scotland. *Palaeontology*, 26: 605-639.
- 1986. Top Ordovician and lowest Silurian of Dob's Linn. *Geological Society of London Special Publication*, 20: 165-171.
- Xu, D., Zhang, Q., Sun, Y., Yan, Z., Chai, Z. and He, J., 1989. *Astrogeological Events in China*. Scottish Academic Press, Edinburgh, 264 pp.
- Xu, D., Yan, Z. and Ye, L., 1991. Organic carbon isotope perturbation across the Ordovician-Silurian boundary layer of the Wangjiawan Section, Yichang, China. In: *Event Makers in Earth History. Program and Abstracts of the Joint Meeting of the IGCP Projects 216, 293 and 303*, Calgary, Alberta, Canada, pp. 78.
- Yan, Z., Ye, L. and Hou, H., In press. Carbon isotope anomalies near the Frasnian/Famennian boundary at the Xiantian Section, Guangxi, China. *Palaeo*<sup>3</sup>.
- Yapp, C.J. and Poths, H., 1992. Ancient atmospheric CO<sub>2</sub> pressures inferred from natural goethites. *Nature*, 355: 342-344.
- Zachos, J.C., Arthur, M.A. and Dean, W.E., 1989. Geochemical evidence for suppression of pelagic marine productivity at the Cretaceous/Tertiary boundary. *Nature*, 337: 61-64.



## Chapter 5

### Geochemical evidence for a catastrophic biotic event at the Frasnian/Famennian boundary in South China

(A version of this chapter has been published. Wang, K., Orth, C.J., Attrep, M. Jr., Chatterton, B.D.E., Hou, H. and Geldsetzer, H.H.J., 1991. *Geology*, 19: 776-779.)

#### Introduction

It has long been known that there was a massive biotic event close to the boundary between the Frasnian and Famennian stages of the Upper Devonian (McLaren, 1970). Only recently have the timing, in terms of the standard Upper Devonian conodont zones, and the global occurrence and synchronism of the event been well established (Sandberg et al., 1988; McLaren and Goodfellow, 1990). Evidence has been obtained from North America, Europe, China, Australia, and North Africa for a globally synchronous F/F mass extinction event, which is marked in the field by the disappearance of many taxa at a bedding plane in shelf sections (McLaren, 1988). Recent work on conodont dating of the F/F event in Euramerica, consistent with the global evidence, has demonstrated that the crisis took place very near the end of the latest Frasnian linguiformis conodont zone, shortly before the earliest Famennian lower triangularis zone (Sandberg et al., 1988). This horizon coincides with the upper Kellwasser limestone of Germany, which has long been identified as the latest Frasnian "Kellwasser event" (Walliser et al., 1989; Sandberg et al., 1988). The previously reported geochemical anomalies in the upper triangularis zone in the Canning basin, Western Australia (Playford et al., 1984) and in the crepida zone in Hunan, south China (Wang and Bai, 1988) postdate the F/F event by at least 1 and 1.5 m.y., respectively (using 0.5 m.y. for each Late Devonian conodont zone).

According to a recent study of the F/F event in the western United States, Germany, Belgium, and Morocco (Sandberg et al., 1988), the biotic crisis was accompanied by drastic eustatic and

sedimentary events, including major storms, slumping, debris flows, and tsunami deposits, and the mass extinction took place in far less time than a few tens of thousands of years and was probably instantaneous. No Ir anomaly has been found in any European and American section at this extinction horizon (McGhee et al., 1984, 1986), although anomalies of a positive  $\delta^{34}\text{S}$  (Geldsetzer et al., 1987) and some chalcophile elements and a negative  $\delta^{13}\text{C}$  (Goodfellow et al., 1989) are associated with the extinction in Canadian sections. The only Ir anomaly in the Canning basin of Australia was the result of biological concentration (Orth, 1989), and is independent of the adjacent platform extinction event (McLaren and Goodfellow, 1990).

The F/F extinction event has been recognized in south China from nearshore (inner shelf), carbonate platform, slope, and basinal settings (Hou et al., 1988; Ji, 1988). As in other parts of the world, the extinction in south China is best documented in shallow-water shelf facies. In basinal or slope facies, more complete sequences of deposition and the presence of the standard conodont zones allow precise correlation of the F/F extinction horizon globally. Basinal facies are also ideal for the documentation of geochemical anomalies across the extinction interval because relatively quiet water conditions would increase the potential for the preservation of fragile geochemical signatures of a physical event, such as an impact.

### **Geologic setting and stratigraphy**

The Devonian sediments were deposited in an epicontinental sea on the southern margin of the south China plate, whereas the northern part of the south China plate was a landmass that provided clastics deposited in the sea to the south. This South China Sea covered a carbonate platform, which was formed during Emsian-Eifelian time, and a northwest-trending trough developed during the Givetian transgression, which extended marine conditions progressively farther northward. Several subparallel, northeast-trending troughs were established in the Frasnian by cutting of the carbonate platform as a result of subsidence. This unique

paleogeographic pattern of carbonate platform alternating with submarine troughs persisted to the end of the Devonian despite the apparent occurrence of regressions during the Famennian (Fig. 5.1). A brief summary of the regional paleotectonic evolution of the Devonian in South China was given by Tsien et al.(1988).

There are four major Upper Devonian facies from the north to the south: littoral clastic facies, nearshore (inner shelf) argillaceous carbonate, carbonate platform (middle and outer shelf), and trough (basinal) siliceous carbonate and shale (Fig. 5.1). A slope (platform margin) facies and a reef facies are also identified in some areas. The F/F extinction is best documented in nearshore, carbonate platform and reef facies, where one can actually see the sudden disappearance of brachiopods, corals, stromatoporoids, bryozoans, and other benthos. The horizon of this biotic crisis in these facies appears to coincide stratigraphically with the base of the triangularis zone (Ji, 1988). For example, an inner shelf facies at Xikuangshan in Hunan (Fig. 5.1) contains a very abundant fauna of benthos consisting of 16 coral, 8 brachiopod, 2 bryozoan and some stromatoporoid species in the topmost 1 m of the Frasnian Shetianqiao Formation (Wang and Bai, 1988; Hou et al., 1988). The entire fauna, except two or three brachiopod species, died out before the deposition of the overlying Famennian Xikuangshan Formation. Recent work on conodont biostratigraphy at this locality indicates that the extinction horizon may correspond to the F/F boundary (Ji, 1988).

The F/F boundary section that was selected for geochemical analyses is located at Xiangtian Village, Luoxiu Town, Xiangzhou County, Guangxi Province (Fig. 5.1). This section was deposited in a northeast-trending trough in the Late Devonian, and therefore is composed of basinal facies. The Upper Devonian consists of deep-water siliceous rocks of the Frasnian Liujiang Formation and of nodular or thick-bedded limestones of the Famennian Wuzhishan Formation. The faunas are mainly pelagic in both Frasnian and Famennian strata, including conodonts, ammonoids, and tentaculitids. A distinct lithologic unit was recently distinguished within the Frasnian Liujiang Formation and named the Xiangtian

Member to represent the uppermost part of the formation (Hou et al., 1988). This unit, with a wide geographic distribution, is characterized by limestone breccias and debris which are angular, poorly sorted, and probably derived from the nearby carbonate platform as debris flows.

A generalized geologic column of the measured interval of the Xiangtian section (Fig. 5.2) shows lithologies and conodont zones established by Ji (1988). The F/F boundary is marked by bed E which separates strata with Frasnian conodonts below from strata with Famennian conodonts above. *Palmatolepis gigas* and *Palmatolepis subrecta* occur throughout beds B, C, and D, and *Palmatolepis linguiformis* occurs only in bed D. These three species extend to the top of Bed D, where they disappear before the deposition of bed E. Bed E, a 20-cm-thick mudstone, is a barren zone where no fossils are found. *Palmatolepis triangularis*, which marks the beginning of the triangularis zone, first appears at the base of bed F. *Palmatolepis delicatula clarki*, marking the start of the middle triangularis zone, first appears in the lower part of bed G. The relative abundances of the conodont genera indicate a deep-water palmatolepid-polygnathid conodont biofacies, which is consistent with the deep-water basinal setting at this locality. The only macrofossils that have been found in this section are a small quantity of Frasnian benthos in the upper part of bed C, including some solitary corals and small brachiopods, among which *Temnophyllum* and *Spinatrypa* have been identified (Hou et al., 1988)

### Sample preparations

Forty five samples were collected continuously from about 2 m above to 3.4 m below the F/F boundary for neutron activation analysis. Samples from bed E and adjacent parts of beds D and F are the most closely spaced, with no gaps between samples. Duplicate samples from beds D, E, and F were collected for sedimentologic and paleontologic determinations, and portions of these were measured for carbon and oxygen isotope ratios. Thin sections of these samples were made for sedimentary microfacies analysis and the cutoffs

were dissolved in a 10% acetic acid solution. The sieved residues of the different size fractions were carefully checked under a microscope for microspherules and shocked minerals, as well as for conodonts and other microfossils. Samples for O and C isotopic analyses were carefully selected by using thin sections. The excellent preservation of original fabrics, the relatively minor amount of recrystallization of calcite cements, and the absence of dolomitization suggest that the isotopic composition of the original sea-water is probably well represented.

### Geochemical results and discussion

Values of  $\delta^{13}\text{C}$  and  $\delta^{18}\text{O}$  expressed relative to Peedee belemnite for carbonates from the Xiangtian section are plotted in Figure 5.3. From the base upwards, values of  $\delta^{13}\text{C}$  are fairly uniform in beds D and F (average = +1‰) but decrease markedly to -2.49‰ in bed E before returning to the background values in bed F. The maximum shift of  $\delta^{13}\text{C}$  in bed E is about -3.5‰. Values of  $\delta^{18}\text{O}$  increase upward across the extinction interval in general, but decrease at the top of bed D and base of bed F.

A decrease in  $\delta^{13}\text{C}$  values in carbonate at the F/F boundary is similar to carbon isotopic patterns described for three other major time-boundaries: Cretaceous/Tertiary (K/T), Permian/Triassic, and Precambrian/Cambrian. The  $\delta^{13}\text{C}$  values characteristically decrease to minimum values at and immediately following the mass extinction, and then increase to more positive values with the recovery of biomass (Magaritz, 1989). The carbon isotopic shifts are considered to reflect changes in the near-surface-water reservoir, which is dominated by biomass carbon. A decrease in  $^{13}\text{C}$  in dissolved carbonate is best explained by a decrease in biomass of living organisms that preferentially fix  $^{12}\text{C}$  in the ocean (Hsü et al., 1985). This "Strangelove ocean" model of Hsü et al. (1985) is well represented by a strong negative  $\delta^{13}\text{C}$  anomaly of -3.5‰ shift in the Xiangtian section at the F/F extinction horizon, which provides further geochemical evidence for a major biotic crisis at the close of

the Frasnian Stage. The  $\delta^{18}\text{O}$  data might suggest a cooling trend at and across the extinction boundary.

Elemental abundances and ratios are plotted in Figure 5.4. Bed E is significantly enriched in Ir and other siderophile (Fe, Co, Cr) and chalcophile (As, Sb) elements. All samples from bed E have high Ir contents with a 0.23 parts per billion (ppb) maximum (0.35 ppb on a carbonate-free basis). The average Ir content is about 0.016 ppb in the overlying beds F and G, and about 0.044 ppb in the underlying bed D. Thus, the Ir content in the extinction horizon is about 14 times and 5 times, on a bulk-rock basis, more than that of the overlying and underlying strata, respectively. Bed E is also enriched in lithophile elements Al, U, Hf, Th, and V, but not in rare earth elements. Ni abundances in a few samples (not shown) follow the Co pattern and peak within bed E ( $\text{Ni/Co} = 1.3$ ).

The relatively abundant Al in bed E may suggest a high clay content. However, X-ray diffraction (XRD) shows no clay mineral peaks. Mass balance calculations based on XRD and chemical data indicate the presence of 4-8% mica and 6-8% K-feldspar in bed E, with much lower values above and below. These minerals are not likely to cause a considerable enrichment of the siderophiles and chalcophiles. Further examination of our data indicates that Ir, V, Cl, Co, As, and U show similar abundance patterns and Mn correlates with calcite (Ca) in general. We plotted Mn/Ca to look for deviations from the norm. The dip in this ratio and the peaks in V, Co, As, and U led us to consider that reducing conditions during deposition of bed E might have been responsible for the elemental enrichments. This hypothesis is supported by the fact that bed E is not enriched in the rare earths (e.g., La) or in alkali and alkaline earth elements (not shown). However, the black shales in bed D contain higher contents of organic C (3-7%), S, and pyrite, suggesting even more reducing conditions during deposition of bed D, which is not enriched in the elements.

The presence of anomalously high concentrations (over local background) of Ir may indicate it resulted from a bolide impact. The K/T boundary is a classic example where unusually high Ir values

have been observed around the globe (Alvarez et al., 1980). Physical evidence of impact in the form of shocked quartz grains and microspherules is also associated with the K/T boundary (Bohor et al., 1987).

At the F/F boundary in south China, Ir contents in bed E are above local backgrounds, but not nearly so much as in the K/T example. Therefore, we have examined Ir contents as ratios to several other elements to look for clues about its origin. No matter what combination we choose, Ir/Al, Ir/Sc, Ir/U, Ir/Th, or Ir/As, a small excess of Ir remains in bed E. Although there may indeed be a causal relationship of Ir enrichment and a reducing environment, high Ir values are consistently associated with extraterrestrial impacts.

Unlike the situation in the Canning basin, bed E in Xiangtian section was deposited at the time of a sterile "Strangelove ocean" and is devoid of any fossils. Therefore, the excess Ir in bed E is unlikely to have been concentrated by organisms. If we use 300 ka as the duration for the linguiformis zone (Sandberg et al., 1988), the 20-cm-thick bed E represents a maximum of 27 ka, and the calculated sedimentation rate is about 7.3 mm/ka, which is much faster than that calculated for the Canning basin (0.6 mm/ka; Playford et al., 1984). Thus, the excess Ir in bed E can not be attributed to a low sedimentation rate.

We have searched the residues and thin sections of all samples for microspherules and shocked minerals. No microspherules have been found from any samples. Some of the quartz grains we found from the boundary seem to show multiple sets of lamellae, but petrographic study indicates that they are not shock lamellae. However, an impact into an ocean floor with minor sediment cover would not generate shocked quartz grains.

Immediately below the F/F boundary, a sedimentary sequence (beds D and C), characterized by limestone breccias and debris in the lower part, and distributed laterally over several hundred kilometres, has been found in at least three sections (Xiangtian, Liuqing, Yangdi; Fig. 5.1) of basinal or slope facies in the Late Devonian South China Sea (Hou et al., 1988; Ji, 1988). This unit,

consisting of a fining-upward sequence which is similar to that of a tsunami deposit at the K/T boundary (Bourgeois et al., 1988), might have been formed during a strong storm or tsunami generated by some unusual event. Wave deposits at the F/F boundary were also described from Devil's Gates section in Nevada (Sandberg et al., 1988).

Previous studies of the F/F event in Australia, Europe, and North America found no evidence of an impact-related Ir anomaly, microspherules, or shocked mineral grains (Playford et al., 1984; McGhee et al., 1984, 1986; Goodfellow et al., 1989; Geldsetzer et al., 1987). Our study indicates that there is a strong shift to the lighter isotope of carbon and moderate enrichment of some chemical elements (including Ir) in the extinction interval. A widely distributed breccia unit of possible wave-deposit origin occurs just below the extinction boundary. These observations provide strong evidence that something unusual happened at the time of the F/F boundary. Some of us (K.W., B.D.E.C., H.H., and H.H.J.G.) believe that a terminal Frasnian oceanic impact(s) near south China could have provided the Ir, the biotic crisis, and the breccia and debris flows (from tsunami and/or earthquake), although the projectile(s) might have been much smaller than the K/T impactor(s). Two of us (C.J.O. and M.A.) suspect that the elemental anomalies might be associated with the reducing conditions in the boundary sediments but can not preclude an impact origin.

### Conclusions

A strong  $\delta^{13}\text{C}$  anomaly coincides with a weak Ir anomaly at the Frasnian-Famennian (F/F) boundary exposed at Xiangtian, Guangxi, south China. The maximum whole-rock Ir abundance is 0.23 ppb (0.35 ppb on a carbonate-free basis) compared with averages of 0.016 and 0.044 ppb above and below the boundary interval. The  $\delta^{13}\text{C}$  in carbonate abruptly shifts from a Late Frasnian level of about +1‰ to -2.49‰ in the boundary interval and then abruptly returns to pre-boundary levels, suggesting a temporary reduction of surface-water biomass. A widely distributed (at least



over several hundred kilometres) limestone breccia unit of possible wave-deposit origin occurs right below the boundary in south China. Enrichments of Al, V, Cr, As, and U, and a dip in the Mn abundance in the boundary interval indicate that reducing conditions might have been responsible for the elemental enrichment. However, an alternative hypothesis is that an oceanic impact(s) at the F/F boundary near south China provided the excess Ir, the biotic crisis, and the breccia deposits observed in the Late Devonian South China Sea.

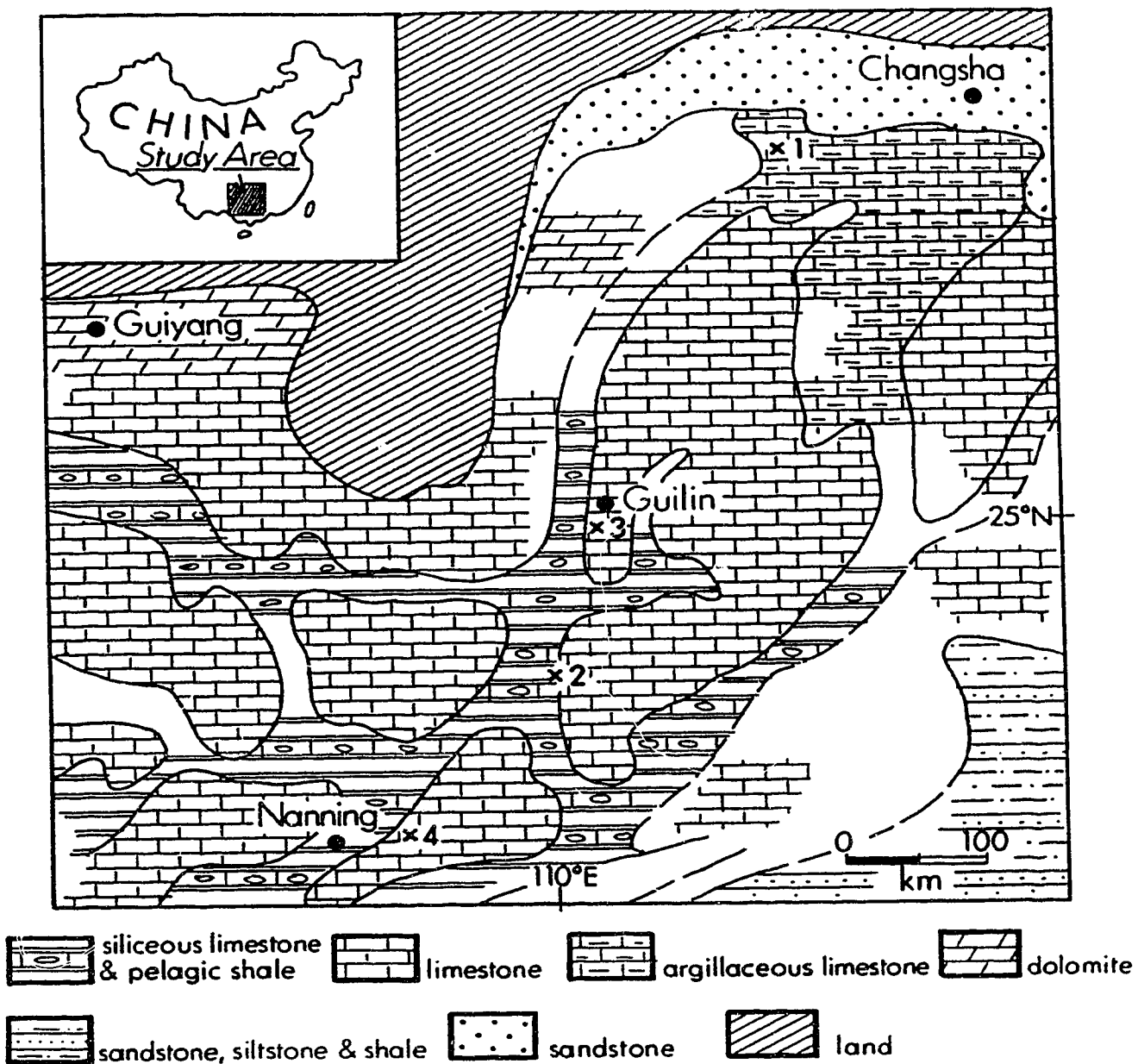


Fig. 5.1. Late Devonian paleogeography and facies distribution in south China. Section localities: 1, Xikuangshan; 2, Xiangtian; 3, Yangdi; 4, Liuqing.


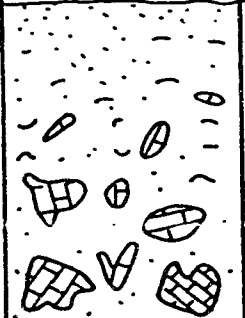
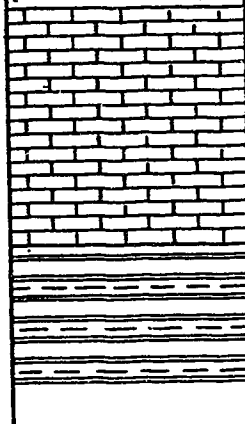
| STAGE          | CONODONT ZONE | LITHOLOGY                               | BED   | FM.  |                  |   |
|----------------|---------------|---|---|--|------------------|---|
| UPPER DEVONIAN | FAMENNIAN     | Middle <i>Palmatolepis triangularis</i> | G   | Wuzhishan Fm   |                  |   |
|                |               | Lower <i>Palmatolepis triangularis</i>  |   |  |                  |   |
|                | FRASNIAN      | <i>Palmatolepis linguiformis</i>        |   | E  | Xiangtian Member |   |
|                |               |   |   | D  |                  |   |
|                |               | <i>Palmatolepis gigas</i>               |  | C  |                  |   |
|                |               |   |   |  |                  | B |
|                |               |   |   |  |                  | A |
|                | 1 m           |   |   | Liujiang Formation   |                  |   |

Fig. 5.2. Geochemically studied section at Xiangtian, Guangxi, south China. Rock types: A, siliceous rocks and shale; B, limestone; C, limestone breccias and debris; D, black shaly mudstone with marl concretions (size = 10-15 X 25-60 cm); E, mudstone; F, limestone with nodules; G, nodular limestone.

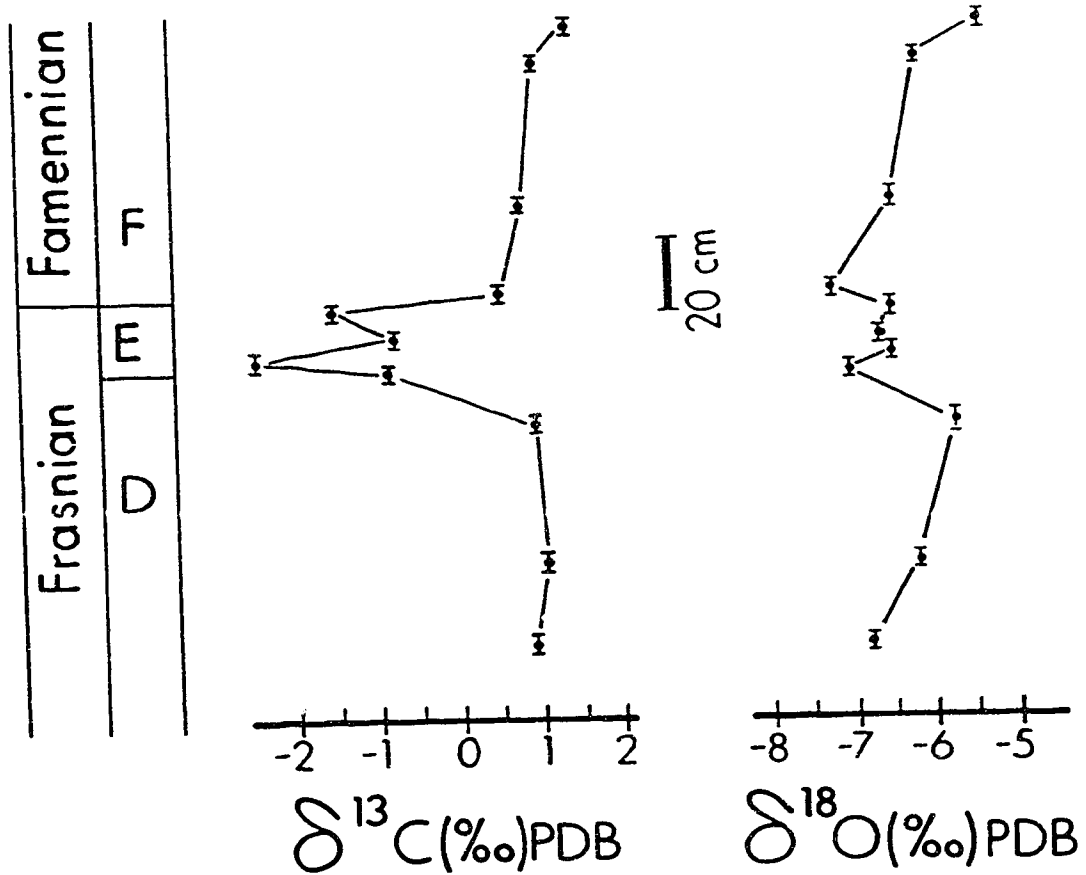
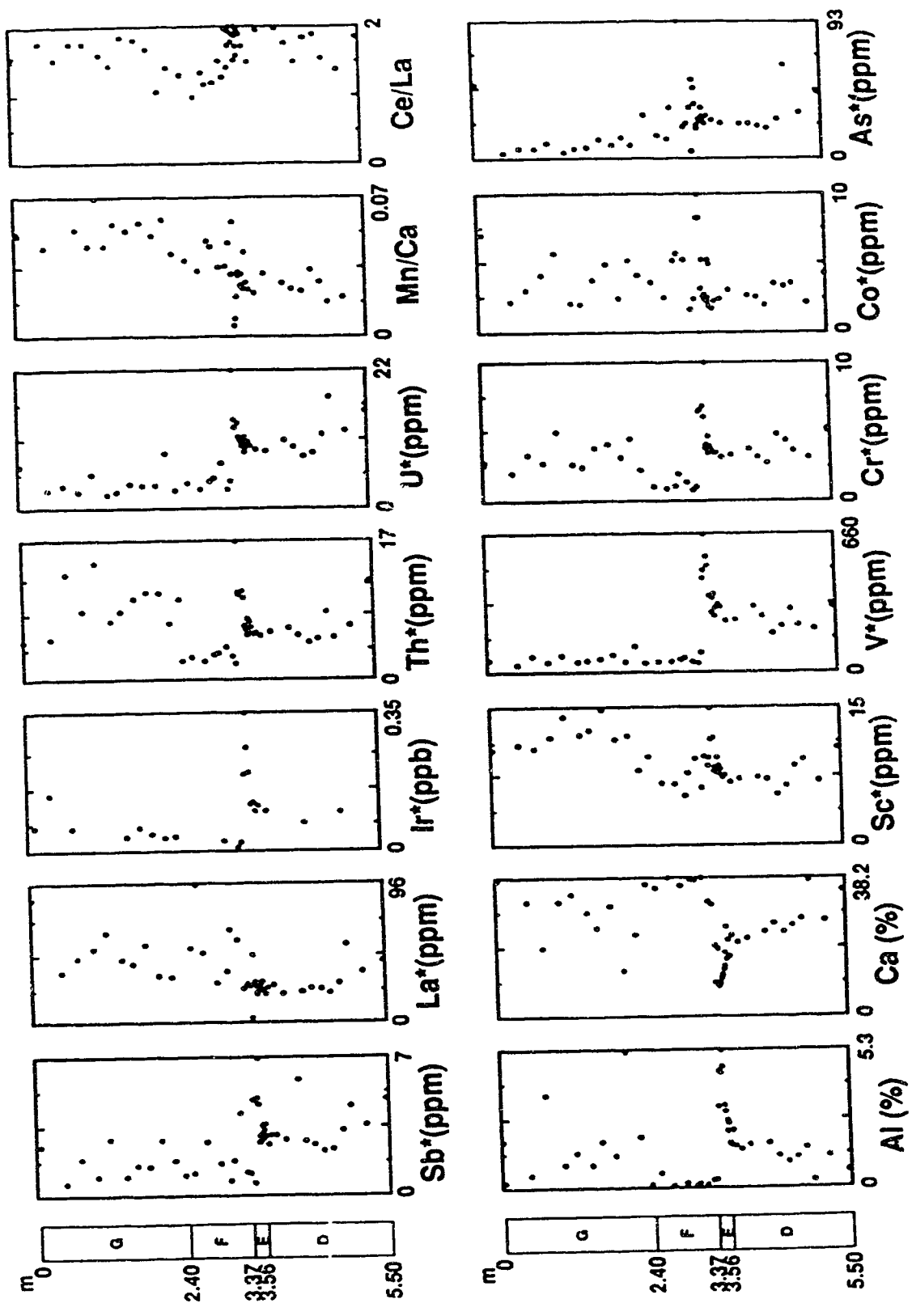


Fig. 5.3. Carbon and oxygen isotopic profile of Xiangtian section. See Figure 2 for rock types.

**Fig. 5.4.** Abundances and ratios of some significant elements. See Figure 2 for rock types. Stratigraphic dimensions given in metres. asterisk = abundances on carbonate-free basis.



## References

- Alvarez, L.W., Alvarez, W., Asaro, F., and Michel, H.V., 1980. Extraterrestrial cause for the Cretaceous-Tertiary extinction. *Science*, 208: 1095-1108.
- Bohor, B.F., Modreski, P.J., and Foord, E.E., 1987. Shocked quartz in the Cretaceous-Tertiary boundary clays: Evidence for a global distribution. *Science*, 236: 705-709.
- Bourgeois, J., Hansen, T.A., Wiberg, P.L., and Kauffman, E.G., 1988. A tsunami deposit at the Cretaceous-Tertiary boundary in Texas. *Science*, 241: 567-570.
- Geldsetzer, H.H.J., Goodfellow, W.D., McLaren, D.J., and Orchard, M.J., 1987. Sulfur-isotope anomaly associated with the Frasnian-Famennian extinction, Medicine Lake, Alberta, Canada. *Geology*, 15: 393-396.
- Goodfellow, W.D., Geldsetzer, H.H.J., McLaren, D.J., Orchard, M.J., and Klapper, G., 1989. Geochemical and isotopic anomalies associated with the Frasnian-Famennian extinction. *Historical Biology*, 2: 51-72.
- Hou, H., Ji, Q., and Wang, J., 1988. Preliminary report on Frasnian-Famennian events in South China. In: McMillan, N.J., Embry, A.F., and Glass, D.J. (Editors), *Devonian of the world, Volume III*. Canadian Society of Petroleum Geologists Memoir 14: 63-70.
- Hsu, K.J., Czerhansli, H., Gao, J.Y., Shu, S., Haihong, C., and Krahenbul, U., 1985. "Strangelove ocean" before the Cambrian explosion. *Nature*, 316: 809-811.
- Ji, Q., 1988. On the Frasnian-Famennian mass extinction event in South China [Ph.D. thesis]. Chinese Academy of Geological Sciences, Beijing, 140 pp.
- Magaritz, M., 1989.  $^{13}\text{C}$  minima follow extinction events: A clue to faunal radiation. *Geology*, 17: 337-340.
- McGhee, G.R., Jr., Gilmore, J.S., Orth, C.J., and Olsen, E., 1984. No geochemical evidence for an asteroidal impact at Late Devonian mass extinction horizon. *Nature*, 308: 629-631.
- McGhee, G.R., Jr., Orth, C.J., Quintana, L.R., Gilmore, J.S., and Olsen, E.J., 1986. Late Devonian "Kellwasser Event" mass-extinction horizon

- in Germany: No geochemical evidence for a large-body impact. *Geology*, 14: 776-779.
- McLaren, D.J., 1970. Presidential address: Time, life and boundaries. *Journal of Paleontology*, 48: 801-815.
- 1988. Detection and significance of mass killings. In: McMillan, N.J., Embry, A.F., and Glass, D.J. (Editors), *Devonian of the world, Volume III. Canadian Society of Petroleum Geologists Memoir 14*: 1-8.
- McLaren, D.J., and Goodfellow, W.D., 1990. Geological and biological consequences of giant impacts. *Annual Review of Earth and Planetary Sciences*, 18: 123-171.
- Orth, C.J., 1989. Geochemistry of the bio-event horizons. In : S.K. Donovan (Editor), *Mass extinctions: Processes and evidence. Columbia University Press, New York*, pp. 37-72.
- Playford, P.E., McLaren, D.J., Orth, C.J., Gilmore, J.S., and Goodfellow, W.D., 1984. Iridium anomaly in the Upper Devonian of the Canning Basin, Western Australia. *Science*, 226: 437-439.
- Sandberg, C.A., Ziegler, W., Dreesen, R., and Butler, J.L., 1988. Late Devonian mass extinction: Conodont event stratigraphy, global changes, and possible causes. *Courier Forschungsinstitut Senckenberg*, 102: 263-307.
- Tsien, H.H., Hou, H.F., Zhou, W.L., and Wu, Y., 1988. Devonian development and paleogeographic evolution in South China. In: McMillan, N.J., Embry, A.F., and Glass, D.J. (Editors), *Devonian of the world, Volume I. Canadian Society of Petroleum Geologists Memoir 14*: 619-633.
- Walliser, O.H., Groos-Uffenorde, H., Schindler, E., and Ziegler, W., 1989. On the Upper Kellwasser horizon (boundary Frasnian-Famennian): *Courier Forschungsinstitut Senckenberg*, v. 110, p. 247-256.
- Wang, K., and Bai, S., 1988. Faunal changes and events in the Upper Devonian of Hunnan, South China. In: McMillan, N.J., Embry, A.F., and Glass, D.J. (Editors), *Devonian of the world, Volume III. Canadian Society of Petroleum Geologists Memoir 14*: 71-78.



## Chapter 6

### **Glassy Microspherules (Microtektites) from an Upper Devonian Limestone**

(A version of this chapter has been published. K. Wang, 1992. *Science*, 256: 1547-1550.)

#### **Introduction**

Recognition of ancient bolide impacts and their influence on biota is important for understanding the evolution of Earth and its biosystem. Signatures of an impact in the pre-Cenozoic rock record are difficult to recognize because of their long history.

Microspherules were discovered in a marine limestone from the Late Devonian conodont lower *crepida* zone in South China (Wang, 1991). The conodont lower *crepida* zone has an age of about 365 million years, and each Late Devonian conodont zone represents a duration of less than 0.5 million years (Ziegler and Sandberg, 1990). Chemostratigraphic and paleontological studies indicate that a geochemical anomaly, a negative carbon isotope excursion, and a brachiopod faunal turnover are associated with the occurrence of the microspherules in South China (Figs. 6.1, 6.2) (Wang and Geldsetzer, 1992). An iridium anomaly (about 20 times the background values) and a negative carbon isotope excursion were originally reported in the conodont upper *triangularis* zone in the Canning Basin, Western Australia (Playford et al., 1984). An evaluation of the conodont fauna showed that the anomaly is actually in the subsequent lower *crepida* zone (Nicoll and Playford, 1988). Thus, the Australian geochemical anomalies (iridium and carbon isotope) were found in the same conodont zone as those in South China. Based on these results and the presence of a probable Late Devonian impact crater under Taihu Lake in South China (Fu et al., 1990; He et al., 1991), it is proposed that a bolide impact occurred about 365 million years ago on the South China Plate and probably caused a regional extinction in the southern hemisphere (eastern Gondwana) (Wang and Geldsetzer, 1992). In this paper, I

describe glassy microspherules from South China and provide evidence that they are of impact origin.

### Discovery of microtektites

Microspherules were recovered from a marine limestone that is immediately below a geochemical anomaly that occurs in a 3-cm-thick claystone between the Shetianqiao and Xikuangshan formations at Qidong, Hengyang, Hunan Province, South China (Figs. 6.1, 6.2). The Qidong Section is exposed in a quarry behind an elementary school about 1.5 km east of the center of the small town. The section was sampled when the quarry was being mined by local residents for paving stones. Samples from 25 stratigraphic horizons were collected over a 20-m span along a fresh exposure of the section. The samples were cleaned and then dissolved in 10% acetic acid. Conodonts and microspherules were picked from the 60 to 250  $\mu\text{m}$  size fraction of the sieved residues. Microspherules were only found in the residues from one horizon, which is immediately below the geochemical anomaly that was revealed later by neutron activation analysis (Fig. 6.2). All samples were processed in the same fashion at the same time in the same laboratory, but no microspherules were observed in the samples from the other 24 horizons. There are no signs of contamination of the samples both at the outcrop and in the laboratory. Conodonts from the section indicate that the microspherules occur in the lower *crepida* zone (Wang and Bai, 1988; Ji, 1988), which is three zones above (or about 1.5 million years after) the Frasnian-Famennian boundary extinction event in South China (Wang et al., 1991).

### Description

About 60 microspherules were picked and studied in detail. The microspherules range from 80 to 160  $\mu\text{m}$  in diameter; most are  $\sim 100$   $\mu\text{m}$  across. Although most of them are spherical, a few are in the form of a teardrop or a pear, with a protruding tail (Fig. 6.3). These so-called "splash form" shapes are the most common form in known microtektites (Glass, 1974). Some specimens have two or more spherules welded together by material that has a similar

chemical composition to the spherules and is probably derived from the same parental material (Fig. 6.3D). The microspherules vary in translucence and color. They are opaque black and white, translucent dark brown, or transparent yellowish brown, but a few are colorless and transparent. Surface textures vary from smooth with a glassy luster to pitted and corroded with a dull or frosted luster. Elevated small caps were also observed (Fig. 6.3B, D). Broken fragments of the microspherules showed a conchoidal fracture when two specimens were crushed. The appearance of the microspherules is similar to that of known microtektites (Glass, 1974).

Petrographically, the microspherules are isotropic, except for a few quartz inclusions present in some specimens. X-ray microdiffraction (XRMD) (Wicks and Zussman, 1975) performed on individual specimens confirmed that the microspherules are amorphous; the only mineral phase identified in the XRMD patterns was quartz (Fig. 6.4). Oil-immersion technique applied to four fragments from two microspherules gave refractive indices ranging between 1.544 and 1.548; this is consistent with tektite glass having about 61-65% SiO<sub>2</sub> (Izett, 1991; Glass, 1969). The refractive index of natural glasses varies inversely with SiO<sub>2</sub> content (Berry et al., 1983). A plot of refractive indices of tektites against SiO<sub>2</sub> showed that they define a curve that lies above the curve for igneous glasses (Izett, 1991; Glass, 1969). The refractive index of the Qidong microspherules plotted against the analyzed SiO<sub>2</sub> also lies above the curve for igneous glasses.

## Chemistry

Energy dispersive x-ray analysis was performed on all of the microspherules. All showed a silicate composition; Si, Al, Ca, Fe, K, Na, and Mg were the major elements. Seven randomly selected microspherules were analyzed with an electron microprobe, including both random point analyses and more detailed elemental mapping. The analysis revealed that the microspherules contain up to three phases: a matrix glass (SiO<sub>2</sub> ≈ 62%), a high-silica glass (SiO<sub>2</sub> ≈ 86%), and pure silica inclusions (SiO<sub>2</sub> > 99%) (Table 6.1). The matrix glass is dominant and makes up some microspherules entirely (Fig.

6.5A). The other two phases, when present, occur as isolated SiO<sub>2</sub>-rich areas in the matrix glass (Fig. 6.5B). These areas appeared darker than matrix glass under the microprobe. Petrographically, the pure silica inclusions are largely isotropic and partially crystalline. The isotropic pure silica inclusions have a lower refractive index than the surrounding glass; they are lechatelierite (SiO<sub>2</sub> glass). The crystalline silica inclusions are quartz. Silica inclusions were found in three of the seven microspherules analyzed. Some North American microtektites and Muong Nong-type tektites also contain inclusions of quartz and lechatelierite (Glass and Zwart, 1979; Glass, 1972). It is widely held that lechatelierite particles in tektites were formed by melting of quartz grains during an impact (Chao, 1963). The presence of both lechatelierite and quartz inclusions is probably a result of partial melting of quartz grains in the molten melt that had a temperature near the melting point of quartz. The presence of spherical vesicles in the microspherules implies their original molten state.

The chemical compositions of the microspherules are given in Table 6.1. A plot of SiO<sub>2</sub> versus other major oxides for the microspherules indicates that Al<sub>2</sub>O<sub>3</sub>, CaO (Fig. 6.6), MgO, TiO<sub>2</sub> and FeO all decrease with increasing SiO<sub>2</sub>. The microspherules show similar oxide variation trends to those in known microtektites (Fig. 6.6). North American microtektites plotted in Figure 6.6 appear to fill the gap between the matrix glass and the high-silica glass on the trends for the Qidong microspherules. FeO is the only oxide in the microspherules that falls off the variation trend of North American microtektites. This may reflect a slightly different, iron-poorer source material for the microspherules. The oxide variation patterns of the Qidong microspherules presented in Figure 6.6 are distinct from those documented for the Cynthia glasses that were believed to be flyash spherules (Byerly, et al., 1990).

## Discussion

Natural glasses are known to be thermodynamically unstable; with time and under a variety of conditions, they become crystalline. Water and temperature are important factors (Marshall,

1961). Although rare, there are reports of unaltered volcanic glasses of Precambrian (Palmer, et al., 1988), Carboniferous (Schmincke and Pritchard, 1981), Triassic (Brew and Muffler, 1966), and Jurassic (Shervais and Hanan, 1989) age.

Like known microtektites, the microspherules are volatile-poor as is evident from their high oxide totals. The microspherule glasses survived 365 million years undevitrified suggesting that they must have contained very little water. In contrast, volcanic glass shards found in marine sediments tend to be water-rich; volcanic glass shards may contain as much as 5% water (Izett, 1991). The microspherules contain lechatelierite, and, except for quartz, are devoid of microlites and other minute crystals commonly found in volcanic glasses. These observations essentially exclude the possibility that the microspherules are of volcanic origin.

Survival of the microspherules for 365 million years implies that there is an unusual preservation mechanism preventing devitrification of the glass. Preservation of the microspherules may have been aided by their inclusion in a diagenetic limestone, as petrographic examination of thin sections of the limestone indicates that it underwent several stages of diagenesis. Early diagenesis may have greatly reduced permeability of the limestone and thus shielded the microspherules from fluid interaction preventing devitrification. The Qidong Section may never have been deeply buried.

The microspherules closely resemble microtektites in many respects. I suggest that the Qidong microspherules are Late Devonian microtektites, on the basis of their physical and chemical characteristics, such as the splash form shapes, spherical inner vesicles, presence of lechatelierite, absence of primary crystallites (except for a few quartz inclusions in some specimens), and chemical compositions that have similar variations to those in microtektites.

The compositions of impact glasses may reflect those of target rocks. A target of a sedimentary rock assemblage of arkose, dolomite (high CaO and MgO/FeO ratios) and shale (high Al<sub>2</sub>O<sub>3</sub>) could account for the compositions of the microspherules. The observed silica

inclusions could be derived from the arkose as a result of partial melting of quartz grains in a molten melt after the impact. The high-silica glass could result from chemical reaction or incomplete mixing between the original impact-melt and included silica.

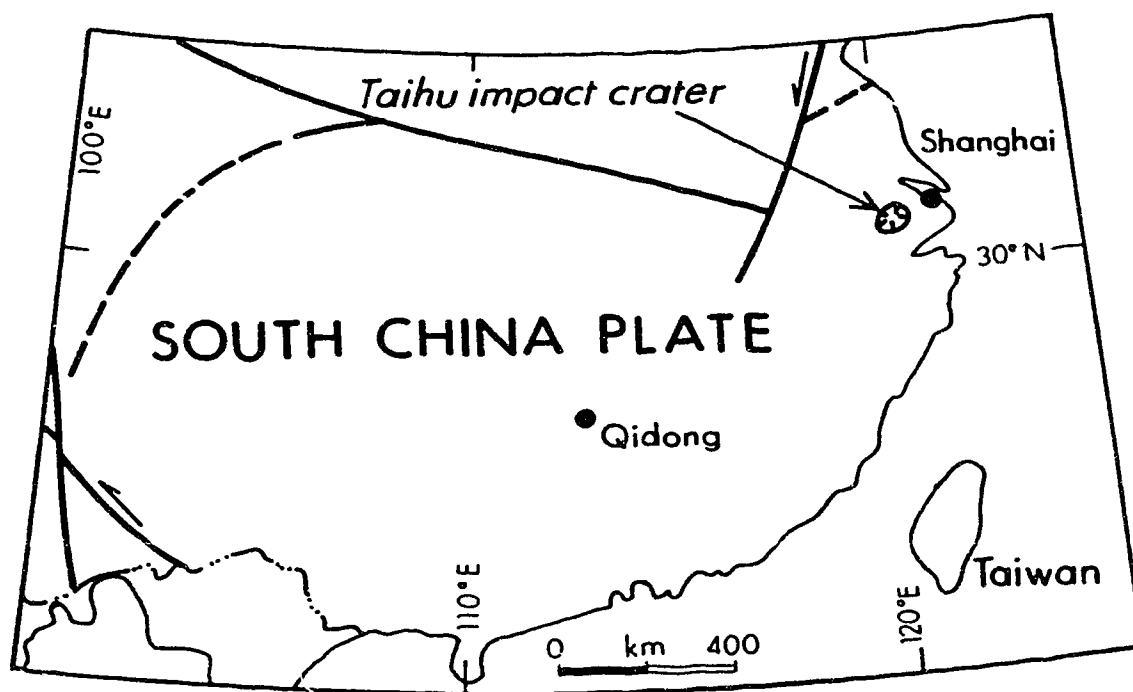
### **Conclusions**

Microspherules recovered from a Late Devonian marine limestone immediately overlain by a geochemical anomaly of siderophile and chalcophile elements have properties similar to those of impact-derived microtektites. They are glass, have splash-form shapes, contain spherical vesicles and lechatelierite inclusions, and show oxide compositional variations similar to those in known microtektites. These characteristics suggest that these Late Devonian microspherules are microtektites having an impact origin. A bolide impact may have occurred about 365 million years ago on the South China Plate and caused a faunal extinction on eastern Gondwana.

**Table 6.1.** Major oxide composition of Qidong microspherules with comparison to microtektites. Data in weight percent based on 80 microprobe analyses (50 on matrix glass, 10 on high-silica glass and 20 on silica inclusions) performed on seven randomly selected specimens. Data for microtektites (excluding bottle-green microtektites) are from Koeberl (1990) except the ranges for Australasian (Glass, 1972) and Ivory Coast (Glass and Zwart, 1979) microtektites.

|                                | Qidong Microspherules |             |                   |             |                    |             |              |          |                |          |              |          |
|--------------------------------|-----------------------|-------------|-------------------|-------------|--------------------|-------------|--------------|----------|----------------|----------|--------------|----------|
|                                | Matrix glass          |             | High-silica glass |             | Silica Inclusions* |             | Australasian |          | North American |          | Ivory Coast  |          |
|                                | Ave.                  | Range (%)   | Ave.              | Range (%)   | Ave.               | Range (%)   | Microtektite | Range(%) | Microtektite   | Range(%) | Microtektite | Range(%) |
| SiO <sub>2</sub>               | 61.77                 | 58.19-67.16 | 86.33             | 79.79-93.04 | 99.68              | 99.3-100.45 | 55.0-81.0    | 72.0     | 64.4-75.9      | 70.7     | 59.7-69.8    | 65.6     |
| Al <sub>2</sub> O <sub>3</sub> | 21.82                 | 20.58-24.01 | 7.38              | 3.53-9.96   | 0.19               | 0.00-0.39   | 7.4-23.4     | 13.6     | 13.1-17.5      | 15.4     | 14.1-18.4    | 15.6     |
| FeO**                          | 1.48                  | 0.46-2.80   | 0.56              | 0.33-1.15   | 0.02               | 0.00-0.04   | 2.78-9.68    | 4.9      | 2.73-6.79      | 5.00     | 5.81-8.26    | 6.9      |
| MgO                            | 2.91                  | 1.15-4.14   | 0.71              | 0.31-1.65   | 0.01               | 0.00-0.03   | 1.2-12.7     | 2.4      | 0.78-2.87      | 1.77     | 3.0-8.45     | 4.6      |
| CaO                            | 5.15                  | 3.37-6.83   | 1.45              | 0.56-3.54   | 0.02               | 0.00-0.04   | 0.5-6.18     | 3.6      | 0.92-2.49      | 1.61     | 0.3-2.31     | 1.4      |
| K <sub>2</sub> O               | 3.23                  | 2.66-4.45   | 1.97              | 1.29-2.71   | 0.05               | 0.00-0.11   | 0.19-3.7     | 1.9      | 2.16-3.96      | 3.02     | 0.94-2.4     | 1.8      |
| Na <sub>2</sub> O              | 2.48                  | 2.31-2.70   | 1.08              | 0.59-1.41   | 0.00               | 0.00-0.01   | 0.32-2.8     | 0.6      | 0.63-1.52      | 1.05     | 1.15-4.0     | 1.9      |
| TiO <sub>2</sub>               | 0.55                  | 0.20-0.70   | 0.24              | 0.14-0.55   | 0.07               | 0.00-0.33   | 0.3-2.09     | 0.8      | 0.52-0.99      | 0.80     | 0.44-0.85    | 0.7      |
| MnO                            | 0.04                  | 0.00-0.09   | 0.02              | 0.00-0.07   | 0.01               | 0.00-0.05   | 0.03-0.15    | 0.1      | 0.03-0.09      | 0.07     | 0.05-0.13    | 0.1      |
| Cr <sub>2</sub> O <sub>3</sub> | 0.05                  | 0.00-0.14   | 0.05              | 0.00-0.15   | 0.00               | 0.00-0.00   |              |          |                |          |              |          |
| Total                          | 99.48                 |             | 99.79             |             | 100.05             |             |              |          |                |          |              |          |

\* Silica inclusions are largely glassy (lechatelierite) and partially crystalline (quartz). \*\*All Fe expressed as FeO.



**Fig. 6.1.** Tectonic map of the South China Plate with locations of the Qidong microspherules and Taihu Lake impact crater. Two localities are about 900 km apart.



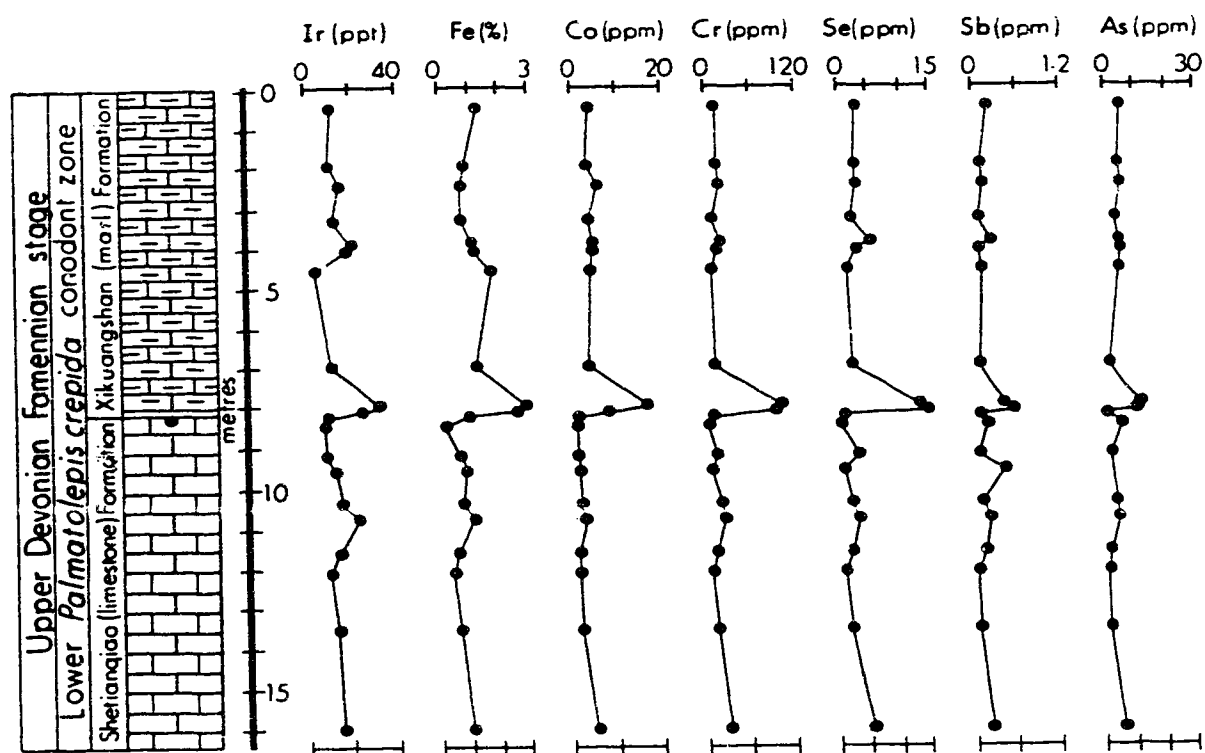
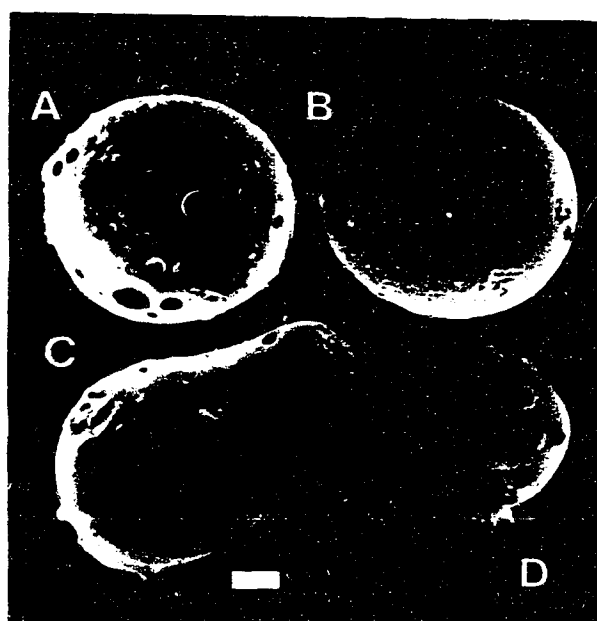
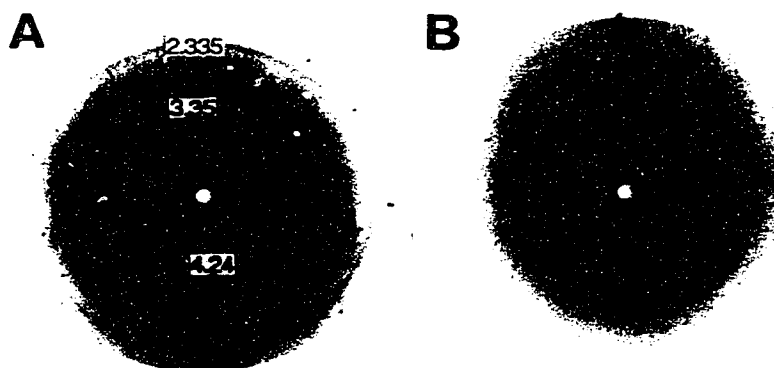


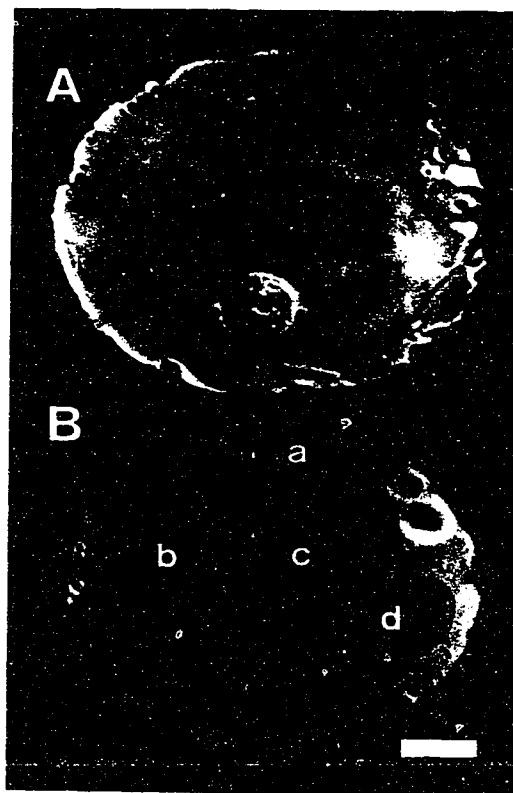
Fig. 6.2. Chemostratigraphy of the Qidong Section showing a geochemical anomaly of siderophile and chalcophile elements in a 3-cm-thick claystone (50% illite, 25% calcite, 25% quartz) between the two formations. The claystone is immediately above the limestone containing the microspherules (indicated by a solid circle in the stratigraphic column).



**Fig. 6.3.** Scanning electron micrographs of surfaces of the Qidong microspherules. (A) Surface with "crater-like" big shallow pits and caps. (B) Finely pitted surface with two caps on top. (C) Pear-shaped spherule with a few small pits. (D) Welded spherules with caps on the surface that is slightly pitted (welding material = impact melt?). Caps are composed of silica as revealed by energy dispersive x-ray analysis. Scale bar = 20  $\mu\text{m}$  .



**Fig. 6.4.** X-ray microdiffraction patterns of the Qidong microspherules. (A) Pattern showing that the only crystalline phase in this microspherule is quartz (3.35 Å, 4.24 Å); sample to film distance corrected with the  $d_{111}$  (2.355 Å) of gold used as the internal standard. (B) Amorphous pattern of a purely glassy microspherule. For comparison, an Australasian tektite was also analyzed which showed the same amorphous pattern as in B. Film exposure times for these analyses were between 24 and 48 hours.



**Fig. 6.5.** Scanning electron micrographs in backscattered mode of polished sections of the Qidong microspherule. (A) Rather homogeneous glassy spherule with a vesicle. (B) Inhomogeneous spherule showing vesicles (black holes) and silica-rich areas (a, b, c, d) within a glass matrix. a, high-silica glass (see Table 1); b, high-silica glass (25%) + silica glass (50%) + quartz (25%); c, quartz; d, silica glass (80%) + quartz (20%) (modal estimates). Small bright spots are burns caused by electron beam during microprobe mapping. Scale bar = 20  $\mu\text{m}$ .

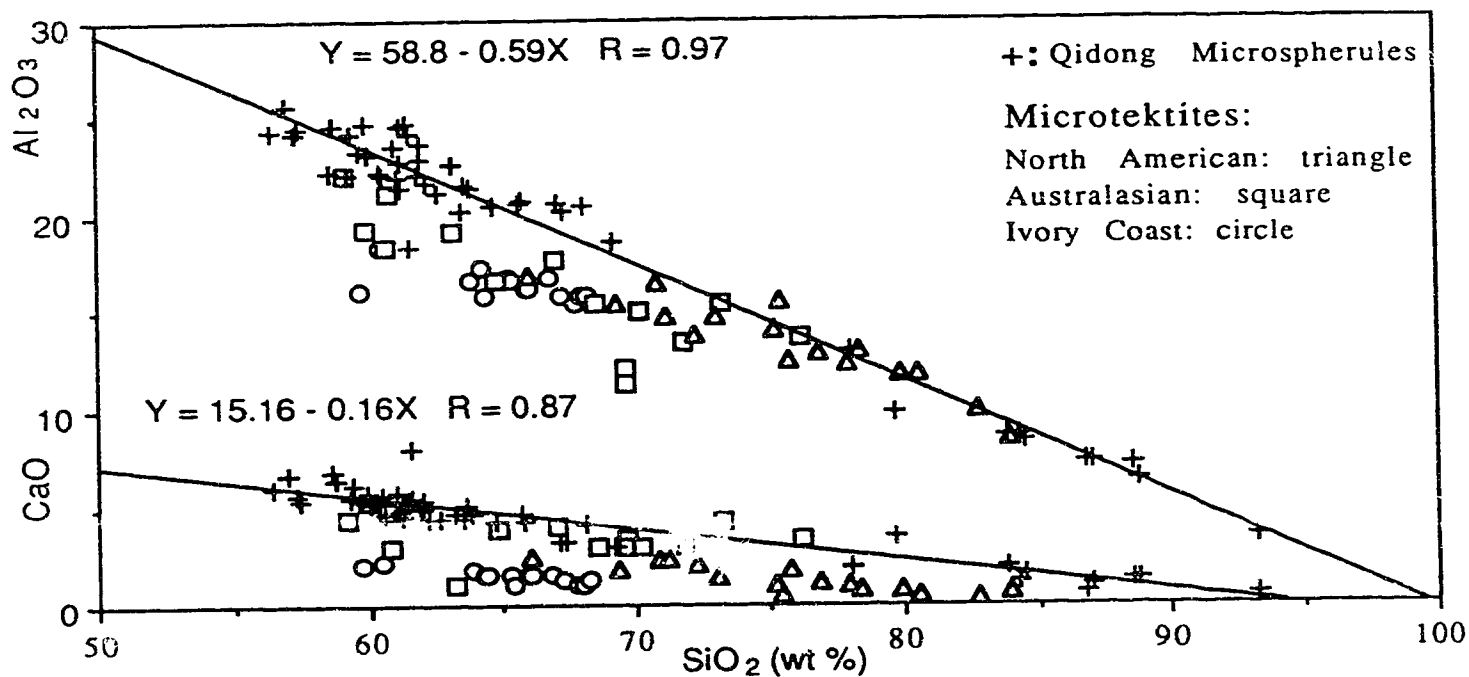


Fig. 6.6. Oxide compositional variation diagram comparing the Qidong microspherules (cross) to microtektites from three known strewn fields. Data for microtektites: North American (triangle) (20), Australasian (square) (21), and Ivory Coast (circle) (22). Note the excellent correlations between SiO<sub>2</sub> and Al<sub>2</sub>O<sub>3</sub> ( $R=0.97$ ), and SiO<sub>2</sub> and CaO ( $R=0.87$ ) for the microspherules.

## References

- Berry, L. G., Mason, B. and Dietrich, R. V., 1983. *Mineralogy*. W. H. Freeman and Company, New York, 542 pp.
- Brew, D.A. and Muffler, L.J.P, 1966. Upper Triassic undevitrified volcanic glass from Howard Island, Keku Strait, southeastern Alaska. *U.S. Geol. Surv. Prof. Paper 525C*: 38-43.
- Byerly, G.R., Hazel, J.E. and McCabe, C., 1990. Discrediting the late Eocene microspherule layer at Cynthia, Mississippi. *Meteoritics*, 25: 89-92.
- Cassidy, W. A., Glass, B.P. and Heezen, B.C., 1969. Physical and chemical properties of Australasian microtektites. *Journal of Geophysical Research*, 74: 1009-1025.
- Chao, E.C.T., 1963. The petrographic and chemical characteristics of tektites. In: J.A. O'Keefe (Editor), *Tektites*. Univ. of Chicago Press, Chicago, pp.51-94.
- Fu, C., Yu, J., Wang, C., Yen, Z., Yin, L., Hu, Z., Li, X., and Fu, G., 1990. The discovery of shock metamorphic rocks at Sanshan Island of Taihu Lake and its significance. *Acta Geographica Sinica*, 45: 253-258.
- Glass, B. P., 1969. Chemical composition of Ivory Coast microtektites. *Geochim. Cosmochim. Acta*, 33: 1135-1147.
- 1972. Crystalline inclusions in a Muong Nong-type tektite. *Ear. Planet. Sci. Lett.*, 16: 23-26.
- 1974. Microtektites surface sculpturing. *Geol. Soc. Am. Bull.*, 85: 1305-1314.
- Glass, B.P., Burns, C.A., Crosbie, J.R. and DuBois, D.L., 1985. Late Eocene North American microtektites and clinopyroxene-bearing spherules. *J. Geophys. Res.*, 90: D175-D196.
- Glass, B. P., and Zwart, M. J., 1979. North American microtektites in DSDP cores from the Caribbean Sea and Gulf of Mexico. *Geol. Soc. Am. Bull.*, 90: 595-602.
- Glass, B. P., and Zwart, P. A., 1979. The Ivory Coast microtektites strewnfield: New data. *Ear. Planet. Sci. Lett.*, 43: 336-342.
- He, Y., Xu, D., Lu, D., Shen, Z., Lin, C., and Shi, L., 1991. Preliminary study on the origin of Taihu Lake: Inference from shock

- deformation features in Quartz. Chinese Science Bulletin, 36: 847-851.
- Izett, G.A., 1991. Tektites in Cretaceous/Tertiary boundary rocks on Haiti and their bearing on the Alvarez impact extinction hypothesis. *J. Geophys. Res.*, 96: 20879-20905.
- Ji, Q., 1988. On the Frasnian-Famennian mass extinction event in South China [Ph.D. thesis]. Chinese Academy of Geological Sciences, Beijing, 140 pp.
- Koeberl, C., 1990. The geochemistry of tektites: an overview. *Tectonophysics*, 171: 405-422.
- Marshall, R.R., 1961. Devitrification of natural glass. *Geol. Soc. Am. Bull.*, 72: 1493-1520.
- Nicoll, R. S., and Playford, P. E., 1988. Upper Devonian iridium anomalies, conodont zonation and the Frasnian-Famennian boundary in the Canning Basin, Western Australia. *Geol. Soc. Austral. Abstr.* 21: 296.
- Palmer, H.C., Tazaki, K., Fyfe, W.S. and Zhou, Z., 1988. Precambrian glass. *Geology*, 16: 221-224.
- Playford, P.E., McLaren, D.J., Orth, C.J., Gilmore, J.S., and Goodfellow, W.D., 1984. Iridium anomaly in the Upper Devonian of the Canning Basin, Western Australia. *Science*, 226: 437-439.
- Schmincke, H.U. and Pritchard, G., 1981. Carboniferous volcanic glass from submarine hyaloclastite, Lahn-Dill area, Germany. *Naturwissenschaften*, 68: 615-616.
- Shervais, J.W. and Hanan, B.B., 1989. Jurassic volcanic glass from the Stonyford volcanic complex, Franciscan assemblage, northern California Coast Ranges. *Geology*, 17: 510-514.
- Wang, K., 1991. Glassy silicate microspherules from an Upper Devonian sediment: Microtektites? *Geol. Soc. Am. Abstr. Progr.*, 23: A227.
- Wang, K., and Bai, S., 1988. Faunal changes and events in the Upper Devonian of Hunnan, South China. In: McMillan, N.J., Embry, A.F., and Glass, D.J. (Editors), *Devonian of the world, Volume III*. Canadian Society of Petroleum Geologists Memoir 14: 71-78.
- Wang, K., and Geldsetzer, H.H.J., 1992. A Late Devonian impact event and its association with a possible extinction event on eastern

- Gondwana. Lunar and Planetary Institute Contribution, 790: 77-78.
- Wang, K., Orth, C.J., Attrep, M., Chatterton, B.D.E., Hou, H., and Geldsetzer, H. H.J., 1991. Geochemical evidence for a catastrophic biotic event at the Frasnian/Famennian boundary in south China. *Geology*, 19: 776-779.
- Wicks, F. J., and Zussman, J., 1975. Microbeam X-ray diffraction patterns of the serpentine minerals. *Can. Mineral.* 13: 244-258.
- Ziegler, W., and Sandberg, C. A., 1990. The Late Devonian Standard conodont zonation. *Courier Forschungsinstitut Senckenberg*, 121: 7-115.



## Chapter 7

### **A Late Devonian impact event with a probable extinction event on eastern Gondwana**

(A version of this chapter has been published. Wang, K., and Bai, S., 1989. *CSPG Memoir*, 14(3): 71-79)

#### **Introduction**

Astronomical estimation has shown, in agreement with the cratering record on Earth and Moon, that impact of large Earth-crossing bodies, such as the one documented at the Cretaceous/Tertiary (K/T) boundary (Alvarez et al., 1980), occur once about every 40 Ma (Wetherill and Shoemaker, 1982). Over one hundred terrestrial hypervelocity impact structures are currently known on land (Grieve, 1982). Many more of these structures are yet to be found on the sea floors, and many have almost certainly disappeared as a result of oceanic plate subduction. It is clear that extraterrestrial bodies bombarded Earth many times during geologic time.

After the proposal of the impact hypothesis at the K/T boundary (Alvarez et al., 1980), scientists have shown great interest in documenting relationships between impacts and extinctions in geologic time (Donovan, 1989). During the last decade, a number of bio-event horizons and stratigraphic boundaries have been scrutinized by paleontologists and geochemists for evidence of impacts (Orth, 1989). So far, several other impact events have been fairly well documented in the sedimentary record, including impacts in the late Pliocene (Kyte et al., 1988; Margolis et al., 1991a), late Eocene (Ganapathy, 1982; Alvarez et al., 1982; Keller et al., 1987), late Precambrian (Gostin et al., 1989), and possibly at the F/F (Wang et al., 1991) and Cenomanian/Turonian (Orth et al., 1988) boundaries. Some of these impacts were associated with major extinction events and some were not.

Evidence from sedimentary rocks suggesting an impact includes wide distribution of Ir anomalies (Alvarez et al., 1980),

shocked minerals (Bohor et al., 1987), tektites and microtektites (Glass, 1990), impact ejecta deposits and craters (Hildebrand et al., 1991), and other shock-metamorphic features. However, an impact is not always associated with a detectable Ir anomaly, because a highly differentiated meteorite or a cometary impact could have left no significant Ir anomalies in sediments. Also, the thin fallout layers from an impact could be very sensitive to erosion and mixing processes, especially in older horizons. On the other hand, it appears that some terrestrial processes can also produce small Ir anomalies in sedimentary rocks. Of all the documented ancient impact events, the K/T impact is a typical example; just about all the evidence suggesting an impact has been found (Alvarez et al., 1980; Bohor et al., 1987; Margolis et al., 1991b; Hildebrand et al., 1991).

The Late Devonian Epoch appears to have been a very dynamic time interval, characterized by a high rate of biological evolution. Rapid diversification, faunal turnovers, and extinctions have been known throughout the late Devonian (Walliser, 1984); and these have offered the best time resolution in the Paleozoic. Thirty two Upper Devonian conodont zones have been identified over a time span of 15 Ma (Ziegler and Sandberg, 1990), giving a biostratigraphic time resolution better than 0.5 Ma on average. The most prominent biotic events in the late Devonian are the mass extinctions at the end of the Frasnian (F/F extinction) and of the Famennian (Devonian/Carboniferous extinction) (McLaren and Goodfellow, 1990; Sandberg et al., 1988), although a series of smaller-scale events are also known in the late Devonian (Walliser, 1984).

In the southern hemisphere, geochemical anomalies (including Ir) were previously reported in the lower Famennian in the Canning basin of western Australia (Playford et al., 1984) and in Hunan, south China (Wang and Bai, 1989); and at the F/F boundary in Guangxi, south China (Wang et al., 1991). Subsequent interpretations of the Famennian geochemical anomalies were that the Canning basin Ir anomaly was a result of biological concentration and unrelated to bolide impact (Orth, 1989; Wallace et al., 1991), and the Hunan geochemical anomaly was a local phenomenon (Hou et al.,

1988). Our recent work indicates that a reevaluation is necessary. This paper presents evidence for a lower Famennian impact event, about 1.5 Ma after the F/F extinction, affecting south China and western Australian of eastern Gondwana. We also posit an association between this impact and a possible extinction in eastern Gondwana.

### **Paleo-reconstruction**

It has been recognized that China consisted of three major Paleozoic continents (Scotese and McKerrow, 1990): north China (Sino-Korea), south China and Tarim (Fig. 7.1). The biogeographic affinities with eastern Gondwana suggest that south China was located very close to Australia during most of the Paleozoic. The latest world paleo-map for the late Devonian (Famennian) positioned south China very close to and facing western Australia (Scotese and McKerrow, 1990).

The studied stratigraphic section is located at Qidong, Hunan, south China, and the newly confirmed late Devonian impact crater is at Taihu Lake, 100 km west of Shanghai (Fig. 7.1). These two localities are some 900 km apart.

### **The Qidong Section**

According to a late Devonian paleogeographic reconstruction of south China (Tsien et al., 1988), the Qidong section was deposited in an outer-shelf setting, between a shallow-water clastic facies to the north and a deep-water siliceous carbonate facies to the south. This paleogeographic location has provided an excellent yield of both benthic (brachiopods) and pelagic (conodonts) faunas for this study. These two fossil groups are important to examine faunal changes and to establish biostratigraphic constraints, respectively.

A 20-m-thick carbonate section, containing the top part of the Shetianqiao Formation (limestone) and the basal Xikuangshan Formation (marl), was measured and sampled for this study (Fig. 7.2). Brachiopods and conodonts were studied, elemental abundances were determined, C and O stable isotopic ratios were measured, and microfacies thin-sections were made on all samples

collected across the Shetianqiao/Xikuangshan boundary, which is marked by a 3-cm-thick clay bed.

### BIOSTRATIGRAPHY

Fairly abundant conodonts were recovered in this section. A typical early Famennian conodont fauna was found, which includes species of *Palmatolepis quadrantinodosalobata*, *Polygnathus nodocostatus*, *Icriodus iowaensis*, *Icriodus cornutus*, *Icriodus alternatus*, and *Pelekysgnathus inclinatus* (Wang and Bai, 1988). Ji (1989) resampled this section interval for conodonts and found *Palmatolepis minuta minuta*, *Palmatolepis quadrantinodosalobata*, *Palmatolepis crepida*, *Icriodus iowaensis*, *Icriodus alternatus helmsi* and *Icriodus alternatus alternatus*. *Palmatolepis crepida* is the zonal species of the Lower *crepida* zone in the standard late Devonian conodont zonation, and *Palmatolepis quadrantinodosalobata* and *Pelekysgnathus inclinatus* are characteristic elements of that zone (Ziegler and Sandberg, 1990). All other species are important elements in the Lower *crepida* zone. There is no doubt that this section interval at Qidong is in the Lower *crepida* zone, which is three zones above (or 1.5 Ma after) the F/F boundary.

Two distinct brachiopod faunas were recognized in this section. *Yunnanellina hanburyi*, *Dmitria hunanensis*, *Athyris gurdoni transversalis*, *Tenticospirifer kwangsiensis*, *Productellana linglingensis*, and *Productella* sp. were recovered in the Shetianqiao Formation, and *Yunnanella synplicata*, *Yunnanellina hanburyi*, *Tenticospirifer mesosulcata*, and *Athyris hunanensis* were found in the Xikuangshan Formation (Wang and Bai, 1988). These two brachiopod faunas may belong to the long-recognized Famennian *Yunnanellina* and *Yunnanella* faunas of Tien (1938). They were established from a detailed study of the brachiopods found in a more clastic facies in central Hunan, about 200 km north of Qidong. Tien (1938) also established these two faunas as two adjacent zones of his brachiopod zonation for the late Devonian of south China.

Paleontological data show that the boundary (clay bed) between the Shetianqiao and Xikuangshan Formations separates two different brachiopod faunas, and therefore coincides with a

brachiopod faunal changeover. This brachiopod faunal turnover occurred in the Lower *crepida* conodont zone.

### MICROTEKTITES

Abundant microspherules were discovered in the 60-250  $\mu\text{m}$  fraction of the acetic-acid-treated residues of a carbonate sample, which is immediately below and in direct contact with the boundary clay above, when the Qidong samples were searched and hand-picked for conodonts under a binocular microscope. No microspherules were found in any other samples. More than 60 spherules were picked out and studied individually using combined light microscopic, SEM, X-ray energy dispersive, and microprobe analytical methods. This work has shown that these microspherules are microtektites with an impact origin (Wang, 1991).

The microspherules range from 80 to 160  $\mu\text{m}$  in diameter, most being around 100  $\mu\text{m}$ . Most of them are spherical in shape, but several are in the form of a teardrop or a pear, with a protruding tail (Fig. 7.3). These shapes are called "splash form" in tektites and are the most common form in known microtektites (Glass, 1990). A few specimens (Fig. 7.3, F) have two or more spherules cemented together by material, which has a similar chemical composition to the spherules. The microspherules vary in translucence and colour, including opaque black and white, translucent dark brown, transparent yellowish brown, and a few colourless, transparent ones. Their surface appearances and textures vary from perfectly smooth with a glassy lustre to pitted and corroded with a dull or frosted lustre. Elevated small caps were also observed on some (Fig. 7.3, B, C). The overall appearance of these microspherules is quite similar to that of known microtektites (Glass, 1974).

Semi-quantitative X-ray energy dispersive analysis was performed on all microspherules when they were photographed under the SEM. All showed a silicate compositional pattern, with Si, Al, Ca, Fe, K and Mg comprising the major elements. Seven randomly selected microspherules were then mounted in epoxy and thin-sectioned for microprobe analysis to quantitatively obtain their chemical composition. Detailed elemental mapping has revealed that

the microspherules consist of three chemical phases: a silicate matrix, an intermediate silicate, and silica inclusions ( $\text{SiO}_2 > 99\%$ ). They were marked out individually under the microprobe and then studied with a petrographic microscope.

Petrographic studies indicate that, like microtektites, the microspherules are glassy (totally isotropic), except for some crystalline spots on the silica inclusions. It is interesting to find that part of the silica inclusions is glass, and part is crystalline silica, assumed to be quartz or one of its polymorphs. Thus, like the North American microtektites (Glass and Zwart, 1979), the microspherules contain inclusions of both silica glass (lechatelierite) and "quartz". Except for the "quartz", the microspherules appear to be free of crystalline inclusions. The presence of lechatelierite and absence of primary crystallites are the main characteristics of tektites. It has been suggested that the lechatelierite particles in tektites were formed by melting of quartz grains during an impact, and that the tektites containing lechatelierite particles must have been melted at above  $1710^\circ\text{C}$  (Chao, 1963).

Table 7.1 gives the chemical composition of the microspherules. It is quite different from the compositions of various volcanic glasses (provided by B. P. Glass). Besides, volcanic glasses do not contain lechatelierite inclusions (Chao, 1963). Thus, the non-volcanic composition and the silica-rich glass inclusions are suggestive of an impact origin, and indicate that the microspherules are microtektites.

To approximate a source rock for the microtektites, the CIPW norm was calculated on the matrix glass (quartz, 18.75; orthoclase, 19.09; albite, 20.99; anorthite, 25.55; corundum, 4.88; hypersthene, 9.13; ilmenite, 1.04). The presence of normative corundum, the high CaO content and the high MgO/FeO ratio indicate a sedimentary target is most probable. A rock assemblage of arkose, dolomite, and shale could account for the composition of the matrix glass. The observed quartz crystals could be derived from the arkose, and the silica glass would result from partial melting of the quartz in a molten melt after the impact. The intermediate glass is interpreted as representing chemical reaction between the original impact-

generated melt and included quartz; it is a mixture of the silicate matrix glass and the silica glass inclusions.

### GEOCHEMICAL ANOMALIES

25 samples from the Qidong section were analyzed for about 40 major, minor and trace elements by both instrumental and radiochemical neutron activation analyses at the Los Alamos National Laboratory, New Mexico. C and O isotopic ratios in whole-rock were determined in all samples and in 17 additional carbonate samples at the Institute of Geology, Beijing.

As shown in figure 7.2, siderophile (Ir, Fe, Co, Cr) and chalcophile (Se, Sb, As) elements are apparently enriched in the boundary clay by factors of one to several orders of magnitude over their background values. In addition, U, Th, W, V, Ta, Cs, Ru, Rb, Sc, K, Al, and Na (not shown) are also enriched in the clay, but Ca, Ba, and Mn (not shown) are depleted in it. Near the base of the section, there seems to be another elemental enrichment level. However, except for Ir and Sb, the enrichment is not as prominent for most elements.

The enrichment of siderophiles in normal sediments may indicate excess influxes of extraterrestrial material, such as an impact (Alvarez et al., 1980). However, the geochemical anomalies here alone do not tell us anything about an impact, because the peak Ir (0.038 ppb) is so low that it falls well within the terrestrial range of Ir for normal sediments. The high Al and low Ca abundances suggest that the Ir peak in the clay might be due to a higher percentage of clay in the rock. The high chalcophile abundances and a dip in Mn indicate that the boundary clay was deposited in a reducing environment, which might be the consequence of a mass mortality, presumably associated with the brachiopod faunal turnover at this locality.

The  $\delta^{13}\text{C}$  maintains constantly positive values in the Shetianqiao Formation, but shifts suddenly to a minimum of -1.97‰ in the boundary clay and above. Negative  $\delta^{13}\text{C}$  excursions ("strangelove ocean" excursions) in carbonate have been consistently reported to be associated with a biomass destruction at several mass

extinction boundaries: K/T (Zachos et al., 1989), Permian/Triassic (Holser et al., 1989), F/F (Wang et al., 1991), and Precambrian/Cambrian (Hsü et al., 1985). The  $\delta^{13}\text{C}$  excursion of 2.7‰ at the boundary in the Qidong section is consistent with the paleontological data suggesting that an extinction might have terminated the *Yunnanellina* fauna which in turn gave rise to the *Yunnanella* fauna. Although the carbonate rocks we analyzed were altered in some degree by diagenesis (as seen in the thin sections), we believe that the trend of the carbon isotopic change is still preserved. This has been shown in a recent study (Sass et al., 1991) that carbon isotopic curves derived for whole-rock and diagenetic calcite samples mimic that for unaltered skeletal samples. The carbon isotope data in the Qidong section provides the further geochemical evidence for a possible extinction between the two brachiopod faunas. Oxygen isotope values are too sensitive to diagenesis to be conclusive.

### Taihu impact crater

The Taihu Lake, a 70-km-diameter circular structure, has long been speculated to be a probable impact crater. Its northern side is in the Wuxi City, about 100 km west of Shanghai. Recent work, on the basis of shock metamorphism found in the target rocks, has confirmed that it is an impact crater (Sharpton, personal communication, 1991). The target rocks are sedimentary with a late Devonian age, which confirms our estimation about the nature of the source rocks for the microtektites. The location, type of target rocks, and age of the Taihu crater all qualify its being the crater of this late Devonian impact event.

### Geochemical anomalies in Western Australia

A strong iridium anomaly was initially reported in the Famennian Upper *triangularis* conodont zone in the Canning basin, western Australia (Playford et al., 1984). Recent work on conodont dating of this anomalous bed proved that the Ir anomaly is actually in the Lower *crepida* zone, on the basis of occurrence of *Palmatolepis crepida* in the bed (Nicoll and Playford, 1988). This is the same level



as the Qidong microtektite and geochemical anomaly horizon, in terms of the best biostratigraphic time-resolution at the moment.

Because this Ir anomaly is associated with a *Frutexites* stromatolite, the subsequent interpretation was that the Ir was concentrated biologically by cyanobacteria (Orth, 1989, Wallace et al., 1991). We appreciate this scenario but further propose that there must have been abundant Ir available in the environment for the biological concentration to take place. The most apparent source for the Ir is an impact(s) near the region, such as the impact in south China. The presence of *Frutexites* stromatolites is probably the reason why there is a stronger Ir anomaly in the Canning basin than that in the Qidong section, where no stromatolites are found.

A negative  $\delta^{13}\text{C}$  excursion of about 1.5‰ is coincident with the Ir anomaly in the Canning basin, and has been suggested to indicate a decrease in biomass (Playford et al., 1984). The carbon isotopic excursions, which occur at the same stratigraphic level, in both south China and western Australia can not be explained as being coincidental. The  $\delta^{13}\text{C}$  excursions and the brachiopod faunal turnover in south China indicate that there might have been an at least regional-scaled (possibly global) extinction at the time of the geochemical anomalies and the microtektites in the Lower *crepida* zone.

### Discussion and interpretations

Microtektites, elemental geochemical anomalies (including a small Ir), and a  $\delta^{13}\text{C}$  excursion are found in the Lower *crepida* zone (365 Ma) in south China, and a strong Ir anomaly and a  $\delta^{13}\text{C}$  excursion are present at the same horizon in western Australia. The microtektites are unequivocal evidence of an impact, which may be responsible for the 70-km-diameter late Devonian Taihu impact crater, about 900 km away in south China. This impact left a weak Ir signature in south China but a stronger one in western Australia, where cyanobacteria might have played an important role in concentrating Ir. A paleo-reconstruction has shown that south China was very close to and facing western Australia in the late Devonian (Scotese and McKerrow, 1990). The presence of the microtektites at

Qidong is apparently due to its proximal location to the impact crater and its unusual preservation, which might be due to early diagenesis in the host rock that has allowed the microtektites to be preserved as glass.

A brachiopod faunal turnover in south China and the "strangelove ocean"-like  $\delta^{13}\text{C}$  excursions in both south China and western Australia are strongly suggestive of a regional (possibly global) extinction event in eastern Gondwana that might have occurred at the time of the impact.

### Conclusions

Evidence from south China and western Australia for a late Devonian impact event in the lower *crepida* conodont zone (365 Ma) of the Famennian stage includes microtektites, geochemical anomalies (including Ir), a 70-km-diameter Taihu impact crater in south China, and a strong Ir anomaly in western Australia. A brachiopod faunal turnover in south China, and the "strangelove ocean"-like  $\delta^{13}\text{C}$  excursions in both Chinese and Australian sections indicate that at least a regional-scale extinction might have occurred at the time of the impact, although a direct association between the impact and the extinction is still conjectural. This impact event occurred about 1.5 Ma after the great Frasnian/Famennian (F/F) extinction.

Table 7.1. Major oxide composition of the Qidong microspherules. Data in weight percent based on 80 microprobe analyses (50 on matrix glass, 10 on high-silica glass and 20 on silica inclusions) performed on seven randomly selected specimens.

| Oxide                          | Matrix glass |             | High-silica glass |             | Silica inclusions* |             |
|--------------------------------|--------------|-------------|-------------------|-------------|--------------------|-------------|
|                                | Ave.         | Range (%)   | Ave.              | Range (%)   | Ave.               | Range (%)   |
| SiO <sub>2</sub>               | 61.77        | 58.19-67.16 | 86.33             | 79.79-93.04 | 99.68              | 99.3-100.45 |
| Al <sub>2</sub> O <sub>3</sub> | 21.82        | 20.58-24.01 | 7.38              | 3.53-9.96   | 0.19               | 0.00-0.39   |
| FeO**                          | 1.48         | 0.46-2.80   | 0.56              | 0.33-1.15   | 0.02               | 0.00-0.04   |
| MgO                            | 2.91         | 1.15-4.14   | 0.71              | 0.31-1.65   | 0.01               | 0.00-0.03   |
| CaO                            | 5.15         | 3.37-6.83   | 1.45              | 0.56-3.54   | 0.02               | 0.00-0.04   |
| K <sub>2</sub> O               | 3.23         | 2.66-4.45   | 1.97              | 1.29-2.71   | 0.05               | 0.00-0.11   |
| Na <sub>2</sub> O              | 2.48         | 2.31-2.70   | 1.08              | 0.59-1.41   | 0.00               | 0.00-0.01   |
| TiO <sub>2</sub>               | 0.55         | 0.20-0.70   | 0.24              | 0.14-0.55   | 0.07               | 0.00-0.33   |
| MnO                            | 0.04         | 0.00-0.09   | 0.02              | 0.00-0.07   | 0.01               | 0.00-0.05   |
| Cr <sub>2</sub> O <sub>3</sub> | 0.05         | 0.00-0.14   | 0.05              | 0.00-0.15   | 0.00               | 0.00-0.00   |
| Total                          | 99.48        |             | 99.79             |             | 100.05             |             |

\*Silica inclusions are largely isotropic (lechatelierite) and partially crystalline (quartz). \*\*All Fe expressed as FeO.

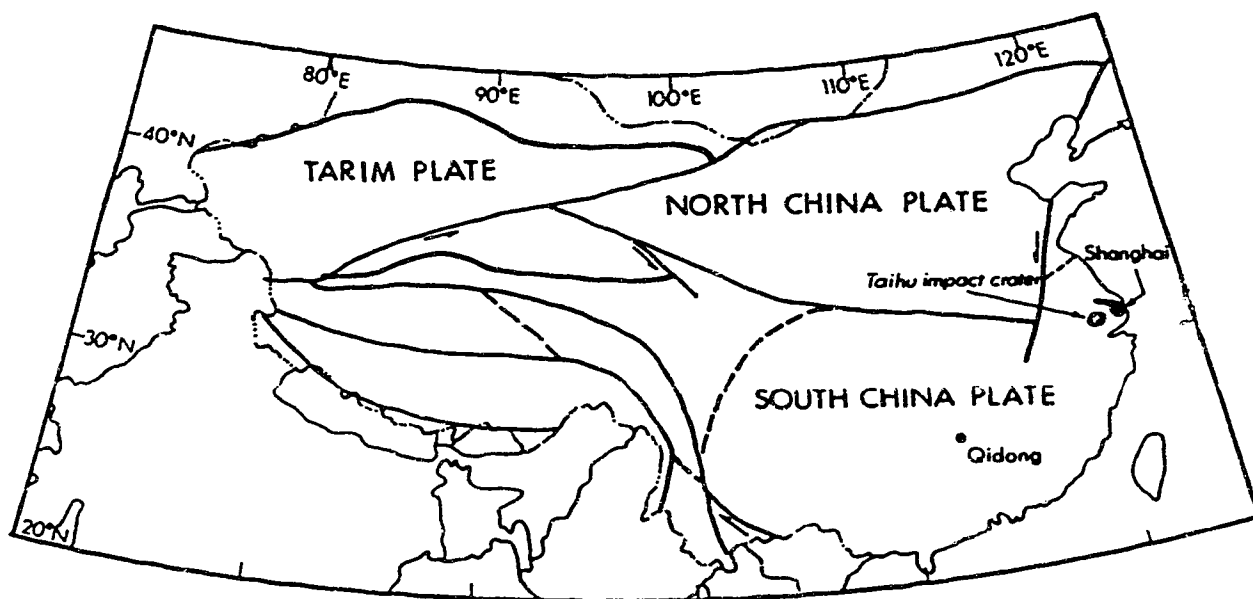
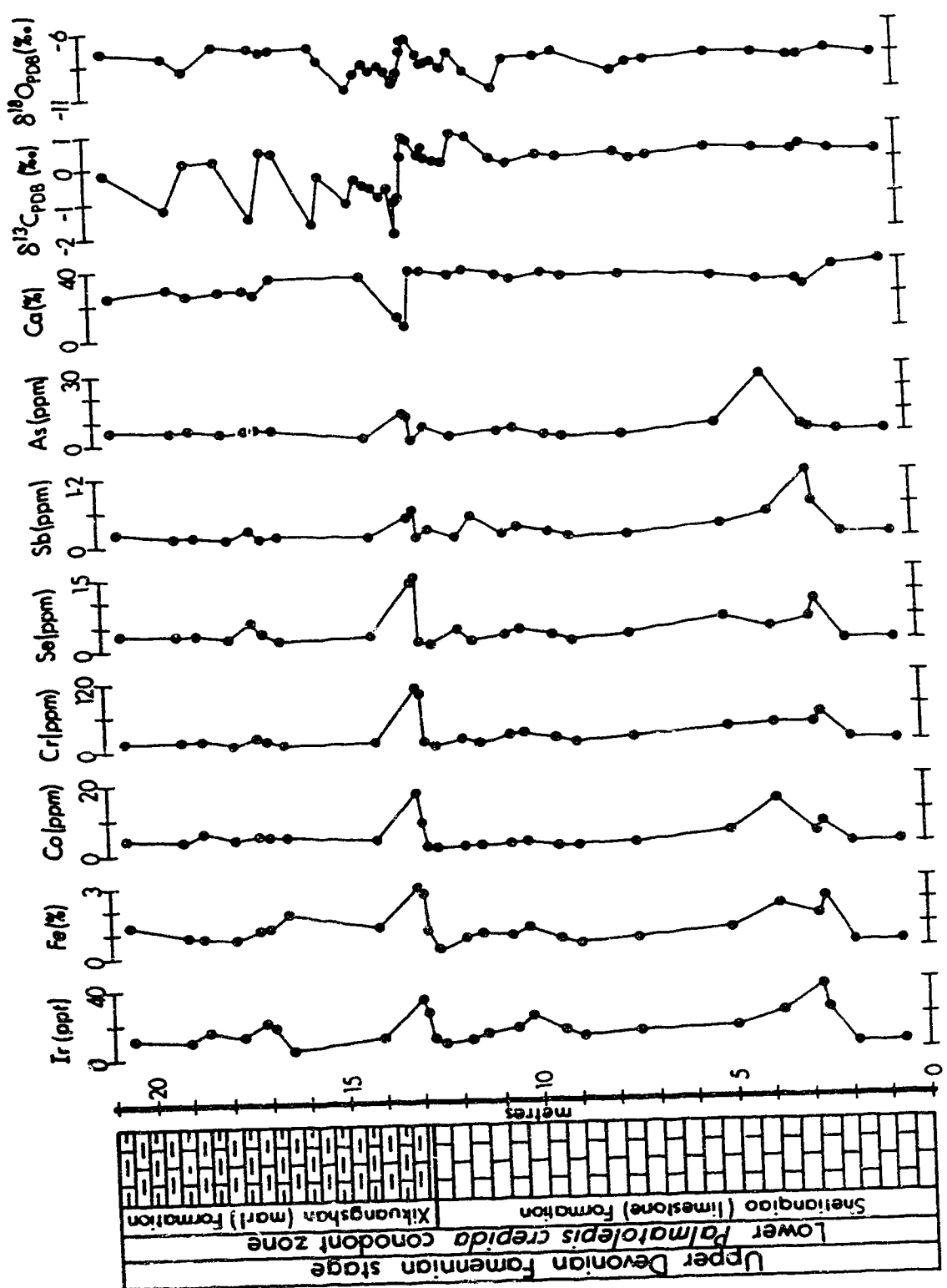
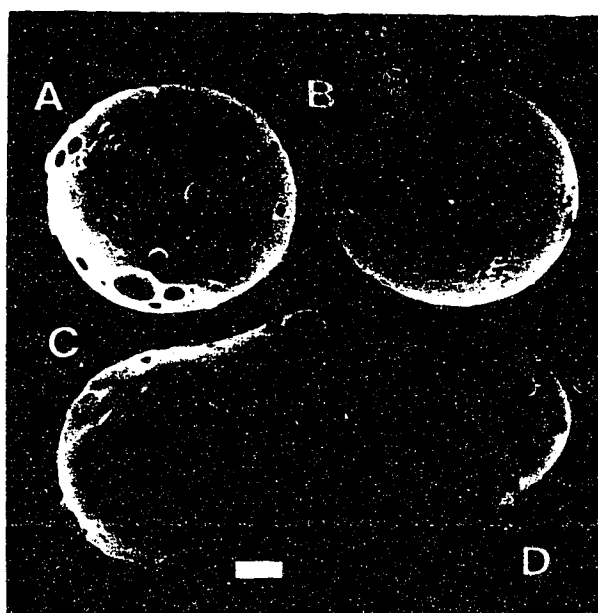


Fig. 7.1. Tectonic units of China.

**Fig. 7.2.** Stratigraphic column of Qidong section, along with some significant elemental abundances and stable isotope (C,O) values. A heavy dot marks microtektite horizon right below boundary clay.





**Fig. 7.3.** Scanning electron micrographs of surfaces of the Qidong microspherules. (A) Surface with "crater-like" big shallow pits and caps. (B) Finely pitted surface with two caps on top. (C) Pear-shaped spherule with a few small pits. (D) Welded spherules with caps on the surface that is slightly pitted (welding material = impact melt?). Caps are composed of silica as revealed by energy dispersive x-ray analysis. Scale bar = 20  $\mu\text{m}$  .

### References

- Alvarez, L.W., Alvarez, W., Asaro, F., and Michel, H.V., 1980. Extraterrestrial cause for the Cretaceous-Tertiary extinction. *Science*, 208: 1095-1108.
- Alvarez, W., Asaro, F., Michel, H.V., and Alvarez, L.W., 1982. Iridium anomaly approximately synchronous with terminal Eocene extinctions. *Science*, 216: 886-888.
- Bohor, B.F., Modreski, P.J., and Foord, E.E., 1987. Shocked quartz in the Cretaceous-Tertiary boundary clays: Evidence for a global distribution. *Science*, 236: 705-709.
- Chao, E.C.T., 1963. The petrographic and chemical characteristics of tektites. In: J.A., O'Keefe (Editor), *Tektites*. University of Chicago Press, Chicago, pp. 51-94.
- Donovan, S.K., 1989. *Mass extinctions: Processes and evidence*. Columbia University Press, New York, 265 pp.
- Ganapathy, R., 1982. Evidence for a major meteorite impact on the Earth 34 million years ago: implication for Eocene extinctions. *Science*, 216: 885-886.
- Glass, B.P., 1974. Microtektite surface sculpturing. *Geological Society of America Bulletin*, 85: 1305-1314.
- 1990. Tektites and microtektites: key facts and inferences. *Tectonophysics*, 171: 393-404.
- Glass, B.P. and Zwart, M.J., 1979. North American microtektites in DSDP cores from the Caribbean Sea and Gulf of Mexico. *Geological Society of America Bulletin*, 90: 595-602.
- Gostin, V.A., Keays, R.R., and Wallace, M.W., 1989. Iridium anomaly from the Acraman impact ejecta horizon: Impact can produce sedimentary iridium peaks. *Nature*, 340: 542-544.
- Grieve, R.A., 1982. The record of impact on Earth: implication for a major Cretaceous/Tertiary impact event. *Geological Society of America Special Paper* 190: 25-37.
- Hildebrand, A.L., Penfield, G.T., Kring, D.A., Pilkington, M., Camargo, A., Jacobsen, S.B., and Boynton, W.V., 1991. Chicxulub Crater: A possible Cretaceous/Tertiary boundary impact crater on the Yucatán Peninsula, Mexico. *Geology*, 19: 867-871.



- Holser, T.H., and 14 others, 1989. A unique geochemical record at the Permian/Triassic boundary. *Nature*, 337: 39-44.
- Hou, H., Ji., Q., and Wang, J., 1988. Preliminary report on Frasnian-Famennian events in South China. *Canadian Society of Petroleum Geologists Memoir*, 14(3): 63-70.
- Hsü, K.J., Oberhansli, H., Gao, J.Y., Shu, S., Haihong, C., and Krahenbul, U., 1985. "Strangelove ocean" before the Cambrian explosion. *Nature*, 316: 809-811.
- Ji., Q., 1988. On the Frasnian-Famennian mass extinction event in South China {Ph.D. thesis}. Chinese Academy of Geological Sciences, Beijing, 140 pp.
- Keller, G., D'Hondt, S.L., Orth, C.J., Gilmore, J.S., Oliver, P.O., Shoemaker, E.M., and Molina, E., 1987. Late Eocene impact microtektites: Stratigraphy, age and geochemistry. *Meteoritics*, 22: 25-60.
- Kyte, F.T., Zhou, Z., and Wasson, J.T., 1988. New evidence on the size and possible effects of a late Pliocene oceanic asteroid impact. *Science*, 241: 63-64.
- Margolis, S.V., Claeys, P., and Kyte, F.T., 1991a. Microtektites, microkrystites, and spinels from a late Pliocene asteroid impact in the southern ocean. *Science*, 251: 1594-1597.
- Margolis, S.V., Claeys, P., Alvarez, W., Montanari, A., Swinburne, N.H.M., Smit J., and Hildebrand, A.R., 1991b. Tektite glass from the Cretaceous-Tertiary boundary, proximal to the proposed impact crater in northern Yucatán Peninsula, Mexico. *Geological Society of American Abstracts with Programs*, 23(5): A420.
- McLaren, D.J., and Goodfellow, W.D., 1990. Geological and biological consequences of giant impacts. *Annual Reviews of Earth and Planetary Sciences*, 18: 123-171.
- Nicoll, R. S., and Playford, P. E., 1988. Upper Devonian iridium anomalies, conodont zonation and the Frasnian-Famennian boundary in the Canning Basin, Western Australia. *Geol. Soc. Austral. Abstr.* 21: 296.
- Orth, C.J., 1989. Geochemistry of the bio-event horizons. In: S.K. Donovan (Editor), *Mass extinctions: Processes and evidence*. Columbia University Press, New York, pp. 37-72.

- Orth, C.J., Attrep, A., Jr., Mao, X.Y., Kauffman, E.G., Diner, R., and Elder, W.P., 1988. Iridium abundance maxima in the upper Cenomanian extinction interval. *Geophysical Research Letters*, 15: 346-349.
- Playford, P.E., McLaren, D.J., Orth, C.J., Gilmore, J.S., and Goodfellow, W.D., 1984. Iridium anomaly in the Upper Devonian of the Canning Basin, Western Australia. *Science*, 226: 437-439.
- Sandberg, C.A., Ziegler, W., Dreesen, R., and Butler, J.L., 1988. Late Devonian mass extinction: Conodont event stratigraphy, global changes, and possible causes. *Courier Forschungsinstitut Senckenberg*, 102: 263-307.
- Saas, E., Bein, A., and Almogi-Labin, A., 1991. Oxygen-isotope composition of diagenetic calcite in organic-rich rocks: Evidence for  $^{18}\text{O}$  depletion in marine anaerobic pore water. *Geology*, 19: 839-842.
- Scotese, C.R., and McKerrow, W.S., 1990. Revised world maps and introduction, In: W.S., McKerrow and C.R., Scotese (Editor), *Paleozoic, Palaeogeography and biogeography*. Geological Society of London Memoir 12, pp. 1-21.
- Tien, C.C., 1938. Devonian brachiopods of Hunan. *Palaeontologia Sinica*, new series B, 4: 1-192.
- Tsien, H.H., Hou, H.F., Zhou, W.L., and Wu, Y., 1988. Devonian development and paleogeographic evolution in South China. *Canadian Society of Petroleum Geologists Memoir*, 14(1): 619-633.
- Wallace, M.W., Keays, R.R., and Gostin, V.A., 1991. Stromatolitic iron oxides: Evidence that sea-level changes can cause sedimentary iridium anomalies. *Geology*, 19: 551-554.
- Walliser, O.H., 1984. Geologic processes and global events. *Terra Cognita*, 4: 17-20.
- Wang, K., 1991. Glassy silicate microspherules from an Upper Devonian sediment: Microtektites? *Geological Society of American Abstracts with Programs*, 23(5): A277.
- Wang, K., and Bai, S., 1988. Faunal changes and events near the Frasnian-Famennian boundary of South China. *Canadian Society of Petroleum Geologists Memoir*, 14(3): 71-78.

- Wang, K., Orth, C.J., Attrep, M., Jr., Chatterton, B.D.E., Hou, H., and Geldsetzer, H.H.J., 1991. Geochemical evidence for a catastrophic biotic event at the Frasnian/Famennian boundary in south China. *Geology*, 19: 776-779.
- Wetherill, G.W. and Shoemaker, E.M., 1982. Collision of astronomically observable bolides with the Earth. *Geological Society of America Special Paper* 190: 1-13.
- Zachos, J.C., Arthur, M.A., and Dean, W.E., 1989. Geochemical evidence for suppression of pelagic marine productivity at the Cretaceous/Tertiary boundary. *Nature*, 337: 61-64.
- Ziegler, W., and Sandberg, C.A., 1990. The Late Devonian standard conodont zonation. *Courier Forschungsinstitut Senckenberg*, 121: 7-115.

## Chapter 8

### **Microspherules from Paleozoic marine sediments: Their origins and significance as geologic event and sedimentary markers**

(A version of this chapter has been submitted for publication. Wang, K. and Chatterton, B.D.E. *Sedimentary Geology*, 08/92)

#### **Introduction**

Fossils have been used to date rocks, correlate strata, and define stratigraphic boundaries since the beginning of geology. Subsequent methods of numerical dating and magnetostratigraphy have greatly complemented biostratigraphy. Stratigraphy is now on the brink of another revolution, owing to the advance in several rapidly-developing fields (e.g., stable-isotope stratigraphy, trace-element stratigraphy, sequence stratigraphy, and event stratigraphy). Markers of stratigraphic events (MSE) of global/regional extent documented in the sedimentary record have been used in stratigraphic correlations, with extremely high time-resolution. Although the present application of MSE in stratigraphy is limited, MSEs have been demonstrated to be important because of their wide geographic extent (some are global). These MSEs include: 1) global geochemical anomalies of elemental abundances (e.g., the iridium spike at the Cretaceous/Tertiary boundary, Alvarez and Asaro, 1990); 2) carbon isotope excursions at major stratigraphic boundaries (Magaritz, 1991) and secular changes (Williams et al., 1988); and some distinctive sedimentary markers, e.g., 3) thin clay layers at the Cretaceous/Tertiary (Alvarez and Asaro, 1990) and Permian/Triassic (Xu et al., 1986, 1989; Yin et al., 1989) boundaries; 4) black shales at the Frasnian/Famennian and Devonian/Carboniferous boundaries (Walliser, 1984; Sandberg et al., 1988); and 5) microtektite (and microkrystite) horizons in the late Eocene and at the Cretaceous/Tertiary boundary (Glass and Burns, 1988).

Microspherules of different origins have been reported from various sedimentary rocks in the Precambrian (Lowe and Byerly, 1986; Simonson, 1992; Wallace et al., 1990), Silurian (Mutch, 1966), Devonian (Wang, 1991; Casier, 1987, 1989; Bai and Ning, 1988; Glenister et al., 1976; Leuteritz et al., 1972), Permian/Triassic boundary (Holser, 1991; Gao et al., 1987, Yin et al., 1989; He, 1989), Jurassic (Czajkowski, 1987; Jehanno et al., 1988), Cretaceous/Tertiary boundary (Smit and Klaver, 1981; Smit and Kyte, 1984; Montanari et al., 1983; Montanari, 1986; Hansen et al., 1986; Naslund et al., 1986; Izett, 1987, 1991), Late Eocene (Glass et al., 1985; D'Hondt et al., 1987; Byerly et al., 1990), and Late Pliocene (Margolis et al., 1991). These reported microspherules have been attributed to a variety of origins, including organic or inorganic precipitates, volcanic or impact droplets, micro-meteorites or meteoroid ablation spherules, and secondary contaminants. Some workers claimed that microspherules can be used as sedimentary, stratigraphic and event markers for the purposes of stratigraphic correlation, boundary recognition, and event identification (e.g., Xu et al., 1989). The validity of some types of microspherules, such as microtektites and microkrystites, being an important event marker has been tested in studies of Late Pliocene (Margolis et al., 1991), Late Eocene (Glass et al., 1985; Keller et al., 1983; D'Hondt et al., 1987), and Cretaceous/Tertiary boundary (Smit and Klaver, 1981; Smit and Kyte, 1984; Montanari et al., 1983; Izett, 1991; Sigurdsson et al., 1991; Kring and Boynton, 1991; Maurrasse and Sen, 1991; Koeberl and Sigurdsson, 1992; Smit et al., 1992) impact events. However, few studies are available that discuss the significance of older microspherules recovered from Paleozoic sediments. In this paper, we describe microspherules that we found primarily in Devonian marine sediments from various localities in Canada and China, and evaluate the validity of using microspherules as sedimentary, stratigraphic and event markers in the Paleozoic.

## Methods

Most microspherules we found were from carbonate residues during micropaleontological studies. Samples were dissolved in 10%

acetic acid, and the insoluble residues were washed and sieved with water. After the residues of different size fractions (1 mm to 65  $\mu\text{m}$ ) were air dried, they were searched under a binocular microscope for microspherules and microfossils.

When microspherules were found, they were picked out with a wet fine-tipped brush and placed in a pre-numbered mount which can be covered with a glass slide. To prevent microspherules from accidentally moving out of the mount, we used water-soluble gum tragacanth to fix microspherules in place.

Microspherules were first examined under binocular and petrographic microscopes, and they were then photographed with a scanning electron microscope (SEM) to examine the morphology. Energy dispersive X-ray analyzer (EDX) provided qualitative elemental compositions of the microspherules. Selected microspherules were mounted in epoxy and polished to expose a flat surface. These polished sections were analyzed with an electron microprobe to obtain quantitative chemical compositions. Thin sections of microspherules were also examined with a petrographic microscope to acquire information on their crystallinity and internal textures (inclusions, vesicles, etc.). If necessary, X-ray micro-diffraction (XRMD) was performed on microspherules individually to determine the mineral phases present. In some cases, microspherules were crushed and their refractive indices were measured by oil-immersion methods. All investigations were carried out at the University of Alberta.

### Origins of microspherules

Microspherules that we found in Devonian marine sediments are from various localities, including Alexandra Falls and English Chief Dome in the Northwest Territories and Cinquefoil Mountain of Jasper area, Alberta in Canada, and Qidong of Hunan in China. These microspherules are generally spherical and are similar in external appearance. They are normally smaller than 0.5 mm in diameter, and range from transparent to opaque, and from light (white) to dark (black). A combined petrographic, SEM, EDX, electron microprobe, and XRMD analysis enables us to separate the

microspherules into different groups in terms of their probable origins ("conodont pearls", microtektites, suspected cosmic spherules, glue balls and steel slag). The following is a discussion of each group.

#### "Conodont pearls"

Microspherules of this group (Fig. 8.1) are very similar to those described by Glenister et al. (1976) and Leuteritz et al. (1972). They are generally spherical and range from 0.12 to 0.44 mm in diameter, which is within the range of 0.1 to 0.7 mm reported by Glenister et al. (1976) for Silurian and Devonian microspherules (these authors believed that they were conodont pearls). Surface conditions of the microspherules vary from shiny smooth to dull and rough. Small pits can be seen on the surface of some spherules.

Microspherules of this group commonly have a distinctive shallow concave area ("dimple") on the surface (Fig. 8.1). This feature may be important in distinguishing them morphologically from other types of microspherules. It has been interpreted to be the result of draping around a resistant area beneath the tissue of the conodont animal that secreted the pearl (Glenister et al., 1976). The cross section of a broken specimen is shown in Figure 1D. As described by Glenister et al. (1976) and Leuteritz et al. (1972), there is a nucleus, with some radial lines extending outwards, in the solid interior which consists of concentric layers. The central nucleus, concentric layers, and radiating lines (filled secondary cracks? of Glenister et al., 1976) are more clearly defined when cross sections of the microspherules are etched with acid (see Glenister et al., 1976; Leuteritz et al., 1972).

The typical EDX spectra of the microspherules and fossil conodonts are shown in Figure 8.2. EDX analysis performed on 13 microspherules gave the same spectrum as that shown in Figure 8.2A, with only calcium and phosphorus comprising the major elements. Results of quantitative electron microprobe analyses performed on polished sections are given in Table 8.1. The chemical data suggest that the microspherules are composed of fluorapatite  $\text{Ca}_5(\text{PO}_4)_3\text{F}$ , with about 1.5 mole percent substitution of  $\text{PO}_4$  by

SO<sub>4</sub>OH. Results of XRMD analysis of the microspherules are given in Table 8.2, which confirms that the mineral phase is fluorapatite. Analyses of some Devonian conodonts revealed that they have a similar EDX spectrum (Fig. 8.2B) and XRMD patterns to those of the microspherules. These results support the idea that the microspherules were probably associated with the conodont-bearing animal (Glenister et al., 1976). There is evidence (e.g., concentric accretion of phosphatic lamellae around a nucleus) suggesting that the spherules may have been pearls secreted internally by the conodont-bearing animal (Glenister et al., 1976) through a process similar to that of pearl secretion by modern bivalves (Taburiaux, 1985).

Phosphatic "conodont pearls" have been found in sediments ranging in age from Cambrian to Carboniferous (Stauffer, 1935, 1940; Youngquist and Miller, 1948; Leuteritz et al., 1972; Glenister et al., 1976; Casier, 1987). It was proposed that these microspherules are inorganic precipitates (Leuteritz et al., 1972), or organic structures, such as conodont otoliths (Youngquist and Miller, 1948), cnidarian statoliths (Bischoff, 1973), egg cases (Stauffer, 1935), or conodont pearls (Glenister et al., 1976). It was noted that the occurrences of "conodont pearls" are always in association with conodonts (Glenister et al., 1976) and their abundance is approximately proportional to that of associated conodonts (Youngquist and Miller, 1948). This association and the chemical and petrographic characteristics identical to conodonts appears to indicate that the microspherules, like conodonts, were formed biologically. They could very well be pearls secreted by the conodont-bearing animal, although it is difficult to prove unequivocally.

We have noted a tendency for these "conodont pearls" to be found preferentially in samples where conodonts are particularly abundant. These samples are often obtained from condensed strata. It is not clear whether this association was caused by the environmental conditions in an area where the rate of sedimentation was very low or by the fact that these "pearls" were comparatively rare and were more likely to be found in sediments which contain



a large number of remains of the conodont animal. These condensed horizons are usually close to or at the boundaries between rock units, and thus are frequently located at sequence boundaries. Hence, the presence of a large number of these distinctive "conodont pearls" may have some significance for sequence stratigraphy.

### Microtektites

Microtektites are microscopic tektites that are naturally occurring silicate glass bodies generally believed to be produced by meteorite impact (Glass, 1982, 1990). Microtektites are well known in Cenozoic strata from three areas on Earth (called strewn fields): the Australasian ( $\approx 0.7$  Ma), Ivory Coast ( $\approx 1$  Ma) and North American ( $\approx 34$  Ma) strewn fields. A new strewn field is emerging from the recent intense study of the Cretaceous/Tertiary boundary event. Glass microtektites and tektites have been recently found in the Cretaceous/Tertiary boundary sediments from Haiti and northeastern Mexico (Izett, 1991; Sigurdsson et al., 1991; Kring and Boynton, 1991; Maurrasse and Sen, 1991; Koeberl and Sigurdsson, 1992; Smit et al., 1992; but see Jehanno et al., 1992; Lyons and Officer, 1992). Paleozoic microtektites were found in the Famennian (Upper Devonian) of South China (Wang, 1991, 1992) and Belgium (Kerr, 1992; Claeys et al., 1992; Casier, 1989), and possibly in the lowest Carboniferous of South China (Bai and Ning, 1988). The microtektites discussed here are from South China, and the detailed evidence for an impact origin was presented in Wang (1992).

The microspherules range from 0.08 to 0.16 mm in diameter, most being around 0.1 mm. Although most of them are spherical in shape, some are in the form of a teardrop or a pear (Figs. 8.3, 8.4). These so-called "splash form" shapes are commonly seen in Cenozoic microtektites (Glass, 1982, 1990). The microspherules vary in translucence and colour, including opaque white, translucent dark brown, transparent yellowish brown, and a few that are colourless and transparent. The surface textures vary from perfectly smooth with a glassy lustre to pitted with a dull or frosted lustre. Some microspherules have shallow craters (or pits) and protrusions on the

surface. Compound or fused microspherules are also observed (Fig. 8.3; also see Casier, 1989).

Petrographic and EDX analyses indicate that the microspherules are glass, except for a few small quartz inclusions present in some specimens. A silicate composition for the microspherules was revealed by EDX analysis indicating that Si, Al, Ca, Fe, K, Mg and Na comprise the major elements (Fig. 8.5A). Electron microprobe analyses indicate that the microspherules contain up to three phases: silicate matrix glass, high-silica glass and pure silica inclusions. Table 8.3 gives quantitative chemical compositions of these phases in a representative microspherule. Petrographically, the pure silica inclusions are largely glass (lechatelierite, with the lowest refractive index) and partly crystalline (quartz). The high-silica glass and pure silica inclusions, when present, occur as patches within the silicate glass matrix (Fig. 8.4). The microspherules differ from volcanic glasses in lacking primary crystallites and water, in containing lechatelierite inclusions, and in having similar oxide compositional variations to those of known microtektites (Wang, 1992). The presence of lechatelierite inclusions in a glass matrix is characteristic of all tektites and suggests that the microspherules have an impact origin, because lechatelierite inclusions in microtektites were formed by melting of quartz grains at high temperature during an impact (Chao, 1963). The co-existence of both quartz and lechatelierite in the microspherules suggests that the impact-generated melt had a temperature that was slightly above the melting point of quartz.

It has been noticed that natural glasses are thermodynamically unstable; with time and under a variety of conditions (e.g., water and temperature), they devitrify (Marshall, 1961). Therefore, the chances of preservation of ancient glasses are small. However, there are reports of unaltered volcanic glasses of Jurassic (Shervais and Hanan, 1989), Triassic (Brew and Muffler, 1966), Carboniferous (Schmincke and Pritchard, 1981), and Precambrian (Palmer et al., 1988) age. Preservation of the Devonian glass microspherules that we discussed here was probably aided by

their inclusion in a limestone that may have had a very low permeability (see Wang, 1992).

If impact-produced microspherules, which were originally glass, have devitrified and become crystalline, they are then called microkrystites (Glass and Burns, 1988). Microkrystites have been found from the late Pliocene (Margolis et al., 1991), late Eocene (Glass et al., 1985; Keller et al., 1983), Cretaceous/Tertiary boundary (Montanari et al., 1983; Smit and Kyte, 1984; Smit and Romein, 1985; Kyte and Smit, 1986), and Precambrian (Lowe and Byerly, 1986; Lowe et al., 1989; Simonson, 1992; Wallace et al., 1990) impact horizons.

### Suspected cosmic spherules

Cosmic spherules are subspherical to spherical objects (generally  $< 2$  mm in diameter) produced by melting of incoming interplanetary dust and large bodies during atmospheric entry (Brownlee, 1985). Today, they can be collected both in space and in terrestrial environments, such as the deep-sea floor, and Greenland or Antarctic ice sheets (Brownlee, 1985). Ancient cosmic spherules, although significantly altered, have been found in various types of sedimentary deposits, ranging in age from early Paleozoic to Quaternary (e.g., Taylor and Brownlee, 1991; Czajkowski, 1987; Jehanno et al., 1988; Mutch, 1966; Mutch and Garrison, 1967; Crozier, 1960; Hunter and Parkin, 1961; Skolnik, 1961). There are two general types of spherules identified as of cosmic origin: 1) black, magnetic iron-spherules composed of iron oxide(s) (normally magnetite/wustite) that sometimes contain a metallic (Ni/Fe) core; and 2) stony spherules composed of magnetite, olivine and glass similar in composition to chondrules (Brownlee, 1985; Kyte, 1988). Although both types of cosmic spherules occur in similar abundance in modern deep-sea sediments (Brownlee, 1985), most cosmic spherules found in ancient sediments belong to the first group, probably as a result of greater resistance of iron-type cosmic spherules to alteration (Kyte, 1988).

Probable cosmic spherules that we found in Devonian sediments from China are black, magnetic iron-spherules with

beautiful surface textures (Fig. 8.6). They are spherical and 200-300  $\mu\text{m}$  in diameter. One of them has a distinctive dendritic surface texture (Fig. 8.6A; Fig. 8.7), similar to the ablation texture on the surface of some typical iron-type cosmic spherules (Czajkowski, 1987; Jehanno et al., 1988). Another spherule shown in Fig. 8.6B has a polygonal surface texture, similar to that of some cosmic spherules recovered from East Antarctic ice sheet (Hagen et al., 1990). EDX analysis of these spherules showed the iron (Fig. 8.5B) and oxygen spectra, indicating that, like most other iron-spherules found in ancient sediments, they are composed of iron oxide(s), such as magnetite and wustite. Polished sections of the two spherules were analyzed with an electron microprobe and the results are shown in Table 8.4.

Magnetite/wustite is formed through the oxidation of molten meteoritic metal (FeNi) at high temperature during atmospheric entry, while more refractory elements (e.g., Ni and PGEs) are concentrated into a shrinking Ni-rich metallic core (Blanchard et al., 1980; Czajkowski, 1987). When oxidation is nearly complete, most of the Fe and Ni leave the core, resulting in a small nugget (5-10  $\mu\text{m}$ ) of almost pure platinum group elements (Brownlee et al., 1984). The presence of an FeNi core or a PGE nugget in iron-spherules clearly indicates their cosmic origin. However, a lower nickel content in iron-spherules does not preclude a cosmic origin because during oxidation of Fe and Ni metals at high temperature, the Ni tends to be concentrated in the metallic phase leaving the oxide phase depleted in Ni (Marvin and Einaudi, 1967). Although the Devonian iron-spherules we found are very similar to iron-type cosmic spherules, we did not observe an FeNi core or a PGE nugget in these spherules, and therefore we can only call them probable cosmic spherules at this time. It has been noticed that most common iron-type cosmic spherules larger than 300  $\mu\text{m}$  do not contain an FeNi core, but instead contain a PGE nugget (Brownlee et al., 1984). Because of the small size of a PGE nugget, we can not preclude the possibility that it was missed when the spherules were sectioned.

#### Man-made microspherules

Unlike natural microspherules formed in geologic time, these microspherules are believed to be modern contaminants. Fortunately, they can be recognized on the basis of their chemical and physical properties.

### 1. Glue balls

Two mounts containing natural microspherules were taken to a thin-sectioning lab where the microspherules were buried in epoxy and polished to expose a flat surface for petrographic and microprobe analyses. After the mounts were returned from the lab, we found that there were many tiny, clean and transparent "microspherules" (Fig. 8.8) in the mounts.

These clear microspherules were not present in the mounts originally, and thus they must have come from the thin-sectioning lab. We were informed that the technician in the lab used a fine-tipped brush with some sort of glue to pick up the natural microspherules in the mounts. We suspect that these tiny, clear microspherules came from the glue on the brush, and we call them glue balls here.

These glue balls are small (34-104  $\mu\text{m}$  across) and spherical (Fig. 8.8), but one of them is in compound form (Fig. 8.8C). EDX analysis of the glue balls gave a flat spectrum (Fig. 8.5C), indicating that they are composed of light elements, probably hydrocarbon compounds. The electron beam easily burned a hole on the surface of a glue ball analyzed (Fig. 8.8D), suggesting that they are relatively soft. Indeed, continuous exposure to the beam caused them to "boil" and collapse. The results of these analyses are consistent with our inference that they are glue balls which came from the thin-sectioning lab.

### 2. Industrial slag

Fly ash and industrial slag can be a source of microspherule contaminants. Our microspherule-containing samples were obtained from fresh, solid limestones, and we cleared the surfaces of the samples to remove any possible contamination before processing them. Containers for microspherules were always covered up with a

lid before and after examination. However, one of our microspherules (Fig. 8.9) is believed to be a steel slag, probably coming from a steel plant. It occurs in a sample independently from other microspherule-containing samples, and is the only spherule in our collection that does not fall into any of the other categories discussed above.

This spherule is about 380  $\mu\text{m}$  across and has two protrusions on the surface (Fig. 8.9). It is dark, with a semi-metallic lustre. There are several holes visible on the surface; a large, deep hole indicates that it is probably hollow. The EDX spectrum of this spherule is given in Figure 8.5D. Results of semi-quantitative energy-dispersive analysis revealed that this spherule has high Ti and Mn contents (Table 8.5), as is common in industrial slags. The chemical composition of this spherule is very similar to that of the Port Kembla steel slag analyzed by Heaton (1979).

## Discussion

Microspherules occasionally found in sedimentary rocks of the Paleozoic apparently have different origins. When properly studied, the origins of most of these microspherules can be determined. Those microspherules with determined origins are most valuable because they can provide important (sometimes unique) information on paleo-environmental conditions and on geologic and sedimentary events, which may be otherwise undetectable. For example, the presence of microtektites in the Late Devonian would indicate impact events some 360 Ma ago (Wang, 1992; Claeys et al., 1992; Kerr, 1992).

Owing to their small size and scarcity of occurrences, microspherules from Paleozoic sediments have not been the subject of extensive studies. There are very few reported Paleozoic microspherules, and most of them were found by paleontologists as by-products of micropaleontological studies (e.g., Stauffer, 1935, 1940; Youngquist and Miller, 1948; Leuteritz et al., 1972; Glenister et al, 1976; Casier, 1987, 1989; Bai and Ning, 1988). Conventional equipment, used by most paleontologists, such as the binocular microscope, are not sufficient for identifying the different types of

microspherules. External morphology and appearance, in most cases, are not distinct enough between different microspherule groups. Studies of microspherules found in ancient sediments must employ modern techniques of micro-sectioning, SEM, EDX, XRMD, electron microprobe, and even ultra-sensitive neutron activation analysis (Czajkowski, 1987; Jehanno et al., 1988).

In this study, we have identified three groups of natural microspherules and two groups of artificial microspherules. They are similar in size (<0.5 mm) and in appearance under a light microscope. But there are some criteria that can be used to distinguish them. Morphologically (particularly the SEM image), "conodont pearls" always have a "dimple" on the surface; microtektites commonly have "splash form" shapes, such as sphere, teardrop, dumbbell, rod and disc; suspected cosmic spherules have distinctive surface textures (ablation texture), such as dendritic and polygonal patterns; glue balls are clear and smooth; and steel slag has a semi-metallic lustre. Internally, "conodont pearls" show concentric growth layering around a central nucleus; microtektites have spherical bubble cavities and lechatelierite inclusions; suspected cosmic spherules have a solid matrix of iron oxide (magnetite/wustite) crystallites; and the steel slag is probably hollow. Mineralogically, "conodont pearls" are composed of fluorapatite; microtektites are glass; and suspected cosmic spherules consist of magnetite/wustite. Compositionally, "conodont pearls" are primarily  $\text{Ca}_5(\text{PO}_4)_3\text{F}$ ; microtektites are acidic silicate; suspected cosmic spherules are  $\text{Fe}_3\text{O}_4/\text{FeO}$ ; glue balls are probably made up of hydrocarbon compounds; and steel slag contains high contents of Ti, Fe, Si, Al, Mn and Ca. Therefore, there are wide differences between these five groups of microspherules.

The geological significance of natural microspherules from the sedimentary record depends on the type of microspherules. Microtektites are most valuable because they imply the occurrence of an important geologic process: meteorite impact on the surface of Earth. Although an impact can also be indicated by other lines of evidence, such as iridium anomalies, shocked quartz, and impact craters (KYTE, 1988), microtektites are more useful in identifying

target materials and in locating impact sites. Microtektite glasses can be used to determine the time of impact by measuring  $^{40}\text{Ar}/^{39}\text{Ar}$  ages in the glass which was formed during the impact. The geographic distribution of microtektites of an impact event would define a strewn field, and ultimately provide an estimate of the amount of material thrown up from the impact crater (Glass, 1990). There are not many microtektite horizons known in the geologic record. In addition to the classic microtektites found in the Cenozoic, new occurrences of microtektites may include Late Pliocene microtektites found in the southeast Pacific (Margolis et al., 1991), Cretaceous/Tertiary boundary microtektites found in Haiti and northeastern Mexico (Izett, 1991; Sigurdsson et al., 1991; Kring and Boynton, 1991; Maurrasse and Sen, 1991; Koeberl and Sigurdsson, 1992; Smit et al., 1992), Lower Famennian (Upper Devonian) microtektites recently reported from South China (Wang, 1992) and Belgium (Claeys et al., 1992; Kerr, 1992), and possibly lowest Carboniferous microtektites previously reported from South China (Bai and Ning, 1988). It is known that meteorite impacts occurred many times in geologic past, and thus we would expect more occurrences of microtektites in the sedimentary record. However, long and complex geologic history makes signatures of an ancient impact (such as microtektites), which may be destroyed or altered, difficult to recognize. Therefore, once unaltered microtektites are found in the sedimentary record, they are extremely valuable and good indicators of ancient impact events. However, most ancient microtektites have been altered and the glass has been devitrified to form crystallites (Glass and Burns, 1988). Microkrystites are known to be associated with impact events in the Late Pliocene (Margolis et al., 1991), Late Eocene (Glass et al., 1985; Keller et al., 1983), Cretaceous-Tertiary boundary (Montanari et al., 1983; Smit and Kyte, 1984; Smit and Romein, 1985; Kyte and Smit, 1986), and Precambrian (Lowe et al., 1989; Lowe and Byerly, 1986; Simonson, 1992; Wallace et al., 1990).

Ancient cosmic spherules are also valuable geologic material, since they record the accretion event of extra-terrestrial material to Earth in the geologic past. The rate of influx of extra-terrestrial



material on Earth can be estimated on the basis of abundance of cosmic spherules in sedimentary deposits. Therefore, cosmic spherules found in the sedimentary record can be used to estimate the rate of ancient influx of extra-terrestrial material. For example, from the study of cosmic iron spherules recovered from Silurian salt, Mutch (1964) was able to come up with a Silurian accumulation rate of extra-terrestrial material to be  $10^8$ - $10^9$  tons/year some 400 Ma ago, which is much greater than the present day rate  $10^4$ - $10^5$  tons/year (Glass, 1982). It has been noticed that the proportions of cosmic spherule types change as a function of time, with the number of iron spherules increasing with age. This change may reflect a real change in meteoroid compositions through time, or alternatively a result of differential preservation favouring iron-spherules in geologic environments (Taylor and Brownlee, 1991). It is quite obvious that, with a given influx rate, cosmic spherules would be concentrated in strata in which the sedimentation rate was low. This is why greater abundances of cosmic spherules were found in Jurassic hardgrounds (Czajkowski, 1987; Jehanno et al., 1988) which represent a significant amount of time. Mutch and Garrison (1967) applied the abundance of cosmic spherules to the determination of sedimentation rates.

"Conodont pearls" are commonly associated with the occurrences of conodonts. The stratigraphic significance of "conodont pearls" are not fully understood at the moment. "Conodont pearls" were reported to occur only in strata ranging in age from Cambrian to Carboniferous (Glenister et al., 1976). However, calcium-phosphatic spherules described by Gao et al. (1987) and Yin et al. (1989) from the latest Permian of South China are probably also "conodont pearls". These latter spherules are also associated with conodonts, and they were interpreted to be of organic origin (Yin et al., 1989). It was noticed by Glenister et al. (1976) that the only fossils invariably associated with "conodont pearls" are conodonts. In our Devonian samples containing "conodont pearls", we found that conodonts are always abundant. But in samples with abundant conodonts, "conodont pearls" do not always occur. For example, among 27 conodont-bearing samples collected across the

Frasnian/Famennian boundary at the Cinquefoil Mountain Section, western Canada, only one sample also contains "conodont pearls". If these phosphatic spherules are indeed pearls secreted by the conodont animal as suggested, rocks containing "conodont pearls" would represent time periods (or living environments) when (or where) secretion of pearls by the conodont animal was encouraged, such as summer times (or warm areas). The best conditions under which modern molluscs secrete pearls are warm, stable and shallow waters, and of course an appropriate irritant under the tissue (Tabouriaux, 1985). "Conodont pearls" may be useful paleoecologically, particularly when other lines of evidence are available to aid interpretations. Apparently, more studies are needed before the geological significance of "conodont pearls" can be fully understood.

It is clear that geologic samples sometimes can be contaminated by man-made microspherules either at the outcrop or in the laboratory. Therefore, great care must be taken to eliminate any possible contamination during the processing of samples for natural microspherules. Fortunately, in most cases, man-made microspherules can be distinguished chemically and petrographically from natural microspherules, and their sources can be traced. Industrial slags are the main source of contamination at the outcrop, while glue balls can be a source of contamination during sample preparations.

In summary, we have studied the microspherules that we found in Paleozoic marine sediments from various localities in Canada and China. Although these microspherules look similar in appearance, they have different origins which we have determined through combined SEM, EDX, XRMD, and electron microprobe analyses. On the basis of these analyses and observations, we have classified the microspherules, in terms of their origins, into the following groups (three groups of natural microspherules and two groups of man-made microspherules): "conodont pearls" of biological origin; microtektites of terrestrial meteorite-impact origin; suspected cosmic spherules of probable extra-terrestrial origin; contaminant microspherules (glue balls and steel slag) of artificial origin.

Although some microspherules have distinctive external morphological features (e.g., the "dimple" on "conodont pearls"), this study shows that external morphology and appearance, without information on internal structures and on chemical and petrographic characteristics, are inadequate to characterize the nature and origins of various types of microspherules.

Once their origins are determined, ancient natural microspherules can provide invaluable geological information. "Conodont pearls" have been found to have close associations with conodonts, and they were probably formed in such environments (warm, stable waters) in which the conodont animal was encouraged to secrete pearls. Microtektites are glass droplets of quenched splash melt-material produced by meteorite-impact on Earth, and they therefore can be used as an impact event marker. However, their occurrence in the sedimentary record is rather rare because of the small chance of long-time preservation of glasses in geologic environments. Ancient cosmic spherules can be used to determine changes in the composition and influx rate of extra-terrestrial material in geologic time. These spherules can occur anywhere in the Paleozoic sedimentary record, but they tend to occur in greater abundance in condensed strata (slow sedimentation), such as in hardgrounds. Their occurrence, together with other evidence, may indicate reduced rate of deposition. Man-made microspherules have been found to contaminate geologic samples. Great care must be paid during the processing of geologic samples for natural microspherules.

### Conclusions

Microspherules (<0.5 mm) are occasionally found in Paleozoic marine sediments during micropaleontological studies (e.g., conodont-picking). The microspherules are similar in appearance, but they can be quite different in origin. A combined scanning electron microscope, energy dispersive X-ray, X-ray micro-diffraction and electron microprobe analysis enables us to separate them into four groups of different origins: 1) phosphatic "conodont pearls" of biological origin; 2) silicate glass microtektites of

terrestrial meteorite-impact origin; 3) black, magnetic iron-spherules of probable extra-terrestrial origin (suspected cosmic spherules); and 4) contaminant spherules (glue balls and industrial slag) of artificial origin. "Conodont pearls" have been found to have close associations with conodonts, and they were probably formed in the environments in which the conodont animal was able to secrete pearls. Microtektites are glass products of quenched splash melt-material resulting from meteorite-impact on the surface of Earth, and they therefore can be used as an impact event marker. However, their occurrence in the sedimentary record is rather rare because of the small chance of long-time preservation of glasses in geologic environments. Cosmic spherules (cosmic dust) can occur anywhere in the Paleozoic sedimentary record, but they tend to occur in greater abundance in a condensed sequence (low sedimentation rate), such as in a hardground. Their occurrence, together with other evidence, may indicate sedimentary condensation. Man-made microspherules have been found to contaminate geologic samples. Great care must be paid during the processing of geologic samples for natural microspherules. Although some microspherules have distinctive external morphologic features (e.g., the "dimple" on "conodont pearls"), this study shows that external morphology and appearance, without information on internal structures and on chemical and petrographic characteristics, are inadequate to characterize the nature and origins of various microspherules. Ancient microspherules are valuable geological materials; once their origins are determined, they can provide important geological information.

**Table 8.1.** Chemical composition (wt. %) of "conodont pearls" by electron microprobe analysis. Analyzed "conodont pearls" are from the Cinquefoil Mountain, Jasper, Alberta, Canada.

| SiO <sub>2</sub> | Al <sub>2</sub> O <sub>3</sub> | FeO  | CaO   | P <sub>2</sub> O <sub>5</sub> | SO <sub>3</sub> | Cl   | F    |
|------------------|--------------------------------|------|-------|-------------------------------|-----------------|------|------|
| 0.04             | 0.04                           | 0.00 | 55.28 | 39.28                         | 1.61            | 0.08 | 3.65 |
| 0.11             | 0.07                           | 0.10 | 55.56 | 38.76                         | 1.56            | 0.17 | 3.66 |
| 0.15             | 0.08                           | 0.02 | 55.32 | 39.13                         | 1.42            | 0.07 | 3.81 |
| 0.14             | 0.06                           | 0.01 | 55.28 | 38.80                         | 1.48            | 0.06 | 4.15 |
| 0.15             | 0.04                           | 0.04 | 55.31 | 39.00                         | 1.50            | 0.07 | 3.89 |
| 0.09             | 0.05                           | 0.00 | 55.46 | 38.92                         | 1.51            | 0.07 | 3.88 |

**Table 8.2.** Results of X-ray microdiffraction analysis of "conodont pearls", best matching fluorapatite.

| Conodont Pearl<br>(This study) |                  | Fluorapatite<br>JCPDS (1980) |                  |
|--------------------------------|------------------|------------------------------|------------------|
| d(Å)                           | I/I <sub>0</sub> | d(Å)                         | I/I <sub>1</sub> |
| 8.15                           | 5                | 8.12                         | 8                |
| 5.19                           | 6                | 5.25                         | 4                |
| 4.04                           | 6                | 4.035                        | 8                |
| 3.87                           | 6                | 3.872                        | 8                |
| 3.46                           | 6                | 3.442                        | 40               |
| 3.14                           | 9                | 3.167                        | 14               |
| 3.06                           | 7                | 3.067                        | 18               |
| 2.80                           | 10               | 2.800                        | 100              |
| 2.71                           | 4                | 2.702                        | 60               |
| 2.63                           | 5                | 2.624                        | 30               |
| 2.254                          | 5                | 2.250                        | 20               |
| 2.135                          | 5                | 2.140                        | 6                |
| 1.938                          | 7                | 1.937                        | 25               |
| 1.88                           | 6                | 1.884                        | 14               |
| 1.83                           | 7                | 1.837                        | 30               |

Table 8.3. Oxide compositions (wt. %) of three different phases within a typical Upper Devonian Qidong microtektite from South China, by electron microprobe analysis.

| Oxide\Phase                    | Matrix glass | High-silica glass | Silica inclusions* |
|--------------------------------|--------------|-------------------|--------------------|
| SiO <sub>2</sub>               | 62.63        | 86.38             | 99.67              |
| Al <sub>2</sub> O <sub>3</sub> | 21.41        | 7.14              | 0.33               |
| FeO*                           | 1.39         | 0.64              | 0.01               |
| MgO                            | 2.66         | 0.77              | 0.00               |
| CaO                            | 4.89         | 1.54              | 0.04               |
| K <sub>2</sub> O               | 3.38         | 1.91              | 0.07               |
| Na <sub>2</sub> O              | 2.51         | 1.02              | 0.00               |
| TiO <sub>2</sub>               | 0.49         | 0.29              | 0.00               |
| MnO                            | 0.04         | 0.03              | 0.00               |
| Cr <sub>2</sub> O <sub>3</sub> | 0.05         | 0.03              | 0.00               |
| Total                          | 99.45        | 99.75             | 100.12             |

\* Silica inclusions are largely isotropic (lechatelierite) and partially crystalline (quartz). + All Fe expressed as FeO

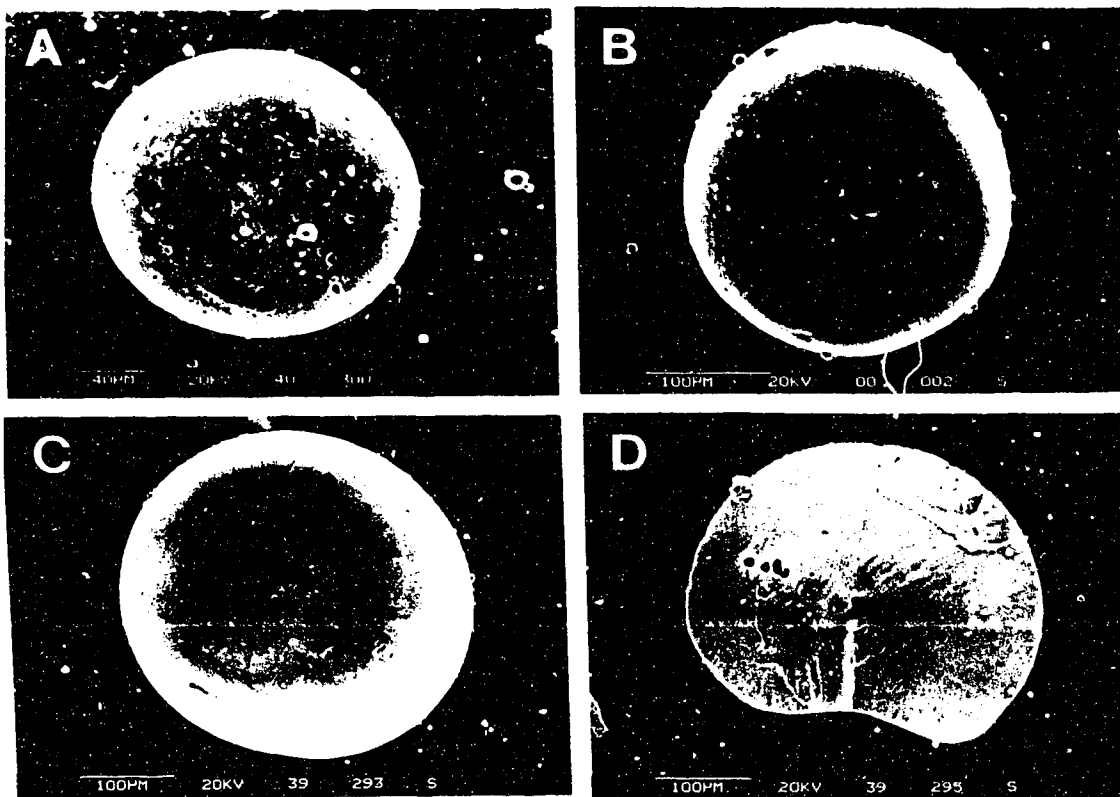
Table 8.4. Chemical composition (wt.%) of two black, magnetic iron-spherules (suspected cosmic spherules) by electron microprobe analysis.

| Oxide                          | Spherule A | Spherule B |
|--------------------------------|------------|------------|
| SiO <sub>2</sub>               | 0.10       | 0.07       |
| TiO <sub>2</sub>               | 0.03       | 0.24       |
| Al <sub>2</sub> O <sub>3</sub> | 0.11       | 0.04       |
| Cr <sub>2</sub> O <sub>3</sub> | 0.11       | 0.06       |
| FeO*                           | 99.14      | 99.31      |
| MnO                            | 0.31       | 0.11       |
| MgO                            | 0.07       | 0.03       |
| NiO                            | 0.12       | 0.07       |
| Total                          | 99.99      | 99.93      |

\* All Fe expressed as FeO

Table 8.5. Elemental composition (wt. %) of semi-quantitative energy dispersive analysis of the steel slag pictured in Fig. 9.

| Al-ka | Si-ka | Ca-ka | Ti-ka | Mn-ka | Fe-ka |
|-------|-------|-------|-------|-------|-------|
| 9.00  | 18.25 | 7.50  | 32.52 | 8.28  | 24.45 |



**Fig. 8.1.** Scanning electron micrographs of Devonian "conodont pearls" recovered from (A) near the Frasnian-Famennian boundary in the Cinquefoil Mountain, Jasper, Alberta, Canada; (B) the Frasnian at the Alexandra Falls, N.W.T., Canada; and (C, D) the Eifelian at English Chief Dome, N.W.T., Canada. A big, shallow concave area ("dimple") is clearly shown on the surface of each specimen. Picture in (D) shows a cross-section cutting through the "dimple" on the bottom and a nucleus in the centre.

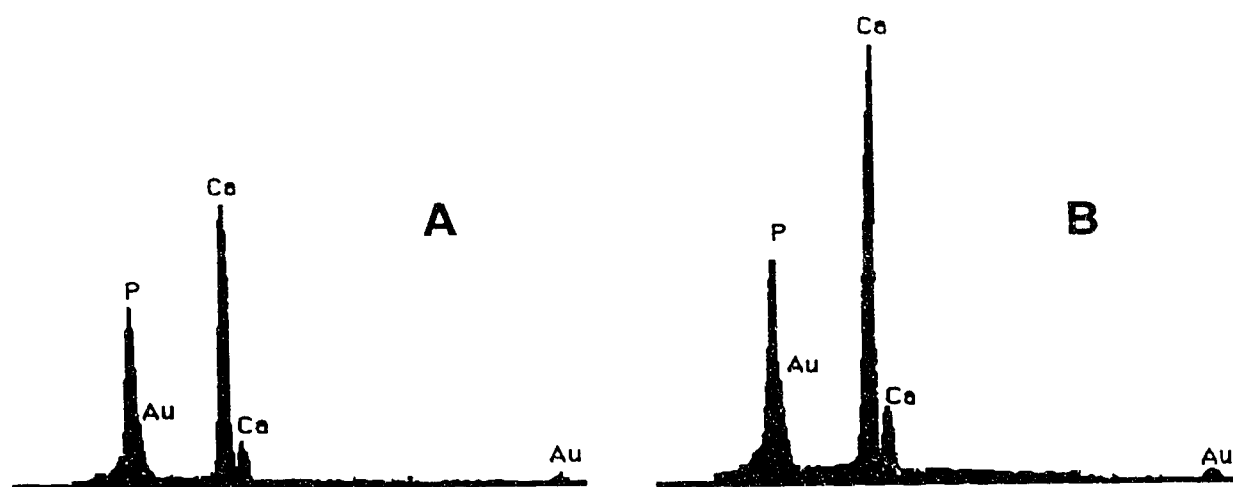
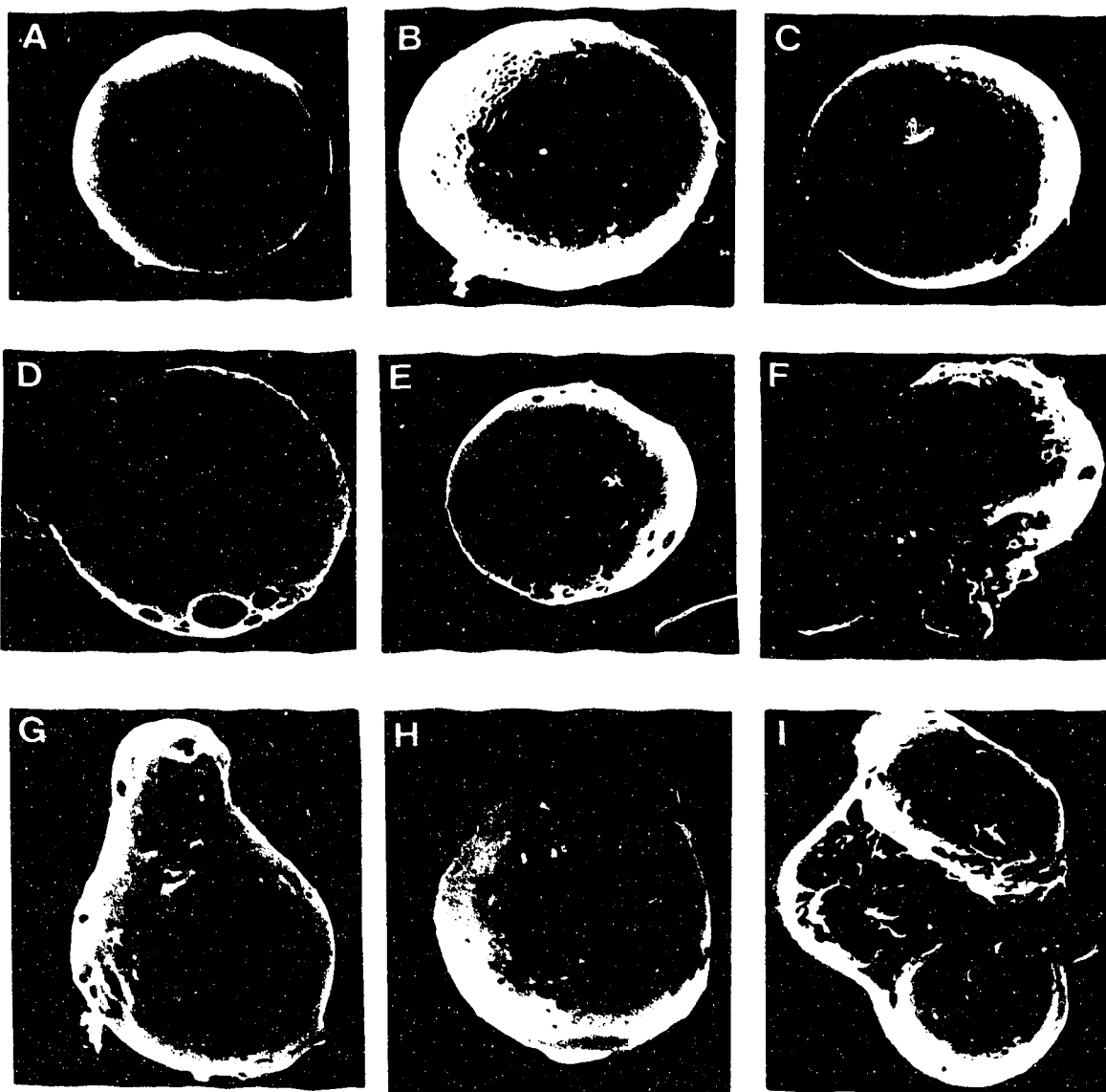
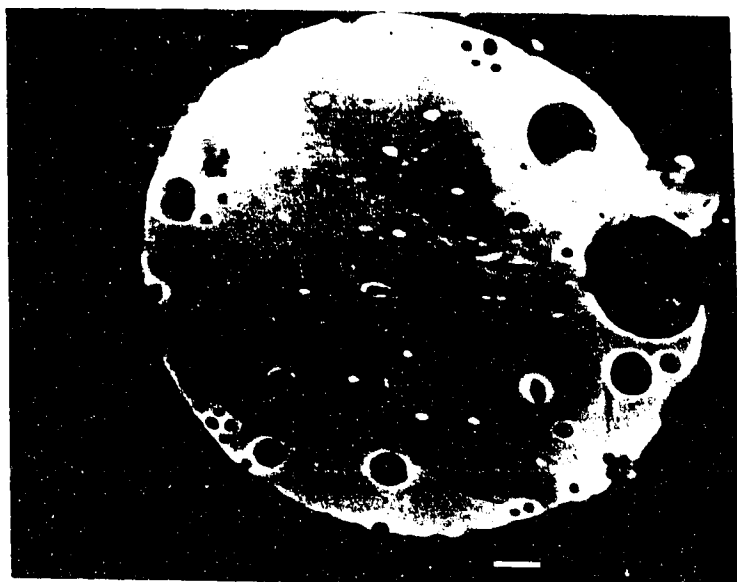


Fig. 8.2. EDX spectra of "conodont pearls" (A) and fossil conodonts (B). The gold spectra are from coating.



**Fig. 8.3.** Scanning electron micrographs of surfaces of Famennian (Upper Devonian) microtektites recovered from Qidong, Hunan, China. Typical forms are spherical, teardrop or pear-shaped, and compound. Scale, the sphere in (A) is  $\sim 80 \mu\text{m}$  in diameter.





**Fig. 8.4.** Scanning electron micrograph in the backscattered mode of the polished section of a Qidong microtektite, showing spherical bubble vesicles (black holes), glass matrix (light phase) and silica-rich areas (dark phase) which are composed of two phases (high-silica and pure silica, see Table 3). Scale bar, 10  $\mu\text{m}$ .

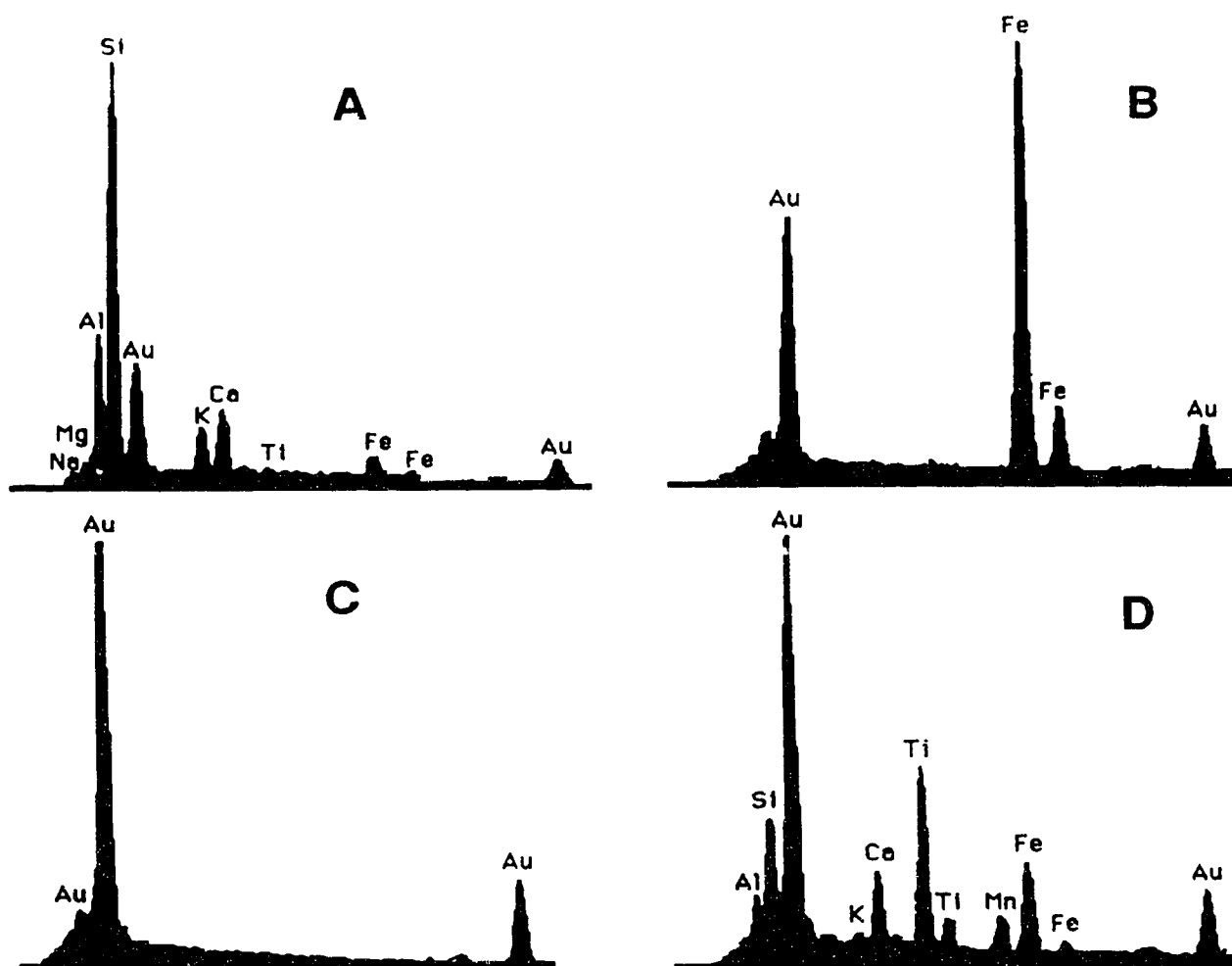
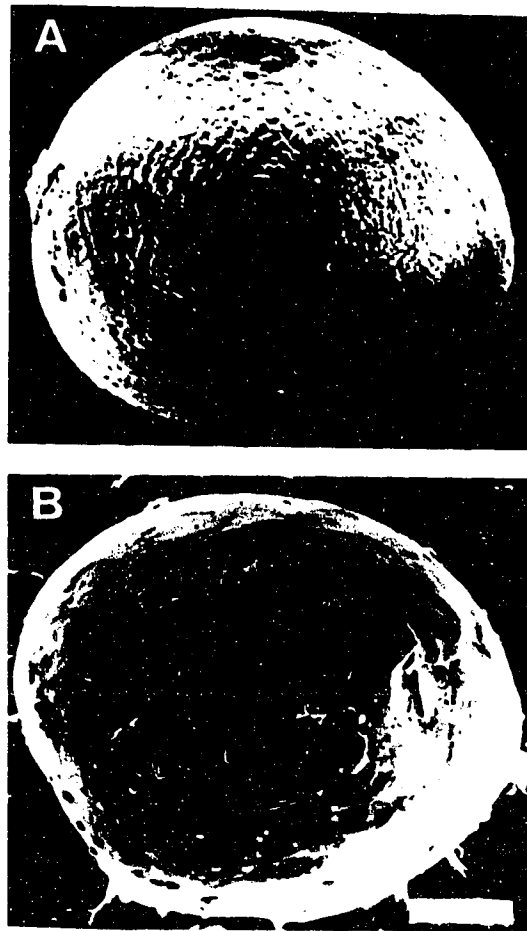
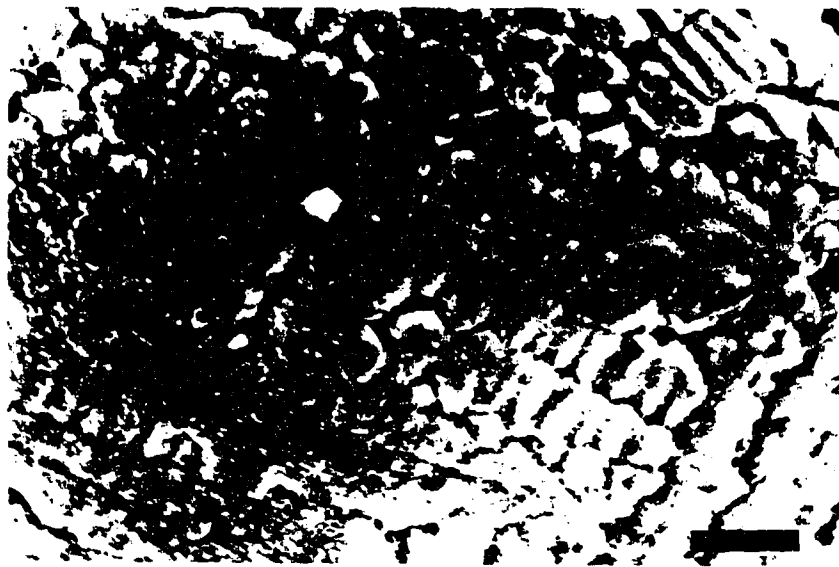


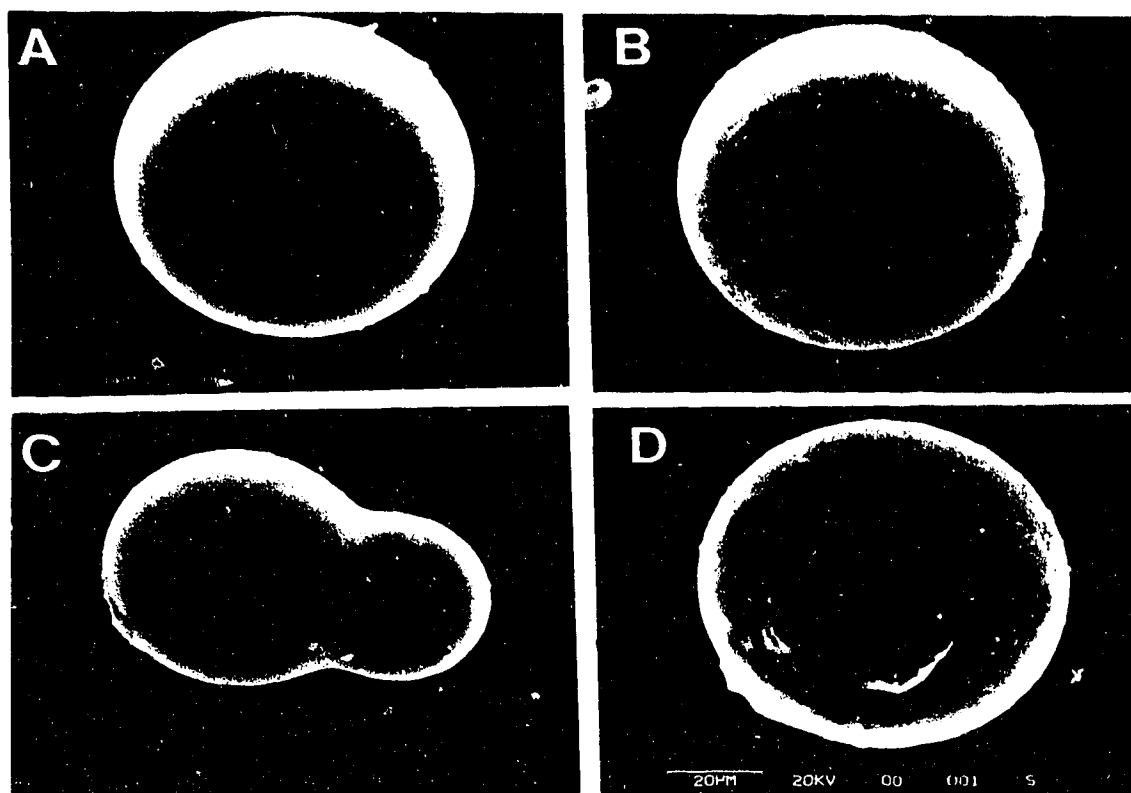
Fig. 8.5. EDX spectra of (A) Qidong microtektites, (B) suspected cosmic spherules, (C) glue balls, and (D) steel slag. The gold spectra are from coating.



**Fig. 8.6.** Scanning electron micrographs of surfaces of two black, magnetic iron-spherules (suspected cosmic spherules) recovered from the Devonian of South China. (A) Dendritic surface pattern (caused by ablation?); (B) Polygonal surface pattern. Scale bar, 50  $\mu\text{m}$ .



**Fig. 8.7.** Magnified surface texture of the suspected cosmic spherule in Fig. 6A, showing iron oxide (magnetite) crystals. Scale bar, 10  $\mu\text{m}$ .



**Fig. 8.8.** Scanning electron micrographs of small, clean and smooth-surfaced glue balls. The broken surface in (D) was caused by the electron beam.



**Fig. 8.9.** Scanning electron micrograph of a spherule interpreted as steel slag. Scale bar, 100  $\mu\text{m}$ .



## References

- Alvarez, W. and Asaro, F., 1990. An extraterrestrial impact. *Scientific American*, 10: 78-84.
- Bai, S. and Ning, Z., 1988. Faunal changes and events across the Devonian-Carboniferous boundary of Huangmao Section, Guangxi, South China. *Can. Soc. Petrol. Geol. Memoir*, 14 (3): 147-158.
- Bischoff, G.C.O., 1973. On the nature of the conodont animal. *Geol. Palaeont.*, 7: 147-174.
- Blanchard, M.B., Brownlee, D.E., Bunch, T.E., Hodge, P.W. and Kyte, F.T., 1980. Meteoroid ablation spheres from deep-sea sediments. *Earth Planet. Sci. Lett.*, 46: 178-190.
- Brew, D.A. and Muffler, L.J.P., 1966. Upper Triassic undevitrified volcanic glass from Howard Island, Keku Strait, southeastern Alaska. *U.S. Geol. Surv. Prof. Paper*, 525C: 38-43.
- Brownlee, D.E., 1985. Cosmic dust: Collection and research. *Ann. Rev. Earth Planet. Sci.*, 13: 147-173.
- Brownlee, D.E., Bates, B.A. and Wheelock, M., 1984. Extraterrestrial platinum group nuggets in deep sea sediments. *Nature*, 309: 693-695.
- Byerly, G.R., Hazel, J.E. and McCabe, C., 1990. Discrediting the late Eocene microspherule layer at Cynthia, Mississippi. *Meteoritics*, 25: 89-92.
- Casier, J.G., 1987. Etude biostratigraphique et paleoecologique des ostracodes du recif de marbre rouge du hautmont a vodelle. *Revue de Paleobiologie*, 6: 193-204.
- Casier, J.G., 1989. Paleoecologie des Ostracodes au niveau de la limite des etages Frasnian et Famennian, a Senzeilles. *Bull. de L'institut Royal des Sci. Naturelles de Belgique*, 59: 79-93.
- Chao, E.C.T., 1963. The petrographic and chemical characteristics of tektites. In: J.A. O'Keefe (Editor), *Tektites*. Univ. of Chicago Press, Chicago, pp.51-94.
- Claeys, P., Casier, J.G., and Margolis, S.V., 1992. Microtektites and mass extinctions: Evidence for a Late Devonian asteroid impact. *Science*, 257: 1102-1104.

- Crozier, W.D., 1960. Black, magnetic spherules in sediments. *J. Geophys. Res.*, 65: 2971-2977.
- Czajkowski, J., 1987. Cosmo and geochemistry of the Jurassic hardgrounds (Ph.D. thesis). University of California, San Diego, 418pp.
- D'Hondt, S.L., Keller, G. and Stallard, R.F., 1987. Major element compositional variation within and between different late Eocene microtektite strewn fields. *Meteoritics*, 22: 61-79.
- Gao, Z., Xu, D., Zhang, Q. and Sun, Y., 1987. Discovery and study of microspherules at the Permian-Triassic boundary of the Shangsi Section, Guangyuan, Sichuan (in Chinese, with English abstract). *Geological Review*, 33: 203-211.
- Glass, B.P., 1982. *Introduction to Planetary Geology*. Cambridge Univ. Press, Cambridge, 469 pp.
- Glass, B.P., 1990. Tektites and microtektites: Key facts and inferences. *Tectonophysics*, 171: 393-404.
- Glass, B.P. and Burns, C.A., 1988. Microkrystites: A new term for impact-produced glassy spherules containing primary crystallites. *Proc. 18th Lun. Planet. Sci. Conf.*, 18: 455-458.
- Glass, B.P., Burns, C.A., Crosbie, J.R. and DuBois, D.L., 1985. Late Eocene North American microtektites and clinopyroxene-bearing spherules. *J. Geophys. Res.*, 90: D175-D196.
- Glenister, B.F., Klapper, G. and Chauff, K.M., 1976. Conodont pearls? *Science*, 193: 571-573.
- Hagen, E.H., Koeberl, C. and Faure, G., 1990. Extraterrestrial spherules in glacial sediments, Beardmore Glacier area, Transantarctic Mountains. *Antarctic Research Series*, 50: 19-24.
- Hansen, H.J., Gwozdz, R., Bromley, R.G., Rasmussen, K.L., Voegensen, E.W. and Pedersen, K.R., 1986. Cretaceous-Tertiary boundary spherules from Denmark, New Zealand, and Spain. *Bull. Geol. Soc. Denmark*, 35: 75-82.
- He, J., 1989. Restudy of the Permian-Triassic boundary clay in Meishan, Changxing, Zhejiang, China. *Historical Biology*, 2: 73-87.
- Heaton, B.S., 1979. Steel furnace slag as an aggregate in asphaltic concrete. In: I. Branch (Editor), *Utilisation of Steelplant Slags*.

- Australasian Institute of Mining and Metallurgy, Victoria, pp. 81-85.
- Holser, W.T., 1991. The Permian-Triassic of the Gartnerkofel-1 Core (Carnic Alps, Austria): Sulfur, organic carbon and microspherules. *Abh. Geol. B.-A.*, 45: 139-148.
- Hunter, W. and Parkin, D.W., 1961. Cosmic dust in Tertiary rock and the lunar surface. *Geochim. Cosmochim. Acta*, 24: 32-39.
- Izett, G.A., 1987. Authigenic spherules in K-T boundary sediments at Caravaca, Spain, and Raton Basin, Colorado and New Mexico, may not be impact derived. *Geol. Soc. Am. Bull.*, 99: 78-86.
- Izett, G.A., 1991. Tektites in Cretaceous/Tertiary boundary rocks on Haiti and their bearing on the Alvarez impact extinction hypothesis. *J. Geophys. Res.*, 96: 20879-20905.
- Jehanno, C., Boclet, D., Bonte, P., Castellarin, A. and Rocchia, R., 1988. Identification of two populations of extraterrestrial particles in a Jurassic hardground of the Southern Alps. *Proc. Lunar Planet. Sci. Conf.*, 20: 623-630.
- Jehanno, C., Boclet, Froget, L., Lambert, B., Robin, E., Rocchia, R. and Turpin, L., 1992. The Cretaceous/Tertiary boundary at Beloc, Haiti: No evidence for an impact in the Caribbean area. *Eur. Planet. Sci. Lett.*, 109: 229-241.
- Keller, G., D'Hondt, S. and Vallier, T.L., 1983. Multiple microtektite horizons in upper Eocene marine sediments: No evidence for mass extinctions. *Science*, 221: 150-152.
- Kerr, R.A., 1992. Another impact extinction? *Science*, 256: 1280.
- Koeberl, C. and Sigurdsson, H., 1992. Geochemistry of impact glasses from the K/T boundary in Haiti: Relation to smectites and a new type of glass. *Geochim. Cosmochim. Acta*, 56: 2113-2129.
- Kring, D. A. and Boynton, W.V., 1991. Altered spherules of impact melt and associated relic glass from the Cretaceous/Tertiary boundary sediments in Haiti. *Geochim. Cosmochim. Acta*, 55: 1737-1742.
- Kyte, F.T., 1988. The extraterrestrial component in marine sediments: Description and interpretation. *Paleoceanography*, 2: 235-247.

- Kyte, F.T. and Smit, J., 1986. Regional variations in spinel compositions: an important key to the Cretaceous/Tertiary boundary event. *Geology*, 14: 485-487.
- Leuteritz, K., Pietzner, H., Vahl, J. and Ziegler, W., 1972. Aufbau zusammensetzung und entstehung von calciumphosphat sphaeren in Palaozoischen kalken. *Geol. Palaeontol.*, 6: 111-137.
- Lowe, D.R. and Byerly, G.R., 1986. Early Archean silicate spherules of probable impact origin, South Africa and Western Australia. *Geology*, 14: 83-86.
- Lowe, D.R., Byerly, G.R., Asaro, F. and Kyte, F.J., 1989. Geological and Geochemical record of 3400-million-year-old terrestrial meteorite impacts. *Science*, 245: 959-962.
- Lyons, J.B. and Officer, C.B., 1992. Mineralogy and petrology of the Haiti Cretaceous/Tertiary section. *Eur. Planet. Sci. Lett.*, 109: 205-224.
- Magaritz, M., 1991. Carbon isotopes, time boundaries and evolution. *Terra Nova*, 3: 251-256.
- Margolis, S.V., Claeys, P. and Kyte, F.K., 1991. Microtektites, mikrokrystites, and spinels from a Late Pliocene asteroid impact in the Southern Ocean. *Science*, 251: 1594-1597.
- Marshall, R.R., 1961. Devitrification of natural glass. *Geol. Soc. Am. Bull.*, 72: 1493-1520.
- Marvin, V.B. and Einaudi, M.T., 1967. Black magnetic spherules from Pleistocene beach sands. *Geochim. Cosmochim. Acta*, 31: 1871-1884.
- Maurrasse, F.J.M. and Sen, G., 1991. Impacts, tsunamis, and the Haitian Cretaceous-Tertiary boundary layer. *Science*, 252: 1690-1693.
- Montanari, A., 1986. Spherules from the Cretaceous/Tertiary boundary clay at Gubbio, Italy: The problem of outcrop contamination. *Geology*, 14: 1024-1026.
- Montanari, A., Hay, R.L., Alvarez, W., Asaro, F., Michel, H.V. and Alvarez, L.W., 1983. Spheroids at the Cretaceous/Tertiary boundary are altered impact droplets of basaltic composition. *Geology*, 11: 668-671.

- Mutch, T.A., 1964. Volcanic ashes compared with Paleozoic salts containing extraterrestrial spherules. *J. Geophys. Res.*, 69: 4735-4740.
- Mutch, T.A., 1966. Abundances of magnetic spherules in Silurian and Permian salt samples. *Earth Planet. Sci. Lett.*, 1: 325-329.
- Mutch, T.A. and Garrison, R.E., 1967. Determination of sedimentation rates by magnetic spherule abundances. *J. Sediment. Petrol.*, 37:1139-1146.
- Naslund, H.R., Officer, C.B. and Johnson, G.D., 1986. Microspherules in Upper Cretaceous and lower Tertiary clay layers at Gubbio, Italy. *Geology*, 14: 923-926.
- Palmer, H.C., Tazaki, K., Fyfe, W.S. and Zhou, Z., 1988. Precambrian glass. *Geology*, 16: 221-224.
- Sandberg, C.A., Ziegler, W., Dreesen, R. and Butler, J.L., 1988. Late Devonian mass extinctions: Conodont event stratigraphy, global changes, and possible causes. *Courier Forschungsinstitut Senckenberg*, 102: 263-307.
- Schmincke, H.U. and Pritchard, G., 1981. Carboniferous volcanic glass from submarine hyaloclastite, Lahn-Dill area, Germany. *Naturwissenschaften*, 68: 615-616.
- Shervais, J.W. and Hanan, B.B., 1989. Jurassic volcanic glass from the Stonyford volcanic complex, Franciscan assemblage, northern California Coast Ranges. *Geology*, 17: 510-514.
- Sigurdsson, H., D'Hondt, S., Arthur, M.A., Bralower, T.J. Zachos, J.C., Fossen, V. and Channell, J.E.T., 1991. Glass from the Cretaceous/Tertiary boundary in Haiti. *Nature*, 349: 482-487.
- Simonson, B.M., 1992. Geological evidence for a strewn field of impact spherules in the early Precambrian Hamersley Basin of Western Australia. *Geol. Soc. Am. Bull.*, 104: 829-839.
- Skolnik, H., 1961. Ancient meteoritic dust. *Geol. Soc. Am. Bull.*, 72: 1837-1841.
- Smit, J. and Klaver, G., 1981. Sanidine spherules at the Cretaceous/Tertiary boundary indicate a large impact event. *Nature*, 292: 47-49.

- Smit, J. and Kyte, F.T., 1984. Siderophile-rich magnetic spheroids from the Cretaceous/Tertiary boundary in Umbria, Italy. *Nature*, 310: 403-405.
- Smit, J., Montanari, A., Swinburne, N.H.M., Alvarez, W., Hildebrand, A.R., Margolis, S.V., Claeys, P., Lowrie, W. and Asaro, F., 1992. Tektite-bearing, deep-water clastic unit at the Cretaceous/Tertiary boundary in northern Mexico. *Geology*, 20: 99-103.
- Smit, J. and Romein, A.J.T., 1985. A sequence of events across the Cretaceous/Tertiary boundary. *Eur. Planet. Sci. Lett.*, 74: 155-170.
- Stauffer, C.R., 1935. The conodont fauna of the Decorah Shale (Ordovician). *J. Paleont.*, 9: 596-620.
- Stauffer, C.R., 1940. Conodonts from the Devonian and associated clays of Minnesota. *J. Paleont.*, 14: 417-435.
- Taburiaux, J., 1985. *Pearls: Their Origins, Treatment and Identification*. N.A.G. Press, Ipswich, 247 pp.
- Taylor, S. and Brownlee, D.E., 1991. Cosmic spherules in the geologic record. *Meteoritics*, 26: 203-211.
- Wallace, M.W., Gostin, V.A. and Keays, R.R., 1990. Spherules and shard-like clasts from the late Proterozoic Acraman impact ejecta horizon, South Australia. *Meteoritics*, 25: 161-165.
- Walliser, O.H., 1984. Geologic processes and global events. *Terra Cognita*, 4: 17-20.
- Wang, K., 1991. Glassy silicate microspherules from an Upper Devonian sediment: Microtektites? *Geol. Soc. Am. Abstr. Progr.*, 23: A227.
- Wang, K., 1992. Glassy microspherules (microtektites) from an Upper Devonian limestone. *Science*, 256: 1547-1550.
- Williams, D.F., Lerche, I. and Full, W.F., 1988. *Isotope Chronostratigraphy: Theory and Methods*. Academic Press, San Diego, 345 pp.
- Xu, D., Zhang, Q., Sun, Y. and Yan, Z., 1986. Three mass extinctions: Significant indicators of major natural division of geological history in the Phanerozoic. *Modern Geology*, 10: 365-375.

- Xu, D., Zhang, Q., Sun, Y., Yan, Z., Chai, Z. and He, J., 1989. Astrogeological Events in China. Scottish Academic Press, Edinburgh, 264 pp.
- Yin, H., Huang, S., Zhang, K., Yang, F., Ding, M., Bi, X. and Zhang, S., 1989. Volcanism at the Permian-Triassic boundary in South China and its effects on mass extinction (in Chinese, with English abstract). *Acta Geologica Sinica*, 63: 169-181.
- Youngquist, W. and Miller, A.K., 1948. Additional conodonts from the Sweetland Creek Shale of Iowa. *J. Paleont.*, 22: 440-450.

## Chapter 9

### Conclusions

This Ph.D. thesis study has dealt with three global (and near global) scale geologic events in the middle Paleozoic, using an integrated approach which combines geochemistry (trace elements, carbon and oxygen stable isotopes), sedimentology (microfacies), and paleontology to analyze sedimentary rocks collected from the most important intervals of these events in stratigraphic sections from both Canada and China. In addition, microspherules with different origins found in Paleozoic sediments were evaluated as to their significance as geologic event and/or stratigraphic markers.

A general picture for the latest Ordovician mass extinction seems clear. There exists a global geochemical anomaly associated with the extinction in many sections around the world, e.g., South China (Wang et al., 1992, in press), Northwestern Canada (Wang et al., submitted; Goodfellow et al., 1992), Quebec (Orth et al., 1986), and Scotland (Wilde et al., 1986). However, this geochemical anomaly is probably terrestrial in origin, most likely owing to a condensed sequence near the base of a global transgression (Wang et al., 1992, in press, submitted). Carbon isotope data from many sections around the world suggest that the main episodes of the late Ordovician extinction may have occurred at times when there were dramatic changes in the atmospheric and oceanic CO<sub>2</sub> levels, associated with the growth (low CO<sub>2</sub> levels) and decay (high CO<sub>2</sub> levels) of the Gondwanan ice sheets (Wang et al., in press). But what was driving the CO<sub>2</sub> levels up and down during that period of time remains uncertain.

After many years of search for iridium at the Frasnian-Famennian extinction boundary in many areas in the world, an Ir anomaly has been found to be associated with a  $\delta^{13}\text{C}$  excursion at the Frasnian-Famennian boundary in South China (Wang et al., 1991) that is suggestive of a meteorite impact at the time of the Frasnian-Famennian extinction. Although the Ir was the only evidence at the time of publication of the paper, the impact



hypothesis has now received strong support from the recent discovery of Frasnian-Famennian microtektites in Belgium (Claeys et al., 1992).

For the first time, 365-ma-old microtektites have been found in the early Famennian conodont crepida Zone (Wang, 1992), which documents the earliest known impact tektite glass to date (Science News, 1992). The microtektites occur together with a minor Ir anomaly, a  $\delta^{13}\text{C}$  excursion, and a brachiopod faunal turnover in South China (Wang and Bai, 1989). A strong Ir anomaly and a  $\delta^{13}\text{C}$  excursion were previously reported to occur in the same conodont zone in Western Australia (Playford et al., 1984) which was located then very close to the South China Plate. Based on these additional geochemical and paleontological data from South China and Australia, an impact-extinction model was proposed, hypothesizing that an impact occurred in the early Famennian on the South China Plate and probably caused a regional extinction on eastern Gondwana (Wang and Geldsetzer, 1992).

A study of different types of microspherules found in Paleozoic sediments (Wang and Chatterton, submitted) indicates that, after the spherules are properly studied, their origins can be inferred with confidence. Natural spherules have varying significance as geologic event and sedimentary (or stratigraphic) markers.

## References

- Claeys, P., Casier, J.G., and Margolis, S.V., 1992. Microtektites and mass extinctions: Evidence for a Late Devonian asteroid impact. *Science*, 257: 1102-1104.
- Goodfellow, W.D., Nowlan, G.S., McCracken, A.D., Lenz, A.C. and Grégoire, D.C., 1992. Geochemical anomalies near the Ordovician-Silurian boundary, northern Yukon Territory, Canada. *Historical Biology*, 6: 1-23.
- Orth, C.J., Gilmore, L.R., Quintana, L.R. and Sheehan, P.M., 1986. Terminal Ordovician extinction: Geochemical analysis of the Ordovician/Silurian boundary, Anticosti Island, Quebec. *Geology*, 14: 433-436.

- Playford, P.E., McLaren, D.J., Orth, C.J., Gilmore, J.S., and Goodfellow, W.D., 1984. Iridium anomaly in the Upper Devonian of the Canning Basin, Western Australia. *Science*, 226: 437-439.
- Science News*, 1992. Glassy evidence for multiple crashes. 142.1: 15.
- Wang, K., 1992. Glassy microspherules (microtektites) from an Upper Devonian limestone. *Science*, 256: 1547-1550.
- Wang, K. and Bai, S., 1989. Faunal changes and events near the Frasnian-Famennian boundary of South China. *Canadian Society of Petroleum Geologists Memoir*, 14(3): 71-78.
- Wang, K. and Chatterton, B.D.E., Submitted. Microspherules from Paleozoic marine sediments. *Sedimentary Geology*.
- Wang, K., Chatterton, B.D.E., Orth, C.J., and Attrep, M., 1992. Iridium abundance maxima at the latest Ordovician mass extinction horizon: Terrestrial or extra-terrestrial? *Geology*, 20: 39-42.
- Wang, K., Chatterton, B.D.E., Attrep, M. Jr., and Orth, C.J., Submitted. Late Ordovician mass extinction event on northwestern Laurentia: Geochemical, paleontological, and sedimentological analyses of the Ordovician-Silurian boundary interval, Mackenzie Mountains, N.W.T. *Canadian Journal of Earth Sciences*.
- Wang, K. and Geldsetzer, H.H.J., 1992. A Late Devonian impact event and its association with a possible extinction event on eastern Gondwana. *Lunar and Planetary Institute Contribution*, 790: 77-78.
- Wang, K., Orth, C.J., Attrep, M., Jr., Chatterton, B.D.E., Hou, H., and Geldsetzer, H.H.J., 1991. Geochemical evidence for a catastrophic biotic event at the Frasnian/Famennian boundary in south China. *Geology*, 19: 776-779.
- Wang, K., Orth, C.J., Attrep, M. Jr., Chatterton, B.D.E., Wang, X., and Li, J., In press, The great latest Ordovician extinction on the South China Plate: Chemostratigraphic studies of the Ordovician-Silurian boundary interval on the Yangtze Platform. *Palaeogeography, Palaeoclimatology, Palaeoecology*.
- Wilde, P., Berry, W.B.N., Quinby-Hunt, M.S., Orth, C.J., Quintana, L.R. and Gilmore, J.S., 1986. Iridium abundances across the Ordovician-Silurian stratotype. *Science*, 233: 339-341.

## Appendix 1

Analytical results of  $\delta^{13}\text{C}$ ,  $\delta^{18}\text{O}$  and Ir in carbonate samples from the AV 4B Section, Mackenzie Mountains, N.W.T.

| Sample | Lab number | $\delta^{13}\text{C}$ | $\delta^{18}\text{O}$ | Ir   |
|--------|------------|-----------------------|-----------------------|------|
| AV 43  | 905001     | 0.10                  | -6.49                 | 2.0  |
| AV 42  | 905002     | 0.69                  | -6.90                 | 9.3  |
| AV 41  | 905003     | 0.88                  | -7.07                 |      |
| AV 39A | 905004     | 0.68                  | -7.48                 | 13.7 |
| AV 40  | 905006     | 0.74                  | -6.47                 |      |
| AV 38  | 905007     | 1.66                  | -6.69                 |      |
| AV 37  | 905008     | 0.83                  | -8.86                 | 1.5  |
| AV 36  | 905009     | 1.09                  | -6.68                 |      |
| AV 35  | 905010     | 1.65                  | -7.08                 |      |
| AV 34  | 905011     | 1.11                  | -6.76                 |      |
| AV 33  | 905012     | 0.92                  | -7.59                 | 3.3  |
| AV 32  | 905013     | 1.32                  | -5.99                 |      |
| AV 31  | 905014     | 2.11                  | -6.41                 |      |
| AV 30  | 905015     | 1.11                  | -8.82                 |      |
| AV 29  | 905016     | 1.92                  | -5.77                 | 1.3  |
| AV 28  | 905017     | 2.13                  | -6.79                 | 9.4  |
| AV 27  | 905018     | 1.70                  | -9.05                 | 5.1  |
| AV 26  | 905019     | 1.78                  | -7.56                 | 8.4  |
| AV A   | 905062     |                       |                       | 9    |
| AV E   | 905063     |                       |                       | 3.4  |
| AV 25A | 905020     | 2.19                  | -6.90                 | 1.7  |
| AV B   | 905064     |                       |                       | 1.0  |
| AV 25B | 905021     | 1.70                  | -7.16                 | 1.8  |
| AV C   | 905065     | 1.55                  | -6.56                 | 1.1  |
| AV 23A | 905022     | 1.50                  | -6.81                 | 3.6  |
| AV 23B | 905023     | 1.56                  | -7.00                 | 3.5  |
| AV 23C | 905024     | 1.49                  | -6.44                 | 3.2  |
| AV 22A | 905025     | 0.20                  | -6.49                 | 1.0  |
| AV 22B | 905026     | -0.13                 | -6.81                 | 8.7  |
| AV 22C | 905027     | 1.98                  | -6.05                 | 3.2  |

$\delta^{13}\text{C}$  and  $\delta^{18}\text{O}$  are in per mil relative to PDB standard.  
Ir is in ppt ( $10^{-12}\text{g/g}$ ).

| Sample | Lab number | $\delta^{13}\text{C}$ | $\delta^{18}\text{O}$ | Ir  |
|--------|------------|-----------------------|-----------------------|-----|
| AV 22D | 905028     | 2.03                  | -6.12                 | 2.4 |
| AV 22E | 905029     | 1.37                  | -6.56                 | 5.7 |
| AV 22F | 905030     | 0.27                  | -6.85                 | 10  |
| AV 22G | 905031     | 0.37                  | -6.81                 | 7   |
| AV 21  | 905032     | 0.34                  | -7.26                 | 15  |
| AV D   | 905068     |                       |                       | 24  |
| AV 1A  | 905033     | -0.17                 | -6.27                 | 7   |
| AV 1B  | 905034     | 0.11                  | -7.65                 | 4.3 |
| AV 1C  | 905035     | -1.31                 | -7.06                 | 3.6 |
| AV 1D  | 905036     | -0.94                 | -6.86                 | 4   |
| AV 1E  | 905037     | 2.28                  | -6.18                 | 2.6 |
| AV 1F  | 905038     | 1.87                  | -6.62                 | 3.1 |
| AV 2A  | 905039     | 0.56                  | -6.74                 | 3.7 |
| AV 2B  | 905040     | 0.39                  | -6.77                 | 2.2 |
| AV 2C  | 905041     | 0.28                  | -6.26                 | 3.5 |
| AV 2D  | 905042     | 1.04                  | -6.31                 |     |
| AV 3A  | 905043     | 1.12                  | -6.79                 | 5   |
| AV 3B  | 905044     | 0.44                  | -7.31                 | 5.8 |
| AV 4A  | 905045     | 0.88                  | -6.57                 | 6.2 |
| AV 4B  | 905046     | 0.14                  | -6.58                 |     |
| AV 4C  | 905047     | 0.23                  | -6.38                 | 4.6 |
| AV 4D  | 905048     | -0.49                 | -6.51                 |     |
| AV 6A  | 905049     | 0.47                  | -6.19                 | 4.9 |
| AV 6B  | 905050     | 0.07                  | -6.61                 |     |
| AV 7A  | 905051     | -0.05                 | -6.89                 |     |
| AV 7B  | 905052     | -0.39                 | -6.78                 | 16  |
| AV 7C  | 905053     | -0.58                 | -7.07                 |     |
| AV 7D  | 905054     | -0.02                 | -7.34                 |     |
| AV 8   | 905055     | -0.05                 | -7.16                 | 16  |
| AV 9   | 905056     | -0.45                 | -6.88                 |     |
| AV 10  | 905057     | -0.37                 | -6.60                 |     |
| AV 11  | 905058     | 0.32                  | -6.91                 | 4.4 |
| AV 12A | 905059     | 0.41                  | -6.26                 |     |
| AV 12B | 905060     | 0.44                  | -6.25                 | 8   |
| AV 13  | 905061     | 0.54                  | -6.15                 |     |

$\delta^{13}\text{C}$  and  $\delta^{18}\text{O}$  are in per mil relative to PDB standard.  
Ir is in ppt ( $10^{-12}\text{g/g}$ ).

## **Appendix 2**

NAA results of elemental abundances (all in ppm) in samples from the AV 4B Section, Mackenzie Mountains, N.W.T.

|        | 905001        | 905002         | 905003         | 905004        | 905005         |
|--------|---------------|----------------|----------------|---------------|----------------|
| Na-23  | 159 ± 8       | 2010 ± 80      | 1700 ± 70      | 1050 ± 50     | 1510 ± 60      |
| Mg-27  | 13700 ± 700   | 7600 ± 500     | 7800 ± 500     | 8300 ± 400    | 9900 ± 500     |
| Al-28  | 25000 ± 700   | 11700 ± 400    | 13500 ± 400    | 12800 ± 400   | 15000 ± 500    |
| Cl-38  | <40           | <60            | 63 ± 14        | <50           | <60            |
| K-42   | 18300 ± 1200  | 6700 ± 500     | 8900 ± 600     | 8200 ± 500    | 10300 ± 700    |
| Ca-49  | 111000 ± 5000 | 304000 ± 12000 | 293000 ± 12000 | 228000 ± 9000 | 244000 ± 10000 |
| Sc-46  | 4.52 ± 0.24   | 2.36 ± 0.13    | 2.84 ± 0.15    | 2.78 ± 0.15   | 3.09 ± 0.16    |
| Ti-51  | 1890 ± 250    | 740 ± 130      | 860 ± 140      | 760 ± 110     | 840 ± 130      |
| V-52   | 60 ± 3        | 23.0 ± 1.3     | 29.2 ± 1.5     | 27.1 ± 1.4    | 29.3 ± 1.5     |
| Cr-51  | 74 ± 4        | 27.5 ± 1.7     | 36.6 ± 2.2     | 37.1 ± 2.2    | 46 ± 3         |
| Mn-56  | 56 ± 3        | 90 ± 4         | 84 ± 4         | 80 ± 4        | 77 ± 4         |
| Fe-59  | 8200 ± 500    | 4100 ± 300     | 5300 ± 300     | 6000 ± 300    | 8700 ± 600     |
| Co-60  | 2.11 ± 0.14   | 1.89 ± 0.11    | 1.61 ± 0.16    | 2.35 ± 0.13   | 3.07 ± 0.18    |
| Cu-66  | <80           | <90            | <90            | <90           | <90            |
| Zn-65  | 20 ± 4        | 11.9 ± 2.4     | <4             | 19 ± 3        | <5             |
| Ga-72  | 6.3 ± 0.9     | <6             | <6             | <5            | <6             |
| As-76  | 2.9 ± 0.3     | 1.24 ± 0.17    | 1.70 ± 0.22    | 1.86 ± 0.22   | 1.91 ± 0.22    |
| Se-75  | <3            | 0.52 ± 0.23    | <1.5           | <1.7          | <2.3           |
| Br-82  | <0.8          | <1.1           | <0.9           | 0.25 ± 0.10   | <1.0           |
| Rb-86  | 43 ± 3        | 15.1 ± 1.4     | 20.8 ± 1.6     | 20.1 ± 1.4    | 24.1 ± 1.7     |
| Sr-87  | 260 ± 40      | 800 ± 70       | 790 ± 70       | 630 ± 60      | 650 ± 60       |
| Zr-95  | <100          | <70            | <80            | <70           | <80            |
| Ag-110 | <1.8          | <1.4           | <1.3           | <1.2          | <1.6           |
| In-116 | <0.07         | <0.10          | <0.08          | <0.07         | <0.07          |
| Sb-122 | 0.154 ± 0.025 | <0.11          | <0.11          | <0.09         | <0.11          |
| I-128  | <7            | <7             | <6             | <6            | <8             |
| Cs-134 | 1.73 ± 0.12   | 0.70 ± 0.08    | 0.87 ± 0.07    | 1.02 ± 0.07   | 1.05 ± 0.11    |
| Ba-131 | 110 ± 30      | <120           | <110           | 36 ± 12       | 70 ± 30        |
| Ba-139 | <1500         | <1700          | <1600          | <1500         | <1600          |
| La-140 | 15.1 ± 0.8    | 12.2 ± 0.6     | 11.8 ± 0.6     | 8.5 ± 0.4     | 12.8 ± 0.6     |
| Ce-141 | 23.8 ± 1.4    | 16.7 ± 1.1     | 18.7 ± 1.1     | 12.9 ± 0.8    | 19.2 ± 1.2     |
| Nd-147 | 11.1 ± 1.1    | 8.1 ± 0.8      | 6.1 ± 0.6      | 6.8 ± 0.7     | 9.3 ± 0.9      |
| Sm-153 | 1.74 ± 0.08   | 1.84 ± 0.09    | 1.36 ± 0.07    | 1.17 ± 0.06   | 1.68 ± 0.08    |
| Eu-152 | 0.30 ± 0.06   | 0.29 ± 0.05    | 0.30 ± 0.06    | 0.281 ± 0.013 | 0.32 ± 0.06    |
| Tb-160 | 0.20 ± 0.04   | 0.224 ± 0.022  | 0.07 ± 0.03    | 0.211 ± 0.023 | 0.200 ± 0.024  |
| Dy-165 | 1.36 ± 0.15   | 1.65 ± 0.19    | 1.20 ± 0.14    | 1.32 ± 0.14   | 1.41 ± 0.17    |
| Yb-175 | 0.83 ± 0.06   | 0.78 ± 0.12    | 0.72 ± 0.07    | 0.92 ± 0.08   | 0.93 ± 0.08    |
| Lu-177 | 0.117 ± 0.009 | 0.098 ± 0.007  | 0.101 ± 0.008  | 0.105 ± 0.007 | 0.114 ± 0.008  |
| Hf-181 | 1.67 ± 0.16   | 0.60 ± 0.04    | 0.80 ± 0.05    | 0.75 ± 0.05   | 0.91 ± 0.05    |
| Ta-182 | 0.34 ± 0.11   | <0.15          | 0.107 ± 0.023  | 0.149 ± 0.023 | <0.20          |
| W-187  | <1.3          | <1.5           | <1.5           | <1.3          | <1.6           |
| Au-198 | <0.004        | <0.004         | <0.003         | <0.004        | <0.004         |
| Hg-203 | <0.3          | <0.24          | <0.20          | <0.21         | <0.3           |
| Th-233 | 3.81 ± 0.16   | 1.26 ± 0.06    | 1.92 ± 0.22    | 1.80 ± 0.08   | 2.22 ± 0.10    |
| U-235  | 2.05 ± 0.08   | 1.26 ± 0.05    | 1.27 ± 0.05    | 1.28 ± 0.05   | 1.49 ± 0.06    |

|        | 905006        | 905007         | 905008        | 905009        | 905010         |
|--------|---------------|----------------|---------------|---------------|----------------|
| Na-24  | 850 ± 40      | 2370 ± 100     | 165 ± 10      | 700 ± 30      | 1300 ± 60      |
| Mg-27  | 11600 ± 600   | 6500 ± 500     | 5700 ± 300    | 11000 ± 700   | 3680 ± 250     |
| Al-28  | 24800 ± 700   | 13700 ± 400    | 17900 ± 500   | 19700 ± 600   | 5110 ± 200     |
| Cl-38  | <50           | <70            | <30           | <50           | 54 ± 11        |
| K-42   | 17700 ± 1100  | 8400 ± 600     | 13900 ± 900   | 13700 ± 900   | 2400 ± 200     |
| Ca-49  | 175000 ± 7000 | 306000 ± 12000 | 75000 ± 3000  | 121000 ± 5000 | 364000 ± 14000 |
| Sc-46  | 4.13 ± 0.22   | 2.99 ± 0.16    | 3.41 ± 0.18   | 3.79 ± 0.20   | 1.32 ± 0.07    |
| Ti-51  | 1470 ± 200    | 560 ± 110      | 880 ± 120     | 1290 ± 170    | <1700          |
| V-52   | 47 ± 5        | 26.5 ± 1.5     | 39.9 ± 1.8    | 45.2 ± 2.0    | 11.0 ± 0.9     |
| Cr-51  | 70 ± 4        | 43 ± 3         | 60 ± 4        | 79 ± 5        | 15.3 ± 1.0     |
| Mn-56  | 63 ± 3        | 67 ± 3         | 32.9 ± 1.4    | 45.6 ± 2.0    | 77 ± 3         |
| Fe-59  | 11000 ± 600   | 5500 ± 300     | 8300 ± 500    | 7900 ± 500    | 10000 ± 600    |
| Co-60  | 4.20 ± 0.23   | 1.76 ± 0.17    | 3.46 ± 0.19   | 2.02 ± 0.13   | 1.46 ± 0.09    |
| Cu-66  | <90           | <90            | <70           | <70           | <80            |
| Zn-65  | 18 ± 3        | <4             | 35 ± 5        | 24 ± 4        | 11.1 ± 2.2     |
| Ga-72  | 5.2 ± 1.0     | <7             | <4            | <5            | <5             |
| As-76  | 3.7 ± 0.4     | 1.88 ± 0.24    | 2.8 ± 0.3     | 2.08 ± 0.23   | 1.73 ± 0.21    |
| Se-75  | <2.2          | <1.6           | 1.3 ± 0.3     | 0.7 ± 0.3     | <1.4           |
| Br-82  | <1.0          | <1.0           | 0.42 ± 0.08   | <0.8          | <0.9           |
| Rb-86  | 36.9 ± 2.4    | 19.9 ± 1.7     | 32.3 ± 2.1    | 38.8 ± 2.2    | 5.5 ± 1.2      |
| Sr-87  | 610 ± 60      | 630 ± 60       | 140 ± 30      | 320 ± 40      | 880 ± 70       |
| Zr-95  | <100          | <90            | <80           | <90           | <60            |
| Ag-110 | <1.9          | <1.4           | <1.4          | <1.6          | <1.2           |
| In-116 | <0.09         | <0.08          | <0.05         | <0.06         | <0.09          |
| Sb-122 | 0.14 ± 0.04   | <0.12          | 0.155 ± 0.025 | 0.147 ± 0.023 | <0.09          |
| I-128  | <6            | <6             | <4            | <6            | <6             |
| Cs-134 | 1.48 ± 0.12   | 0.88 ± 0.11    | 1.29 ± 0.08   | 1.79 ± 0.12   | 0.28 ± 0.03    |
| Ba-131 | 70 ± 30       | 62 ± 12        | 74 ± 14       | 70 ± 30       | <100           |
| Ba-139 | 83 ± 21       | <1700          | 70 ± 13       | <1500         | <1500          |
| La-140 | 19.3 ± 1.0    | 13.8 ± 0.8     | 5.4 ± 0.3     | 7.9 ± 0.4     | 10.9 ± 0.6     |
| Ce-141 | 24.0 ± 1.5    | 19.5 ± 1.1     | 7.7 ± 0.7     | 12.0 ± 1.1    | 13.2 ± 0.9     |
| Nd-147 | 9.2 ± 1.0     | 7.9 ± 0.8      | 4.4 ± 0.5     | 7.7 ± 0.9     | 5.5 ± 0.6      |
| Sm-153 | 1.92 ± 0.09   | 1.39 ± 0.07    | 0.74 ± 0.03   | 1.33 ± 0.07   | 1.55 ± 0.08    |
| Eu-152 | 0.32 ± 0.06   | 0.39 ± 0.07    | 0.19 ± 0.05   | 0.27 ± 0.05   | 0.27 ± 0.05    |
| Tb-160 | 0.20 ± 0.03   | <0.06          | <0.18         | 0.160 ± 0.019 | 0.172 ± 0.018  |
| Dy-165 | 1.49 ± 0.18   | 1.32 ± 0.17    | 0.87 ± 0.10   | 1.13 ± 0.13   | 1.26 ± 0.15    |
| Yb-175 | 0.99 ± 0.08   | 0.87 ± 0.14    | 0.44 ± 0.05   | 0.72 ± 0.05   | 0.82 ± 0.06    |
| Lu-177 | 0.114 ± 0.010 | 0.118 ± 0.009  | 0.080 ± 0.006 | 0.109 ± 0.009 | 0.096 ± 0.007  |
| Hf-181 | 1.32 ± 0.09   | 0.61 ± 0.04    | 0.97 ± 0.09   | 1.16 ± 0.11   | 0.19 ± 0.03    |
| Ta-182 | 0.32 ± 0.03   | 0.121 ± 0.021  | 0.20 ± 0.03   | 0.30 ± 0.13   | <0.18          |
| W-187  | <1.5          | <1.7           | <1.1          | <1.3          | <1.3           |
| Au-198 | <0.004        | <0.004         | <0.003        | <0.004        | <0.004         |
| Hg-203 | <0.3          | <0.22          | <0.23         | <0.3          | <0.21          |
| Th-233 | 3.17 ± 0.13   | 1.64 ± 0.18    | 2.31 ± 0.23   | 2.51 ± 0.10   | 0.44 ± 0.03    |
| U-235  | 1.89 ± 0.07   | 1.51 ± 0.06    | 1.54 ± 0.06   | 2.20 ± 0.08   | 1.01 ± 0.04    |

|        | <i>905011a</i> | <i>905012</i> | <i>905013</i> | <i>905014</i>  | <i>905015</i> |
|--------|----------------|---------------|---------------|----------------|---------------|
| Na-24  | 970 ± 40       | 1100 ± 50     | 480 ± 20      | 1240 ± 50      | 670 ± 30      |
| Mg-27  | 7900 ± 400     | 9000 ± 500    | 7800 ± 500    | 4700 ± 500     | 13800 ± 700   |
| Al-28  | 18400 ± 600    | 25400 ± 800   | 16900 ± 500   | 9700 ± 300     | 33500 ± 1000  |
| Cl-38  | <60            | <50           | <50           | <60            | 81 ± 16       |
| K -42  | 15200 ± 1000   | 19700 ± 1200  | 13700 ± 900   | 6000 ± 400     | 26900 ± 1700  |
| Ca-49  | 228000 ± 9000  | 182000 ± 7000 | 211000 ± 8000 | 351000 ± 14000 | 177000 ± 7000 |
| Sc-46  | 3.66 ± 0.19    | 4.24 ± 0.22   | 3.41 ± 0.18   | 2.08 ± 0.11    | 5.2 ± 0.3     |
| Ti-51  | 1120 ± 160     | 1760 ± 240    | 950 ± 140     | 400 ± 90       | 2200 ± 300    |
| V -52  | 41.3 ± 1.9     | 60 ± 3        | 38.9 ± 1.8    | 19.6 ± 1.2     | 80 ± 3        |
| Cr-51  | 73 ± 4         | 97 ± 6        | 64 ± 4        | 29.8 ± 1.8     | 120 ± 7       |
| Mn-56  | 59.5 ± 2.5     | 60 ± 3        | 57.7 ± 2.4    | 66 ± 3         | 53 ± 3        |
| Fe-59  | 7400 ± 400     | 9000 ± 500    | 6000 ± 300    | 4600 ± 300     | 10200 ± 600   |
| Co-60  | 2.09 ± 0.14    | 2.33 ± 0.19   | 2.57 ± 0.14   | 1.78 ± 0.12    | 3.82 ± 0.23   |
| Cu-66  | <80            | <100          | <80           | <90            | <90           |
| Zn-65  | <6             | <4            | 21 ± 3        | 21 ± 3         | 23 ± 4        |
| Ga-7   | <5             | 4.3 ± 1.1     | 3.8 ± 0.7     | <5             | 5.2 ± 1.3     |
| As-76  | 1.87 ± 0.21    | 2.2 ± 0.3     | 1.68 ± 0.19   | 1.17 ± 0.17    | 2.6 ± 0.3     |
| Se-75  | 0.6 ± 0.3      | <1.9          | 1.3 ± 0.4     | <1.9           | 1.0 ± 0.4     |
| Br-82  | <0.9           | <0.9          | <0.8          | <0.9           | <0.9          |
| Rb-86  | 34.2 ± 2.2     | 46 ± 3        | 30.0 ± 1.9    | 12.9 ± 1.3     | 61 ± 3        |
| Sr-87  | 500 ± 50       | 360 ± 40      | 520 ± 50      | 1130 ± 90      | 340 ± 40      |
| Zr-95  | <90            | <60           | <80           | <70            | <110          |
| Ag-110 | <1.6           | <1.7          | <1.3          | <1.2           | <2.1          |
| In-116 | <0.07          | <0.08         | <0.07         | <0.09          | <0.08         |
| Sb-122 | <0.09          | 0.16 ± 0.03   | 0.11 ± 0.03   | <0.09          | <0.11         |
| I -128 | <7             | <6            | <6            | <6             | <6            |
| Cs-134 | 1.37 ± 0.09    | 1.87 ± 0.11   | 1.29 ± 0.10   | 0.50 ± 0.05    | 2.51 ± 0.15   |
| Ba-131 | 80 ± 30        | 80 ± 40       | 80 ± 14       | <120           | 120 ± 40      |
| Ba-139 | <1500          | 131 ± 23      | <1500         | <1700          | <1600         |
| La-140 | 9.5 ± 0.5      | 10.0 ± 0.5    | 8.5 ± 0.4     | 11.2 ± 0.6     | 10.4 ± 0.6    |
| Ce-141 | 14.0 ± 1.1     | 13.8 ± 1.2    | 11.8 ± 0.8    | 14.7 ± 1.0     | 13.5 ± 1.3    |
| Nd-147 | 7.0 ± 0.8      | 5.7 ± 0.7     | 6.7 ± 0.7     | 7.1 ± 0.8      | 9.3 ± 1.1     |
| Sm-153 | 1.54 ± 0.07    | 1.34 ± 0.07   | 1.24 ± 0.06   | 1.44 ± 0.07    | 1.31 ± 0.07   |
| Eu-152 | 0.32 ± 0.06    | 0.36 ± 0.08   | 0.28 ± 0.06   | 0.33 ± 0.06    | 0.37 ± 0.08   |
| Tb-160 | 0.20 ± 0.03    | <0.06         | 0.132 ± 0.019 | 0.190 ± 0.020  | 0.18 ± 0.03   |
| Dy-165 | 1.43 ± 0.15    | 1.66 ± 0.17   | 1.25 ± 0.14   | 1.10 ± 0.16    | 1.62 ± 0.18   |
| Yb-175 | 0.82 ± 0.07    | 1.07 ± 0.08   | 0.76 ± 0.05   | 0.83 ± 0.08    | 0.91 ± 0.08   |
| Lu-177 | 0.117 ± 0.010  | 0.161 ± 0.011 | 0.117 ± 0.009 | 0.113 ± 0.007  | 0.122 ± 0.010 |
| Hf-181 | 1.16 ± 0.10    | 1.60 ± 0.11   | 1.08 ± 0.13   | 0.43 ± 0.03    | 1.99 ± 0.18   |
| Ta-182 | 0.27 ± 0.03    | 0.33 ± 0.11   | 0.208 ± 0.024 | <0.22          | <0.4          |
| W -187 | <1.4           | <0.8          | <1.2          | <1.3           | <1.5          |
| Au-198 | <0.004         | <0.004        | <0.003        | <0.004         | <0.003        |
| Hg-203 | <0.3           | <0.3          | <0.23         | <0.23          | <0.4          |
| Th-233 | 2.74 ± 0.11    | 3.52 ± 0.14   | 2.50 ± 0.10   | 0.96 ± 0.05    | 4.48 ± 0.18   |
| U -235 | 2.02 ± 0.07    | 2.81 ± 0.10   | 1.86 ± 0.07   | 1.00 ± 0.04    | 3.33 ± 0.12   |



|        | 905016         | 905017         | 905018        | 905019         | 905020         |
|--------|----------------|----------------|---------------|----------------|----------------|
| Na-24  | 1080 ± 50      | 1240 ± 50      | 470 ± 20      | 1140 ± 50      | 580 ± 30       |
| Mg-27  | 5900 ± 300     | 5500 ± 300     | 14400 ± 800   | 4500 ± 300     | 2610 ± 180     |
| Al-28  | 12800 ± 400    | 8500 ± 300     | 36900 ± 1100  | 6700 ± 300     | 2330 ± 130     |
| Cl-38  | <60            | 79 ± 11        | <50           | <70            | 245 ± 25       |
| K-42   | 8200 ± 500     | 5200 ± 400     | 29300 ± 1800  | 3700 ± 300     | 950 ± 140      |
| Ca-49  | 326000 ± 13000 | 405000 ± 16000 | 134000 ± 6000 | 385000 ± 15000 | 327000 ± 13000 |
| Sc-46  | 2.85 ± 0.15    | 2.23 ± 0.12    | 5.9 ± 0.3     | 1.57 ± 0.08    | 0.66 ± 0.03    |
| Ti-51  | 820 ± 130      | 530 ± 100      | 2700 ± 300    | 430 ± 100      | <1400          |
| V-52   | 28.7 ± 1.5     | 19.3 ± 1.2     | 91 ± 4        | 17.6 ± 1.2     | 16.8 ± 1.0     |
| Cr-51  | 39.0 ± 2.3     | 30.3 ± 1.8     | 141 ± 8       | 23.8 ± 1.5     | 17.8 ± 1.2     |
| Mn-56  | 67 ± 3         | 64 ± 3         | 47 ± 3        | 66 ± 3         | 40.0 ± 2.2     |
| Fe-59  | 3800 ± 200     | 2990 ± 160     | 12700 ± 800   | 2560 ± 140     | 5600 ± 300     |
| Co-60  | 0.78 ± 0.13    | 0.98 ± 0.06    | 4.06 ± 0.24   | 1.16 ± 0.07    | 0.87 ± 0.13    |
| Cu-66  | <90            | <90            | <90           | <80            | <80            |
| Zn-65  | <3             | 21 ± 3         | <8            | 19 ± 3         | 170 ± 30       |
| Ga-72  | <5             | <5             | 8.0 ± 1.2     | <5             | <6             |
| As-76  | 1.07 ± 0.15    | 0.83 ± 0.12    | 5.3 ± 0.6     | 1.43 ± 0.19    | 3.1 ± 0.4      |
| Se-75  | <1.4           | <1.6           | 1.2 ± 0.4     | <1.8           | <3             |
| Br-82  | <0.8           | 0.60 ± 0.13    | <1.0          | 0.51 ± 0.14    | 1.52 ± 0.24    |
| Rb-86  | 16.9 ± 1.6     | 12.4 ± 1.2     | 68 ± 4        | 9.5 ± 1.2      | <4             |
| Sr-87  | 670 ± 60       | 740 ± 70       | 190 ± 40      | 900 ± 70       | 1120 ± 80      |
| Zr-95  | <70            | <70            | <60           | <60            | <70            |
| Ag-110 | <1.3           | <1.1           | <2.1          | <1.2           | <1.1           |
| In-116 | <0.07          | <0.07          | <0.09         | <0.07          | 0.118 ± 0.016  |
| Sb-122 | <0.09          | <0.09          | 0.39 ± 0.04   | 0.08 ± 0.03    | 0.29 ± 0.05    |
| I-128  | <6             | <8             | <6            | <6             | <5             |
| Cs-134 | 0.79 ± 0.06    | 0.53 ± 0.04    | 3.35 ± 0.22   | 0.45 ± 0.06    | <0.4           |
| Ba-131 | 39 ± 10        | <80            | 124 ± 24      | <18            | <170           |
| Ba-139 | <1500          | <1700          | 127 ± 24      | <1600          | <1500          |
| La-140 | 11.5 ± 0.5     | 10.5 ± 0.5     | 16.0 ± 0.8    | 17.7 ± 1.0     | 69 ± 3         |
| Ce-141 | 13.7 ± 1.0     | 13.1 ± 0.9     | 21.2 ± 1.4    | 21.0 ± 1.2     | 78 ± 4         |
| Nd-147 | 5.2 ± 0.6      | 5.7 ± 0.6      | 14.3 ± 1.4    | 7.8 ± 1.0      | 36 ± 3         |
| Sm-153 | 1.10 ± 0.05    | 1.16 ± 0.05    | 2.51 ± 0.12   | 1.61 ± 0.08    | 6.9 ± 0.7      |
| Eu-152 | 0.31 ± 0.06    | 0.303 ± 0.013  | 0.61 ± 0.08   | 0.61 ± 0.06    | 2.86 ± 0.18    |
| Tb-160 | <0.06          | 0.180 ± 0.020  | 0.28 ± 0.03   | 0.230 ± 0.024  | 1.05 ± 0.10    |
| Dy-165 | 1.41 ± 0.16    | 0.92 ± 0.12    | 1.85 ± 0.21   | 1.65 ± 0.17    | 6.8 ± 0.5      |
| Yb-175 | 0.98 ± 0.10    | 0.78 ± 0.07    | 1.04 ± 0.08   | 0.82 ± 0.07    | 1.76 ± 0.24    |
| Lu-177 | 0.130 ± 0.009  | 0.116 ± 0.008  | 0.162 ± 0.011 | 0.098 ± 0.008  | 0.145 ± 0.015  |
| Hf-181 | 0.55 ± 0.04    | 0.44 ± 0.03    | 2.34 ± 0.20   | 0.28 ± 0.09    | <0.3           |
| Ta-182 | 0.128 ± 0.021  | 0.098 ± 0.017  | 0.46 ± 0.04   | <0.19          | <0.22          |
| W-187  | <1.4           | <1.4           | 0.95 ± 0.21   | <1.4           | <2.0           |
| Au-198 | <0.004         | <0.004         | <0.004        | <0.003         | <0.006         |
| Hg-203 | <0.19          | <0.18          | <0.4          | <0.25          | <0.4           |
| Th-233 | 1.20 ± 0.18    | 0.91 ± 0.04    | 4.87 ± 0.20   | 0.79 ± 0.05    | 0.92 ± 0.07    |
| U-235  | 1.48 ± 0.06    | 1.32 ± 0.05    | 4.08 ± 0.15   | 2.42 ± 0.09    | 13.4 ± 0.5     |

|        | 905021         | 905022         | 905023         | 905024         | 905025         |
|--------|----------------|----------------|----------------|----------------|----------------|
| Na-24  | 296 ± 13       | 521 ± 24       | 140 ± 7        | 67 ± 3         | 79 ± 3         |
| Mg-27  | 4700 ± 300     | 16000 ± 900    | 4600 ± 400     | 4100 ± 400     | 7900 ± 400     |
| Al-28  | 3430 ± 160     | 10800 ± 400    | 2400 ± 140     | 2060 ± 130     | 7400 ± 300     |
| Cl-38  | 178 ± 24       | 29 ± 8         | <60            | 57 ± 11        | <60            |
| K-42   | 3100 ± 230     | 6000 ± 400     | 1100 ± 110     | 1320 ± 120     | 4900 ± 300     |
| Ca-49  | 369000 ± 14000 | 303000 ± 12000 | 359000 ± 14000 | 359000 ± 14000 | 312000 ± 12000 |
| Sc-46  | 0.78 ± 0.04    | 2.32 ± 0.12    | 0.454 ± 0.024  | 0.56 ± 0.03    | 1.66 ± 0.09    |
| Ti-51  | <1600          | 810 ± 130      | <1600          | <1500          | 570 ± 100      |
| V-52   | 5.2 ± 2.0      | 27.6 ± 1.4     | 4.1 ± 0.6      | 4.1 ± 0.6      | 14.3 ± 1.0     |
| Cr-51  | 12.8 ± 0.8     | 20.6 ± 1.3     | 3.0 ± 0.3      | 3.2 ± 0.3      | 17.4 ± 1.1     |
| Mn-56  | 56 ± 3         | 107 ± 4        | 77 ± 4         | 83 ± 4         | 89 ± 4         |
| Fe-59  | 1990 ± 110     | 11800 ± 700    | 1360 ± 70      | 1500 ± 100     | 5100 ± 300     |
| Co-60  | 0.62 ± 0.05    | 2.16 ± 0.13    | 0.58 ± 0.05    | 0.31 ± 0.12    | 1.25 ± 0.10    |
| Cu-66  | <70            | <80            | <70            | <80            | <80            |
| Zn-65  | 50 ± 7         | 30 ± 4         | 17 ± 3         | <1.5           | 55 ± 7         |
| Ga-72  | <4             | 3.0 ± 0.8      | <3             | <3             | <3             |
| As-76  | 1.73 ± 0.20    | 7.7 ± 0.8      | 0.56 ± 0.09    | 0.75 ± 0.10    | 2.5 ± 0.3      |
| Se-75  | <2.5           | <0.38          | <1.0           | <0.9           | <1.9           |
| Br-82  | 1.03 ± 0.15    | 0.45 ± 0.11    | 0.22 ± 0.06    | 0.52 ± 0.07    | <0.6           |
| Rb-86  | 3.8 ± 1.2      | 16.8 ± 1.5     | <2.5           | 3.0 ± 0.8      | 16.0 ± 1.5     |
| Sr-87  | 1160 ± 80      | 820 ± 70       | 770 ± 60       | 680 ± 60       | 610 ± 50       |
| Zr-95  | <50            | <70            | <16            | <40            | <70            |
| Ag-110 | <0.8           | <1.4           | <0.7           | <0.7           | <1.2           |
| In-116 | <0.06          | <0.08          | <0.07          | <0.06          | <0.07          |
| Sb-122 | <0.09          | 0.50 ± 0.04    | <0.06          | <0.06          | 0.246 ± 0.025  |
| I-128  | <7             | <7             | <6             | <5             | <7             |
| Cs-134 | 0.185 ± 0.025  | 0.75 ± 0.06    | 0.084 ± 0.020  | 0.137 ± 0.019  | 0.59 ± 0.06    |
| Ba-131 | <22            | 51 ± 14        | <60            | <60            | <40            |
| Ba-139 | <1600          | <1700          | <1500          | <1500          | <1700          |
| La-140 | 27.0 ± 1.3     | 6.3 ± 0.3      | 6.6 ± 0.3      | 7.2 ± 0.4      | 9.4 ± 0.4      |
| Ce-141 | 32.8 ± 1.8     | 8.8 ± 1.0      | 7.1 ± 0.7      | 7.8 ± 0.8      | 11.6 ± 1.0     |
| Nd-147 | 18.9 ± 1.7     | 4.3 ± 0.5      | 2.1 ± 0.4      | 2.5 ± 0.3      | 4.9 ± 0.5      |
| Sm-153 | 3.41 ± 0.16    | 0.66 ± 0.04    | 0.378 ± 0.022  | 0.47 ± 0.03    | 0.82 ± 0.04    |
| Eu-152 | 1.21 ± 0.05    | 0.26 ± 0.06    | 0.22 ± 0.04    | 0.33 ± 0.04    | 0.42 ± 0.06    |
| Tb-160 | 0.42 ± 0.04    | <0.18          | 0.039 ± 0.007  | <0.11          | <0.16          |
| Dy-165 | 2.50 ± 0.24    | 0.74 ± 0.16    | 0.50 ± 0.10    | 0.66 ± 0.11    | 1.04 ± 0.15    |
| Yb-175 | 0.78 ± 0.09    | 0.46 ± 0.08    | 0.24 ± 0.03    | 0.35 ± 0.04    | 0.67 ± 0.05    |
| Lu-177 | 0.092 ± 0.009  | 0.091 ± 0.007  | 0.037 ± 0.004  | 0.028 ± 0.004  | 0.084 ± 0.006  |
| Hf-181 | 0.116 ± 0.019  | 0.89 ± 0.08    | 0.074 ± 0.016  | 0.09 ± 0.03    | 0.47 ± 0.03    |
| Ta-182 | <0.15          | <0.19          | <0.12          | <0.14          | 0.115 ± 0.020  |
| W-187  | <1.3           | <1.1           | <0.8           | <0.8           | <1.0           |
| Au-198 | <0.004         | <0.003         | <0.0018        | <0.0022        | <0.003         |
| Hg-203 | <0.25          | <0.3           | <0.14          | <0.11          | <0.23          |
| Th-233 | 1.15 ± 0.05    | 1.41 ± 0.14    | 0.188 ± 0.017  | 0.33 ± 0.06    | 1.15 ± 0.20    |
| U-235  | 6.09 ± 0.21    | 2.65 ± 0.10    | 1.55 ± 0.06    | 2.00 ± 0.07    | 2.96 ± 0.11    |

|        | 905026         | 905027         | 905028         | 905029         | 905030         |
|--------|----------------|----------------|----------------|----------------|----------------|
| Na-24  | 82 ± 4         | 91 ± 5         | 55 ± 3         | 66 ± 3         | 50.4 ± 2.3     |
| Mg-27  | 5900 ± 300     | 4700 ± 300     | 3620 ± 220     | 5500 ± 300     | 6800 ± 500     |
| Al-28  | 4340 ± 180     | 2830 ± 150     | 1760 ± 110     | 3210 ± 160     | 4490 ± 190     |
| Cl-38  | <50            | <70            | 46 ± 12        | <70            | <50            |
| K-42   | 2950 ± 210     | 1550 ± 130     | 1430 ± 120     | 2710 ± 190     | 3150 ± 230     |
| Ca-49  | 274000 ± 11000 | 349000 ± 14000 | 400000 ± 16000 | 424000 ± 21000 | 346000 ± 14000 |
| Sc-46  | 1.04 ± 0.06    | 0.66 ± 0.04    | 0.48 ± 0.03    | 0.85 ± 0.04    | 1.07 ± 0.06    |
| Ti-51  | 270 ± 70       | <1600          | <1400          | <1800          | 430 ± 100      |
| V-52   | 7.7 ± 0.7      | 3.8 ± 0.6      | 2.8 ± 0.6      | 5.0 ± 0.7      | 8.4 ± 0.8      |
| Cr-51  | 9.2 ± 0.6      | 5.5 ± 0.4      | 4.0 ± 0.3      | 7.0 ± 0.5      | 10.3 ± 0.7     |
| Mn-56  | 81 ± 3         | 79 ± 3         | 68 ± 3         | 75 ± 3         | 92 ± 4         |
| Fe-59  | 3770 ± 220     | 1990 ± 120     | 1500 ± 80      | 2100 ± 110     | 2910 ± 170     |
| Co-60  | 1.29 ± 0.08    | 0.35 ± 0.13    | 0.48 ± 0.04    | 0.48 ± 0.08    | 0.89 ± 0.07    |
| Cu-66  | <70            | <70            | <80            | <70            | <70            |
| Zn-65  | 22 ± 3         | <3             | 28 ± 4         | 25 ± 4         | 17 ± 3         |
| Ga-72  | <3             | <3             | <2.5           | <3             | <3             |
| As-76  | 1.68 ± 0.19    | 0.67 ± 0.10    | 0.53 ± 0.08    | 0.71 ± 0.09    | 0.98 ± 0.12    |
| Se-75  | <1.2           | <1.0           | <1.0           | <1.4           | <1.3           |
| Br-82  | <0.5           | 0.40 ± 0.07    | 0.52 ± 0.08    | 0.56 ± 0.09    | 0.43 ± 0.09    |
| Rb-86  | 8.6 ± 1.1      | 3.1 ± 1.0      | 3.0 ± 0.8      | 5.2 ± 0.9      | 8.2 ± 1.1      |
| Sr-87  | 560 ± 50       | 830 ± 70       | 1150 ± 80      | 960 ± 70       | 870 ± 70       |
| Zr-95  | <50            | <50            | <40            | <30            | <50            |
| Ag-110 | <1.0           | <0.8           | <0.6           | <0.9           | <1.0           |
| In-116 | <0.07          | <0.06          | <0.06          | <0.06          | <0.07          |
| Sb-122 | 0.102 ± 0.020  | 0.055 ± 0.016  | 0.200 ± 0.021  | 0.101 ± 0.015  | 0.084 ± 0.018  |
| I-128  | <6             | <6             | <5             | <7             | <6             |
| Cs-134 | 0.48 ± 0.04    | 0.19 ± 0.03    | 0.116 ± 0.024  | 0.21 ± 0.03    | 0.46 ± 0.05    |
| Ba-131 | <30            | <13            | <50            | <90            | <90            |
| Ba-139 | <1500          | <1500          | <1300          | <1700          | <1700          |
| La-140 | 7.4 ± 0.4      | 6.2 ± 0.3      | 5.4 ± 0.3      | 5.4 ± 0.3      | 6.0 ± 0.3      |
| Ce-141 | 7.7 ± 0.8      | 6.9 ± 0.8      | 5.9 ± 0.6      | 6.2 ± 0.8      | 6.1 ± 0.8      |
| Nd-147 | 2.8 ± 0.5      | 3.0 ± 0.4      | 2.7 ± 0.3      | 3.6 ± 0.4      | 3.4 ± 0.5      |
| Sm-153 | 0.67 ± 0.04    | 0.43 ± 0.03    | 0.393 ± 0.019  | 0.60 ± 0.03    | 0.65 ± 0.04    |
| Eu-152 | 0.29 ± 0.04    | 0.28 ± 0.05    | 0.331 ± 0.014  | 0.38 ± 0.05    | 0.42 ± 0.05    |
| Tb-160 | 0.079 ± 0.010  | <0.038         | 0.076 ± 0.010  | <0.13          | 0.086 ± 0.013  |
| Dy-165 | <2.0           | 0.60 ± 0.10    | <1.8           | 0.62 ± 0.11    | <2.2           |
| Yb-175 | 0.47 ± 0.04    | 0.38 ± 0.04    | 0.28 ± 0.03    | 0.35 ± 0.03    | 0.38 ± 0.04    |
| Lu-177 | 0.051 ± 0.010  | 0.049 ± 0.005  | 0.044 ± 0.004  | 0.049 ± 0.004  | 0.049 ± 0.005  |
| Hf-181 | 0.23 ± 0.04    | 0.123 ± 0.018  | 0.091 ± 0.013  | 0.19 ± 0.04    | 0.26 ± 0.03    |
| Ta-182 | <0.17          | <0.15          | <0.12          | <0.17          | <0.18          |
| W-187  | <0.7           | <0.8           | <0.7           | <0.8           | <0.8           |
| Au-198 | <0.0022        | <0.0018        | <0.0020        | <0.0022        | <0.0022        |
| Hg-203 | <0.18          | <0.12          | <0.11          | <0.17          | <0.19          |
| Th-233 | 0.59 ± 0.03    | 0.40 ± 0.07    | 0.267 ± 0.017  | 0.52 ± 0.10    | 0.67 ± 0.04    |
| U-235  | 2.08 ± 0.08    | 2.33 ± 0.09    | 1.66 ± 0.06    | 1.94 ± 0.07    | 2.09 ± 0.08    |

|        | 905031         | 905032         | 905033        | 905034        | 905035        |
|--------|----------------|----------------|---------------|---------------|---------------|
| Na-24  | 46 ± 3         | 69 ± 3         | 28.4 ± 1.3    | 25.6 ± 1.2    | 25.9 ± 1.6    |
| Mg-27  | 6100 ± 400     | 10400 ± 600    | 7400 ± 700    | 5900 ± 300    | 5500 ± 400    |
| Al-28  | 3400 ± 160     | 7900 ± 300     | 2420 ± 120    | 1500 ± 100    | 1100 ± 80     |
| Cl-38  | <60            | <60            | <50           | 31 ± 8        | <40           |
| K-42   | 2690 ± 200     | 6100 ± 400     | 1420 ± 110    | 840 ± 80      | 620 ± 70      |
| Ca-49  | 347000 ± 14000 | 349000 ± 14000 | 194000 ± 8000 | 79000 ± 3000  | 95000 ± 4000  |
| Sc-46  | 1.03 ± 0.05    | 1.52 ± 0.08    | 0.77 ± 0.04   | 0.331 ± 0.018 | 0.279 ± 0.015 |
| Ti-51  | <1700          | 500 ± 90       | <1400         | <1400         | <1100         |
| V-52   | 6.4 ± 0.7      | 15.0 ± 1.0     | 4.3 ± 0.5     | <2.0          | 1.5 ± 0.3     |
| Cr-51  | 7.3 ± 0.5      | 19.3 ± 1.2     | 7.9 ± 0.5     | 3.4 ± 0.3     | 3.3 ± 0.3     |
| Mn-56  | 84 ± 4         | 97 ± 5         | 58.3 ± 2.4    | 103 ± 4       | 42.0 ± 1.9    |
| Fe-59  | 2380 ± 130     | 4800 ± 300     | 2910 ± 170    | 1700 ± 110    | 1810 ± 100    |
| Co-60  | 0.43 ± 0.12    | 1.08 ± 0.07    | 0.49 ± 0.07   | 0.49 ± 0.04   | <0.009        |
| Cu-66  | <60            | <90            | <50           | <50           | <40           |
| Zn-65  | <5             | 20 ± 3         | 9.6 ± 2.0     | 5.7 ± 0.9     | <0.024        |
| Ga-72  | <3             | <3             | <2.1          | <1.6          | <1.8          |
| As-76  | 0.47 ± 0.09    | 1.74 ± 0.20    | 1.20 ± 0.13   | 1.55 ± 0.17   | 1.66 ± 0.18   |
| Se-75  | <1.0           | <1.5           | <1.3          | <0.8          | <0.7          |
| Br-82  | <0.5           | 0.26 ± 0.06    | <0.4          | 0.17 ± 0.05   | <0.3          |
| Rb-86  | 5.5 ± 1.0      | 13.6 ± 1.3     | 4.8 ± 0.9     | 2.3 ± 0.5     | <2.2          |
| Sr-87  | 690 ± 60       | 1180 ± 90      | 550 ± 50      | 890 ± 130     | 250 ± 30      |
| Zr-95  | <50            | <24            | <40           | <30           | <30           |
| Ag-110 | <0.8           | <1.0           | <0.8          | <0.6          | <0.5          |
| In-116 | <0.06          | <0.06          | <0.05         | <0.05         | <0.04         |
| Sb-122 | <0.06          | 0.195 ± 0.023  | 0.116 ± 0.014 | 0.75 ± 0.05   | 0.197 ± 0.017 |
| I-128  | <6             | <6             | <6            | <5            | <4            |
| Cs-134 | 0.33 ± 0.03    | 0.66 ± 0.05    | 0.54 ± 0.04   | 0.12 ± 0.03   | <0.19         |
| Ba-131 | <80            | <80            | <80           | <60           | <50           |
| Ba-139 | <1500          | <1700          | <1300         | <1500         | <1100         |
| La-140 | 5.4 ± 0.3      | 6.5 ± 0.3      | 2.26 ± 0.12   | 1.10 ± 0.06   | 1.10 ± 0.05   |
| Ce-141 | 5.9 ± 0.7      | 7.7 ± 0.7      | 2.9 ± 0.6     | <0.9          | 1.2 ± 0.4     |
| Nd-147 | 2.8 ± 0.4      | 3.5 ± 0.4      | 1.7 ± 0.3     | 0.9 ± 0.3     | 0.78 ± 0.19   |
| Sm-153 | 0.411 ± 0.024  | 0.57 ± 0.03    | 0.302 ± 0.018 | 0.238 ± 0.015 | 0.115 ± 0.010 |
| Eu-152 | 0.44 ± 0.05    | 0.52 ± 0.07    | 0.20 ± 0.03   | <0.040        | 0.068 ± 0.024 |
| Tb-160 | <0.12          | 0.096 ± 0.013  | <0.12         | <0.10         | <0.10         |
| Dy-165 | 0.69 ± 0.12    | <2.1           | <1.7          | 0.64 ± 0.12   | <1.4          |
| Yb-175 | 0.31 ± 0.03    | 0.44 ± 0.06    | 0.21 ± 0.03   | 0.109 ± 0.021 | 0.075 ± 0.019 |
| Lu-177 | 0.045 ± 0.005  | 0.066 ± 0.005  | 0.027 ± 0.003 | 0.009 ± 0.003 | 0.011 ± 0.003 |
| Hf-181 | 0.158 ± 0.020  | 0.45 ± 0.03    | 0.15 ± 0.04   | 0.073 ± 0.014 | 0.060 ± 0.012 |
| Ta-182 | <0.15          | 0.102 ± 0.021  | <0.14         | <0.11         | <0.11         |
| W-187  | <0.8           | <0.9           | <0.6          | <0.5          | <0.5          |
| Au-198 | <0.0017        | <0.0025        | <0.0017       | <0.0014       | <0.0012       |
| Hg-203 | <0.13          | <0.18          | <0.16         | <0.12         | <0.09         |
| Th-233 | 0.54 ± 0.10    | 1.16 ± 0.05    | 0.53 ± 0.10   | 0.236 ± 0.017 | 0.225 ± 0.017 |
| U-235  | 2.01 ± 0.07    | 1.85 ± 0.07    | 1.46 ± 0.06   | 1.52 ± 0.06   | 0.60 ± 0.03   |

|        | 905036         | 905037         | 905038         | 905039         | 905040          |
|--------|----------------|----------------|----------------|----------------|-----------------|
| Na-24  | 41.1 ± 1.9     | 41.5 ± 2.0     | 44.9 ± 2.2     | 41.4 ± 2.3     | 73 ± 3          |
| Mg-27  | 4100 ± 300     | 5100 ± 400     | 4500 ± 300     | 4800 ± 300     | 5300 ± 300      |
| Al-28  | 870 ± 90       | 570 ± 70       | 360 ± 70       | 720 ± 90       | 1010 ± 90       |
| Cl-38  | <60            | <60            | <50            | <60            | 30 ± 9          |
| K-42   | 540 ± 60       | 510 ± 60       | 460 ± 70       | <400           | 560 ± 70        |
| Ca-49  | 408000 ± 16000 | 448000 ± 17000 | 429000 ± 17000 | 414000 ± 20000 | 275000 ± 11000  |
| Sc-46  | 0.289 ± 0.016  | 0.266 ± 0.014  | 0.241 ± 0.013  | 0.250 ± 0.014  | 0.258 ± 0.014   |
| Ti-51  | <1500          | <1500          | <1500          | <1500          | <1200           |
| V-52   | <2.3           | <2.2           | <2.4           | <2.4           | <1.9            |
| Cr-51  | 3.5 ± 0.3      | 2.75 ± 0.23    | 2.56 ± 0.22    | 2.68 ± 0.23    | 3.35 ± 0.24     |
| Mn-56  | 53.0 ± 2.3     | 41.7 ± 1.8     | 41.5 ± 2.0     | 49.4 ± 2.1     | 41.3 ± 1.8      |
| Fe-59  | 850 ± 50       | 710 ± 40       | 650 ± 40       | 750 ± 40       | 910 ± 60        |
| Co-60  | 0.32 ± 0.04    | <0.12          | 0.43 ± 0.04    | <0.0009        | 0.34 ± 0.04     |
| Cu-66  | <80            | <60            | <70            | <60            | <60             |
| Zn-65  | 16.0 ± 2.1     | 3.7 ± 1.3      | 6.3 ± 1.0      | <0.023         | 12.7 ± 1.7      |
| Ga-72  | <2.3           | <2.5           | <2.4           | <3             | <3              |
| As-76  | 0.36 ± 0.07    | 0.25 ± 0.05    | <0.3           | 0.29 ± 0.07    | 0.43 ± 0.07     |
| Se-75  | <0.9           | <1.1           | <0.9           | <0.8           | <0.8            |
| Br-82  | 0.44 ± 0.08    | 0.48 ± 0.08    | 0.53 ± 0.10    | <0.5           | 0.22 ± 0.06     |
| Rb-86  | <2.0           | <2.2           | <2.3           | <2.3           | <1.9            |
| Sr-87  | 880 ± 70       | 1280 ± 90      | 1720 ± 120     | 820 ± 60       | 520 ± 40        |
| Zr-95  | <30            | <30            | <30            | <30            | <30             |
| Ag-110 | <0.5           | <0.5           | <0.6           | <0.5           | <0.5            |
| In-116 | <0.06          | <0.05          | <0.06          | <0.06          | <0.05           |
| Sb-122 | <0.05          | <0.05          | <0.05          | <0.05          | <0.05           |
| I-128  | <5             | <6             | <5             | <5             | <4              |
| Cs-134 | 0.078 ± 0.017  | <0.17          | 0.077 ± 0.016  | <0.14          | <0.15           |
| Ba-131 | <40            | <60            | <50            | <50            | <40             |
| Ba-139 | <1400          | <1500          | <1400          | <1400          | <1200           |
| La-140 | 4.7 ± 0.3      | 3.41 ± 0.25    | 3.0 ± 0.3      | 3.68 ± 0.21    | 2.24 ± 0.12     |
| Ce-141 | 4.9 ± 0.5      | 3.3 ± 0.5      | 2.6 ± 0.4      | 3.2 ± 0.6      | 2.7 ± 0.4       |
| Nd-147 | 2.3 ± 0.3      | 1.4 ± 0.3      | 0.98 ± 0.24    | 1.6 ± 0.3      | 1.14 ± 0.21     |
| Sm-153 | 0.334 ± 0.019  | 0.366 ± 0.022  | 0.322 ± 0.022  | 0.264 ± 0.018  | 0.197 ± 0.010   |
| Eu-152 | 0.15 ± 0.03    | 0.09 ± 0.03    | <0.06          | 0.08 ± 0.03    | <0.05           |
| Tb-160 | 0.061 ± 0.007  | 0.055 ± 0.008  | 0.038 ± 0.007  | <0.11          | 0.046 ± 0.006   |
| Dy-165 | <1.8           | 0.30 ± 0.07    | <1.9           | 0.42 ± 0.09    | 0.38 ± 0.07     |
| Yb-175 | 0.22 ± 0.03    | 0.227 ± 0.023  | 0.186 ± 0.025  | 0.19 ± 0.03    | 0.16 ± 0.03     |
| Lu-177 | 0.025 ± 0.003  | 0.025 ± 0.003  | 0.025 ± 0.003  | 0.021 ± 0.003  | 0.0206 ± 0.0024 |
| Hf-181 | <0.09          | <0.11          | 0.050 ± 0.011  | 0.065 ± 0.013  | 0.061 ± 0.009   |
| Ta-182 | <0.11          | <0.11          | <0.11          | <0.11          | <0.09           |
| W-187  | <0.7           | <0.7           | <0.7           | <0.8           | <0.7            |
| Au-198 | <0.0019        | <0.0019        | <0.0018        | <0.0016        | <0.0018         |
| Hg-203 | <0.10          | <0.12          | <0.12          | <0.10          | <0.09           |
| Th-233 | 0.207 ± 0.016  | 0.245 ± 0.017  | 0.206 ± 0.018  | 0.185 ± 0.017  | 0.204 ± 0.013   |
| U-235  | 1.23 ± 0.05    | 0.85 ± 0.03    | 0.71 ± 0.03    | 1.32 ± 0.05    | 0.89 ± 0.04     |

|        | 905041          | 905042         | 905043          | 905044         | 905045         |
|--------|-----------------|----------------|-----------------|----------------|----------------|
| Na-24  | 53 ± 3          | 57 ± 3         | 48 ± 3          | 57 ± 3         | 160 ± 7        |
| Mg-27  | 7900 ± 400      | 4800 ± 300     | 3600 ± 240      | 7900 ± 400     | 7400 ± 400     |
| Al-28  | 980 ± 70        | 1010 ± 90      | 840 ± 100       | 2720 ± 140     | 4260 ± 180     |
| Cl-38  | <40             | <50            | <60             | <50            | <70            |
| K-42   | 410 ± 60        | 560 ± 70       | 920 ± 100       | 1570 ± 140     | 2090 ± 170     |
| Ca-49  | 137000 ± 6000   | 318000 ± 13000 | 432000 ± 17000  | 344000 ± 14000 | 428000 ± 17000 |
| Sc-46  | 0.276 ± 0.015   | 0.279 ± 0.015  | 0.233 ± 0.013   | 0.74 ± 0.04    | 0.90 ± 0.05    |
| Ti-51  | <1100           | <1400          | <1500           | <1500          | 290 ± 80       |
| V-52   | 1.8             | <2.2           | <2.5            | 6.8 ± 0.7      | 8.5 ± 0.8      |
| Cr-51  | 4.0 ± 0.3       | 3.6 ± 0.3      | 2.40 ± 0.22     | 7.3 ± 0.5      | 11.6 ± 0.7     |
| Mn-56  | 29.6 ± 1.3      | 45.7 ± 2.0     | 34.8 ± 1.9      | 64 ± 3         | 65 ± 3         |
| Fe-59  | 1130 ± 60       | 9900 ± 600     | 580 ± 50        | 2250 ± 110     | 3530 ± 190     |
| Co-60  | 0.15 ± 0.07     | 0.65 ± 0.05    | <0.06           | 0.67 ± 0.05    | 0.60 ± 0.08    |
| Cu-66  | <50             | <60            | <60             | <70            | <70            |
| Zn-65  | 2.3 ± 1.0       | 4.0 ± 0.9      | <0.022          | 14.8 ± 2.0     | 9.4 ± 2.0      |
| Ga-72  | <2.2            | <3             | <3              | <3             | <4             |
| As-76  | 0.48 ± 0.07     | 1.29 ± 0.15    | 0.27 ± 0.06     | 0.98 ± 0.13    | 1.42 ± 0.17    |
| Se-75  | <0.9            | <1.1           | <0.7            | <1.1           | <1.5           |
| Br-82  | <0.4            | <0.5           | <0.4            | <0.5           | <0.6           |
| Rb-86  | <1.9            | <3             | <2.3            | 5.0 ± 0.8      | 5.6 ± 0.9      |
| Sr-87  | 340 ± 30        | 1300 ± 90      | 1820 ± 120      | 1300 ± 90      | 1620 ± 110     |
| Zr-95  | <30             | <50            | <30             | <40            | <50            |
| Ag-110 | <0.5            | <0.9           | <0.5            | <0.7           | <0.9           |
| In-116 | <0.04           | <0.06          | <0.06           | <0.06          | <0.06          |
| Sb-122 | <0.04           | 0.110 ± 0.016  | <0.05           | 0.111 ± 0.022  | 1.29 ± 0.07    |
| I-128  | <4              | <5             | <5              | <5             | <7             |
| Cs-134 | <0.17           | 0.046 ± 0.015  | 0.104 ± 0.015   | 0.175 ± 0.019  | 0.18 ± 0.04    |
| Ba-131 | <50             | <70            | <50             | <60            | <90            |
| Ba-139 | <1200           | <1400          | <1400           | <1500          | <1600          |
| La-140 | 0.99 ± 0.07     | 2.21 ± 0.23    | 1.44 ± 0.07     | 5.1 ± 0.3      | 6.6 ± 0.3      |
| Ce-141 | 1.1 ± 0.3       | 2.0 ± 0.5      | 1.6 ± 0.3       | 7.3 ± 0.5      | 10.0 ± 0.6     |
| Nd-147 | <0.8            | 1.4 ± 0.4      | <0.5            | 2.7 ± 0.4      | 3.9 ± 0.5      |
| Sm-153 | 0.129 ± 0.009   | 0.214 ± 0.017  | 0.122 ± 0.007   | 0.46 ± 0.03    | 0.78 ± 0.04    |
| Eu-152 | <0.04           | 0.051 ± 0.008  | <0.05           | 0.191 ± 0.008  | 0.22 ± 0.05    |
| Tb-160 | <0.08           | <0.13          | <0.09           | 0.092 ± 0.011  | <0.14          |
| Dy-165 | <1.5            | <1.7           | <1.7            | 0.59 ± 0.10    | 0.66 ± 0.11    |
| Yb-175 | 0.072 ± 0.014   | <0.11          | <0.09           | 0.32 ± 0.04    | 0.29 ± 0.04    |
| Lu-177 | 0.0131 ± 0.0023 | 0.021 ± 0.004  | 0.0101 ± 0.0022 | 0.029 ± 0.003  | 0.035 ± 0.004  |
| Hf-181 | <0.08           | 0.061 ± 0.016  | 0.055 ± 0.010   | 0.223 ± 0.018  | 0.295 ± 0.022  |
| Ta-182 | <0.11           | <0.14          | <0.10           | <0.14          | <0.16          |
| W-187  | <0.6            | <0.7           | <0.7            | <0.9           | <1.0           |
| Au-198 | <0.0016         | <0.0018        | <0.0014         | <0.0023        | <0.003         |
| Hg-203 | <0.11           | <0.15          | <0.09           | <0.13          | <0.18          |
| Th-233 | 0.220 ± 0.015   | 0.183 ± 0.020  | 0.166 ± 0.016   | 0.49 ± 0.03    | 0.81 ± 0.13    |
| U-235  | 0.403 ± 0.020   | 0.76 ± 0.03    | 0.309 ± 0.016   | 0.64 ± 0.03    | 0.79 ± 0.03    |

|        | 905046         | 905047         | 905048         | 905049         | 905050         |
|--------|----------------|----------------|----------------|----------------|----------------|
| Na-24  | 245 ± 11       | 900 ± 40       | 326 ± 17       | 568 ± 24       | 740 ± 30       |
| Mg-27  | 4300 ± 300     | 6700 ± 500     | 24700 ± 1400   | 8900 ± 500     | 6600 ± 400     |
| Al-28  | 3380 ± 160     | 4510 ± 190     | 12300 ± 400    | 5840 ± 220     | 5250 ± 210     |
| Cl-38  | <50            | <70            | <50            | <70            | <60            |
| K-42   | 1900 ± 160     | 1760 ± 200     | 7500 ± 500     | 2550 ± 210     | 2090 ± 190     |
| Ca-49  | 415000 ± 16000 | 393000 ± 20000 | 294000 ± 12000 | 405000 ± 16000 | 388000 ± 15000 |
| Sc-46  | 0.79 ± 0.04    | 1.27 ± 0.07    | 2.90 ± 0.15    | 1.64 ± 0.09    | 1.37 ± 0.07    |
| Ti-51  | <1700          | 220 ± 70       | 540 ± 90       | 230 ± 60       | <1800          |
| V-52   | 5.4 ± 0.6      | 8.1 ± 0.8      | 28.6 ± 1.5     | 9.3 ± 0.8      | 7.0 ± 0.7      |
| Cr-51  | 6.6 ± 0.5      | 7.9 ± 0.5      | 27.2 ± 1.7     | 11.8 ± 0.8     | 9.6 ± 0.6      |
| Mn-56  | 59.2 ± 2.5     | 63 ± 3         | 92 ± 4         | 64 ± 3         | 67 ± 3         |
| Fe-59  | 2940 ± 160     | 3840 ± 250     | 7900 ± 400     | 5100 ± 300     | 4900 ± 300     |
| Co-60  | 0.80 ± 0.05    | 0.61 ± 0.13    | 1.95 ± 0.11    | 0.77 ± 0.08    | 1.03 ± 0.07    |
| Cu-66  | <70            | <70            | <90            | <80            | <80            |
| Zn-65  | 6.6 ± 1.5      | <3             | 18 ± 3         | <4             | 10.3 ± 1.5     |
| Ga-72  | <4             | <5             | <5             | <5             | <5             |
| As-76  | 0.80 ± 0.11    | 0.88 ± 0.14    | 1.23 ± 0.16    | 0.78 ± 0.11    | 0.92 ± 0.14    |
| Se-75  | <1.1           | <1.1           | <1.8           | <1.6           | <1.3           |
| Br-82  | <0.7           | <0.8           | <0.7           | <0.8           | <0.9           |
| Rb-86  | 4.1 ± 0.9      | 2.9 ± 0.8      | 17.2 ± 1.5     | 4.7 ± 0.9      | 4.7 ± 0.9      |
| Sr-87  | 1260 ± 90      | 1270 ± 90      | 770 ± 60       | 1280 ± 90      | 1330 ± 100     |
| Zr-95  | <40            | <60            | <80            | <60            | <60            |
| Ag-110 | <0.9           | <0.9           | <1.3           | <1.1           | <1.1           |
| In-116 | <0.07          | <0.07          | <0.07          | <0.06          | <0.08          |
| Sb-122 | <0.07          | <0.09          | 0.27 ± 0.03    | <0.08          | <0.08          |
| I-128  | <6             | <6             | <6             | <7             | <6             |
| Cs-134 | 0.129 ± 0.018  | 0.13 ± 0.03    | 0.60 ± 0.07    | <0.3           | 0.18 ± 0.04    |
| Ba-131 | <22            | <80            | <90            | <110           | <90            |
| Ba-139 | <1500          | <1500          | <1800          | <1700          | <1700          |
| La-140 | 7.3 ± 0.4      | 7.3 ± 0.3      | 8.6 ± 0.4      | 8.3 ± 0.4      | 8.8 ± 0.4      |
| Ce-141 | 11.0 ± 0.6     | 11.2 ± 0.7     | 14.3 ± 0.7     | 13.8 ± 0.8     | 13.4 ± 0.8     |
| Nd-147 | 3.4 ± 0.4      | 4.1 ± 0.5      | 5.9 ± 0.6      | 5.3 ± 0.6      | 5.2 ± 0.6      |
| Sm-153 | 0.86 ± 0.05    | 0.65 ± 0.03    | 0.95 ± 0.04    | 0.97 ± 0.05    | 1.04 ± 0.05    |
| Eu-152 | 0.20 ± 0.04    | 0.20 ± 0.05    | 0.25 ± 0.06    | 0.23 ± 0.05    | 0.197 ± 0.013  |
| Tb-160 | 0.070 ± 0.010  | 0.046 ± 0.018  | 0.11 ± 0.03    | 0.131 ± 0.017  | 0.120 ± 0.016  |
| Dy-165 | 0.44 ± 0.13    | 0.57 ± 0.11    | 0.89 ± 0.13    | 0.75 ± 0.13    | 0.78 ± 0.15    |
| Yb-175 | 0.23 ± 0.03    | 0.42 ± 0.06    | 0.62 ± 0.06    | 0.39 ± 0.05    | 0.34 ± 0.05    |
| Lu-177 | 0.029 ± 0.004  | 0.037 ± 0.005  | 0.066 ± 0.006  | 0.057 ± 0.005  | 0.042 ± 0.005  |
| Hf-181 | 0.129 ± 0.018  | 0.177 ± 0.019  | 0.62 ± 0.06    | 0.240 ± 0.022  | 0.20 ± 0.05    |
| Ta-182 | <0.15          | <0.16          | 0.113 ± 0.020  | <0.17          | <0.17          |
| W-187  | <1.0           | <1.3           | <1.4           | <1.3           | <1.3           |
| Au-198 | <0.003         | <0.003         | <0.003         | <0.003         | <0.003         |
| Hg-203 | <0.16          | <0.14          | <0.21          | <0.20          | <0.20          |
| Th-233 | 0.49 ± 0.03    | 0.54 ± 0.06    | 1.59 ± 0.07    | 0.73 ± 0.04    | 0.63 ± 0.03    |
| U-235  | 0.517 ± 0.024  | 0.409 ± 0.020  | 0.65 ± 0.03    | 0.468 ± 0.022  | 0.346 ± 0.018  |

|        | <i>905051a</i> | <i>905052</i>  | <i>905053</i>  | <i>905054a</i> | <i>905055</i>  |
|--------|----------------|----------------|----------------|----------------|----------------|
| Na-24  | 162 ± 8        | 158 ± 9        | 138 ± 6        | 980 ± 40       | 296 ± 13       |
| Mg-27  | 34400 ± 1700   | 28200 ± 1400   | 32800 ± 1900   | 7900 ± 600     | 30200 ± 1500   |
| Al-28  | 20100 ± 600    | 19400 ± 600    | 16800 ± 500    | 7700 ± 300     | 16000 ± 500    |
| Cl-38  | <50            | <60            | <60            | <70            | <60            |
| K-42   | 12700 ± 800    | 12200 ± 800    | 10900 ± 700    | 2860 ± 240     | 8100 ± 600     |
| Ca-49  | 261000 ± 10000 | 276000 ± 11000 | 289000 ± 12000 | 408000 ± 16000 | 265000 ± 11000 |
| Sc-46  | 3.88 ± 0.21    | 3.80 ± 0.20    | 3.65 ± 0.20    | 2.02 ± 0.11    | 3.48 ± 0.18    |
| Ti-51  | 1290 ± 190     | 1330 ± 190     | 840 ± 130      | <1900          | 1070 ± 160     |
| V-52   | 46.4 ± 2.1     | 44.7 ± 2.1     | 34.0 ± 1.6     | 13.2 ± 1.0     | 36.2 ± 1.7     |
| Cr-51  | 43 ± 3         | 39.0 ± 2.4     | 34.6 ± 2.1     | 11.9 ± 0.8     | 38.3 ± 2.3     |
| Mn-56  | 99 ± 4         | 90 ± 4         | 92 ± 5         | 67 ± 3         | 84 ± 3         |
| Fe-59  | 11300 ± 700    | 10100 ± 600    | 9500 ± 500     | 3350 ± 190     | 9900 ± 600     |
| Co-60  | 2.09 ± 0.18    | 1.86 ± 0.18    | 2.39 ± 0.13    | 1.12 ± 0.07    | 1.94 ± 0.13    |
| Cu-66  | <100           | <100           | <80            | <80            | <80            |
| Zn-65  | <4             | <0.03          | 25 ± 4         | 14.4 ± 2.0     | 15 ± 3         |
| Ga-72  | 6.5 ± 1.3      | <7             | <5             | <6             | <6             |
| As-76  | 2.3 ± 0.3      | 1.71 ± 0.21    | 1.52 ± 0.18    | 0.51 ± 0.10    | 0.92 ± 0.14    |
| Se-75  | <1.7           | <1.8           | <2.0           | <1.4           | <2.3           |
| Br-82  | <0.8           | 0.73 ± 0.12    | <0.8           | <0.9           | <0.8           |
| Rb-86  | 28.8 ± 2.1     | 26.3 ± 2.2     | 24.6 ± 1.7     | 6.7 ± 0.9      | 23.6 ± 1.8     |
| Sr-87  | 660 ± 60       | 780 ± 70       | 730 ± 70       | 1290 ± 90      | 710 ± 60       |
| Zr-95  | 63 ± 24        | <100           | <90            | <60            | <90            |
| Ag-110 | <1.7           | <1.7           | <1.5           | <1.0           | <1.6           |
| In-116 | <0.07          | <0.07          | <0.07          | <0.07          | <0.07          |
| Sb-122 | 0.059 ± 0.020  | 0.24 ± 0.03    | <0.09          | <0.09          | <0.09          |
| I-128  | <7             | <7             | <8             | <7             | <7             |
| Cs-134 | 1.17 ± 0.18    | 0.94 ± 0.07    | 0.89 ± 0.06    | 0.23 ± 0.04    | 0.79 ± 0.06    |
| Ba-131 | 85 ± 18        | <150           | 72 ± 12        | <90            | 49 ± 20        |
| Ba-139 | 90 ± 30        | <1900          | <2000          | <1700          | <1800          |
| La-140 | 9.2 ± 0.4      | 10.0 ± 0.5     | 9.5 ± 0.4      | 9.5 ± 0.4      | 7.9 ± 0.4      |
| Ce-141 | 15.3 ± 1.0     | 16.1 ± 1.0     | 16.8 ± 1.0     | 14.6 ± 0.7     | 14.9 ± 1.0     |
| Nd-147 | 4.5 ± 0.6      | 5.0 ± 0.7      | 7.2 ± 0.7      | 5.7 ± 0.6      | 6.8 ± 0.8      |
| Sm-153 | 1.09 ± 0.05    | 1.12 ± 0.05    | 1.47 ± 0.07    | 1.13 ± 0.05    | 0.98 ± 0.05    |
| Eu-152 | 0.27 ± 0.07    | 0.27 ± 0.07    | 0.297 ± 0.022  | 0.236 ± 0.012  | 0.27 ± 0.07    |
| Tb-160 | <0.043         | <0.23          | 0.185 ± 0.024  | 0.139 ± 0.017  | 0.120 ± 0.021  |
| Dy-165 | 1.01 ± 0.14    | 1.07 ± 0.16    | 0.96 ± 0.13    | 0.73 ± 0.13    | 0.91 ± 0.13    |
| Yb-175 | 0.77 ± 0.06    | 0.66 ± 0.06    | 0.55 ± 0.05    | 0.52 ± 0.05    | 0.55 ± 0.07    |
| Lu-177 | 0.056 ± 0.008  | 0.081 ± 0.010  | 0.077 ± 0.007  | 0.064 ± 0.006  | 0.080 ± 0.007  |
| Hf-181 | 1.04 ± 0.09    | 0.96 ± 0.06    | 0.93 ± 0.11    | 0.29 ± 0.03    | 0.97 ± 0.15    |
| Ta-182 | 0.26 ± 0.03    | 0.24 ± 0.04    | 0.18 ± 0.03    | <0.16          | <0.21          |
| W-187  | <1.6           | <1.7           | <1.4           | <1.5           | <1.5           |
| Au-198 | <0.004         | <0.004         | <0.003         | <0.004         | <0.003         |
| Hg-203 | <0.25          | <0.25          | <0.24          | <0.18          | <0.3           |
| Th-233 | 3.19 ± 0.20    | 2.52 ± 0.20    | 2.39 ± 0.11    | 0.73 ± 0.04    | 2.59 ± 0.11    |
| U-235  | 0.80 ± 0.04    | 0.77 ± 0.03    | 0.63 ± 0.03    | 0.375 ± 0.019  | 0.73 ± 0.03    |



|        | 905056         | 905057         | 905058        | 905059a        | 905060a        |
|--------|----------------|----------------|---------------|----------------|----------------|
| Na-24  | 132 ± 6        | 146 ± 6        | 315 ± 13      | 1440 ± 60      | <5             |
| Mg-27  | 26600 ± 1300   | 41800 ± 2100   | 9400 ± 500    | 11000 ± 800    | 8900 ± 500     |
| Al-28  | 15300 ± 500    | 18800 ± 600    | 3160 ± 150    | 7500 ± 300     | 6900 ± 300     |
| Cl-38  | <60            | <60            | <40           | <50            | <70            |
| K-42   | 9600 ± 600     | 11300 ± 700    | 1710 ± 170    | 3100 ± 300     | <700           |
| Ca-49  | 285000 ± 11000 | 272000 ± 11000 | 197000 ± 8000 | 317000 ± 13000 | 336000 ± 13000 |
| Sc-46  | 3.37 ± 0.18    | 3.74 ± 0.20    | 0.97 ± 0.05   | 2.06 ± 0.11    | 1.79 ± 0.10    |
| Ti-51  | 970 ± 150      | 1410 ± 200     | <1600         | 290 ± 80       | 250 ± 80       |
| V-52   | 33.9 ± 1.7     | 40.1 ± 1.8     | 6.7 ± 0.6     | 15.0 ± 1.0     | 11.3 ± 0.9     |
| Cr-51  | 33.7 ± 2.1     | 42 ± 3         | 10.1 ± 0.6    | 14.8 ± 0.9     | 12.6 ± 0.8     |
| Mn-56  | 86 ± 4         | 92 ± 4         | 49.1 ± 2.2    | 69 ± 3         | 67 ± 3         |
| Fe-59  | 8200 ± 500     | 9100 ± 500     | 5700 ± 300    | 6900 ± 400     | 5600 ± 300     |
| Co-60  | 1.97 ± 0.11    | 1.83 ± 0.16    | 1.15 ± 0.07   | 1.43 ± 0.11    | 1.35 ± 0.08    |
| Cu-66  | <90            | <80            | <60           | <90            | <80            |
| Zn-65  | 14 ± 3         | <4             | 8.2 ± 1.3     | <4             | 6.8 ± 1.8      |
| Ga-72  | <6             | 4.6 ± 0.9      | <4            | <6             | <7             |
| As-76  | 1.13 ± 0.16    | 1.22 ± 0.15    | 0.72 ± 0.11   | 0.68 ± 0.13    | <0.8           |
| Se-75  | <2.0           | <1.6           | <1.2          | <1.8           | <1.4           |
| Br-82  | <0.7           | <0.8           | <0.6          | <1.0           | <1.0           |
| Rb-86  | 20.0 ± 1.6     | 21.9 ± 1.7     | 6.9 ± 0.9     | 7.8 ± 1.1      | 4.9 ± 0.9      |
| Sr-87  | 800 ± 70       | 600 ± 60       | 730 ± 60      | 1160 ± 90      | 1130 ± 90      |
| Zr-95  | <90            | <90            | <50           | <70            | <60            |
| Ag-110 | <1.7           | <1.5           | <0.9          | <1.3           | <1.2           |
| In-116 | <0.07          | <0.07          | <0.06         | <0.08          | <0.08          |
| Sb-122 | <0.09          | 0.126 ± 0.025  | <0.06         | <0.10          | <0.11          |
| I-128  | <7             | <8             | <5            | <7             | <6             |
| Cs-134 | 0.78 ± 0.10    | 1.04 ± 0.08    | 0.32 ± 0.03   | 0.31 ± 0.03    | 0.24 ± 0.03    |
| Ba-131 | 64 ± 20        | <130           | <60           | <130           | <120           |
| Ba-139 | <1800          | <1900          | <1500         | <1700          | <1600          |
| La-140 | 9.3 ± 0.4      | 9.0 ± 0.4      | 2.24 ± 0.13   | 8.0 ± 0.4      | 8.5 ± 0.4      |
| Ce-141 | 15.6 ± 1.0     | 14.7 ± 1.0     | 4.0 ± 0.3     | 12.9 ± 0.8     | 13.6 ± 0.9     |
| Nd-147 | 5.1 ± 0.7      | 5.8 ± 0.7      | <0.8          | 4.5 ± 0.6      | 4.1 ± 0.6      |
| Sm-153 | 1.08 ± 0.05    | 1.41 ± 0.06    | 0.359 ± 0.018 | 1.01 ± 0.05    | 0.82 ± 0.04    |
| Eu-152 | 0.27 ± 0.07    | 0.25 ± 0.07    | <0.08         | 0.20 ± 0.05    | 0.22 ± 0.05    |
| Tb-160 | 0.15 ± 0.03    | <0.03          | <0.13         | 0.109 ± 0.017  | 0.122 ± 0.016  |
| Dy-165 | 1.05 ± 0.13    | 0.90 ± 0.12    | 0.43 ± 0.10   | 0.74 ± 0.14    | 0.77 ± 0.13    |
| Yb-175 | 0.68 ± 0.08    | 0.69 ± 0.05    | 0.25 ± 0.04   | 0.57 ± 0.06    | <0.23          |
| Lu-177 | 0.078 ± 0.008  | 0.081 ± 0.007  | 0.026 ± 0.004 | 0.052 ± 0.006  | 0.059 ± 0.006  |
| Hf-181 | 0.75 ± 0.06    | 0.94 ± 0.08    | 0.208 ± 0.023 | 0.33 ± 0.05    | 0.23 ± 0.03    |
| Ta-182 | 0.16 ± 0.03    | 0.21 ± 0.03    | <0.15         | <0.20          | 0.067 ± 0.017  |
| W-187  | <1.5           | <1.5           | <1.0          | <1.5           | <1.8           |
| Au-198 | <0.003         | <0.003         | <0.0024       | <0.004         | <0.004         |
| Hg-203 | <0.3           | <0.23          | <0.15         | <0.23          | <0.22          |
| Th-233 | 2.17 ± 0.09    | 3.10 ± 0.21    | 0.63 ± 0.08   | 0.84 ± 0.04    | 0.66 ± 0.04    |
| U-235  | 0.65 ± 0.03    | 0.80 ± 0.03    | 0.316 ± 0.017 | 0.364 ± 0.019  | 0.298 ± 0.016  |

|        | 905061         | 905062         | 905063        | 905064         | 905065         |
|--------|----------------|----------------|---------------|----------------|----------------|
| Na-24  | 401 ± 17       | 1200 ± 50      | 380 ± 16      | 590 ± 30       | 600 ± 30       |
| Mg-27  | 20400 ± 1100   | 4600 ± 400     | 15300 ± 800   | 3900 ± 300     | 4800 ± 400     |
| Al-28  | 10400 ± 300    | 8500 ± 300     | 17100 ± 500   | 4330 ± 180     | 4590 ± 190     |
| Cl-38  | <60            | <60            | 46 ± 11       | 132 ± 13       | 184 ± 17       |
| K-42   | 5300 ± 400     | 5300 ± 400     | 13000 ± 900   | 2900 ± 300     | 3400 ± 300     |
| Ca-49  | 309000 ± 12000 | 385000 ± 15000 | 228000 ± 9000 | 303000 ± 12000 | 368000 ± 15000 |
| Sc-46  | 2.50 ± 0.13    | 2.12 ± 0.11    | 2.85 ± 0.15   | 1.04 ± 0.06    | 0.96 ± 0.05    |
| Ti-51  | 630 ± 110      | 430 ± 90       | 1190 ± 180    | 160 ± 50       | <1800          |
| V-52   | 22.9 ± 1.2     | 20.2 ± 1.2     | 41.2 ± 1.9    | 13.6 ± 0.9     | 8.5 ± 0.7      |
| Cr-51  | 22.9 ± 1.4     | 30.6 ± 1.9     | 31.9 ± 1.9    | 13.0 ± 0.9     | 14.0 ± 1.0     |
| Mn-56  | 75 ± 3         | 73 ± 4         | 112 ± 6       | 62 ± 3         | 66 ± 4         |
| Fe-59  | 7700 ± 400     | 3950 ± 220     | 12400 ± 800   | 6600 ± 400     | 2730 ± 140     |
| Co-60  | 1.59 ± 0.11    | 1.37 ± 0.09    | 2.68 ± 0.20   | 1.12 ± 0.08    | 0.60 ± 0.08    |
| Cu-66  | <70            | <90            | <80           | <80            | <80            |
| Zn-65  | <5             | 17 ± 3         | <3            | 60 ± 8         | 69 ± 9         |
| Ga-72  | <5             | <7             | <10           | <7             | <7             |
| As-76  | 1.39 ± 0.17    | 1.46 ± 0.20    | 13.9 ± 1.4    | 10.4 ± 1.1     | 2.2 ± 0.3      |
| Se-75  | <2.0           | <1.8           | <1.7          | <3             | <4             |
| Br-82  | <0.8           | 0.64 ± 0.20    | 0.79 ± 0.15   | 0.89 ± 0.14    | 0.73 ± 0.15    |
| Rb-86  | 14.7 ± 1.3     | 12.3 ± 1.4     | 26.7 ± 2.3    | 6.1 ± 1.9      | 6.0 ± 1.7      |
| Sr-87  | 980 ± 80       | 920 ± 70       | 460 ± 50      | 930 ± 70       | 1030 ± 80      |
| Zr-95  | <70            | <70            | <90           | <60            | <60            |
| Ag-110 | <1.4           | <1.4           | <1.5          | <1.0           | <1.1           |
| In-116 | <0.06          | <0.10          | <0.07         | <0.05          | <0.07          |
| Sb-122 | <0.08          | <0.11          | 0.97 ± 0.05   | 0.36 ± 0.04    | 0.19 ± 0.03    |
| I-128  | <7             | <7             | <7            | <5             | <7             |
| Cs-134 | 0.51 ± 0.06    | 0.51 ± 0.04    | 1.10 ± 0.08   | 0.234 ± 0.025  | 0.21 ± 0.04    |
| Ba-131 | 60 ± 16        | <30            | 63 ± 17       | <32            | <180           |
| Ba-139 | <1700          | <1700          | <1700         | <1500          | <1600          |
| La-140 | 8.6 ± 0.4      | 13.3 ± 0.7     | 9.4 ± 0.4     | 28.4 ± 1.4     | 38.8 ± 2.1     |
| Ce-141 | 15.0 ± 0.9     | 16.3 ± 1.0     | 10.5 ± 1.3    | 34.0 ± 2.4     | 52 ± 3         |
| Nd-147 | 6.6 ± 0.6      | 7.5 ± 0.9      | 4.2 ± 0.6     | 21.9 ± 1.9     | 34 ± 3         |
| Sm-153 | 1.12 ± 0.06    | 1.71 ± 0.09    | 0.98 ± 0.05   | 2.6 ± 0.3      | 5.23 ± 0.25    |
| Eu-152 | 0.24 ± 0.06    | 0.42 ± 0.07    | 0.39 ± 0.07   | 1.29 ± 0.11    | 1.79 ± 0.12    |
| Tb-160 | 0.151 ± 0.019  | 0.190 ± 0.022  | <0.20         | 0.43 ± 0.04    | 0.70 ± 0.06    |
| Dy-165 | 0.78 ± 0.11    | 1.30 ± 0.17    | 1.12 ± 0.14   | 2.57 ± 0.21    | 3.6 ± 0.3      |
| Yb-175 | 0.54 ± 0.07    | 0.84 ± 0.07    | 0.83 ± 0.06   | 0.83 ± 0.08    | 1.03 ± 0.09    |
| Lu-177 | 0.073 ± 0.007  | 0.110 ± 0.009  | 0.111 ± 0.009 | 0.091 ± 0.010  | 0.109 ± 0.011  |
| Hf-181 | 0.50 ± 0.04    | 0.35 ± 0.03    | 1.18 ± 0.08   | 0.142 ± 0.024  | 0.19 ± 0.06    |
| Ta-182 | 0.132 ± 0.023  | <0.22          | 0.32 ± 0.05   | <0.18          | <0.21          |
| W-187  | <1.4           | <1.7           | <1.8          | <1.8           | <1.9           |
| Au-198 | <0.003         | <0.004         | <0.003        | <0.005         | <0.005         |
| Hg-203 | <0.25          | <0.3           | <0.23         | <0.3           | <0.4           |
| Th-233 | 1.37 ± 0.06    | 0.91 ± 0.05    | 1.98 ± 0.23   | 1.00 ± 0.05    | 1.15 ± 0.06    |
| U-235  | 0.53 ± 0.03    | 2.06 ± 0.08    | 5.03 ± 0.18   | 18.7 ± 0.6     | 11.2 ± 0.4     |

|        | 905066         | 905067         | 905068         | 905069        | 905070        |
|--------|----------------|----------------|----------------|---------------|---------------|
| Na-24  | 44.8 ± 2.2     | 58 ± 3         | 74 ± 4         | 36 ± 3        | 47.9 ± 2.3    |
| Mg-27  | 7200 ± 500     | 6600 ± 600     | 8200 ± 600     | 5300 ± 400    | 5500 ± 400    |
| Al-28  | 3640 ± 160     | 4630 ± 190     | 7200 ± 300     | 2080 ± 110    | 1260 ± 90     |
| Cl-38  | <50            | <60            | <60            | <40           | <30           |
| K-42   | 2100 ± 180     | 3700 ± 300     | 5500 ± 400     | 1650 ± 150    | 770 ± 90      |
| Ca-49  | 310000 ± 12000 | 337000 ± 13000 | 344000 ± 14000 | 162000 ± 6000 | 154000 ± 6000 |
| Sc-46  | 0.95 ± 0.05    | 1.15 ± 0.06    | 1.52 ± 0.08    | 0.61 ± 0.03   | 0.302 ± 0.017 |
| Ti-51  | <1700          | 180 ± 70       | 390 ± 80       | <1300         | <1200         |
| V-52   | 5.9 ± 0.7      | 7.7 ± 0.8      | 12.3 ± 0.9     | 3.0 ± 0.5     | <1.9          |
| Cr-51  | 9.4 ± 0.6      | 10.3 ± 0.7     | 19.5 ± 1.2     | 6.3 ± 0.4     | 3.3 ± 0.3     |
| Mn-56  | 88 ± 4         | 86 ± 4         | 97 ± 5         | 47.3 ± 2.0    | 39.1 ± 1.9    |
| Fe-59  | 2730 ± 140     | 2850 ± 170     | 4800 ± 300     | 2270 ± 150    | 1590 ± 80     |
| Co-60  | 0.78 ± 0.07    | 0.51 ± 0.13    | 1.21 ± 0.07    | 0.45 ± 0.08   | 0.56 ± 0.05   |
| Cu-66  | <70            | <70            | <80            | <50           | <40           |
| Zn-65  | 17 ± 3         | <0.024         | 22 ± 3         | 6.7 ± 1.7     | 5.7 ± 0.9     |
| Ga-72  | <4             | <4             | <5             | <3            | <3            |
| As-76  | 0.75 ± 0.11    | 0.68 ± 0.12    | 1.53 ± 0.19    | 0.67 ± 0.09   | 0.42 ± 0.07   |
| Se-75  | <1.2           | <0.23          | <1.6           | <1.2          | <0.8          |
| Br-82  | <0.6           | <0.6           | 0.35 ± 0.07    | <0.5          | <0.5          |
| Rb-86  | 6.8 ± 1.1      | 8.6 ± 1.2      | 11.9 ± 1.2     | 4.8 ± 0.9     | <2.2          |
| Sr-87  | 750 ± 70       | 790 ± 70       | 1180 ± 90      | 480 ± 40      | 360 ± 40      |
| Zr-95  | <50            | <60            | <60            | <40           | <30           |
| Ag-110 | <1.0           | <0.9           | <1.0           | <0.7          | <0.6          |
| In-116 | <0.07          | <0.06          | <0.06          | <0.04         | <0.05         |
| Sb-122 | 0.101 ± 0.019  | <0.07          | 0.159 ± 0.024  | 0.073 ± 0.014 | 0.078 ± 0.015 |
| I-128  | <6             | <6             | <6             | <5            | <4            |
| Cs-134 | 0.29 ± 0.05    | 0.36 ± 0.03    | 0.53 ± 0.04    | 0.157 ± 0.017 | 0.112 ± 0.017 |
| Ba-131 | <23            | <90            | <46            | <80           | <50           |
| Ba-139 | <1600          | <1600          | <1700          | <1300         | <1300         |
| La-140 | 5.4 ± 0.3      | 6.0 ± 0.3      | 6.4 ± 0.3      | 2.72 ± 0.13   | 1.97 ± 0.09   |
| Ce-141 | 6.2 ± 0.7      | 6.6 ± 0.8      | 7.3 ± 0.6      | 3.4 ± 0.6     | 2.3 ± 0.5     |
| Nd-147 | 2.9 ± 0.5      | 3.3 ± 0.4      | 3.2 ± 0.4      | 1.9 ± 0.3     | 1.2 ± 0.3     |
| Sm-153 | 0.54 ± 0.03    | 0.44 ± 0.03    | 0.58 ± 0.03    | 0.347 ± 0.022 | 0.252 ± 0.019 |
| Eu-152 | 0.349 ± 0.016  | 0.41 ± 0.05    | 0.50 ± 0.07    | 0.17 ± 0.03   | 0.09 ± 0.03   |
| Tb-160 | 0.093 ± 0.012  | <0.14          | 0.097 ± 0.017  | <0.11         | <0.10         |
| Dy-165 | 0.56 ± 0.12    | 0.48 ± 0.11    | <2.1           | 0.35 ± 0.07   | <1.5          |
| Yb-175 | 0.39 ± 0.04    | 0.36 ± 0.04    | 0.38 ± 0.04    | 0.21 ± 0.03   | 0.17 ± 0.04   |
| Lu-177 | 0.047 ± 0.005  | 0.047 ± 0.005  | 0.058 ± 0.005  | 0.031 ± 0.004 | 0.017 ± 0.003 |
| Hf-181 | 0.25 ± 0.04    | 0.195 ± 0.022  | 0.40 ± 0.04    | 0.119 ± 0.016 | 0.055 ± 0.013 |
| Ta-182 | <0.17          | <0.17          | 0.111 ± 0.017  | <0.13         | <0.11         |
| W-187  | <0.9           | <1.0           | <1.2           | <0.8          | <0.7          |
| Au-198 | <0.0022        | <0.0020        | <0.003         | <0.0019       | <0.0016       |
| Hg-203 | <0.18          | <0.14          | <0.18          | <0.15         | <0.12         |
| Th-233 | 0.64 ± 0.03    | 0.70 ± 0.12    | 1.03 ± 0.05    | 0.351 ± 0.021 | 0.22 ± 0.03   |
| U-235  | 2.10 ± 0.08    | 2.24 ± 0.08    | 1.45 ± 0.06    | 1.20 ± 0.05   | 0.92 ± 0.04   |

**905071**

|               |                |
|---------------|----------------|
| <b>Na-24</b>  | 69 ± 3         |
| <b>Mg-27</b>  | 4500 ± 300     |
| <b>Al-28</b>  | 880 ± 90       |
| <b>Cl-38</b>  | <60            |
| <b>K-42</b>   | 590 ± 100      |
| <b>Ca-49</b>  | 411000 ± 16000 |
| <b>Sc-46</b>  | 0.267 ± 0.014  |
| <b>Ti-51</b>  | <1600          |
| <b>V-52</b>   | <2.3           |
| <b>Cr-51</b>  | 2.86 ± 0.24    |
| <b>Mn-56</b>  | 45.4 ± 2.0     |
| <b>Fe-59</b>  | 960 ± 60       |
| <b>Co-60</b>  | <0.08          |
| <b>Cu-66</b>  | <70            |
| <b>Zn-65</b>  | <0.023         |
| <b>Ga-72</b>  | <5             |
| <b>As-76</b>  | 0.40 ± 0.07    |
| <b>Se-75</b>  | <0.8           |
| <b>Br-82</b>  | 0.42 ± 0.07    |
| <b>Rb-86</b>  | <2.3           |
| <b>Sr-87</b>  | 1020 ± 80      |
| <b>Zr-95</b>  | <30            |
| <b>Ag-110</b> | <0.5           |
| <b>In-116</b> | <0.06          |
| <b>Sb-122</b> | <0.04          |
| <b>I-128</b>  | <5             |
| <b>Cs-134</b> | <0.18          |
| <b>Ba-131</b> | <60            |
| <b>Ba-139</b> | <1500          |
| <b>La-140</b> | 3.6 ± 0.3      |
| <b>Ce-141</b> | 2.7 ± 0.6      |
| <b>Nd-147</b> | 2.0 ± 0.3      |
| <b>Sm-153</b> | 0.368 ± 0.024  |
| <b>Eu-152</b> | 0.13 ± 0.03    |
| <b>Tb-160</b> | <0.10          |
| <b>Dy-165</b> | <1.9           |
| <b>Yb-175</b> | 0.220 ± 0.024  |
| <b>Lu-177</b> | 0.021 ± 0.004  |
| <b>Hf-181</b> | <0.10          |
| <b>Ta-182</b> | <0.11          |
| <b>W-187</b>  | <0.8           |
| <b>Au-198</b> | <0.0016        |
| <b>Hg-203</b> | <0.10          |
| <b>Th-233</b> | 0.204 ± 0.016  |
| <b>U-235</b>  | 1.38 ± 0.05    |

## Appendix 3

Analytical results of  $\delta^{13}\text{C}$  of organic matter in samples from the Jinxian Section, Anhui.

| Sample | Lab number | $\delta^{13}\text{C}$ |
|--------|------------|-----------------------|
| S-8    | 987001     | -28.12                |
| S-7    | 987002     | -28.00                |
| S-6    | 987003     | -25.23                |
| S-5    | 987004     | -24.79                |
| S-4    | 987005     | -25.56                |
| S-3    | 987006     | -26.36                |
| S-2    | 987007     | -25.95                |
| S-1    | 987008     | -24.34                |
| E-9    | 987009     | -24.75                |
| E-8    | 987010     | -24.88                |
| E-7    | 987011     | -24.11                |
| E-6    | 987012     | -25.64                |
| E-5    | 987013     | -24.73                |
| E-4    | 987014     | -23.84                |
| E-3    | 987015     | -26.44                |
| E-2    | 987016     | -23.96                |
| E-1    | 987017     | -25.55                |
| E-0    | 987018     | -26.73                |
| O-1    | 987019     | -27.11                |
| O-2    | 987020     | -27.12                |
| O-3    | 987021     | -26.69                |
| O-5    | 987023     | -26.38                |
| O-6    | 987024     | -26.07                |
| O-7    | 987025     | -26.33                |
| O-8    | 987026     | -24.98                |
| O-9    | 987027     | -24.98                |
| O-10   | 987028     | -24.26                |
| O-11   | 987029     | -26.52                |
| O-12   | 987030     | -24.57                |
| O-13   | 987031     | -26.77                |

$\delta^{13}\text{C}$  is in per mil relative to PDB standard.

#### **Appendix 4**

**NAA results of elemental abundances (all in ppm) in samples from the Jinxian Section, Anhui.**

|        | 987001       | 987002       | 987003       | 987004       | 987005       |
|--------|--------------|--------------|--------------|--------------|--------------|
| Na-24  | 420 ± 20     | 334 ± 17     | 305 ± 13     | 294 ± 13     | 277 ± 14     |
| Mg-27  | 8000 ± 500   | 5200 ± 300   | 9100 ± 500   | 8700 ± 600   | 5400 ± 300   |
| Al-28  | 86000 ± 2000 | 54100 ± 1500 | 64600 ± 1800 | 64300 ± 1800 | 62800 ± 1800 |
| Cl-38  | <30          | <30          | <30          | <30          | <30          |
| K-42   | 34000 ± 2000 | 23800 ± 1600 | 23400 ± 1600 | 23400 ± 1600 | 21700 ± 1500 |
| Ca-49  | <700         | <600         | <500         | <600         | <600         |
| Sc-46  | 15.2 ± 0.8   | 12.6 ± 0.7   | 11.5 ± 0.6   | 10.7 ± 0.6   | 10.3 ± 0.6   |
| Ti-51  | 3800 ± 500   | 2600 ± 300   | 2900 ± 400   | 3100 ± 400   | 2800 ± 400   |
| V-52   | 238 ± 9      | 466 ± 17     | 630 ± 20     | 700 ± 30     | 650 ± 20     |
| Cr-51  | 82 ± 5       | 77 ± 5       | 76 ± 5       | 77 ± 5       | 74 ± 4       |
| Mn-56  | 131 ± 5      | 78 ± 3       | 182 ± 7      | 149 ± 6      | 95 ± 4       |
| Fe-59  | 16300 ± 900  | 22100 ± 1100 | 10500 ± 500  | 11500 ± 600  | 22100 ± 1200 |
| Co-60  | 2.44 ± 0.15  | 5.8 ± 0.3    | 1.86 ± 0.16  | 3.35 ± 0.18  | 2.64 ± 0.17  |
| Cu-66  | <150         | <170         | <180         | <180         | <160         |
| Zn-65  | <12          | 53 ± 8       | 30 ± 20      | 45 ± 6       | 58 ± 8       |
| Ga-72  | 25 ± 4       | 20 ± 4       | 18 ± 3       | 20 ± 3       | 18 ± 4       |
| As-76  | 25 ± 3       | 46 ± 5       | 15.1 ± 1.6   | 15.9 ± 1.7   | 110 ± 12     |
| Se-75  | 0.6 ± 0.5    | 1.8 ± 0.7    | 0.8 ± 0.8    | 1.3 ± 0.5    | 1.6 ± 0.9    |
| Br-82  | <1.9         | <2.0         | <1.4         | <1.4         | <1.7         |
| Rb-86  | 172 ± 9      | 128 ± 7      | 135 ± 7      | 123 ± 6      | 111 ± 6      |
| Sr-87  | <170         | <150         | <150         | <150         | <160         |
| Zr-95  | 160 ± 40     | 210 ± 50     | 190 ± 90     | 180 ± 40     | 120 ± 70     |
| Mo-99  | 10 ± 2       | 10.8 ± 2.0   | 9.1 ± 1.5    | 56 ± 6       | 31 ± 3       |
| Ag-110 | <3           | <4           | <3           | <3           | <3           |
| In-116 | <0.11        | <0.13        | <0.16        | <0.14        | 0.10 ± 0.02  |
| Sb-122 | 7.2 ± 0.4    | 4.6 ± 0.3    | 5.1 ± 0.3    | 4.5 ± 0.2    | 12.6 ± 0.6   |
| I-128  | <11          | <12          | <11          | <10          | <11          |
| Cs-134 | 8.1 ± 0.5    | 7.2 ± 0.5    | 6.6 ± 0.4    | 5.8 ± 0.4    | 5.8 ± 0.3    |
| Ba-131 | 4200 ± 300   | 3290 ± 160   | 3280 ± 150   | 3200 ± 200   | 2910 ± 150   |
| Ba-139 | 4400 ± 300   | 3100 ± 200   | <6000        | 3200 ± 200   | 3000 ± 200   |
| La-140 | 43 ± 2       | 39 ± 2       | 36 ± 2       | 40 ± 2       | 36.9 ± 1.9   |
| Ce-141 | 83 ± 4       | 76 ± 4       | 72 ± 3       | 72 ± 3       | 75 ± 4       |
| Nd-147 | 26 ± 5       | 27 ± 5       | 32 ± 6       | 29 ± 5       | 26 ± 5       |
| Sm-153 | 5.9 ± 0.3    | 5.8 ± 0.3    | 5.4 ± 0.3    | 6.8 ± 0.3    | 5.0 ± 0.2    |
| Eu-152 | 1.15 ± 0.06  | 1.16 ± 0.06  | 1.12 ± 0.06  | 1.01 ± 0.05  | 0.97 ± 0.05  |
| Tb-160 | 0.82 ± 0.08  | 0.88 ± 0.09  | 0.69 ± 0.07  | 0.61 ± 0.06  | 0.66 ± 0.06  |
| Dy-165 | 4.9 ± 0.4    | 5.3 ± 0.5    | 4.9 ± 0.4    | 5.0 ± 0.4    | 4.4 ± 0.4    |
| Yb-175 | 3.13 ± 0.18  | 2.64 ± 0.16  | 2.77 ± 0.16  | 2.83 ± 0.16  | 2.25 ± 0.13  |
| Lu-177 | 0.40 ± 0.03  | 0.41 ± 0.03  | 0.37 ± 0.03  | 0.36 ± 0.02  | 0.37 ± 0.02  |
| Hf-181 | 5.0 ± 0.3    | 3.7 ± 0.2    | 3.8 ± 0.4    | 3.9 ± 0.2    | 3.7 ± 0.3    |
| Ta-187 | 0.89 ± 0.07  | 0.91 ± 0.07  | 0.74 ± 0.07  | 0.92 ± 0.07  | 0.88 ± 0.08  |
| W-187  | 3.0 ± 0.5    | 2.6 ± 0.9    | 2.1 ± 0.6    | 3.6 ± 0.6    | 2.2 ± 0.4    |
| Au-198 | <0.007       | <0.007       | <0.005       | <0.006       | <0.007       |
| Hg-203 | <0.7         | <0.8         | <0.5         | <0.5         | <0.5         |
| Th-233 | 14.4 ± 0.6   | 13.8 ± 0.5   | 13.3 ± 0.5   | 12.2 ± 0.5   | 11.9 ± 0.5   |
| U-235  | 4.63 ± 0.16  | 16.2 ± 0.6   | 12.2 ± 0.4   | 11.0 ± 0.4   | 11.9 ± 0.4   |

|        | 987006       | 987007       | 987008       | 987009        | 987010       |
|--------|--------------|--------------|--------------|---------------|--------------|
| Na-24  | 274 ± 12     | 255 ± 14     | 328 ± 15     | 311 ± 14      | 250 ± 16     |
| Mg-27  | 5100 ± 300   | 4900 ± 300   | 6000 ± 400   | 4600 ± 300    | 3000 ± 200   |
| Al-28  | 55200 ± 1500 | 54100 ± 1500 | 67400 ± 1900 | 73000 ± 2000  | 54700 ± 1500 |
| Cl-38  | <30          | <20          | <30          | <30           | <30          |
| K-42   | 22100 ± 1500 | 20900 ± 1400 | 28300 ± 1900 | 29700 ± 1900  | 21000 ± 1400 |
| Ca-49  | <500         | <400         | <500         | <600          | <400         |
| Sc-46  | 11.5 ± 0.6   | 10.3 ± 0.5   | 9.7 ± 0.5    | 9.3 ± 0.5     | 9.6 ± 0.5    |
| Ti-51  | 2300 ± 300   | 2500 ± 300   | 3300 ± 400   | 2900 ± 400    | 2000 ± 300   |
| V-52   | 530 ± 19     | 620 ± 20     | 580 ± 20     | 620 ± 20      | 542 ± 20     |
| Cr-51  | 80 ± 5       | 72 ± 4       | 70 ± 4       | 71 ± 4        | 73 ± 4       |
| Mn-56  | 89 ± 4       | 109 ± 4      | 84 ± 4       | 66 ± 3        | 49 ± 2       |
| Fe-59  | 46000 ± 2000 | 42000 ± 2000 | 31000 ± 1600 | 49000 ± 3000  | 51000 ± 3000 |
| Co-60  | 4.2 ± 0.2    | 8.2 ± 0.4    | 5.3 ± 0.3    | 5.5 ± 0.3     | 2.18 ± 0.13  |
| Cu-66  | <170         | <150         | <160         | <160          | 90 ± 40      |
| Zn-65  | 98 ± 13      | 290 ± 40     | 170 ± 20     | 51 ± 7        | 56 ± 8       |
| Ga-72  | 24 ± 4       | <17          | 23 ± 5       | <19           | 16 ± 4       |
| As-76  | 174 ± 18     | 300 ± 30     | 220 ± 20     | 270 ± 30      | 220 ± 20     |
| Se-75  | 1.8 ± 0.6    | 2.9 ± 0.9    | 2.3 ± 1.6    | 11 ± 3        | 3.5 ± 1.0    |
| Br-82  | 1.1 ± 0.2    | <1.4         | 0.86 ± 0.16  | 1.3 ± 0.6     | 2.1 ± 0.5    |
| Rb-86  | 121 ± 7      | 115 ± 6      | 143 ± 7      | 147 ± 8       | 114 ± 6      |
| Sr-87  | <150         | <120         | <130         | <160          | <140         |
| Zr-95  | 270 ± 60     | 190 ± 50     | 200 ± 140    | 270 ± 50      | 230 ± 80     |
| Mo-99  | 49 ± 6       | 56 ± 6       | 151 ± 9      | 145 ± 15      | 295 ± 15     |
| Ag-110 | <4           | <3           | <3           | <3            | <4           |
| In-116 | <0.13        | 0.06 ± 0.02  | <0.12        | 0.09 ± 0.03   | <0.12        |
| Sb-122 | 23.0 ± 1.3   | 25.4 ± 1.2   | 19.6 ± 0.9   | 25.2 ± 1.2    | 43 ± 2       |
| I-128  | <12          | <8           | <8           | <10           | <11          |
| Cs-134 | 6.7 ± 0.4    | 5.8 ± 0.3    | 7.6 ± 0.5    | 6.8 ± 0.4     | 7.3 ± 0.4    |
| Ba-134 | 2700 ± 140   | 2710 ± 150   | 3960 ± 200   | 3830 ± 190    | 2270 ± 110   |
| Ba-139 | 2580 ± 180   | 2580 ± 180   | 4100 ± 300   | 4000 ± 300    | 2500 ± 170   |
| La-140 | 33.4 ± 1.9   | 31.7 ± 1.8   | 33 ± 2       | 25.6 ± 1.4    | 29.7 ± 1.6   |
| Ce-141 | 66 ± 3       | 70 ± 3       | 65 ± 3       | 53 ± 3        | 58 ± 3       |
| Nd-147 | 27 ± 6       | 22 ± 5       | 26 ± 5       | 19 ± 5        | 17 ± 5       |
| Sm-153 | 5.2 ± 0.3    | 4.3 ± 0.2    | 6.0 ± 0.3    | 3.23 ± 0.16   | 4.09 ± 0.20  |
| Eu-152 | 1.09 ± 0.05  | 0.99 ± 0.06  | 1.16 ± 0.07  | 0.79 ± 0.06   | 0.86 ± 0.05  |
| Tb-160 | 0.89 ± 0.09  | 0.75 ± 0.08  | 0.71 ± 0.08  | 0.42 ± 0.05   | 0.57 ± 0.07  |
| Dy-165 | 5.8 ± 0.6    | 4.6 ± 0.6    | 5.9 ± 0.8    | 4.0 ± 0.3     | 3.4 ± 0.4    |
| Yb-175 | 3.43 ± 0.19  | 2.52 ± 0.15  | 3.26 ± 0.19  | 2.9 ± 0.2     | 2.12 ± 0.15  |
| Lu-177 | 0.38 ± 0.03  | 0.37 ± 0.03  | 0.42 ± 0.03  | 0.37 ± 0.03   | 0.41 ± 0.03  |
| Hf-181 | 3.8 ± 0.3    | 3.7 ± 0.4    | 5.0 ± 0.5    | 5.4 ± 0.6     | 3.5 ± 0.3    |
| Ta-182 | 0.79 ± 0.06  | 0.91 ± 0.08  | 2.21 ± 0.15  | 2.14 ± 0.15   | 0.84 ± 0.07  |
| W-187  | 3.2 ± 1.2    | 2.4 ± 0.8    | 2.3 ± 0.8    | 5 ± 5         | 2.4 ± 1.3    |
| Au-198 | <0.008       | <0.006       | <0.007       | 0.018 ± 0.002 | <0.008       |
| Hg-203 | <0.8         | <0.5         | <0.5         | <0.6          | <0.8         |
| Th-233 | 12.6 ± 0.5   | 11.7 ± 0.5   | 12.7 ± 0.5   | 14.9 ± 0.6    | 10.7 ± 0.5   |
| U-235  | 20.6 ± 0.7   | 18.6 ± 0.6   | 16.3 ± 0.6   | 16.8 ± 0.6    | 15.7 ± 0.5   |



|        | 987011        | 987012        | 987013       | 987014          | 987015          |
|--------|---------------|---------------|--------------|-----------------|-----------------|
| Na-24  | 251 ± 12      | 274 ± 15      | 266 ± 13     | 214 ± 10        | 238 ± 11        |
| Mg-27  | 4100 ± 300    | 4700 ± 500    | 4500 ± 300   | 3700 ± 200      | 5100 ± 300      |
| Al-28  | 57100 ± 1600  | 63600 ± 1800  | 62500 ± 1700 | 46400 ± 1300    | 60400 ± 1700    |
| Cl-38  | <30           | <30           | <30          | <30             | <30             |
| K-42   | 20700 ± 1400  | 22500 ± 1600  | 22400 ± 1500 | 16000 ± 1100    | 20400 ± 1400    |
| Ca-49  | <500          | <500          | <500         | <600            | <400            |
| Sc-46  | 9.4 ± 0.5     | 10.1 ± 0.5    | 9.3 ± 0.5    | 8.2 ± 0.4       | 8.4 ± 0.4       |
| Ti-51  | 2700 ± 300    | 2900 ± 400    | 3000 ± 400   | 2000 ± 300      | 2600 ± 300      |
| V-52   | 700 ± 30      | 670 ± 20      | 690 ± 20     | 357 ± 13        | 487 ± 18        |
| Cr-51  | 77 ± 5        | 88 ± 5        | 82 ± 5       | 82 ± 5          | 86 ± 5          |
| Mn-56  | 69 ± 3        | 76 ± 3        | 57 ± 2       | 55 ± 2          | 83 ± 3          |
| Fe-59  | 12000 ± 600   | 28300 ± 1400  | 6800 ± 400   | 20300 ± 1100    | 11200 ± 600     |
| Co-60  | 0.80 ± 0.12   | 2.06 ± 0.12   | 0.81 ± 0.07  | 1.76 ± 0.11     | 1.27 ± 0.13     |
| Cu-66  | <160          | <190          | <150         | <150            | <160            |
| Zn-65  | <6            | 42 ± 6        | <8           | 26 ± 4          | 26 ± 19         |
| Ga-72  | 19 ± 6        | 19 ± 4        | 17 ± 3       | 16 ± 3          | 15 ± 6          |
| As-76  | 56 ± 6        | 220 ± 30      | 25 ± 3       | 178 ± 18        | 18.5 ± 2.0      |
| Se-75  | 0.8 ± 0.5     | 2.6 ± 1.3     | 0.5 ± 0.3    | 1.6 ± 0.6       | 1.4 ± 0.6       |
| Br-82  | 1.0 ± 0.3     | 2.4 ± 0.3     | 0.89 ± 0.19  | 1.8 ± 0.3       | 0.8 ± 0.3       |
| Rb-86  | 128 ± 7       | 119 ± 6       | 123 ± 6      | 85 ± 5          | 110 ± 6         |
| Sr-87  | <120          | <140          | <140         | <130            | <120            |
| Zr-95  | 190 ± 50      | 180 ± 110     | 150 ± 30     | 150 ± 50        | 270 ± 50        |
| Mo-99  | 30 ± 4        | 530 ± 30      | 31 ± 3       | 47 ± 3          | 28 ± 2          |
| Ag-110 | <3            | <3            | <2           | <3              | <3              |
| In-116 | <0.14         | 0.12 ± 0.03   | <0.11        | 0.08 ± 0.02     | <0.13           |
| Sb-122 | 8.7 ± 0.4     | 34.0 ± 1.6    | 6.7 ± 0.3    | 15.6 ± 0.9      | 5.0 ± 0.2       |
| I-128  | <8            | <9            | <10          | <11             | <8              |
| Cs-134 | 6.2 ± 0.4     | 6.8 ± 0.4     | 6.2 ± 0.4    | 4.9 ± 0.3       | 6.0 ± 0.4       |
| Ba-131 | 2680 ± 140    | 2830 ± 170    | 2890 ± 150   | 2160 ± 100      | 2570 ± 140      |
| Ba-139 | 2590 ± 180    | 2900 ± 200    | 2890 ± 200   | 2150 ± 150      | <5000           |
| La-140 | 21.8 ± 1.2    | 34 ± 2        | 33.3 ± 1.8   | 29.4 ± 1.6      | 33.2 ± 2.0      |
| Ce-141 | 44 ± 2        | 63 ± 3        | 67 ± 3       | 54 ± 3          | 67 ± 3          |
| Nd-147 | 22 ± 5        | 24 ± 5        | 30 ± 5       | 23 ± 5          | 29 ± 5          |
| Sm-153 | 2.24 ± 0.11   | 5.3 ± 0.3     | 3.57 ± 0.17  | 3.45 ± 0.17     | 3.66 ± 0.18     |
| Eu-152 | 0.56 ± 0.05   | 0.88 ± 0.06   | 0.76 ± 0.05  | 0.72 ± 0.05     | 0.83 ± 0.05     |
| Tb-160 | 0.24 ± 0.04   | 0.32 ± 0.09   | 0.30 ± 0.05  | 0.28 ± 0.04     | 0.45 ± 0.05     |
| Dy-165 | <3            | 3.0 ± 0.7     | 2.3 ± 0.2    | 2.0 ± 0.2       | <3              |
| Yb-175 | 1.58 ± 0.12   | 1.78 ± 0.14   | 1.61 ± 0.13  | 1.30 ± 0.11     | 1.55 ± 0.10     |
| Lu-177 | 0.233 ± 0.020 | 0.33 ± 0.03   | 0.29 ± 0.02  | 0.19 ± 0.02     | 0.226 ± 0.017   |
| Hf-181 | 3.7 ± 0.4     | 3.6 ± 0.4     | 3.8 ± 0.3    | 3.1 ± 0.3       | 3.4 ± 0.4       |
| Ta-182 | 0.81 ± 0.06   | 1.02 ± 0.10   | 0.97 ± 0.07  | 0.76 ± 0.06     | 0.80 ± 0.06     |
| W-187  | 2.3 ± 0.5     | 3.1 ± 1.0     | 1.9 ± 0.5    | 1.6 ± 0.8       | 2.9 ± 0.7       |
| Au-198 | <0.004        | 0.012 ± 0.003 | <0.006       | 0.0074 ± 0.0017 | 0.0057 ± 0.0015 |
| Hg-203 | <0.5          | <0.6          | <0.5         | <0.7            | <0.5            |
| Th-233 | 12.1 ± 0.5    | 11.9 ± 0.5    | 12.7 ± 0.5   | 10.1 ± 0.4      | 11.1 ± 0.6      |
| U-235  | 11.1 ± 0.4    | 14.9 ± 0.5    | 11.5 ± 0.4   | 14.8 ± 0.5      | 16.8 ± 0.6      |

|        | 987016       | 987017       | 987018       | 987019       | 987020       |
|--------|--------------|--------------|--------------|--------------|--------------|
| Na-24  | 303 ± 14     | 188 ± 11     | 365 ± 19     | 303 ± 14     | 374 ± 16     |
| Mg-27  | 23200 ± 1800 | 7400 ± 400   | 5100 ± 300   | 11200 ± 700  | 8100 ± 500   |
| Al-28  | 86000 ± 2000 | 50000 ± 1400 | 69600 ± 1900 | 83000 ± 3000 | 90000 ± 3000 |
| Cl-38  | <30          | <30          | <30          | <30          | <30          |
| K-42   | 21100 ± 1500 | 14300 ± 1100 | 30000 ± 2000 | 25600 ± 1700 | 33000 ± 2000 |
| Ca-49  | <700         | <800         | <500         | <400         | <600         |
| Sc-46  | 14.0 ± 0.7   | 9.8 ± 0.5    | 16.5 ± 0.9   | 14.7 ± 0.8   | 16.0 ± 0.8   |
| Ti-51  | 3400 ± 400   | 2300 ± 300   | 3400 ± 400   | 3300 ± 400   | 4000 ± 500   |
| V-52   | 302 ± 11     | 230 ± 9      | 175 ± 6      | 264 ± 10     | 150 ± 6      |
| Cr-51  | 155 ± 9      | 137 ± 8      | 85 ± 5       | 94 ± 6       | 82 ± 5       |
| Mn-56  | 340 ± 14     | 129 ± 5      | 84 ± 3       | 198 ± 8      | 115 ± 6      |
| Fe-59  | 43000 ± 2000 | 50000 ± 3000 | 34500 ± 1800 | 27600 ± 1400 | 33900 ± 1700 |
| Co-60  | 8.3 ± 0.4    | 2.45 ± 0.14  | 1.73 ± 0.10  | 7.9 ± 0.4    | 2.24 ± 0.14  |
| Cu-66  | <200         | <130         | <140         | 170 ± 50     | <150         |
| Zn-65  | 95 ± 13      | 53 ± 8       | 33 ± 6       | 78 ± 19      | 44 ± 6       |
| Ga-72  | 21 ± 4       | <20          | 28 ± 4       | 22 ± 3       | 22 ± 4       |
| As-76  | 54 ± 6       | 220 ± 20     | 157 ± 17     | 35 ± 4       | 114 ± 12     |
| Se-75  | 1.8 ± 0.7    | 1.9 ± 0.6    | 2.5 ± 0.7    | 1.2 ± 1.2    | 2.9 ± 0.8    |
| Br-82  | 1.6 ± 0.2    | 4.6 ± 0.7    | 0.8 ± 0.3    | 0.92 ± 0.19  | 1.1 ± 0.2    |
| Rb-86  | 112 ± 6      | 76 ± 5       | 166 ± 8      | 140 ± 7      | 178 ± 9      |
| Sr-87  | <190         | <160         | <140         | <140         | <130         |
| Zr-95  | 320 ± 90     | 500 ± 200    | 240 ± 90     | 280 ± 100    | 190 ± 50     |
| Mo-99  | 98 ± 8       | 89 ± 6       | 24 ± 2       | 17.4 ± 1.8   | 83 ± 6       |
| Ag-110 | <3           | <3           | <4           | <3           | <3           |
| In-116 | <0.15        | <0.09        | <0.10        | 0.08 ± 0.03  | <0.11        |
| Sb-122 | 7.2 ± 0.4    | 28.5 ± 1.4   | 18.0 ± 1.0   | 6.6 ± 0.3    | 13.6 ± 0.7   |
| I-128  | <12          | <11          | <11          | <9           | <8           |
| Cs-134 | 5.1 ± 0.3    | 3.4 ± 0.3    | 8.2 ± 0.5    | 6.7 ± 0.4    | 9.1 ± 0.5    |
| Ba-131 | 3230 ± 150   | 3200 ± 200   | 4000 ± 200   | 3500 ± 200   | 4200 ± 200   |
| Ba-139 | 3300 ± 200   | 3200 ± 200   | 4000 ± 300   | 3400 ± 200   | 4400 ± 300   |
| La-140 | 52 ± 3       | 109 ± 6      | 48 ± 3       | 29.7 ± 1.8   | 46 ± 3       |
| Ce-141 | 90 ± 4       | 216 ± 9      | 86 ± 4       | 57 ± 3       | 83 ± 4       |
| Nd-147 | 49 ± 7       | 85 ± 8       | <20          | 18 ± 5       | 27 ± 6       |
| Sm-153 | 12.0 ± 0.6   | 21.4 ± 1.0   | 6.7 ± 0.3    | 5.9 ± 0.3    | 6.1 ± 0.3    |
| Eu-152 | 2.47 ± 0.12  | 6.3 ± 0.3    | 1.39 ± 0.07  | 1.76 ± 0.09  | 1.01 ± 0.06  |
| Tb-160 | 1.38 ± 0.13  | 3.1 ± 0.3    | 0.79 ± 0.08  | 1.24 ± 0.12  | 0.65 ± 0.10  |
| Dy-165 | 10.0 ± 0.9   | 15.7 ± 1.3   | 4.7 ± 0.4    | 7.1 ± 0.5    | 4.5 ± 0.4    |
| Yb-175 | 3.34 ± 0.19  | 5.7 ± 0.3    | 2.45 ± 0.15  | 3.02 ± 0.17  | 2.88 ± 0.17  |
| Lu-177 | 0.50 ± 0.04  | 0.80 ± 0.04  | 0.37 ± 0.03  | 0.41 ± 0.03  | 0.41 ± 0.03  |
| Hf-181 | 4.9 ± 0.4    | 6.7 ± 0.3    | 4.7 ± 0.3    | 4.4 ± 0.5    | 4.5 ± 0.5    |
| Ta-182 | 1.17 ± 0.09  | 2.59 ± 0.19  | 1.11 ± 0.08  | 1.01 ± 0.10  | 1.03 ± 0.08  |
| W-187  | 3.6 ± 1.9    | 2.4 ± 1.9    | 3.6 ± 0.8    | 3.5 ± 1.0    | 4.0 ± 0.9    |
| Au-198 | <0.008       | <0.010       | <0.008       | <0.005       | <0.007       |
| Hg-203 | <0.6         | <0.6         | <0.8         | <0.5         | <0.6         |
| Th-233 | 14.3 ± 0.6   | 14.6 ± 0.6   | 12.8 ± 0.5   | 12.6 ± 0.5   | 13.4 ± 1.0   |
| U-235  | 20.1 ± 0.7   | 37.3 ± 1.3   | 12.9 ± 0.4   | 19.2 ± 0.7   | 8.1 ± 0.3    |

|        | 987021       | 987022        | 987023       | 987024        | 987025       |
|--------|--------------|---------------|--------------|---------------|--------------|
| Na-24  | 350 ± 15     | 382 ± 17      | 384 ± 17     | 413 ± 19      | 390 ± 20     |
| Mg-27  | 7400 ± 400   | 4500 ± 300    | 6100 ± 400   | 6500 ± 400    | 5500 ± 300   |
| Al-28  | 84000 ± 2000 | 73000 ± 2000  | 88000 ± 2000 | 94000 ± 3000  | 90000 ± 3000 |
| Cl-38  | <30          | 21 ± 5        | <30          | <30           | <30          |
| K-42   | 32000 ± 2000 | 32000 ± 2000  | 33000 ± 2000 | 35000 ± 2000  | 34000 ± 2000 |
| Ca-49  | <400         | <500          | <500         | <600          | <600         |
| Sc-46  | 15.1 ± 0.8   | 16.1 ± 0.9    | 16.1 ± 0.9   | 17.4 ± 0.9    | 16.2 ± 0.9   |
| Ti-51  | 3600 ± 500   | 3300 ± 400    | 3800 ± 500   | 4100 ± 500    | 4000 ± 500   |
| V-52   | 142 ± 5      | 115 ± 4       | 129 ± 5      | 140 ± 5       | 138 ± 5      |
| Cr-51  | 78 ± 5       | 83 ± 5        | 85 ± 5       | 86 ± 5        | 83 ± 5       |
| Mn-56  | 117 ± 5      | 66 ± 3        | 105 ± 4      | 85 ± 3        | 77 ± 3       |
| Fe-59  | 27000 ± 1500 | 13800 ± 700   | 9000 ± 500   | 19900 ± 1000  | 15700 ± 1100 |
| Co-60  | 1.77 ± 0.11  | 0.99 ± 0.20   | 0.85 ± 0.12  | 1.17 ± 0.08   | 0.90 ± 0.07  |
| Cu-66  | <120         | <130          | <150         | 170 ± 50      | <120         |
| Zn-65  | <10          | 21 ± 4        | <8           | 30 ± 5        | <10          |
| Ga-72  | 29 ± 4       | 23 ± 4        | 30 ± 5       | 25 ± 5        | 27 ± 4       |
| As-76  | 110 ± 12     | 240 ± 20      | 105 ± 11     | 148 ± 16      | 63 ± 6       |
| Se-75  | 2.1 ± 0.7    | 7.7 ± 1.9     | 11 ± 3       | 28 ± 7        | 9 ± 2        |
| Br-82  | <1.7         | <2            | <1.6         | <1.6          | <1.7         |
| Rb-86  | 157 ± 8      | 166 ± 8       | 177 ± 9      | 187 ± 9       | 175 ± 8      |
| Sr-87  | <140         | <130          | <120         | <120          | <140         |
| Zr-95  | 130 ± 40     | <200          | 180 ± 50     | 180 ± 40      | 130 ± 30     |
| Mo-99  | 28 ± 3       | 8.2 ± 1.4     | 4.1 ± 1.1    | 34 ± 5        | 8.2 ± 1.8    |
| Ag-110 | <3           | 2.1 ± 0.6     | 2.8 ± 0.7    | <3            | <3           |
| In-116 | <0.09        | 0.061 ± 0.016 | <0.12        | <0.11         | <0.09        |
| Sb-122 | 13.7 ± 0.7   | 12.9 ± 0.7    | 7.2 ± 0.4    | 12.8 ± 0.6    | 15.3 ± 0.7   |
| I-128  | <9           | <10           | <9           | <8            | <9           |
| Cs-134 | 8.4 ± 0.5    | 9.5 ± 0.6     | 9.2 ± 0.5    | 10.4 ± 0.6    | 9.6 ± 0.6    |
| Ba-131 | 3900 ± 200   | 4080 ± 190    | 4300 ± 300   | 4800 ± 300    | 4400 ± 300   |
| Ba-139 | 4000 ± 300   | 4200 ± 300    | 4300 ± 300   | 5100 ± 300    | 4700 ± 300   |
| La-140 | 47 ± 2       | 43 ± 2        | 46 ± 3       | 40 ± 2        | 40 ± 2       |
| Ce-141 | 96 ± 4       | 81 ± 4        | 92 ± 4       | 74 ± 3        | 73 ± 3       |
| Nd-147 | 23 ± 4       | 31 ± 6        | 33 ± 6       | 30 ± 5        | 33 ± 5       |
| Sm-153 | 5.1 ± 0.2    | 5.8 ± 0.3     | 5.2 ± 0.2    | 6.4 ± 0.3     | 5.6 ± 0.3    |
| Eu-152 | 1.05 ± 0.05  | 1.08 ± 0.06   | 1.05 ± 0.06  | 0.93 ± 0.06   | 1.08 ± 0.06  |
| Tb-160 | 0.61 ± 0.07  | 0.59 ± 0.07   | 0.70 ± 0.07  | 0.68 ± 0.09   | 0.86 ± 0.09  |
| Dy-165 | 4.4 ± 0.4    | 4.4 ± 0.4     | 4.4 ± 0.4    | 5.9 ± 0.5     | 5.6 ± 0.4    |
| Yb-175 | 2.61 ± 0.15  | 2.8 ± 0.2     | 2.60 ± 0.16  | 3.19 ± 0.19   | 2.90 ± 0.16  |
| Lu-177 | 0.41 ± 0.03  | 0.45 ± 0.03   | 0.42 ± 0.03  | 0.47 ± 0.03   | 0.44 ± 0.03  |
| Hf-181 | 4.0 ± 0.3    | 4.6 ± 0.3     | 4.9 ± 0.4    | 4.9 ± 0.6     | 4.7 ± 0.3    |
| Ta-182 | 1.09 ± 0.08  | 1.00 ± 0.08   | 1.04 ± 0.08  | 1.04 ± 0.12   | 0.99 ± 0.08  |
| W-187  | 3.4 ± 0.6    | 3.2 ± 0.9     | 3.9 ± 1.1    | 3.9 ± 0.6     | 3.2 ± 0.5    |
| Au-198 | <0.007       | <0.008        | <0.006       | 0.007 ± 0.002 | <0.007       |
| Hg-203 | <0.6         | <0.8          | <0.6         | <0.6          | <0.6         |
| Th-233 | 13.5 ± 0.5   | 13.9 ± 0.5    | 14.4 ± 0.6   | 14.1 ± 0.6    | 13.3 ± 0.6   |
| U-235  | 6.7 ± 0.2    | 5.09 ± 0.18   | 6.1 ± 0.2    | 5.37 ± 0.19   | 5.8 ± 0.2    |

|        | 987026        | 987027          | 987028        | 987029          | 987030       |
|--------|---------------|-----------------|---------------|-----------------|--------------|
| Na-24  | 433 ± 19      | 410 ± 20        | 380 ± 20      | 290 ± 19        | 300 ± 14     |
| Mg-27  | 4900 ± 500    | 6300 ± 400      | 6400 ± 400    | 6300 ± 400      | 5100 ± 300   |
| Al-28  | 72000 ± 2000  | 83000 ± 2000    | 83000 ± 2000  | 65700 ± 1800    | 52000 ± 1500 |
| Cl-38  | <30           | <20             | <30           | <30             | <20          |
| K-42   | 39000 ± 3000  | 37000 ± 2000    | 35000 ± 2000  | 26100 ± 1700    | 25900 ± 1700 |
| Ca-49  | <600          | <500            | <500          | <600            | <500         |
| Sc-46  | 18.1 ± 1.0    | 16.9 ± 0.9      | 15.5 ± 0.8    | 13.2 ± 0.7      | 12.8 ± 0.7   |
| Ti-51  | 3800 ± 500    | 4500 ± 600      | 4100 ± 500    | 2900 ± 400      | 2700 ± 300   |
| V-52   | 123 ± 5       | 144 ± 5         | 156 ± 6       | 174 ± 6         | 165 ± 6      |
| Cr-51  | 91 ± 6        | 88 ± 5          | 82 ± 5        | 70 ± 4          | 67 ± 4       |
| Mn-56  | 71 ± 3        | 100 ± 4         | 93 ± 4        | 96 ± 4          | 69 ± 3       |
| Fe-59  | 5300 ± 300    | 7900 ± 400      | 31900 ± 1600  | 9000 ± 500      | 5300 ± 300   |
| Co-60  | 0.62 ± 0.07   | 0.67 ± 0.10     | 3.9 ± 0.2     | 1.39 ± 0.11     | 0.68 ± 0.05  |
| Cu-66  | <130          | <130            | <130          | <110            | <120         |
| Zn-65  | <9            | <7              | 40 ± 6        | <10             | 18 ± 3       |
| Ga-72  | 20 ± 3        | 22 ± 4          | 18 ± 3        | 23 ± 6          | 14 ± 3       |
| As-76  | 4.3 ± 0.5     | 19 ± 2          | 64 ± 7        | 43 ± 4          | 16.8 ± 1.7   |
| Se-75  | <4            | 0.7 ± 0.4       | 4.4 ± 1.4     | 1.7 ± 0.5       | 2.1 ± 0.7    |
| Br-82  | <2            | <1.5            | 1.2 ± 0.5     | <1.7            | <1.6         |
| Rb-86  | 202 ± 10      | 220 ± 11        | 178 ± 9       | 133 ± 7         | 136 ± 7      |
| Sr-87  | <140          | <110            | <120          | <140            | <120         |
| Zr-95  | 190 ± 110     | 360 ± 60        | 170 ± 30      | 240 ± 70        | 230 ± 40     |
| Mo-99  | 0.3 ± 0.3     | 3.5 ± 0.8       | 49 ± 5        | 43 ± 4          | 7.6 ± 1.4    |
| Ag-110 | <4            | <3              | <3            | <3              | <3           |
| In-116 | 0.058 ± 0.017 | <0.11           | <0.10         | <0.09           | <0.09        |
| Sb-122 | 4.4 ± 0.3     | 5.3 ± 0.3       | 13.4 ± 0.7    | 19.3 ± 0.9      | 5.8 ± 0.3    |
| I-128  | <10           | <8              | <7            | <9              | <9           |
| Cs-134 | 10.8 ± 0.6    | 9.9 ± 0.6       | 9.2 ± 0.5     | 7.8 ± 0.4       | 8.5 ± 0.5    |
| Ba-131 | 4900 ± 200    | 4400 ± 200      | 4100 ± 200    | 3100 ± 200      | 2860 ± 150   |
| Ba-139 | 4900 ± 300    | 4400 ± 300      | 4500 ± 300    | 3000 ± 200      | 3000 ± 200   |
| La-140 | 54 ± 3        | 43 ± 3          | 27.6 ± 1.7    | 40 ± 2          | 33.0 ± 1.7   |
| Ce-141 | 106 ± 5       | 89 ± 4          | 50 ± 2        | 85 ± 4          | 61 ± 3       |
| Nd-147 | 38 ± 7        | 27 ± 5          | 26 ± 5        | 30 ± 5          | 18 ± 4       |
| Sm-153 | 8.3 ± 0.4     | 6.2 ± 0.3       | 5.4 ± 0.3     | 5.7 ± 0.3       | 5.3 ± 0.3    |
| Eu-152 | 1.34 ± 0.07   | 0.98 ± 0.06     | 0.77 ± 0.06   | 1.27 ± 0.06     | 1.01 ± 0.05  |
| Tb-160 | 0.83 ± 0.11   | 0.80 ± 0.09     | 0.76 ± 0.09   | 0.99 ± 0.09     | 0.79 ± 0.08  |
| Dy-165 | 6.0 ± 0.5     | 5.4 ± 0.4       | 6.0 ± 0.5     | 6.4 ± 0.5       | 5.1 ± 0.5    |
| Yb-175 | 3.9 ± 0.2     | 3.55 ± 0.19     | 3.54 ± 0.19   | 4.0 ± 0.3       | 3.6 ± 0.3    |
| Lu-177 | 0.49 ± 0.04   | 0.48 ± 0.03     | 0.49 ± 0.03   | 0.58 ± 0.03     | 0.54 ± 0.03  |
| Hf-181 | 5.6 ± 0.4     | 5.6 ± 0.4       | 4.9 ± 0.6     | 4.09 ± 0.18     | 4.2 ± 0.4    |
| Ta-182 | 1.32 ± 0.09   | 1.15 ± 0.08     | 1.18 ± 0.09   | 0.86 ± 0.07     | 1.10 ± 0.08  |
| W-187  | 3.7 ± 0.6     | 3.2 ± 0.5       | 4.2 ± 0.8     | 3.2 ± 1.0       | 2.8 ± 0.6    |
| Au-198 | 0.019 ± 0.003 | 0.0038 ± 0.0014 | 0.022 ± 0.003 | 0.0106 ± 0.0019 | <0.006       |
| Hg-203 | <0.9          | <0.6            | <0.5          | <0.5            | <0.7         |
| Th-233 | 14.6 ± 0.6    | 15.5 ± 0.6      | 12.9 ± 0.8    | 11.7 ± 0.5      | 11.1 ± 0.4   |
| U-235  | 3.39 ± 0.12   | 3.57 ± 0.13     | 6.1 ± 0.2     | 23.2 ± 0.8      | 10.1 ± 0.3   |

## 9870.31

|        |                 |
|--------|-----------------|
| Na-24  | 271 ± 12        |
| Mg-27  | 6800 ± 400      |
| Al-28  | 58600 ± 1600    |
| Cl-38  | <20             |
| K-42   | 23100 ± 1500    |
| Ca-49  | <400            |
| Sc-46  | 11.6 ± 0.6      |
| Ti-51  | 2700 ± 300      |
| V-52   | 246 ± 9         |
| Cr-51  | 67 ± 4          |
| Mn-56  | 108 ± 5         |
| Fe-59  | 11000 ± 600     |
| Co-60  | 0.85 ± 0.10     |
| Cu-66  | <120            |
| Zn-65  | <6              |
| Ga-72  | 17 ± 3          |
| As-76  | 26 ± 3          |
| Se-75  | 1.1 ± 0.6       |
| Br-82  | <1.1            |
| Rb-86  | 124 ± 6         |
| Sr-87  | <100            |
| Zr-95  | 180 ± 60        |
| Mo-99  | 12.5 ± 1.3      |
| Ag-110 | <3              |
| In-116 | <0.11           |
| Sb-122 | 8.0 ± 0.4       |
| I-128  | <7              |
| Cs-134 | 6.5 ± 0.4       |
| Ba-131 | 2710 ± 120      |
| Ba-139 | 2690 ± 180      |
| La-140 | 22.9 ± 1.3      |
| Ce-141 | 45 ± 2          |
| Nd-147 | 20 ± 5          |
| Sm-153 | 3.86 ± 0.18     |
| Eu-152 | 0.79 ± 0.05     |
| Tb-160 | 0.86 ± 0.09     |
| Dy-165 | 6.4 ± 0.7       |
| Yb-175 | 3.37 ± 0.18     |
| Lu-177 | 0.50 ± 0.03     |
| Hf-181 | 3.5 ± 0.4       |
| Ta-182 | 0.76 ± 0.06     |
| W-187  | 2.2 ± 0.7       |
| Au-198 | 0.0040 ± 0.0014 |
| Hg-203 | <0.5            |
| Th-233 | 10.6 ± 1.1      |
| U-235  | 10.0 ± 0.3      |

## Appendix 5

Analytical results of  $\delta^{13}\text{C}$  of organic matter  
in samples from the Fenxiang Section, Hubei.

| Sample | Lab number | $\delta^{13}\text{C}$ |
|--------|------------|-----------------------|
| FOW-29 | 995029     | -29.15                |
| FOW-28 | 995028     | -29.17                |
| FOW-27 | 995027     | -29.18                |
| FOW-26 | 995026     | -28.81                |
| FOW-25 | 995025     | -29.64                |
| FOW-24 | 995024     | -28.45                |
| FOW-23 | 995023     | -30.16                |
| FOW-22 | 995022     | -28.22                |
| FOW-21 | 995021     | -28.42                |
| FOW-20 | 995020     | -27.91                |
| FOW-19 | 995019     | -27.80                |
| FOW-18 | 995018     | -27.74                |
| FOW-17 | 995017     | -28.21                |
| FOW-16 | 995016     | -26.76                |
| FOW-15 | 995015     | -28.67                |
| FOW-14 | 995014     | -27.71                |
| FOW-13 | 995013     | -27.46                |
| FOW-12 | 995012     | -27.02                |
| FOW-11 | 995011     | -27.59                |
| FOW-10 | 995010     | -27.34                |
| FOW-9  | 995009     | -26.92                |
| FOW-8  | 995008     | -26.97                |
| FOW-7  | 995007     | -26.84                |
| FOW-6  | 995006     | -30.00                |
| FOW-5  | 995005     | -28.53                |
| FOW-4  | 995004     | -28.10                |
| FOW-3  | 995003     | -30.39                |
| FOW-2  | 995002     | -29.66                |
| FOW-1  | 995001     | -29.61                |

$\delta^{13}\text{C}$  is in per mil relative to PDB standard.

## **Appendix 6**

NAA results of elemental abundances (all in ppm) in samples from the Fenxiang Section, Hubei.

|        | 995001        | 995002        | 995003        | 995004          | 995005        |
|--------|---------------|---------------|---------------|-----------------|---------------|
| Na-24  | 2920 ± 130    | 499 ± 21      | 513 ± 22      | 880 ± 40        | 1230 ± 60     |
| Mg-27  | 10500 ± 800   | 1700 ± 300    | 970 ± 130     | 4300 ± 300      | 3500 ± 300    |
| Al-28  | 89000 ± 3000  | 19300 ± 600   | 12900 ± 400   | 51400 ± 1400    | 33600 ± 1000  |
| Cl-38  | <50           | 106 ± 11      | 158 ± 13      | <40             | <40           |
| K-42   | 41000 ± 3000  | 5800 ± 400    | 4500 ± 300    | 24300 ± 1600    | 13100 ± 800   |
| Ca-49  | <1100         | <800          | <600          | <900            | <800          |
| Sc-46  | 17.0 ± 0.9    | 3.61 ± 0.19   | 2.48 ± 0.13   | 9.9 ± 0.5       | 6.2 ± 0.3     |
| Ti-51  | 4700 ± 600    | 910 ± 160     | 660 ± 100     | 4400 ± 600      | 1750 ± 230    |
| V-52   | 195 ± 7       | 193 ± 7       | 233 ± 9       | 890 ± 30        | 365 ± 13      |
| Cr-51  | 121 ± 7       | 33.8 ± 2.1    | 25.7 ± 1.6    | 81 ± 5          | 52 ± 3        |
| Mn-56  | 80 ± 3        | 314 ± 13      | 12.0 ± 0.5    | 15.9 ± 0.8      | 37.9 ± 1.7    |
| Fe-59  | 35500 ± 1800  | 7200 ± 400    | 5500 ± 300    | 7700 ± 400      | 14200 ± 800   |
| Co-60  | 15.4 ± 0.8    | 15.0 ± 0.8    | 2.11 ± 0.17   | 3.65 ± 0.20     | 8.1 ± 0.4     |
| Cu-66  | 160 ± 40      | <110          | <70           | <170            | <110          |
| Zn-65  | 240 ± 30      | 81 ± 11       | 47 ± 19       | 58 ± 8          | 183 ± 23      |
| Ga-72  | 27 ± 3        | 5.6 ± 1.3     | <6            | 22.1 ± 2.5      | 9.5 ± 1.6     |
| As-76  | 13.8 ± 1.5    | 5.4 ± 0.6     | 11.8 ± 1.2    | 9.6 ± 1.0       | 19.0 ± 2.0    |
| Se-75  | 5.0 ± 1.4     | <2.3          | <1.4          | <3              | 2.0 ± 0.6     |
| Br-82  | 1.67 ± 0.24   | 0.50 ± 0.12   | 1.07 ± 0.20   | <1.4            | 1.16 ± 0.16   |
| Rb-86  | 189 ± 9       | 32.7 ± 2.4    | 25.1 ± 2.0    | 118 ± 6         | 68 ± 4        |
| Sr-87  | <160          | <170          | <60           | <120            | <110          |
| Zr-95  | 180 ± 50      | <80           | <21           | 410 ± 130       | <100          |
| Mo-99  | <70           | <40           | 7 ± 3         | 24 ± 6          | 33 ± 4        |
| Ag-110 | <4            | <2.0          | <1.4          | <2.5            | <2.3          |
| In-116 | <0.13         | <0.10         | <0.07         | <0.11           | <0.10         |
| Sb-122 | 3.05 ± 0.17   | 0.66 ± 0.05   | 2.13 ± 0.13   | 2.43 ± 0.13     | 4.35 ± 0.22   |
| I-128  | <9            | <10           | <5            | <7              | <7            |
| Cs-134 | 10.8 ± 0.6    | 1.85 ± 0.11   | 1.35 ± 0.09   | 6.1 ± 0.4       | 4.4 ± 0.3     |
| Ba-131 | 1230 ± 70     | 1050 ± 50     | 1130 ± 80     | 1660 ± 130      | 1110 ± 60     |
| Ba-139 | 1160 ± 80     | 1070 ± 80     | 1140 ± 80     | 1440 ± 100      | 1120 ± 80     |
| La-140 | 77 ± 5        | 30.0 ± 1.6    | 19.6 ± 1.1    | 75 ± 5          | 31.1 ± 1.7    |
| Ce-141 | 147 ± 7       | 51.9 ± 2.4    | 36.1 ± 1.8    | 141 ± 6         | 63 ± 3        |
| Nd-147 | 92 ± 10       | 34 ± 5        | 20 ± 4        | 71 ± 8          | 34 ± 7        |
| Sm-153 | 10.3 ± 0.5    | 4.78 ± 0.22   | 4.67 ± 0.21   | 10.0 ± 0.5      | 5.5 ± 0.3     |
| Eu-152 | 1.79 ± 0.08   | 0.93 ± 0.04   | 0.78 ± 0.04   | 1.97 ± 0.11     | 0.98 ± 0.05   |
| Tb-160 | 1.34 ± 0.12   | 0.54 ± 0.05   | 0.50 ± 0.05   | 1.27 ± 0.12     | 0.60 ± 0.06   |
| Dy-165 | 8.5 ± 0.8     | 3.9 ± 0.3     | 3.3 ± 0.3     | 7.7 ± 0.7       | 4.3 ± 0.3     |
| Yb-175 | 5.9 ± 0.3     | 1.90 ± 0.13   | 1.73 ± 0.10   | 4.5 ± 0.3       | 1.70 ± 0.10   |
| Lu-177 | 0.81 ± 0.04   | 0.256 ± 0.014 | 0.213 ± 0.012 | 0.59 ± 0.03     | 0.251 ± 0.016 |
| Hf-181 | 4.5 ± 0.4     | 1.05 ± 0.06   | 0.67 ± 0.08   | 5.6 ± 0.5       | 1.81 ± 0.19   |
| Ta-182 | 1.53 ± 0.10   | 0.22 ± 0.03   | 0.175 ± 0.023 | 1.26 ± 0.08     | 0.50 ± 0.04   |
| W-187  | 2.4 ± 0.4     | <1.8          | 0.40 ± 0.13   | <2.2            | 1.31 ± 0.23   |
| Au-198 | 0.014 ± 0.003 | <0.005        | <0.004        | 0.0062 ± 0.0025 | <0.006        |
| Hg-203 | <0.7          | <0.4          | <0.25         | <0.5            | <0.4          |
| Th-233 | 22.7 ± 0.9    | 3.99 ± 0.16   | 3.01 ± 0.12   | 13.9 ± 0.6      | 8.1 ± 0.3     |
| U-235  | 6.67 ± 0.23   | 4.39 ± 0.15   | 4.38 ± 0.15   | 14.8 ± 0.5      | 6.39 ± 0.22   |



|        | 995006        | 995007        | 995008        | 995009       | 995010       |
|--------|---------------|---------------|---------------|--------------|--------------|
| Na-24  | 585 ± 25      | 1950 ± 80     | 2730 ± 120    | 3410 ± 140   | 4470 ± 200   |
| Mg-27  | 880 ± 110     | 5600 ± 300    | 1400 ± 300    | 6400 ± 700   | 4700 ± 300   |
| Al-28  | 10900 ± 400   | 67400 ± 1900  | 30000 ± 900   | 57200 ± 1600 | 50700 ± 1500 |
| Cl-38  | 120 ± 10      | <50           | <70           | <60          | <50          |
| K-42   | 3400 ± 300    | 26100 ± 1700  | 7600 ± 600    | 18900 ± 1300 | 18900 ± 1200 |
| Ca-49  | <700          | <1400         | <1300         | <1400        | <1600        |
| Sc-46  | 1.96 ± 0.11   | 13.0 ± 0.7    | 6.1 ± 0.3     | 12.3 ± 0.7   | 10.5 ± 0.6   |
| Ti-51  | 530 ± 80      | 3800 ± 500    | 1410 ± 230    | 3200 ± 400   | 3000 ± 500   |
| V-52   | 100 ± 4       | 178 ± 7       | 110 ± 5       | 334 ± 12     | 314 ± 12     |
| Cr-51  | 15.4 ± 1.0    | 73 ± 4        | 38.6 ± 2.4    | 91 ± 5       | 92 ± 6       |
| Mn-56  | 15.2 ± 0.7    | 109 ± 4       | 432 ± 24      | 195 ± 8      | 283 ± 12     |
| Fe-59  | 7700 ± 400    | 34100 ± 1700  | 19800 ± 1000  | 21500 ± 1100 | 22500 ± 1200 |
| Co-60  | 2.75 ± 0.15   | 10.2 ± 0.6    | 69 ± 4        | 25.1 ± 1.3   | 9.9 ± 0.5    |
| Cu-66  | <70           | <130          | <190          | <150         | <170         |
| Zn-65  | 45 ± 6        | 90 ± 30       | 127 ± 17      | 270 ± 30     | 360 ± 50     |
| Ga-72  | <6            | 17 ± 3        | <13           | 18 ± 3       | 18 ± 3       |
| As-76  | 11.6 ± 1.2    | 20.4 ± 2.1    | 15.3 ± 1.6    | 15.8 ± 1.8   | 21.1 ± 2.2   |
| Se-75  | 0.7 ± 0.3     | <1.0          | 1.9 ± 0.8     | 16 ± 4       | 4.0 ± 1.1    |
| Br-82  | 1.03 ± 0.15   | 3.5 ± 0.4     | 3.5 ± 0.4     | 1.7 ± 0.3    | 0.94 ± 0.21  |
| Rb-86  | 21.2 ± 1.9    | 149 ± 8       | 48 ± 4        | 108 ± 6      | 106 ± 6      |
| Sr-87  | <70           | <130          | <220          | <190         | <200         |
| Zr-95  | <120          | <80           | <110          | <100         | <170         |
| Mo-99  | 19 ± 3        | 158 ± 9       | 23 ± 6        | <6           | 14 ± 4       |
| Ag-110 | <1.6          | <4            | <3            | <4           | <4           |
| In-116 | <0.06         | <0.12         | <0.14         | <0.15        | <0.16        |
| Sb-122 | 2.03 ± 0.12   | 4.56 ± 0.24   | 6.5 ± 0.3     | 8.3 ± 0.5    | 12.7 ± 0.6   |
| I-128  | <5            | 5.7 ± 1.3     | <14           | <12          | <12          |
| Cs-134 | 1.14 ± 0.08   | 7.8 ± 0.5     | 3.67 ± 0.23   | 8.4 ± 0.5    | 8.1 ± 0.5    |
| Ba-131 | 1820 ± 140    | 1450 ± 80     | 960 ± 50      | 1580 ± 180   | 1520 ± 80    |
| Ba-139 | 1620 ± 110    | 1450 ± 100    | 880 ± 70      | 1460 ± 110   | 1300 ± 100   |
| La-140 | 24.8 ± 1.4    | 77 ± 5        | 23.1 ± 1.3    | 63 ± 3       | 48 ± 3       |
| Ce-141 | 47.8 ± 2.4    | 144 ± 7       | 54 ± 3        | 141 ± 6      | 82 ± 4       |
| Nd-147 | 36 ± 5        | 56 ± 8        | 34 ± 7        | 105 ± 12     | 52 ± 8       |
| Sm-153 | 5.6 ± 0.3     | 13.4 ± 0.6    | 5.5 ± 0.3     | 16.5 ± 0.8   | 7.4 ± 0.3    |
| Eu-152 | 1.13 ± 0.05   | 2.16 ± 0.11   | 1.12 ± 0.07   | 2.91 ± 0.13  | 1.40 ± 0.07  |
| Tb-160 | 0.86 ± 0.08   | 1.64 ± 0.15   | 0.84 ± 0.09   | 2.07 ± 0.19  | 1.17 ± 0.11  |
| Dy-165 | 5.2 ± 0.4     | 10.2 ± 0.8    | 5.3 ± 0.9     | 13.1 ± 1.0   | 7.0 ± 0.6    |
| Yb-175 | 2.40 ± 0.14   | 6.1 ± 0.3     | 2.26 ± 0.14   | 5.6 ± 0.4    | 4.5 ± 0.3    |
| Lu-177 | 0.328 ± 0.017 | 0.76 ± 0.04   | 0.329 ± 0.020 | 0.76 ± 0.04  | 0.61 ± 0.03  |
| Hf-181 | 0.59 ± 0.05   | 4.4 ± 0.4     | 1.9 ± 0.3     | 3.79 ± 0.21  | 3.7 ± 0.5    |
| Ta-182 | 0.26 ± 0.025  | 1.27 ± 0.09   | 0.49 ± 0.06   | 0.88 ± 0.08  | 0.86 ± 0.07  |
| W-187  | <1.6          | 2.8 ± 0.5     | 1.8 ± 0.4     | 2.5 ± 0.5    | 2.3 ± 0.4    |
| Au-198 | <0.004        | 0.010 ± 0.003 | <0.008        | <0.009       | <0.009       |
| Hg-203 | 0.49 ± 0.15   | <0.6          | <0.6          | <0.6         | <0.7         |
| Th-233 | 2.35 ± 0.10   | 16.5 ± 0.6    | 8.0 ± 0.4     | 15.0 ± 0.6   | 13.9 ± 0.5   |
| U-235  | 4.47 ± 0.16   | 17.7 ± 0.6    | 8.9 ± 0.3     | 8.3 ± 0.3    | 7.5 ± 0.3    |

|        | 995011          | 995012       | 995013        | 995014       | 995015       |
|--------|-----------------|--------------|---------------|--------------|--------------|
| Na-24  | 4750 ± 220      | 4530 ± 190   | 3570 ± 150    | 5030 ± 220   | 4070 ± 170   |
| Mg-27  | 5000 ± 300      | 3100 ± 500   | 8800 ± 800    | 6900 ± 600   | 4200 ± 500   |
| Al-28  | 51300 ± 1500    | 44800 ± 1300 | 132000 ± 4000 | 96000 ± 3000 | 47600 ± 1300 |
| Cl-38  | <70             | <120         | <70           | <60          | <60          |
| K-42   | 17500 ± 1200    | 15000 ± 1000 | 50000 ± 3000  | 34400 ± 2200 | 17400 ± 1100 |
| Ca-49  | <1800           | <3000        | 2300 ± 300    | 2000 ± 300   | <1300        |
| Sc-46  | 9.2 ± 0.5       | 9.1 ± 0.5    | 13.3 ± 0.7    | 15.0 ± 0.8   | 7.8 ± 0.4    |
| Ti-51  | 2800 ± 400      | 2400 ± 300   | 2700 ± 400    | 5100 ± 700   | 3000 ± 400   |
| V-52   | 209 ± 8         | 153 ± 6      | 102 ± 5       | 230 ± 9      | 110 ± 4      |
| Cr-51  | 90 ± 5          | 80 ± 5       | 31.5 ± 2.2    | 64 ± 4       | 38.4 ± 2.4   |
| Mn-56  | 304 ± 13        | 346 ± 16     | 1110 ± 40     | 740 ± 30     | 289 ± 12     |
| Fe-59  | 18600 ± 900     | 22100 ± 1100 | 21600 ± 1100  | 46300 ± 2300 | 16700 ± 900  |
| Co-60  | 12.0 ± 0.6      | 45.3 ± 2.4   | 144 ± 7       | 80 ± 4       | 19.9 ± 1.1   |
| Cu-66  | <150            | <220         | <210          | <220         | <140         |
| Zn-65  | 350 ± 50        | 250 ± 30     | 410 ± 50      | 730 ± 90     | 200 ± 30     |
| Ga-72  | 12.5 ± 2.4      | 12 ± 3       | 27 ± 3        | 18 ± 3       | 11 ± 3       |
| As-76  | 17.0 ± 1.8      | 23.4 ± 2.4   | 24.0 ± 2.5    | 59 ± 6       | 19.5 ± 2.0   |
| Se-75  | 2.4 ± 0.7       | 10 ± 3       | <4            | 4.7 ± 1.3    | 3.1 ± 0.9    |
| Br-82  | <2.0            | <2.2         | 2.6 ± 0.3     | 1.4 ± 0.3    | 2.3 ± 0.4    |
| Rb-86  | 99 ± 6          | 93 ± 5       | 157 ± 9       | 130 ± 8      | 79 ± 9       |
| Sr-87  | <160            | <500         | <300          | <300         | <150         |
| Zr-95  | 160 ± 70        | <280         | 320 ± 90      | 300 ± 140    | <170         |
| Mo-99  | <5              | <9           | 46 ± 8        | 83 ± 10      | <9           |
| Ag-110 | <3              | <3           | <3            | <4           | <2.3         |
| In-116 | <0.14           | <0.3         | <0.20         | <0.20        | <0.12        |
| Sb-122 | 7.5 ± 0.4       | 12.7 ± 0.7   | 7.3 ± 0.4     | 17.8 ± 0.9   | 7.6 ± 0.4    |
| I-128  | 5.0 ± 1.5       | <24          | <21           | <18          | <10          |
| Cs-134 | 6.9 ± 0.4       | 6.3 ± 0.4    | 7.4 ± 0.4     | 7.6 ± 0.5    | 4.6 ± 0.3    |
| Ba-131 | 1330 ± 80       | 1380 ± 160   | 4800 ± 300    | 2850 ± 170   | 3970 ± 210   |
| Ba-139 | 1410 ± 100      | 1150 ± 140   | 5300 ± 400    | 3120 ± 220   | 4700 ± 300   |
| La-140 | 47 ± 3          | 56 ± 3       | 99 ± 7        | 95 ± 5       | 59 ± 3       |
| Ce-141 | 82 ± 4          | 121 ± 6      | 185 ± 8       | 174 ± 8      | 106 ± 5      |
| Nd-147 | 46 ± 6          | 86 ± 9       | 101 ± 12      | 73 ± 11      | 57 ± 7       |
| Sm-153 | 9.2 ± 0.4       | 16.4 ± 0.8   | 22.8 ± 1.1    | 15.2 ± 0.7   | 14.8 ± 0.7   |
| Eu-152 | 1.63 ± 0.08     | 2.98 ± 0.14  | 3.12 ± 0.15   | 2.38 ± 0.11  | 2.30 ± 0.10  |
| Tb-160 | 1.50 ± 0.15     | 2.41 ± 0.22  | 2.8 ± 0.3     | 2.20 ± 0.20  | 1.89 ± 0.17  |
| Dy-165 | 8.6 ± 0.7       | 13.9 ± 1.8   | 17.1 ± 1.4    | 13.3 ± 1.1   | 11.7 ± 1.0   |
| Yb-175 | 4.6 ± 0.3       | 6.5 ± 0.3    | 11.4 ± 0.6    | 8.8 ± 0.5    | 5.9 ± 0.3    |
| Lu-177 | 0.64 ± 0.03     | 0.92 ± 0.04  | 1.21 ± 0.06   | 1.01 ± 0.06  | 0.65 ± 0.04  |
| Hf-181 | 3.5 ± 0.4       | 3.2 ± 0.3    | 12.3 ± 1.2    | 8.8 ± 0.7    | 3.92 ± 0.22  |
| Ta-182 | 0.79 ± 0.08     | 0.79 ± 0.06  | 3.38 ± 0.22   | 3.18 ± 0.20  | 1.25 ± 0.09  |
| W-187  | 2.2 ± 0.5       | 1.4 ± 0.4    | 1.9 ± 0.4     | 3.4 ± 0.5    | 1.9 ± 0.4    |
| Au-198 | 0.0079 ± 0.0024 | <0.005       | 0.010 ± 0.003 | <0.011       | <0.009       |
| Hg-203 | <0.5            | <0.5         | <0.7          | <0.7         | <0.5         |
| Th-233 | 11.3 ± 1.6      | 11.6 ± 0.5   | 46.9 ± 1.9    | 29.3 ± 1.2   | 11.9 ± 0.5   |
| U-235  | 8.0 ± 0.3       | 9.6 ± 0.3    | 33.5 ± 1.1    | 42.2 ± 1.4   | 15.1 ± 0.5   |

|        | 995016       | 995016_1     | 995017          | 995018          | 995019       |
|--------|--------------|--------------|-----------------|-----------------|--------------|
| Na-24  | 3780 ± 170   | 5800 ± 300   | 5950 ± 250      | 4340 ± 180      | 5460 ± 230   |
| Mg-27  | 3050 ± 220   | 3500 ± 400   | 5600 ± 300      | 5600 ± 400      | 5300 ± 400   |
| Al-28  | 38900 ± 1100 | 44800 ± 1300 | 67400 ± 1900    | 73900 ± 2100    | 71900 ± 2000 |
| Cl-38  | <50          | <60          | <50             | <60             | <50          |
| K-42   | 14500 ± 1000 | 14000 ± 1000 | 15300 ± 1000    | 21000 ± 1300    | 26100 ± 1700 |
| Ca-49  | <1000        | <1200        | <1400           | <1300           | <1200        |
| Sc-46  | 7.2 ± 0.4    | 10.5 ± 0.6   | 9.2 ± 0.5       | 11.9 ± 0.6      | 11.7 ± 0.6   |
| Ti-51  | 2600 ± 300   | 2700 ± 400   | 3800 ± 500      | 3900 ± 500      | 4000 ± 500   |
| V-52   | 115 ± 4      | 165 ± 6      | 178 ± 7         | 543 ± 20        | 730 ± 30     |
| Cr-51  | 33.3 ± 2.1   | 41 ± 3       | 46 ± 3          | 103 ± 6         | 116 ± 7      |
| Mn-56  | 69 ± 3       | 127 ± 6      | 109 ± 4         | 51 ± 3          | 29.6 ± 1.4   |
| Fe-59  | 14500 ± 700  | 22200 ± 1100 | 20600 ± 1100    | 38400 ± 2000    | 22300 ± 1100 |
| Co-60  | 5.1 ± 0.3    | 6.2 ± 0.3    | 14.8 ± 0.8      | 16.9 ± 0.9      | 7.5 ± 0.4    |
| Cu-66  | <130         | <140         | <130            | <160            | <200         |
| Zn-65  | 163 ± 21     | 220 ± 30     | 320 ± 40        | 740 ± 90        | 240 ± 30     |
| Ga-72  | <13          | 14 ± 3       | 14.2 ± 2.2      | 23 ± 3          | 24 ± 4       |
| As-76  | 15.6 ± 1.6   | 26 ± 3       | 26 ± 3          | 48 ± 5          | 15.3 ± 1.6   |
| Se-75  | <0.8         | <3           | 1.7 ± 0.6       | 2.5 ± 0.8       | 3.1 ± 1.0    |
| Br-82  | 0.95 ± 0.18  | 1.0 ± 0.3    | 1.4 ± 0.4       | 2.9 ± 0.4       | 2.6 ± 0.3    |
| Rb-86  | 64 ± 4       | 77 ± 5       | 72 ± 4          | 100 ± 6         | 137 ± 7      |
| Sr-87  | <110         | <160         | <130            | 210 ± 40        | <150         |
| Zr-95  | 300 ± 90     | 200 ± 80     | 460 ± 90        | 280 ± 130       | 260 ± 90     |
| Mo-99  | 21 ± 6       | <8           | <7              | 95 ± 9          | 112 ± 9      |
| Ag-110 | <2.2         | <3           | <2.4            | <3              | <3           |
| In-116 | <0.09        | <0.13        | <0.12           | 0.066 ± 0.023   | <0.14        |
| Sb-122 | 6.5 ± 0.3    | 10.1 ± 0.5   | 11.3 ± 0.6      | 23.6 ± 1.1      | 9.6 ± 0.5    |
| I-128  | <7           | <10          | 5.7 ± 1.3       | 7.7 ± 1.3       | <9           |
| Cs-134 | 4.0 ± 0.3    | 4.9 ± 0.3    | 4.6 ± 0.3       | 8.8 ± 0.5       | 10.4 ± 0.6   |
| Ba-131 | 1160 ± 70    | 1290 ± 80    | 1230 ± 220      | 1690 ± 100      | 5500 ± 300   |
| Ba-139 | 1310 ± 90    | 1340 ± 100   | 1450 ± 100      | 1850 ± 130      | 5800 ± 400   |
| La-140 | 45 ± 3       | 44.0 ± 2.3   | 46 ± 3          | 79 ± 5          | 77 ± 5       |
| Ce-141 | 69 ± 4       | 77 ± 4       | 79 ± 3          | 120 ± 6         | 138 ± 6      |
| Nd-147 | 34 ± 7       | 30 ± 8       | 49 ± 6          | 62 ± 9          | 70 ± 10      |
| Sm-153 | 8.3 ± 0.4    | 6.4 ± 0.3    | 9.9 ± 0.5       | 12.2 ± 0.6      | 14.1 ± 0.6   |
| Eu-152 | 1.27 ± 0.06  | 1.10 ± 0.06  | 1.72 ± 0.08     | 2.23 ± 0.10     | 2.39 ± 0.11  |
| Tb-160 | 0.98 ± 0.10  | 0.81 ± 0.08  | 1.21 ± 0.12     | 1.54 ± 0.14     | 1.73 ± 0.16  |
| Dy-165 | 6.8 ± 0.5    | 5.6 ± 0.5    | 10.2 ± 0.8      | 9.1 ± 0.7       | 10.0 ± 0.8   |
| Yb-175 | 4.15 ± 0.24  | 3.80 ± 0.22  | 4.7 ± 0.4       | 4.8 ± 0.3       | 5.2 ± 0.3    |
| Lu-177 | 0.45 ± 0.03  | 0.45 ± 0.03  | 0.47 ± 0.03     | 0.59 ± 0.04     | 0.59 ± 0.04  |
| Hf-181 | 3.5 ± 0.4    | 4.3 ± 0.6    | 4.7 ± 0.4       | 4.87 ± 0.21     | 5.4 ± 0.3    |
| Ta-182 | 0.86 ± 0.07  | 1.01 ± 0.08  | 0.86 ± 0.06     | 1.13 ± 0.08     | 1.37 ± 0.10  |
| W-187  | 1.8 ± 0.4    | 2.3 ± 0.4    | 1.4 ± 0.4       | 2.5 ± 0.4       | 2.6 ± 0.5    |
| Au-198 | <0.008       | <0.010       | 0.0102 ± 0.0024 | 0.0085 ± 0.0021 | <0.010       |
| Hg-203 | <0.5         | <0.5         | <0.5            | <0.6            | <0.6         |
| Th-233 | 9.9 ± 0.4    | 12.8 ± 0.5   | 11.6 ± 0.5      | 16.3 ± 0.6      | 18.9 ± 0.9   |
| U-235  | 14.0 ± 0.5   | 18.1 ± 0.6   | 17.7 ± 0.6      | 34.0 ± 1.1      | 24.9 ± 0.8   |

|        | 995020       | 995021       | 995022       | 995023       | 995024        |
|--------|--------------|--------------|--------------|--------------|---------------|
| Na-24  | 3360 ± 140   | 2950 ± 120   | 3600 ± 150   | 2710 ± 110   | 2360 ± 110    |
| Mg-27  | 6000 ± 400   | 4900 ± 400   | 5300 ± 400   | 4700 ± 300   | 5300 ± 400    |
| Al-28  | 71400 ± 2000 | 66000 ± 3000 | 66900 ± 1900 | 66300 ± 1900 | 70400 ± 2000  |
| Cl-38  | <50          | <40          | 43 ± 12      | <40          | <40           |
| K-42   | 27100 ± 1700 | 26700 ± 1700 | 24000 ± 1600 | 27600 ± 1800 | 26300 ± 1700  |
| Ca-49  | <1100        | <1000        | <1300        | <1100        | <900          |
| Sc-46  | 12.4 ± 0.7   | 10.7 ± 0.6   | 11.4 ± 0.6   | 11.8 ± 0.6   | 9.9 ± 0.5     |
| Ti-51  | 4300 ± 500   | 3500 ± 500   | 4100 ± 500   | 4700 ± 600   | 3500 ± 400    |
| V-52   | 1220 ± 40    | 1010 ± 40    | 1140 ± 40    | 1050 ± 40    | 547 ± 20      |
| Cr-51  | 109 ± 7      | 85 ± 5       | 109 ± 7      | 99 ± 6       | 71 ± 4        |
| Mn-56  | 23.3 ± 1.1   | 19.8 ± 1.0   | 20.7 ± 1.2   | 20.7 ± 1.2   | 37.5 ± 1.7    |
| Fe-59  | 12300 ± 600  | 12000 ± 600  | 18800 ± 1000 | 9800 ± 500   | 47400 ± 2400  |
| Co-60  | 4.5 ± 0.3    | 3.9 ± 0.3    | 3.75 ± 0.22  | 3.57 ± 0.21  | 6.6 ± 0.4     |
| Cu-66  | <190         | <180         | <200         | <200         | <150          |
| Zn-65  | 65 ± 9       | 71 ± 10      | 54 ± 8       | 47 ± 7       | 280 ± 40      |
| Ga-72  | 22 ± 3       | 19 ± 4       | 20 ± 3       | 22 ± 5       | 20 ± 4        |
| As-76  | 8.6 ± 0.9    | 7.7 ± 0.8    | 13.7 ± 1.6   | 4.7 ± 0.6    | 72 ± 8        |
| Se-75  | 1.6 ± 0.6    | <3           | 1.7 ± 0.7    | <4           | 2.7 ± 0.9     |
| Br-82  | 4.0 ± 0.6    | 4.8 ± 0.6    | 2.9 ± 0.4    | 2.9 ± 0.4    | 1.7 ± 0.3     |
| Rb-86  | 137 ± 7      | 119 ± 7      | 139 ± 8      | 131 ± 7      | 117 ± 7       |
| Sr-87  | <190         | <160         | <160         | <150         | <150          |
| Zr-95  | 350 ± 110    | 290 ± 100    | 240 ± 120    | 420 ± 150    | 660 ± 130     |
| Mo-99  | 36 ± 9       | 40 ± 8       | 84 ± 10      | 70 ± 30      | 115 ± 15      |
| Ag-110 | <3           | <3           | <3           | 2.3 ± 0.4    | <3            |
| In-116 | <0.17        | <0.16        | <0.17        | <0.14        | <0.1          |
| Sb-122 | 4.67 ± 0.24  | 4.4 ± 0.3    | 4.49 ± 0.24  | 4.72 ± 0.25  | 20.3 ± 1.0    |
| I-128  | <11          | <10          | <11          | 4.3 ± 1.3    | <10           |
| Cs-134 | 7.9 ± 0.5    | 6.9 ± 0.4    | 8.0 ± 0.5    | 7.4 ± 0.4    | 5.2 ± 0.3     |
| Ba-131 | 1680 ± 90    | 1960 ± 100   | 1850 ± 120   | 2120 ± 110   | 2790 ± 200    |
| Ba-139 | 1690 ± 130   | 2030 ± 140   | 1760 ± 120   | 2250 ± 150   | 2790 ± 190    |
| La-140 | 82 ± 4       | 76 ± 4       | 83 ± 5       | 86 ± 6       | 72 ± 4        |
| Ce-141 | 155 ± 7      | 144 ± 7      | 163 ± 8      | 165 ± 8      | 118 ± 6       |
| Nd-147 | 74 ± 11      | 73 ± 10      | 70 ± 11      | 69 ± 11      | 49 ± 10       |
| Sm-153 | 15.9 ± 0.7   | 16.5 ± 0.8   | 14.6 ± 0.7   | 16.4 ± 0.8   | 10.3 ± 0.5    |
| Eu-152 | 2.86 ± 0.13  | 2.72 ± 0.13  | 2.65 ± 0.13  | 2.72 ± 0.13  | 2.13 ± 0.11   |
| Tb-160 | 1.98 ± 0.18  | 1.91 ± 0.17  | 1.80 ± 0.16  | 2.03 ± 0.18  | 1.46 ± 0.14   |
| Dy-165 | 12.1 ± 1.0   | 11.6 ± 1.0   | 11.0 ± 0.9   | 12.2 ± 1.0   | 10.1 ± 0.8    |
| Yb-175 | 6.5 ± 0.3    | 5.4 ± 0.3    | 6.1 ± 0.4    | 6.9 ± 0.4    | 5.5 ± 0.3     |
| Lu-177 | 0.71 ± 0.04  | 0.69 ± 0.04  | 0.74 ± 0.04  | 0.79 ± 0.05  | 0.61 ± 0.04   |
| Hf-181 | 5.1 ± 0.3    | 4.70 ± 0.21  | 5.5 ± 0.5    | 5.7 ± 0.5    | 10.0 ± 0.8    |
| Ta-182 | 1.47 ± 0.10  | 2.04 ± 0.13  | 1.43 ± 0.11  | 1.59 ± 0.12  | 2.38 ± 0.15   |
| W-187  | 2.8 ± 0.7    | 1.7 ± 0.4    | 2.6 ± 0.7    | 2.7 ± 0.4    | 2.0 ± 0.4     |
| Au-198 | <0.009       | <0.009       | <0.008       | <0.009       | 0.011 ± 0.003 |
| Hg-203 | <0.6         | <0.5         | <0.6         | <0.6         | <0.6          |
| Th-233 | 18.1 ± 0.7   | 16.0 ± 0.6   | 18.8 ± 0.8   | 17.3 ± 0.7   | 21.3 ± 0.8    |
| U-235  | 35.8 ± 1.2   | 33.5 ± 1.1   | 39.5 ± 1.3   | 45.3 ± 1.5   | 49.9 ± 1.7    |

|        | 995025          | 995026       | 995027      | 995028        | 995029        |
|--------|-----------------|--------------|-------------|---------------|---------------|
| Na-23  | 1180 ± 50       | 2600 ± 110   | 1290 ± 60   | 850 ± 40      | 1460 ± 60     |
| Mg-27  | 2100 ± 300      | 3260 ± 240   | 1310 ± 170  | 2150 ± 180    | 1420 ± 170    |
| Al-28  | 26100 ± 800     | 53900 ± 2100 | 25700 ± 700 | 29800 ± 900   | 24600 ± 700   |
| Cl-38  | 67 ± 14         | <50          | 50 ± 6      | 52 ± 7        | 42 ± 6        |
| K-42   | 10100 ± 700     | 17200 ± 1100 | 9300 ± 600  | 10800 ± 700   | 9000 ± 600    |
| Ca-49  | <800            | <1000        | <600        | <600          | <600          |
| Sc-46  | 4.8 ± 0.3       | 8.7 ± 0.5    | 4.8 ± 0.3   | 5.0 ± 0.3     | 4.38 ± 0.23   |
| Ti-51  | 1570 ± 210      | 3000 ± 400   | 1360 ± 180  | 1890 ± 240    | 1780 ± 230    |
| V-52   | 211 ± 8         | 331 ± 12     | 189 ± 7     | 242 ± 9       | 87 ± 3        |
| Cr-51  | 30.9 ± 1.9      | 52 ± 3       | 28.4 ± 1.8  | 32.1 ± 2.0    | 23.3 ± 1.5    |
| Mn-56  | 32.1 ± 1.7      | 17.8 ± 0.9   | 31.6 ± 1.5  | 9.6 ± 0.6     | 5.7 ± 0.4     |
| Fe-59  | 12100 ± 600     | 16200 ± 800  | 13000 ± 700 | 12300 ± 600   | 4900 ± 300    |
| Co-60  | 3.48 ± 0.19     | 2.55 ± 0.15  | 6.6 ± 0.4   | 1.39 ± 0.10   | 0.37 ± 0.07   |
| Cu-66  | <130            | <120         | <100        | <90           | <80           |
| Zn-65  | 50 ± 7          | 54 ± 8       | 66 ± 9      | 33 ± 5        | 8.8 ± 2.4     |
| Ga-72  | 8.6 ± 1.9       | 14 ± 5       | <8          | 7.9 ± 1.3     | 8.8 ± 1.8     |
| As-76  | 16.9 ± 1.7      | 25 ± 3       | 17.4 ± 1.8  | 20.3 ± 2.2    | 4.7 ± 0.5     |
| Se-75  | <2.3            | <3           | <0.7        | <2.2          | <2.1          |
| Br-82  | 1.9 ± 0.3       | 0.82 ± 0.16  | 1.32 ± 0.19 | 0.99 ± 0.15   | 1.29 ± 0.19   |
| Rb-86  | 40 ± 3          | 88 ± 5       | 41 ± 3      | 46 ± 3        | 39 ± 3        |
| Sr-87  | <120            | 180 ± 40     | <80         | <90           | <80           |
| Zr-95  | 360 ± 80        | 390 ± 100    | 280 ± 100   | 130 ± 60      | 260 ± 70      |
| Mo-99  | 33 ± 9          | <35          | 51 ± 7      | 29 ± 6        | 15 ± 6        |
| Ag-110 | <1.7            | <2.2         | <1.7        | <1.7          | <1.5          |
| In-116 | <0.11           | <0.11        | <0.07       | <0.08         | <0.07         |
| Sb-122 | 3.20 ± 0.19     | 3.63 ± 0.19  | 3.69 ± 0.19 | 2.83 ± 0.14   | 1.24 ± 0.09   |
| I-128  | 7.6 ± 1.4       | 5.3 ± 1.0    | 3.2 ± 0.8   | <6            | <5            |
| Cs-134 | 2.23 ± 0.17     | 4.19 ± 0.25  | 2.00 ± 0.13 | 2.20 ± 0.15   | 1.89 ± 0.11   |
| Ba-131 | 1350 ± 150      | 1620 ± 90    | 1270 ± 90   | 1220 ± 70     | 1400 ± 80     |
| Ba-139 | 2860 ± 190      | 1790 ± 130   | 1490 ± 100  | 1440 ± 100    | 1600 ± 110    |
| La-140 | 41.8 ± 2.2      | 66 ± 4       | 43 ± 3      | 37.3 ± 2.0    | 38.4 ± 2.1    |
| Ce-141 | 80 ± 4          | 117 ± 6      | 87 ± 4      | 64 ± 3        | 68 ± 3        |
| Nd-147 | 50 ± 7          | 61 ± 9       | 42 ± 7      | 26 ± 6        | 34 ± 6        |
| Sm-153 | 11.5 ± 0.5      | 11.0 ± 0.5   | 13.0 ± 0.6  | 5.7 ± 0.3     | 6.3 ± 0.3     |
| Eu-152 | 2.06 ± 0.09     | 1.95 ± 0.11  | 2.18 ± 0.10 | 0.95 ± 0.05   | 1.12 ± 0.06   |
| Tb-160 | 1.41 ± 0.13     | 1.31 ± 0.12  | 1.49 ± 0.13 | 0.66 ± 0.07   | 0.80 ± 0.07   |
| Dy-165 | 18.2 ± 1.6      | 8.4 ± 0.7    | 9.4 ± 0.7   | 4.5 ± 0.4     | 5.5 ± 0.4     |
| Yb-175 | 4.41 ± 0.23     | 5.0 ± 0.3    | 4.43 ± 0.23 | 2.20 ± 0.15   | 2.97 ± 0.18   |
| Lu-177 | 0.48 ± 0.03     | 0.56 ± 0.03  | 0.43 ± 0.03 | 0.271 ± 0.021 | 0.326 ± 0.020 |
| Hf-181 | 2.28 ± 0.10     | 5.9 ± 0.7    | 2.67 ± 0.21 | 2.8 ± 0.3     | 5.0 ± 0.3     |
| Ta-182 | 0.49 ± 0.06     | 1.28 ± 0.08  | 0.55 ± 0.05 | 0.71 ± 0.05   | 1.21 ± 0.08   |
| W-187  | 1.2 ± 0.3       | 1.9 ± 0.3    | 0.95 ± 0.19 | 1.25 ± 0.23   | 1.2 ± 0.3     |
| Au-198 | 0.0036 ± 0.0016 | <0.006       | <0.006      | <0.005        | <0.006        |
| Hg-203 | <0.4            | <0.5         | <0.4        | <0.3          | <0.3          |
| Th-233 | 6.6 ± 0.3       | 14.9 ± 0.6   | 6.5 ± 0.3   | 7.4 ± 0.3     | 8.3 ± 0.3     |
| U-235  | 27.5 ± 0.9      | 39.7 ± 1.3   | 27.5 ± 0.9  | 17.1 ± 0.6    | 17.2 ± 0.6    |

## **Appendix 7**

NAA results of elemental abundances (all in ppm) in samples from the sections in Sichuan Province.

|        | 913001       | 913002       | 913003       | 913004        | 913005         |
|--------|--------------|--------------|--------------|---------------|----------------|
| Na-24  | 9200 ± 400   | 8900 ± 400   | 9100 ± 400   | 8900 ± 400    | 870 ± 40       |
| Mg-27  | 8000 ± 600   | 5900 ± 900   | 7900 ± 1500  | 8500 ± 1100   | 3500 ± 300     |
| Al-28  | 75600 ± 2100 | 79100 ± 2200 | 89000 ± 3000 | 115000 ± 3000 | 33600 ± 1000   |
| Cl-38  | <80          | <70          | <90          | <70           | <50            |
| K-42   | 38700 ± 2400 | 39000 ± 3000 | 42000 ± 3000 | 43000 ± 3000  | 18600 ± 1200   |
| Ca-49  | <1600        | <1700        | <1800        | <1900         | <1100          |
| Sc-46  | 13.9 ± 0.7   | 13.4 ± 0.7   | 15.2 ± 0.8   | 14.3 ± 0.8    | 3.47 ± 0.18    |
| Ti-51  | 4600 ± 600   | 5000 ± 600   | 5200 ± 700   | 4700 ± 600    | 2900 ± 400     |
| V-52   | 1100 ± 40    | 1070 ± 40    | 870 ± 30     | 690 ± 30      | 130 ± 8        |
| Cr-51  | 116 ± 7      | 90 ± 5       | 139 ± 8      | 116 ± 7       | 41 ± 3         |
| Mn-56  | 29.5 ± 1.4   | 17.7 ± 2.2   | 35.6 ± 1.7   | 92 ± 4        | 106 ± 5        |
| Fe-59  | 22000 ± 1300 | 18700 ± 1000 | 24200 ± 1400 | 50000 ± 3000  | 303000 ± 23000 |
| Co-60  | 4.02 ± 0.24  | 3.74 ± 0.21  | 2.98 ± 0.25  | 7.9 ± 0.4     | 4.7 ± 0.3      |
| Cu-66  | <220         | <230         | <300         | <250          | <100           |
| Zn-65  | 200 ± 30     | 230 ± 30     | 190 ± 40     | <13           | <15            |
| Ga-72  | 19 ± 3       | <17          | 27 ± 4       | 24 ± 4        | 8.7 ± 2.0      |
| As-76  | 22.5 ± 2.3   | 30 ± 4       | 23 ± 3       | 19.9 ± 2.1    | 116 ± 12       |
| Se-75  | 8.3 ± 2.5    | 6.9 ± 1.8    | <8           | <0.17         | 42 ± 10        |
| Br-82  | <3           | <3           | <4           | <2.5          | 1.4 ± 0.3      |
| Rb-86  | 209 ± 10     | 203 ± 11     | 216 ± 11     | 210 ± 11      | 108 ± 7        |
| Sr-87  | <200         | <200         | <300         | <180          | <130           |
| Zr-95  | <240         | 250 ± 120    | <220         | 420 ± 210     | <300           |
| Ag-110 | <4           | <4           | <6           | <4            | 3.9 ± 0.6      |
| In-116 | <0.17        | <0.22        | <0.24        | <0.17         | <0.08          |
| Sb-122 | 10.3 ± 0.5   | 12.4 ± 0.7   | 11.2 ± 0.7   | 7.8 ± 0.4     | 4.7 ± 0.3      |
| I-128  | <12          | <11          | <17          | <11           | <8             |
| Cs-134 | 12.0 ± 0.7   | 11.1 ± 0.7   | 12.6 ± 0.9   | 12.9 ± 0.9    | 3.12 ± 0.24    |
| Ba-131 | 1370 ± 80    | 1210 ± 70    | 1620 ± 130   | 1170 ± 70     | 3300 ± 180     |
| Ba-139 | 1230 ± 90    | 1180 ± 100   | 1100 ± 90    | 1060 ± 80     | 3030 ± 210     |
| La-140 | 59 ± 3       | 60 ± 3       | 70 ± 4       | 72 ± 4        | 27.6 ± 1.5     |
| Ce-141 | 116 ± 6      | 89 ± 5       | 173 ± 9      | 120 ± 6       | 49 ± 3         |
| Nd-147 | 65 ± 5       | 74 ± 7       | 72 ± 6       | 66 ± 5        | 12.0 ± 1.7     |
| Sm-153 | 8.6 ± 0.4    | 8.1 ± 0.4    | 6.1 ± 0.3    | 9.6 ± 1.0     | 2.30 ± 0.11    |
| Eu-152 | 1.48 ± 0.07  | 1.35 ± 0.08  | 1.38 ± 0.08  | 2.35 ± 0.12   | 0.46 ± 0.10    |
| Tb-160 | 1.23 ± 0.12  | 1.02 ± 0.11  | 1.08 ± 0.11  | 1.48 ± 0.14   | <0.6           |
| Dy-165 | 7.8 ± 0.6    | 7.1 ± 0.6    | 5.7 ± 0.5    | 9.2 ± 0.7     | 1.56 ± 0.17    |
| Yb-175 | 4.4 ± 0.6    | 4.2 ± 0.7    | 3.4 ± 1.0    | 5.6 ± 0.6     | 1.48 ± 0.16    |
| Lu-177 | 0.63 ± 0.04  | 0.48 ± 0.03  | 0.87 ± 0.05  | 0.67 ± 0.04   | 0.226 ± 0.022  |
| Hf-181 | 7.0 ± 0.3    | 7.4 ± 0.3    | 9.3 ± 0.5    | 8.3 ± 0.4     | 6.3 ± 0.8      |
| Ta-182 | 1.34 ± 0.10  | 1.32 ± 0.11  | 1.33 ± 0.10  | 1.43 ± 0.15   | 0.9 ± 0.3      |
| W-187  | 2.9 ± 0.6    | <4           | <7           | 2.4 ± 0.5     | 2.2 ± 0.5      |
| Au-198 | <0.012       | <0.012       | <0.017       | <0.012        | <0.008         |
| Hg-203 | 0.9 ± 0.3    | <0.8         | <1.1         | <0.6          | <0.5           |
| Th-233 | 21.9 ± 0.9   | 20.0 ± 0.8   | 29.3 ± 1.3   | 25.1 ± 1.0    | 7.8 ± 0.5      |
| U-235  | 33.0 ± 1.1   | 31.9 ± 1.1   | 43.4 ± 1.4   | 47.9 ± 1.6    | 4.34 ± 0.15    |

|        | 913006       | 913007       | 913008       | 913009        | 913010        |
|--------|--------------|--------------|--------------|---------------|---------------|
| Na-24  | 9100 ± 400   | 6300 ± 300   | 2630 ± 120   | 2330 ± 100    | 3530 ± 160    |
| Mg-27  | 6800 ± 700   | 5700 ± 1300  | 6700 ± 1200  | 9600 ± 1200   | 9300 ± 600    |
| Al-28  | 79300 ± 2200 | 66600 ± 1900 | 94000 ± 3000 | 103000 ± 3000 | 106000 ± 3000 |
| Cl-38  | <80          | <80          | <60          | <60           | <50           |
| K-42   | 35600 ± 2300 | 33900 ± 2200 | 48000 ± 3000 | 48000 ± 3000  | 47000 ± 3000  |
| Ca-49  | 1900 ± 300   | <1900        | <1000        | <1100         | <1300         |
| Sc-46  | 13.6 ± 0.7   | 13.4 ± 0.7   | 17.4 ± 0.9   | 18.2 ± 1.0    | 16.9 ± 0.9    |
| Ti-51  | 4700 ± 600   | 4100 ± 500   | 6500 ± 800   | 6300 ± 800    | 6300 ± 800    |
| V-52   | 205 ± 8      | 780 ± 30     | 1450 ± 50    | 1650 ± 60     | 1140 ± 40     |
| Cr-51  | 65 ± 4       | 104 ± 6      | 138 ± 8      | 155 ± 9       | 116 ± 7       |
| Mn-56  | 122 ± 6      | 21.2 ± 1.3   | 38 ± 3       | 46.8 ± 2.2    | 44.1 ± 2.4    |
| Fe-59  | 43300 ± 2500 | 21200 ± 1100 | 45000 ± 3000 | 29000 ± 1600  | 20500 ± 1100  |
| Co-60  | 5.2 ± 0.3    | 2.2 ± 0.3    | 4.6 ± 0.3    | 5.6 ± 0.3     | 5.4 ± 0.3     |
| Cu-66  | <220         | <300         | <300         | <300          | <220          |
| Zn-65  | 340 ± 40     | 170 ± 40     | 240 ± 30     | 270 ± 30      | 220 ± 30      |
| Ga-72  | <19          | 14 ± 4       | 29 ± 4       | 25 ± 3        | 20 ± 3        |
| As-76  | 18.2 ± 1.9   | 47 ± 7       | 41 ± 5       | 28 ± 3        | 10.6 ± 1.7    |
| Se-75  | <5           | 2.7 ± 1.2    | 4.0 ± 1.3    | <8            | <4            |
| Br-82  | <3           | <3           | 2.3 ± 0.4    | 4.5 ± 1.3     | 14.9 ± 1.6    |
| Rb-86  | 181 ± 10     | 173 ± 9      | 233 ± 12     | 261 ± 13      | 246 ± 13      |
| Sr-87  | <210         | <230         | <190         | <240          | <190          |
| Zr-95  | 210 ± 70     | 190 ± 90     | 630 ± 180    | 600 ± 300     | 470 ± 160     |
| Ag-110 | <5           | <5           | <4           | <5            | <5            |
| In-116 | <0.21        | <0.22        | <0.19        | <0.19         | <0.21         |
| Sb-122 | 7.0 ± 0.4    | 13.2 ± 0.7   | 13.9 ± 0.8   | 12.4 ± 0.6    | 10.3 ± 0.6    |
| I-128  | <12          | <15          | <11          | <14           | <12           |
| Cs-134 | 8.4 ± 0.5    | 8.9 ± 0.7    | 10.3 ± 0.6   | 10.8 ± 0.7    | 10.4 ± 0.9    |
| Ba-131 | 1070 ± 90    | 1280 ± 80    | 1160 ± 80    | 1190 ± 200    | 1070 ± 80     |
| Ba-139 | 1260 ± 100   | 940 ± 80     | 1230 ± 90    | 1140 ± 90     | 1170 ± 100    |
| La-140 | 64 ± 4       | 54 ± 3       | 92 ± 5       | 93 ± 5        | 88 ± 5        |
| Ce-141 | 88 ± 4       | 125 ± 7      | 157 ± 8      | 168 ± 9       | 125 ± 7       |
| Nd-147 | 87 ± 8       | 49 ± 5       | 79 ± 6       | 113 ± 9       | 121 ± 10      |
| Sm-153 | 14.8 ± 0.7   | 5.4 ± 0.3    | 12.1 ± 1.2   | 15.3 ± 0.7    | 14.3 ± 0.7    |
| Eu-152 | 2.87 ± 0.13  | 1.01 ± 0.07  | 2.63 ± 0.14  | 2.92 ± 0.13   | 2.27 ± 0.11   |
| Tb-160 | 1.95 ± 0.18  | 0.83 ± 0.09  | 1.64 ± 0.15  | 2.04 ± 0.19   | 1.71 ± 0.17   |
| Dy-165 | 13.2 ± 1.1   | 5.1 ± 0.4    | 10.9 ± 0.8   | 13.1 ± 1.0    | 10.9 ± 0.9    |
| Yb-175 | 5.9 ± 0.7    | 3.8 ± 0.6    | 6.0 ± 0.8    | 8.1 ± 0.9     | 5.9 ± 0.7     |
| Lu-177 | 0.62 ± 0.04  | 0.67 ± 0.04  | 0.78 ± 0.04  | 0.88 ± 0.05   | 0.70 ± 0.04   |
| Hf-181 | 8.7 ± 0.4    | 5.33 ± 0.23  | 11.4 ± 0.6   | 11.6 ± 0.6    | 11.0 ± 0.5    |
| Ta-182 | 1.55 ± 0.12  | 1.16 ± 0.11  | 1.55 ± 0.18  | 1.91 ± 0.13   | 1.80 ± 0.17   |
| W-187  | 3.3 ± 0.6    | <6           | 2.7 ± 0.5    | 3.3 ± 1.1     | 3.7 ± 0.8     |
| Au-198 | <0.013       | <0.015       | <0.012       | <0.011        | <0.011        |
| Hg-203 | <0.8         | <1.0         | <0.8         | <0.9          | <0.8          |
| Th-233 | 19.3 ± 0.8   | 22.6 ± 0.9   | 30.9 ± 1.3   | 32.1 ± 1.3    | 26.4 ± 1.2    |
| U-235  | 5.68 ± 0.20  | 19.5 ± 0.6   | 43.5 ± 1.4   | 53.5 ± 1.8    | 58.9 ± 1.9    |



|        | 913011        | 913012        | 913013        | 913014        | 913015        |
|--------|---------------|---------------|---------------|---------------|---------------|
| Na-24  | 7500 ± 300    | 12000 ± 600   | 10700 ± 400   | 8200 ± 400    | 6600 ± 300    |
| Mg-27  | 7500 ± 800    | 7700 ± 800    | 21100 ± 1400  | 14600 ± 1100  | 5500 ± 900    |
| Al-28  | 103000 ± 3000 | 112000 ± 3000 | 47500 ± 1400  | 44400 ± 1300  | 101000 ± 3000 |
| Cl-38  | <100          | <110          | <140          | <110          | <160          |
| K-42   | 48000 ± 3000  | 49000 ± 3000  | 21800 ± 1700  | 19100 ± 1300  | 46000 ± 3000  |
| Ca-49  | <1500         | <2000         | 234000 ± 9000 | 229000 ± 9000 | <3000         |
| Sc-46  | 16.0 ± 0.9    | 21.2 ± 1.1    | 8.2 ± 0.4     | 7.4 ± 0.4     | 18.9 ± 1.0    |
| Ti-51  | 6400 ± 800    | 6200 ± 800    | 2800 ± 400    | 1900 ± 400    | 6000 ± 900    |
| V-52   | 700 ± 30      | 223 ± 9       | 87 ± 4        | 90 ± 5        | 252 ± 10      |
| Cr-51  | 133 ± 8       | 116 ± 7       | 48 ± 3        | 38.0 ± 2.4    | 129 ± 8       |
| Mn-56  | 107 ± 9       | 1600 ± 70     | 1970 ± 80     | 2220 ± 90     | 2550 ± 100    |
| Fe-59  | 19400 ± 1000  | 43200 ± 2400  | 18100 ± 1300  | 18500 ± 1100  | 55000 ± 3000  |
| Co-60  | 5.7 ± 0.4     | 21.7 ± 1.1    | 8.9 ± 0.5     | 7.0 ± 0.4     | 31.6 ± 1.6    |
| Cu-66  | <300          | <300          | <300          | <300          | <500          |
| Zn-65  | 240 ± 40      | 240 ± 30      | 99 ± 13       | 52 ± 8        | 240 ± 40      |
| Ga-72  | 20 ± 5        | 36 ± 6        | 16            | <15           | 27 ± 5        |
| As-76  | 15.1 ± 1.8    | 10.6 ± 1.2    | 3.4 ± 0.4     | 4.7 ± 0.6     | 31 ± 3        |
| Se-75  | <8            | <5            | <5            | <3            | <9            |
| Br-82  | 3.4 ± 1.1     | 3.1 ± 0.8     | <3            | <2.5          | <4            |
| Rb-86  | 250 ± 13      | 257 ± 13      | 113 ± 6       | 106 ± 6       | 260 ± 13      |
| Sr-87  | <300          | <400          | 770 ± 130     | 690 ± 170     | <800          |
| Zr-95  | <220          | 660 ± 120     | 270 ± 60      | 170 ± 50      | 180 ± 70      |
| Ag-110 | <6            | <5            | <3            | <3            | <7            |
| In-116 | <0.3          | <0.3          | <0.25         | <0.3          | <0.4          |
| Sb-122 | 9.2 ± 0.6     | 4.4 ± 0.3     | 1.33 ± 0.10   | 0.64 ± 0.09   | 1.42 ± 0.15   |
| I-128  | <19           | <24           | <30           | <30           | <50           |
| Cs-134 | 10.9 ± 0.8    | 11.2 ± 0.8    | 4.6 ± 0.3     | 4.6 ± 0.3     | 11.1 ± 1.0    |
| Ba-131 | 1160 ± 100    | 1130 ± 90     | 740 ± 230     | 830 ± 190     | 1260 ± 90     |
| Ba-139 | 1150 ± 90     | 1130 ± 120    | 660 ± 90      | 840 ± 110     | 600 ± 110     |
| La-140 | 99 ± 5        | 91 ± 4        | 45.2 ± 2.4    | 39.9 ± 2.2    | 76 ± 4        |
| Ce-141 | 223 ± 11      | 145 ± 7       | 81 ± 4        | 57 ± 3        | 153 ± 7       |
| Nd-147 | 134 ± 11      | 55 ± 5        | 40 ± 4        | 37 ± 3        | 56 ± 6        |
| Sm-153 | 13.4 ± 0.6    | 7.6 ± 0.4     | 7.5 ± 0.3     | 6.7 ± 0.3     | 8.1 ± 0.4     |
| Eu-152 | 2.68 ± 0.16   | 1.40 ± 0.09   | 1.32 ± 0.15   | 1.08 ± 0.14   | 1.63 ± 0.08   |
| Tb-160 | 2.5 ± 0.3     | 1.08 ± 0.11   | 1.00 ± 0.09   | 0.92 ± 0.09   | 1.19 ± 0.13   |
| Dy-165 | 11.9 ± 0.9    | 6.8 ± 0.6     | 6.1 ± 0.6     | 4.0 ± 0.6     | 5.4 ± 0.6     |
| Yb-175 | 5.9 ± 0.9     | 5.0 ± 0.4     | 3.44 ± 0.22   | 2.98 ± 0.21   | 5.7 ± 1.1     |
| Lu-177 | 1.01 ± 0.06   | 0.72 ± 0.04   | 0.461 ± 0.025 | 0.326 ± 0.020 | 0.83 ± 0.05   |
| Hf-181 | 13.6 ± 1.2    | 14.3 ± 1.0    | 6.8 ± 0.4     | 5.12 ± 0.23   | 14.8 ± 0.7    |
| Ta-182 | 1.62 ± 0.11   | 2.09 ± 0.17   | 0.86 ± 0.07   | 0.81 ± 0.07   | 2.34 ± 0.22   |
| W-187  | 4.5 ± 1.4     | 3.0 ± 0.7     | 2.8 ± 0.5     | <4            | <7            |
| Au-198 | <0.017        | <0.015        | <0.011        | <0.010        | <0.016        |
| Hg-203 | <1.1          | <0.8          | <0.5          | <0.5          | <1.3          |
| Th-233 | 33 ± 4        | 36.2 ± 1.4    | 15.6 ± 0.6    | 11.4 ± 0.4    | 38.6 ± 1.5    |
| U-235  | 53.6 ± 1.8    | 11.1 ± 0.4    | 4.30 ± 0.15   | 3.32 ± 0.12   | 8.3 ± 0.3     |

|        | 913016        | 913017       | 913018       | 913019       | 913020        |
|--------|---------------|--------------|--------------|--------------|---------------|
| Na-24  | 8100 ± 400    | 3850 ± 160   | 5360 ± 230   | 8500 ± 400   | 8600 ± 400    |
| Mg-27  | 9300 ± 800    | 8400 ± 1000  | 6000 ± 500   | 5700 ± 600   | 5500 ± 500    |
| Al-28  | 119000 ± 3000 | 85000 ± 2400 | 72000 ± 2000 | 59700 ± 1700 | 69200 ± 1900  |
| Cl-38  | <80           | <60          | <60          | <80          | <60           |
| K-42   | 51000 ± 3000  | 44000 ± 3000 | 34300 ± 2200 | 31100 ± 2100 | 34600 ± 2200  |
| Ca-49  | <2000         | <1300        | <1600        | <1600        | <1300         |
| Sc-46  | 21.0 ± 1.1    | 17.7 ± 0.9   | 11.0 ± 0.6   | 9.1 ± 0.5    | 14.4 ± 0.8    |
| Ti-51  | 6600 ± 800    | 5400 ± 700   | 4500 ± 600   | 3500 ± 500   | 4200 ± 500    |
| V-52   | 511 ± 18      | 195 ± 7      | 234 ± 9      | 143 ± 6      | 159 ± 6       |
| Cr-51  | 132 ± 8       | 107 ± 6      | 73 ± 4       | 84 ± 5       | 77 ± 5        |
| Mn-56  | 261 ± 10      | 30.8 ± 1.5   | 22.6 ± 1.2   | 17.8 ± 2.3   | 29.7 ± 1.6    |
| Fe-59  | 38900 ± 2400  | 14000 ± 800  | 29200 ± 1600 | 28300 ± 1600 | 46000 ± 3000  |
| Co-60  | 13.4 ± 0.7    | 4.2 ± 0.3    | 10.1 ± 0.5   | 4.7 ± 0.3    | 12.8 ± 0.7    |
| Cu-66  | <300          | <160         | <170         | <210         | <190          |
| Zn-65  | 230 ± 30      | <17          | 122 ± 17     | <22          | 138 ± 18      |
| Ga-72  | 28 ± 5        | 24 ± 4       | 16 ± 3       | <30          | 24 ± 5        |
| As-76  | 17.4 ± 2.0    | 12.6 ± 1.4   | 61 ± 7       | 19.9 ± 2.3   | 35 ± 5        |
| Se-75  | <0.10         | <7           | <4           | <6           | <4            |
| Br-82  | 8.3 ± 1.0     | 1.6 ± 0.4    | <3           | <4           | <3            |
| Rb-86  | 264 ± 13      | 230 ± 11     | 190 ± 10     | 150 ± 8      | 170 ± 9       |
| Sr-87  | <230          | <180         | 160 ± 40     | <200         | <140          |
| Zr-95  | 700 ± 170     | 470 ± 130    | 270 ± 90     | 190 ± 70     | 360 ± 150     |
| Ag-110 | <5            | <4           | <4           | <5           | <4            |
| In-116 | <0.20         | <0.14        | <0.17        | <0.18        | <0.14         |
| Sb-122 | 4.2 ± 0.3     | 1.72 ± 0.12  | 3.37 ± 0.22  | 0.68 ± 0.11  | 3.66 ± 0.22   |
| I-128  | <14           | <11          | <9           | <13          | <9            |
| Cs-134 | 13.5 ± 0.9    | 11.2 ± 0.8   | 10.2 ± 0.6   | 8.1 ± 0.6    | 10.8 ± 0.7    |
| Ba-131 | 1320 ± 90     | 1160 ± 80    | 910 ± 60     | 1070 ± 70    | 1250 ± 80     |
| Ba-139 | 1260 ± 100    | 1020 ± 80    | 1060 ± 80    | 1040 ± 80    | 1090 ± 80     |
| La-140 | 88 ± 4        | 80 ± 4       | 61 ± 3       | 59 ± 3       | 71 ± 3        |
| Ce-141 | 143 ± 7       | 154 ± 7      | 100 ± 5      | 166 ± 8      | 139 ± 7       |
| Nd-147 | 81 ± 7        | 82 ± 7       | 71 ± 7       | 60 ± 5       | 67 ± 5        |
| Sm-153 | 11.7 ± 0.8    | 12.9 ± 0.6   | 8.6 ± 0.4    | 7.0 ± 0.3    | 9.8 ± 0.5     |
| Eu-152 | 2.21 ± 0.12   | 2.40 ± 0.11  | 1.40 ± 0.06  | 1.29 ± 0.08  | 2.35 ± 0.11   |
| Tb-160 | 1.58 ± 0.15   | 1.64 ± 0.17  | 0.93 ± 0.09  | 1.03 ± 0.10  | 1.39 ± 0.14   |
| Dy-165 | 10.9 ± 0.8    | 8.7 ± 0.7    | 6.4 ± 0.6    | 4.9 ± 0.5    | 10.3 ± 0.8    |
| Yb-175 | 6.8 ± 0.4     | 5.5 ± 0.4    | 3.54 ± 0.24  | 3.07 ± 0.23  | 6.1 ± 0.4     |
| Lu-177 | 0.92 ± 0.05   | 0.76 ± 0.04  | 0.41 ± 0.03  | 0.50 ± 0.03  | 0.75 ± 0.04   |
| Hf-181 | 12.6 ± 0.9    | 8.1 ± 0.4    | 6.3 ± 0.3    | 5.8 ± 0.4    | 5.7 ± 0.4     |
| Ta-182 | 1.79 ± 0.17   | 1.65 ± 0.12  | 1.20 ± 0.10  | 0.98 ± 0.08  | 1.23 ± 0.13   |
| W-187  | <6            | 3.9 ± 0.8    | 3.3 ± 0.7    | <7           | 2.1 ± 0.6     |
| Au-198 | <0.014        | <0.011       | <0.011       | <0.015       | 0.010 ± 0.004 |
| Hg-203 | <0.8          | <0.8         | <0.7         | <0.9         | <0.6          |
| Th-233 | 35.5 ± 1.4    | 26.2 ± 1.0   | 19.4 ± 0.8   | 22.2 ± 0.9   | 20.1 ± 0.8    |
| U-235  | 15.9 ± 0.5    | 17.6 ± 0.6   | 15.4 ± 0.5   | 14.5 ± 0.5   | 24.5 ± 0.8    |

## 913021

|        |              |
|--------|--------------|
| Na-24  | 2630 ± 110   |
| Mg-27  | 6200 ± 500   |
| Al-28  | 59600 ± 1700 |
| Cl-38  | <50          |
| K-42   | 29400 ± 1900 |
| Ca-49  | <1100        |
| Sc-46  | 11.5 ± 0.6   |
| Ti-51  | 3800 ± 500   |
| V-52   | 750 ± 30     |
| Cr-51  | 92 ± 6       |
| Mn-56  | 18.3 ± 1.2   |
| Fe-59  | 9300 ± 500   |
| Co-60  | 2.49 ± 0.18  |
| Cu-66  | <170         |
| Zn-65  | <13          |
| Ga-72  | 16 ± 3       |
| As-76  | 11.2 ± 1.3   |
| Se-75  | <6           |
| Br-82  | 1.1 ± 0.4    |
| Rb-86  | 161 ± 8      |
| Sr-87  | <160         |
| Zr-95  | <220         |
| Ag-110 | <3           |
| In-116 | <0.13        |
| Sb-122 | 5.9 ± 0.3    |
| I-128  | <10          |
| Cs-134 | 7.9 ± 0.6    |
| Ba-131 | 990 ± 60     |
| Ba-139 | 990 ± 80     |
| La-140 | 55 ± 3       |
| Ce-141 | 113 ± 5      |
| Nd-147 | 61 ± 5       |
| Sm-153 | 10.5 ± 0.5   |
| Eu-152 | 1.97 ± 0.10  |
| Tb-160 | 1.25 ± 0.11  |
| Dy-165 | 7.1 ± 0.6    |
| Yb-175 | 3.5 ± 0.3    |
| Lu-177 | 0.50 ± 0.03  |
| Hf-181 | 5.56 ± 0.24  |
| Ta-182 | 1.18 ± 0.10  |
| W-187  | 2.1 ± 0.5    |
| Au-198 | <0.009       |
| Hg-203 | <0.7         |
| Th-233 | 18.5 ± 0.7   |
| U-235  | 11.5 ± 0.4   |

## Appendix 8

Analytical results of  $\delta^{13}\text{C}$  and Ir in carbonate samples from the Xiantian Section, Guangxi.

| Sample | Lab number | $\delta^{13}\text{C}$ | Ir  |
|--------|------------|-----------------------|-----|
| G-11   | 988001     | 1.03                  | 5   |
| G-10   | 988002     | 1.20                  |     |
| G-9    | 988003     | 0.40                  | 43  |
| G-8    | 988004     | 1.18                  |     |
| G-7    | 988005     | 1.25                  |     |
| G-6    | 988006     | 1.14                  |     |
| G-5    | 988007     | 1.20                  | 23  |
| G-4    | 988008     | 1.39                  | 20  |
| G-3    | 988009     | 0.27                  | 44  |
| G-2    | 988010     | 1.28                  | 24  |
| G-1    | 988011     | 1.38                  | 2   |
| F-7    | 988012     | 1.56                  |     |
| F-6    | 988013     | 1.07                  | 0.8 |
| F-5    | 988014     | 1.33                  |     |
| F-4    | 988015     | 1.63                  |     |
| F-3    | 988016     | 1.04                  | 3   |
| F-2    | 988017     | 0.27                  |     |
| F-1a   | 988018     | 0.67                  | 6   |
| F-1    | 988019     | 0.91                  | 9   |
| E-8a   | 988020     | -5.35                 | 167 |
| E-8b   | 988021     | -5.34                 |     |
| E-8c   | 988022     | -6.57                 | 194 |
| E-7    | 988023     |                       | 226 |
| E-6    | 988024     | -3.33                 | 170 |
| E-5    | 988025     | -0.78                 |     |
| E-4    | 988026     | -1.73                 | 97  |
| E-3    | 988027     | -1.33                 |     |
| E-2    | 988028     | -2.20                 | 94  |

$\delta^{13}\text{C}$  is in per mil relative to PDB standard.

Ir is in ppt ( $10^{-12}\text{g/g}$ ).

| Sample | Lab number | $\delta^{13}\text{C}$ | Ir  |
|--------|------------|-----------------------|-----|
| E-1a   | 988029     | -5.07                 |     |
| E-1b   | 988030     | 0.10                  |     |
| E-1c   | 988031     | -2.09                 | 7.4 |
| D-1a   | 988032     | 0.43                  |     |
| D-1b   | 988033     | 1.14                  | 4.8 |
| D-2    | 988034     | 1.08                  |     |
| D-3    | 988035     | 0.95                  | 5.9 |
| D-4    | 988036     | 0.98                  |     |
| D-5    | 988037     | 1.04                  |     |
| D-6    | 988038     | 1.11                  | 3.3 |
| D-7    | 988039     | 1.06                  |     |
| D-8    | 988040     | 1.09                  |     |
| D-9    | 988041     | 1.15                  |     |
| D-10   | 988042     | 2.05                  | 8   |
| D-11   | 988043     | 1.15                  |     |
| D-12   | 988044     | 1.69                  |     |

$\delta^{13}\text{C}$  is in per mil relative to PDB standard.

Ir is in ppt ( $10^{-12}\text{g/g}$ ).

## **Appendix 9**

**NAA results of elemental abundances (all in ppm) in samples from the Xiantian Section, Guangxi.**

|        | 988001         | 988002         | 988003        | 988004         | 988005         |
|--------|----------------|----------------|---------------|----------------|----------------|
| Na-24  | 36 ± 3         | 82 ± 6         | 250 ± 10      | 112 ± 5        | 90 ± 7         |
| Mg-27  | <3000          | <2000          | 3200 ± 500    | <3000          | <2000          |
| Al-28  | 2100 ± 300     | 4800 ± 400     | 36000 ± 1000  | 8800 ± 500     | 13200 ± 600    |
| Cl-38  | <200           | <100           | <100          | <100           | <100           |
| K-42   | <500           | 2600 ± 300     | 20000 ± 1000  | 4800 ± 400     | 5800 ± 400     |
| Ca-49  | 400000 ± 20000 | 310000 ± 10000 | 176000 ± 8000 | 310000 ± 10000 | 330000 ± 10000 |
| Sc-46  | 0.80 ± 0.04    | 2.5 ± 0.1      | 5.9 ± 0.3     | 2.7 ± 0.1      | 2.5 ± 0.1      |
| Ti-51  | <10000         | <9000          | 1900 ± 400    | <8000          | <9000          |
| V-52   | <10            | <10            | 41 ± 3        | 10 ± 2         | 14 ± 3         |
| Cr-51  | 2.6 ± 0.5      | 5.7 ± 0.7      | 23 ± 2        | 7.7 ± 0.7      | 10.6 ± 0.8     |
| Mn-56  | 1890 ± 80      | 1370 ± 60      | 1280 ± 50     | 1680 ± 70      | 1500 ± 60      |
| Fe-59  | 2800 ± 200     | 4400 ± 200     | 13400 ± 700   | 5600 ± 300     | 7500 ± 400     |
| Co-60  | 2.9 ± 0.3      | 2.7 ± 0.2      | 9.1 ± 0.6     | 5.1 ± 0.3      | 5.5 ± 0.3      |
| Cu-66  | <400           | <400           | <300          | <400           | <300           |
| Zn-65  | 390 ± 50       | 29 ± 4         | <10           | 58 ± 8         | 25 ± 5         |
| Ga-72  | <5             | <8             | <10           | <6             | <7             |
| As-76  | 3.5 ± 0.4      | 0.8 ± 0.1      | 3.4 ± 0.4     | 1.4 ± 0.2      | 1.7 ± 0.2      |
| Se-75  | <2             | <3             | <3            | <2             | <3             |
| Br-82  | <0.6           | 0.3 ± 0.1      | <0.9          | <0.6           | <0.7           |
| Rb-86  | <7             | <10            | 71 ± 5        | 18 ± 3         | 28 ± 3         |
| Sr-87  | <700           | <700           | <400          | <600           | <600           |
| Zr-95  | <100           | <200           | <200          | <100           | <100           |
| Mo-99  | <20            | <10            | 3.7 ± 0.9     | <40            | <20            |
| Ag-110 | <2             | <3             | <4            | <2             | <3             |
| In-116 | <0.3           | <0.3           | <0.3          | <0.3           | <0.2           |
| Sb-122 | 0.17 ± 0.02    | 0.14 ± 0.02    | 0.96 ± 0.06   | 0.23 ± 0.02    | 0.46 ± 0.03    |
| I-128  | <50            | <60            | <30           | <40            | <40            |
| Cs-134 | 0.2 ± 0.1      | <1             | 3.6 ± 0.2     | 1.12 ± 0.09    | 1.5 ± 0.2      |
| Ba-131 | 120 ± 30       | <300           | 160 ± 40      | <300           | 90 ± 30        |
| Ba-139 | <9000          | <9000          | <6000         | <7000          | <8000          |
| La-140 | 6.2 ± 0.3      | 10.0 ± 0.5     | 24 ± 1        | 12.2 ± 0.7     | 10.4 ± 0.5     |
| Ce-141 | 10.2 ± 0.6     | 14.2 ± 0.9     | 37 ± 2        | 20.3 ± 1.0     | 18.7 ± 1.0     |
| Nd-147 | <9             | <10            | 16 ± 4        | 19 ± 4         | <10            |
| Sm-153 | 0.95 ± 0.04    | 1.93 ± 0.09    | 3.9 ± 0.2     | 3.0 ± 0.1      | 1.42 ± 0.06    |
| Eu-152 | 0.37 ± 0.08    | 0.4 ± 0.1      | 0.6 ± 0.1     | 0.5 ± 0.1      | 0.43 ± 0.09    |
| Tb-160 | 0.23 ± 0.03    | 0.34 ± 0.04    | 0.47 ± 0.05   | 0.44 ± 0.05    | 0.30 ± 0.04    |
| Dy-165 | <10            | <10            | 2.4 ± 0.4     | 2.9 ± 0.6      | <10            |
| Yb-175 | 0.67 ± 0.04    | 1.21 ± 0.07    | 2.1 ± 0.1     | 1.43 ± 0.08    | 0.88 ± 0.05    |
| Lu-177 | 0.11 ± 0.01    | 0.14 ± 0.02    | 0.23 ± 0.02   | 0.17 ± 0.01    | 0.17 ± 0.02    |
| Hf-181 | <0.4           | 0.21 ± 0.05    | 1.9 ± 0.2     | 0.39 ± 0.05    | 0.58 ± 0.06    |
| Ta-182 | <0.4           | <0.5           | 0.47 ± 0.07   | <0.4           | <0.5           |
| W-187  | <1             | <2             | 1.5 ± 0.3     | <1             | 0.7 ± 0.2      |
| Au-198 | <0.002         | <0.003         | <0.003        | <0.002         | <0.002         |
| Hg-203 | <0.4           | <0.7           | <0.6          | <0.5           | <0.5           |
| Th-233 | 0.38 ± 0.04    | 1.19 ± 0.09    | 7.4 ± 0.4     | 2.0 ± 0.1      | 2.6 ± 0.1      |
| U-235  | 0.46 ± 0.03    | 0.58 ± 0.04    | 1.83 ± 0.08   | 0.51 ± 0.03    | 0.88 ± 0.05    |

|        | 988006         | 988007          | 988008         | 988009        | 988010        |
|--------|----------------|-----------------|----------------|---------------|---------------|
| Na-24  | 99 ± 5         | 164 ± 8         | 110 ± 6        | 230 ± 20      | 184 ± 8       |
| Mg-27  | <2000          | 3300 ± 600      | <3000          | 4800 ± 600    | 2600 ± 500    |
| Al-28  | 9000 ± 400     | 17600 ± 700     | 12400 ± 600    | 52000 ± 2000  | 19400 ± 700   |
| Cl-38  | <100           | <100            | <100           | <100          | <100          |
| K-42   | 5900 ± 400     | 11000 ± 800     | 6700 ± 500     | 22000 ± 1000  | 12300 ± 900   |
| Ca-49  | 280000 ± 10000 | 217000 ± 9000   | 300000 ± 10000 | 122000 ± 6000 | 226000 ± 9000 |
| Sc-46  | 3.7 ± 0.2      | 5.1 ± 0.3       | 3.8 ± 0.2      | 8.2 ± 0.4     | 5.5 ± 0.3     |
| Ti-51  | <7000          | 800 ± 300       | <9000          | 1800 ± 400    | <8000         |
| V-52   | 13 ± 2         | 19 ± 2          | 15 ± 3         | 53 ± 4        | 21 ± 3        |
| Cr-51  | 9.9 ± 0.9      | 12 ± 1          | 12 ± 1         | 36 ± 3        | 18 ± 1        |
| Mn-56  | 1270 ± 50      | 1370 ± 50       | 1600 ± 60      | 690 ± 30      | 1120 ± 40     |
| Fe-59  | 5800 ± 300     | 9100 ± 500      | 7300 ± 400     | 19000 ± 1000  | 11200 ± 600   |
| Co-60  | 3.1 ± 0.2      | 4.5 ± 0.4       | 5.2 ± 0.3      | 19 ± 1        | 6.1 ± 0.3     |
| Cu-66  | <400           | <300            | <400           | <300          | <400          |
| Zn-65  | 39 ± 5         | <10             | 69 ± 9         | <20           | 61 ± 10       |
| Ga-72  | <8             | <9              | <8             | <10           | <10           |
| As-76  | 1.3 ± 0.2      | 2.4 ± 0.3       | 1.9 ± 0.2      | 8.3 ± 0.9     | 4.1 ± 0.5     |
| Se-75  | <3             | <3              | <3             | <6            | <4            |
| Br-82  | <0.9           | 0.6 ± 0.2       | <0.7           | <1            | 0.6 ± 0.2     |
| Rb-86  | 19 ± 3         | 37 ± 3          | 29 ± 4         | 97 ± 7        | 42 ± 4        |
| Sr-87  | <600           | <500            | <600           | <500          | <600          |
| Zr-95  | <200           | <200            | <200           | <300          | <200          |
| Mo-99  | <10            | <10             | 5 ± 3          | 4 ± 2         | <20           |
| Ag-110 | <3             | <4              | <3             | <6            | <5            |
| In-116 | <0.3           | <0.3            | <0.3           | <0.3          | <0.3          |
| Sb-122 | 0.30 ± 0.03    | 0.59 ± 0.04     | 0.39 ± 0.03    | 1.80 ± 0.10   | 0.86 ± 0.06   |
| I-128  | <50            | <30             | <40            | <40           | <50           |
| Cs-134 | 1.3 ± 0.1      | 2.0 ± 0.2       | 1.7 ± 0.2      | 6.9 ± 0.4     | 3.0 ± 0.2     |
| Ba-131 | <300           | 180 ± 30        | 100 ± 40       | <600          | 180 ± 60      |
| Ba-139 | <8000          | 330 ± 70        | <8000          | <7000         | <8000         |
| La-140 | 14.7 ± 0.8     | 15.9 ± 0.9      | 14.6 ± 0.8     | 22 ± 1        | 16.0 ± 0.8    |
| Ce-141 | 21 ± 1         | 23 ± 1          | 25 ± 1         | 41 ± 2        | 24 ± 1        |
| Nd-147 | <10            | <20             | <20            | <30           | <20           |
| Sm-153 | 2.5 ± 0.1      | 2.8 ± 0.1       | 3.2 ± 0.2      | 1.70 ± 0.08   | 3.3 ± 0.2     |
| Eu-152 | 0.5 ± 0.1      | 0.5 ± 0.1       | 0.6 ± 0.1      | 0.52 ± 0.04   | 0.6 ± 0.1     |
| Tb-160 | 0.31 ± 0.04    | 0.33 ± 0.05     | 0.40 ± 0.05    | 0.36 ± 0.08   | 0.45 ± 0.06   |
| Dy-165 | 1.8 ± 0.5      | 2.9 ± 0.4       | 2.9 ± 0.6      | 2.2 ± 0.5     | <10           |
| Yb-175 | 1.58 ± 0.09    | 1.57 ± 0.09     | 1.62 ± 0.09    | 1.28 ± 0.08   | 1.7 ± 0.1     |
| Lu-177 | 0.18 ± 0.02    | 0.21 ± 0.02     | 0.21 ± 0.02    | 0.17 ± 0.02   | 0.25 ± 0.02   |
| Hf-181 | 0.41 ± 0.05    | 0.7 ± 0.1       | 0.56 ± 0.07    | 2.0 ± 0.2     | 0.84 ± 0.09   |
| Ta-182 | <0.4           | <0.5            | <0.6           | 0.44 ± 0.09   | <0.6          |
| W-187  | 1.0 ± 0.2      | 1.1 ± 0.2       | 0.7 ± 0.2      | 1.8 ± 0.5     | 1.1 ± 0.2     |
| Au-198 | <0.003         | 0.0020 ± 0.0007 | <0.003         | <0.005        | <0.004        |
| Hg-203 | <0.6           | <0.6            | <0.6           | <1            | <0.9          |
| Th-233 | 2.3 ± 0.1      | 3.5 ± 0.2       | 2.6 ± 0.1      | 7.9 ± 0.3     | 5.0 ± 0.2     |
| U-235  | 0.58 ± 0.04    | 0.92 ± 0.05     | 0.89 ± 0.05    | 2.4 ± 0.1     | 1.58 ± 0.08   |



|        | 988011         | 988012         | 988013         | 988014         | 988015         |
|--------|----------------|----------------|----------------|----------------|----------------|
| Na-24  | 34 ± 7         | 80 ± 4         | 30 ± 2         | 51 ± 3         | 26 ± 2         |
| Mg-27  | <3000          | <2000          | <2000          | <2000          | <3000          |
| Al-28  | <2000          | 5800 ± 400     | <1000          | 1900 ± 300     | <2000          |
| Cl-38  | <200           | <100           | <100           | <100           | <200           |
| K-42   | <600           | 2200 ± 200     | <300           | 1100 ± 100     | <500           |
| Ca-49  | 390000 ± 20000 | 350000 ± 10000 | 430000 ± 20000 | 360000 ± 10000 | 380000 ± 20000 |
| Sc-46  | 0.83 ± 0.04    | 1.23 ± 0.07    | 0.31 ± 0.02    | 0.74 ± 0.04    | 0.29 ± 0.02    |
| Ti-51  | <10000         | <8000          | <8000          | <8000          | <10000         |
| V-52   | <10            | <10            | <10            | <10            | <10            |
| Cr-51  | 2.0 ± 0.5      | 3.6 ± 0.5      | <0.9           | 1.3 ± 0.4      | <1             |
| Mn-56  | 2300 ± 100     | 1470 ± 60      | 1470 ± 60      | 1180 ± 50      | 1840 ± 70      |
| Fe-59  | 1900 ± 100     | 3600 ± 200     | 1820 ± 100     | 3100 ± 200     | 1500 ± 100     |
| Co-60  | 1.0 ± 0.4      | 2.8 ± 0.2      | 0.9 ± 0.2      | 1.5 ± 0.1      | 1.5 ± 0.5      |
| Cu-66  | <500           | <400           | <300           | <400           | <400           |
| Zn-65  | <8             | 51 ± 7         | 12 ± 3         | 20 ± 3         | <7             |
| Ga-72  | <6             | <5             | <4             | <6             | <5             |
| As-76  | 0.5 ± 0.1      | 1.2 ± 0.1      | 1.2 ± 0.1      | 1.9 ± 0.2      | 0.7 ± 0.1      |
| Se-75  | <2             | <2             | <2             | <2             | <2             |
| Br-82  | 0.36 ± 0.10    | 0.29 ± 0.07    | <0.4           | <0.6           | <0.5           |
| Rb-86  | <8             | 13 ± 2         | <5             | <7             | <8             |
| Sr-87  | <700           | <500           | <600           | <600           | <700           |
| Zr-95  | <100           | <90            | <60            | <100           | <100           |
| Mo-99  | <10            | <30            | <10            | <10            | <10            |
| Ag-110 | <2             | <2             | <1             | <2             | <2             |
| In-116 | <0.4           | <0.3           | <0.2           | <0.3           | <0.4           |
| Sb-122 | 0.09 ± 0.02    | 0.15 ± 0.02    | 0.11 ± 0.01    | 0.20 ± 0.02    | <0.05          |
| I-128  | <50            | <30            | <40            | <50            | <50            |
| Cs-134 | <0.6           | 0.52 ± 0.10    | <0.4           | 0.36 ± 0.06    | <0.6           |
| Ba-131 | <200           | <200           | 60 ± 60        | <200           | <200           |
| Ba-139 | <10000         | <7000          | <7000          | <8000          | <10000         |
| La-140 | 9 ± 1          | 6.9 ± 0.4      | 2.1 ± 0.1      | 3.4 ± 0.2      | 1.9 ± 0.3      |
| Ce-141 | 9.6 ± 0.5      | 9.0 ± 0.5      | 2.8 ± 0.3      | 3.0 ± 0.4      | 2.5 ± 0.4      |
| Nd-147 | <10            | <10            | <6             | <9             | <9             |
| Sm-153 | 1.58 ± 0.08    | 1.26 ± 0.06    | 0.28 ± 0.01    | 0.58 ± 0.03    | 0.31 ± 0.01    |
| Eu-152 | 0.28 ± 0.09    | 0.27 ± 0.09    | 0.081 ± 0.006  | 0.13 ± 0.10    | 0.08 ± 0.03    |
| Tb-160 | 0.18 ± 0.05    | 0.20 ± 0.03    | <0.2           | <0.3           | 0.04 ± 0.04    |
| Dy-165 | 2.4 ± 0.5      | <10            | <10            | <10            | <10            |
| Yb-175 | 1.24 ± 0.07    | 0.70 ± 0.04    | 0.19 ± 0.02    | 0.40 ± 0.03    | 0.29 ± 0.03    |
| Lu-177 | 0.15 ± 0.01    | 0.10 ± 0.01    | 0.026 ± 0.006  | 0.041 ± 0.008  | <0.08          |
| Hf-181 | <0.4           | 0.28 ± 0.04    | <0.2           | <0.3           | <0.3           |
| Ta-182 | <0.4           | <0.4           | <0.3           | <0.4           | <0.4           |
| W-187  | <1             | 0.4 ± 0.1      | <0.7           | <1             | <1             |
| Au-198 | <0.002         | <0.002         | <0.001         | <0.002         | <0.002         |
| Hg-203 | <0.4           | <0.4           | <0.2           | <0.5           | <0.4           |
| Th-233 | 0.26 ± 0.04    | 1.31 ± 0.07    | 0.14 ± 0.03    | 0.31 ± 0.04    | <0.2           |
| U-235  | 0.29 ± 0.03    | 0.34 ± 0.03    | 0.17 ± 0.02    | 0.32 ± 0.03    | 0.22 ± 0.03    |

|        | 988016        | 988017         | 988018         | 988019         | 988020       |
|--------|---------------|----------------|----------------|----------------|--------------|
| Na-24  | 34 ± 3        | 42 ± 2         | 86 ± 4         | 20 ± 20        | 46 ± 2       |
| Mg-27  | <3000         | <3000          | <2000          | <2000          | 5400 ± 800   |
| Al-28  | <1000         | <1000          | 2800 ± 400     | 3000 ± 300     | 44000 ± 1000 |
| Cl-38  |               | <200           | <200           | <200           | <100         |
| K-42   |               | <400           | 1800 ± 200     | <700           | 3600 ± 300   |
| Ca-49  | 37000 ± 20000 | 420000 ± 20000 | 310000 ± 10000 | 310000 ± 10000 | 85000 ± 4000 |
| Sc-46  | 0.54 ± 0.03   | 0.43 ± 0.02    | 1.41 ± 0.08    | 2.3 ± 0.1      | 7.7 ± 0.4    |
| Ti-51  | <9000         | <9000          | <8000          | <8000          | 2100 ± 300   |
| V-52   | <10           | <10            | <10            | 21 ± 3         | 380 ± 10     |
| Cr-51  | 1.7 ± 0.4     | <1             | 2.4 ± 0.6      | 3.2 ± 0.6      | 65 ± 4       |
| Mn-56  | 1710 ± 70     | 1330 ± 60      | 1110 ± 40      | 1460 ± 70      | 490 ± 20     |
| Fe-59  | 2700 ± 100    | 4200 ± 200     | 6900 ± 400     | 9300 ± 500     | 28000 ± 1000 |
| Co-60  | 2.1 ± 0.2     | 1.3 ± 0.2      | 2.0 ± 0.2      | 3.1 ± 0.4      | 36 ± 2       |
| Cu-66  | <400          | <400           | <400           | <300           | <400         |
| Zn-65  | 52 ± 7        | 13 ± 3         | 80 ± 10        | <9             | 190 ± 30     |
| Ga-72  | <5            | <5             | <8             | <8             | <6           |
| As-76  | 2.4 ± 0.3     | 4.0 ± 0.5      | 5.0 ± 0.5      | 5.4 ± 0.6      | 3.7 ± 0.4    |
| Se-75  | <2            | <2             | <3             | <3             | 5 ± 2        |
| Br-82  | <0.4          | 0.33 ± 0.07    | 0.6 ± 0.1      | <0.7           | 1.2 ± 0.1    |
| Rb-86  | <6            | <6             | <10            | <10            | 116 ± 8      |
| Sr-87  | <600          | <700           | <700           | <500           | <400         |
| Zr-95  | <80           | <90            | <200           | <200           | <300         |
| Mo-99  | <30           | <20            | <10            | 0.7 ± 0.7      | <30          |
| Ag-110 | <2            | <2             | <3             | <3             | <5           |
| In-116 | <0.3          | <0.3           | <0.3           | <0.3           | <0.3         |
| Sb-122 | 0.13 ± 0.02   | 0.18 ± 0.02    | 0.28 ± 0.03    | 0.26 ± 0.03    | 0.53 ± 0.03  |
| I-128  | <40           | <40            | <50            | <40            | <30          |
| Cs-134 | 0.26 ± 0.05   | <0.5           | <1.0           | 0.44 ± 0.07    | 6.5 ± 0.4    |
| Ba-131 | <200          | <200           | <300           | <300           | 160 ± 70     |
| Ba-139 | <8000         | <9000          | <9000          | <8000          | <5000        |
| La-140 | 4.7 ± 0.3     | 2.5 ± 0.1      | 5.9 ± 0.3      | 6.1 ± 0.5      | 3.2 ± 0.3    |
| Ce-141 | 5.0 ± 0.4     | 3.0 ± 0.3      | 7.8 ± 0.7      | 7.8 ± 0.6      | 42 ± 2       |
| Nd-147 | <9            | <8             | <10            | <10            | <30          |
| Sm-153 | 0.89 ± 0.04   | 0.26 ± 0.01    | 1.16 ± 0.05    | 0.98 ± 0.04    | 0.35 ± 0.02  |
| Eu-152 | 0.19 ± 0.01   | 0.10 ± 0.01    | 0.2 ± 0.1      | 0.2 ± 0.1      | 1.1 ± 0.1    |
| Tb-160 | 0.12 ± 0.02   | 0.06 ± 0.02    | 0.11 ± 0.04    | 0.14 ± 0.03    | 0.72 ± 0.10  |
| Dy-165 | <10           | <10            | <10            | 1.3 ± 0.4      | <9           |
| Yb-175 | 0.49 ± 0.03   | 0.35 ± 0.03    | 0.72 ± 0.05    | 0.91 ± 0.06    | 0.17 ± 0.02  |
| Lu-177 | 0.071 ± 0.008 | 0.070 ± 0.009  | 0.14 ± 0.02    | 0.13 ± 0.01    | 0.24 ± 0.03  |
| Hf-181 | <0.3          | <0.3           | 0.19 ± 0.05    | 0.18 ± 0.05    | 2.5 ± 0.2    |
| Ta-182 | <0.3          | <0.3           | <0.5           | <0.4           | 0.6 ± 0.1    |
| W-187  | <0.9          | <1.0           | <2             | <2             | <1           |
| Au-198 | <0.002        | <0.002         | <0.003         | <0.002         | <0.002       |
| Hg-203 | <0.3          | <0.4           | <0.6           | <0.5           | <1.0         |
| Th-233 | 0.25 ± 0.04   | <0.2           | 0.74 ± 0.07    | 0.58 ± 0.06    | 8.7 ± 0.4    |
| U-235  | 0.30 ± 0.03   | 0.31 ± 0.03    | 0.63 ± 0.04    | 0.97 ± 0.06    | 9.9 ± 0.4    |

|        | 988021        | 988022        | 988023       | 988024        | 988025        |
|--------|---------------|---------------|--------------|---------------|---------------|
| Na-24  | 180 ± 10      | 330 ± 10      | 70 ± 20      | 270 ± 10      | 180 ± 10      |
| Mg-27  | 2900 ± 400    | 3500 ± 300    | 5300 ± 400   | 5700 ± 600    | 3300 ± 600    |
| Al-28  | 30800 ± 1000  | 44000 ± 1000  | 53000 ± 2000 | 46000 ± 2000  | 31000 ± 1000  |
| Cl-38  | <80           | <80           | <90          | <100          | <100          |
| K-42   | 15000 ± 1000  | 27000 ± 2000  | <2000        | 23000 ± 2000  | 14500 ± 1000  |
| Ca-49  | 188000 ± 8000 | 18000 ± 1000  | 7800 ± 800   | 8500 ± 1000   | 101000 ± 5000 |
| Sc-46  | 4.6 ± 0.2     | 8.4 ± 0.5     | 9.5 ± 0.5    | 9.4 ± 0.5     | 6.1 ± 0.3     |
| Ti-51  | 1500 ± 300    | 2100 ± 300    | 2700 ± 400   | 2200 ± 300    | 1500 ± 300    |
| V-52   | 232 ± 9       | 360 ± 10      | 440 ± 20     | 400 ± 20      | 260 ± 10      |
| Cr-51  | 43 ± 3        | 69 ± 4        | 69 ± 4       | 60 ± 4        | 36 ± 2        |
| Mn-56  | 600 ± 20      | 93 ± 4        | 69 ± 4       | 169 ± 7       | 310 ± 10      |
| Fe-59  | 17000 ± 1000  | 29000 ± 2000  | 23000 ± 1000 | 42000 ± 2000  | 16900 ± 900   |
| Co-60  | 29 ± 2        | 25 ± 1        | 14.3 ± 0.9   | 23 ± 1        | 10.5 ± 0.6    |
| Cu-66  | <200          | <300          | <300         | <400          | <300          |
| Zn-65  | 120 ± 20      | 160 ± 20      | 230 ± 70     | 260 ± 30      | 90 ± 10       |
| Ga-72  | 6 ± 1         | <20           | <20          | <20           | <10           |
| As-76  | 17 ± 2        | 32 ± 3        | 37 ± 4       | 31 ± 3        | 14 ± 1        |
| Se-75  | 1.8 ± 0.5     | 4 ± 1         | 4 ± 1        | 4 ± 1         | 1.7 ± 0.7     |
| Br-82  | 6.6 ± 0.7     | 6.2 ± 0.7     | 8 ± 3        | 2.7 ± 0.3     | 2.9 ± 0.3     |
| Rb-86  | 68 ± 4        | 110 ± 7       | 128 ± 8      | 103 ± 8       | 60 ± 5        |
| Sr-87  | <400          | <300          | <200         | <300          | <400          |
| Zr-95  | <200          | 240 ± 70      | 200 ± 90     | <300          | <200          |
| Mo-99  | 27 ± 3        | 25 ± 3        | 22 ± 3       | 110 ± 10      | 22 ± 4        |
| Ag-110 | <3            | <6            | <6           | <6            | <5            |
| In-116 | <0.2          | <0.2          | 0.18 ± 0.03  | <0.3          | <0.2          |
| Sb-122 | 2.4 ± 0.1     | 4.2 ± 0.2     | <0.2         | 3.8 ± 0.2     | 1.9 ± 0.1     |
| I-128  | <30           | <20           | <20          | <20           | <30           |
| Cs-134 | 4.1 ± 0.3     | 7.3 ± 0.5     | 5.4 ± 0.3    | 5.9 ± 0.4     | 3.6 ± 0.2     |
| Ba-131 | 150 ± 40      | 220 ± 50      | 200 ± 50     | 230 ± 80      | 170 ± 60      |
| Ba-139 | <5000         | <4000         | 190 ± 40     | <5000         | <5000         |
| La-140 | 12.8 ± 0.6    | 29 ± 2        | 21 ± 5       | 24 ± 1        | 14.5 ± 0.7    |
| Ce-141 | 26 ± 1        | 44 ± 3        | 40 ± 2       | 45 ± 2        | 27 ± 2        |
| Nd-147 | 19 ± 4        | 23 ± 7        | 39 ± 9       | <30           | <20           |
| Sm-153 | 2.5 ± 0.1     | 6.4 ± 0.3     | 4.9 ± 0.2    | 6.8 ± 0.3     | 2.4 ± 0.1     |
| Eu-152 | 0.6 ± 0.1     | 1.10 ± 0.06   | 0.78 ± 0.06  | 1.04 ± 0.08   | 0.56 ± 0.09   |
| Tb-160 | 0.43 ± 0.05   | 0.76 ± 0.09   | 0.67 ± 0.08  | 0.82 ± 0.09   | 0.5 ± 0.1     |
| Dy-165 | 2.6 ± 0.3     | 5.5 ± 0.6     | 4.0 ± 0.6    | <8            | 3.5 ± 0.4     |
| Yb-175 | 0.93 ± 0.06   | 2.0 ± 0.2     | 2.3 ± 0.5    | 2.4 ± 0.1     | 1.3 ± 0.1     |
| Lu-177 | 0.15 ± 0.01   | 0.27 ± 0.03   | 0.30 ± 0.03  | 0.37 ± 0.03   | 0.27 ± 0.03   |
| Hf-181 | 1.6 ± 0.1     | 2.7 ± 0.2     | 2.5 ± 0.3    | 2.6 ± 0.3     | 1.5 ± 0.1     |
| Ta-182 | 0.36 ± 0.06   | 0.65 ± 0.08   | 0.75 ± 0.09  | 0.5 ± 0.1     | <0.8          |
| W-187  | 1.0 ± 0.2     | 2.1 ± 0.5     | 11 ± 3       | 1.5 ± 0.3     | <2            |
| Au-198 | 0.008 ± 0.001 | 0.013 ± 0.002 | <0.004       | 0.018 ± 0.002 | 0.009 ± 0.001 |
| Hg-203 | <0.6          | 0.6 ± 0.4     | <1.0         | <1            | <0.9          |
| Th-233 | 5.9 ± 0.2     | 9.5 ± 0.4     | 9.2 ± 0.4    | 8.3 ± 0.4     | 5.3 ± 0.2     |
| U-235  | 7.2 ± 0.3     | 11.9 ± 0.4    | 10.7 ± 0.4   | 8.7 ± 0.3     | 7.8 ± 0.3     |

|        | 988026          | 988027        | 988028          | 988029          | 988030          |
|--------|-----------------|---------------|-----------------|-----------------|-----------------|
| Na-24  | 193 ± 8         | 189 ± 13      | 191 ± 10        | 180 ± 10        | 132 ± 6         |
| Mg-27  | 2600 ± 400      | 2100 ± 400    | 3400 ± 300      | 3700 ± 600      | <2000           |
| Al-28  | 29000 ± 1000    | 21800 ± 800   | 25500 ± 900     | 24700 ± 900     | 16600 ± 600     |
| Cl-38  | <120            | <130          | <110            | <110            | <120            |
| K-42   | 14100 ± 900     | 13100 ± 1300  | 14300 ± 900     | 11400 ± 700     | 8700 ± 600      |
| Ca-49  | 112000 ± 5000   | 125000 ± 6000 | 130000 ± 6000   | 172000 ± 8000   | 241000 ± 10000  |
| Sc-46  | 6.3 ± 0.3       | 5.5 ± 0.3     | 6.6 ± 0.3       | 4.8 ± 0.3       | 3.54 ± 0.19     |
| Ti-51  | 1300 ± 300      | 1100 ± 200    | 1200 ± 300      | 1000 ± 200      | <6000           |
| V-52   | 258 ± 11        | 191 ± 8       | 236 ± 9         | 200 ± 8         | 146 ± 6         |
| Cr-51  | 37 ± 2          | 30 ± 2        | 40 ± 3          | 29 ± 2          | 20.2 ± 1.5      |
| Mn-56  | 358 ± 16        | 317 ± 13      | 405 ± 17        | 446 ± 19        | 630 ± 30        |
| Fe-59  | 17400 ± 900     | 16000 ± 800   | 19400 ± 1000    | 16800 ± 900     | 11200 ± 600     |
| Co-60  | 11.1 ± 0.6      | 9.0 ± 0.7     | 8.4 ± 0.5       | 7.8 ± 0.5       | 11.6 ± 0.6      |
| Cu-66  | <300            | <300          | <300            | <300            | <300            |
| Zn-65  | 100 ± 15        | <16           | 134 ± 17        | 82 ± 13         | 81 ± 11         |
| Ga-72  | 7.0 ± 1.2       | <6            | 5.3 ± 0.8       | 5.2 ± 0.9       | 4.0 ± 0.9       |
| As-76  | 16.0 ± 1.7      | 18 ± 2        | 19.4 ± 2.0      | 14.1 ± 1.6      | 11.3 ± 1.2      |
| Se-75  | 2.1 ± 1.0       | <5            | 3.5 ± 1.5       | 1.4 ± 0.6       | 1.6 ± 0.5       |
| Br-82  | 2.1 ± 0.3       | 0.71 ± 0.19   | 1.8 ± 0.2       | 5.8 ± 0.6       | 1.8 ± 0.2       |
| Rb-86  | 55 ± 5          | 55 ± 5        | 59 ± 5          | 41 ± 4          | 30 ± 4          |
| Sr-87  | <400            | <500          | <300            | <300            | <400            |
| Zr-95  | <300            | <300          | <200            | <190            | <190            |
| Mo-99  | 15 ± 2          | <19           | 58 ± 6          | 16 ± 3          | 7.6 ± 1.5       |
| Ag-110 | <6              | <5            | <4              | <4              | <4              |
| In-116 | <0.2            | <0.3          | 0.15 ± 0.05     | <0.2            | <0.19           |
| Sb-122 | 2.14 ± 0.13     | 2.09 ± 0.15   | 2.33 ± 0.12     | 1.62 ± 0.08     | 1.28 ± 0.08     |
| I-128  | <30             | <40           | <20             | <20             | <30             |
| Cs-134 | 3.7 ± 0.3       | 3.1 ± 0.2     | 3.7 ± 0.2       | 2.9 ± 0.2       | 2.04 ± 0.17     |
| Ba-131 | <500            | <500          | 210 ± 50        | <400            | <300            |
| Ba-139 | <6000           | <7000         | <5000           | <5000           | <5000           |
| La-140 | 17.6 ± 0.9      | 17.5 ± 1.7    | 17.6 ± 1.1      | 13.0 ± 0.6      | 10.7 ± 0.5      |
| Ce-141 | 33 ± 2          | 26.5 ± 1.8    | 35.1 ± 1.9      | 24.0 ± 1.5      | 17.7 ± 1.2      |
| Nd-147 | <20             | <20           | <20             | <18             | <15             |
| Sm-153 | 3.50 ± 0.16     | <0.3          | 4.20 ± 0.19     | 2.17 ± 0.10     | 2.15 ± 0.10     |
| Eu-152 | 0.62 ± 0.10     | 0.53 ± 0.05   | 0.74 ± 0.14     | 0.50 ± 0.11     | 0.44 ± 0.03     |
| Tb-160 | 0.51 ± 0.07     | 0.43 ± 0.13   | 0.52 ± 0.07     | 0.43 ± 0.05     | 0.30 ± 0.04     |
| Dy-165 | 3.6 ± 0.4       | 2.9 ± 0.8     | 3.3 ± 0.4       | <7              | 2.2 ± 0.4       |
| Yb-175 | 1.54 ± 0.15     | 1.81 ± 0.11   | 1.74 ± 0.14     | 1.34 ± 0.13     | 1.14 ± 0.12     |
| Lu-177 | 0.21 ± 0.03     | 0.21 ± 0.03   | 0.28 ± 0.02     | 0.166 ± 0.017   | 0.141 ± 0.017   |
| Hf-181 | 1.62 ± 0.14     | 1.07 ± 0.10   | 1.35 ± 0.19     | 1.05 ± 0.09     | 0.72 ± 0.07     |
| Ta-182 | 0.35 ± 0.07     | <0.9          | 0.45 ± 0.09     | <0.7            | 0.29 ± 0.15     |
| W-187  | 1.2 ± 0.2       | 2.1 ± 0.6     | 1.0 ± 0.2       | 0.78 ± 0.14     | 0.7 ± 0.2       |
| Au-198 | 0.0074 ± 0.0015 | <0.004        | 0.0050 ± 0.0010 | 0.0064 ± 0.0012 | 0.0055 ± 0.0009 |
| Hg-203 | <1.1            | <0.9          | <0.8            | <0.7            | <0.7            |
| Th-233 | 4.9 ± 0.2       | 4.1 ± 0.2     | 5.4 ± 0.2       | 3.8 ± 0.2       | 2.96 ± 0.15     |
| U-235  | 7.5 ± 0.3       | 6.7 ± 0.3     | 6.7 ± 0.3       | 5.8 ± 0.2       | 4.38 ± 0.18     |

|        | 988031        | 988032          | 988033          | 988034          | 988035        |
|--------|---------------|-----------------|-----------------|-----------------|---------------|
| Na-24  | 206 ± 9       | 143 ± 6         | 153 ± 8         | 141 ± 6         | 171 ± 9       |
| Mg-27  | 2900 ± 400    | <2000           | 2600 ± 400      | 2600 ± 400      | 2200 ± 400    |
| Al-28  | 17400 ± 600   | 16400 ± 700     | 22200 ± 800     | 15800 ± 600     | 14400 ± 500   |
| Cl-38  | 78 ± 16       | <160            | <90             | <100            | <100          |
| K-42   | 13800 ± 900   | 8500 ± 500      | 10600 ± 700     | 8500 ± 500      | 10800 ± 700   |
| Ca-49  | 152000 ± 7000 | 206000 ± 9000   | 163000 ± 7000   | 223000 ± 9000   | 198000 ± 8000 |
| Sc-46  | 4.9 ± 0.3     | 4.1 ± 0.2       | 4.5 ± 0.2       | 3.53 ± 0.19     | 3.47 ± 0.18   |
| Ti-51  | 580 ± 170     | <8000           | 1000 ± 200      | 580 ± 160       | 850 ± 200     |
| V-52   | 162 ± 7       | 146 ± 7         | 185 ± 8         | 136 ± 6         | 119 ± 5       |
| Cr-51  | 27.5 ± 1.9    | 22.6 ± 1.7      | 25.8 ± 1.7      | 20.1 ± 1.4      | 20.2 ± 1.4    |
| Mn-56  | 369 ± 15      | 880 ± 40        | 446 ± 19        | 520 ± 20        | 433 ± 17      |
| Fe-59  | 19800 ± 1000  | 15900 ± 800     | 14800 ± 800     | 14600 ± 700     | 10900 ± 600   |
| Co-60  | 6.7 ± 0.5     | 13.2 ± 0.7      | 5.6 ± 0.3       | 5.6 ± 0.3       | 6.6 ± 0.4     |
| Cu-66  | <300          | <400            | <300            | <200            | <300          |
| Zn-65  | 70 ± 50       | 170 ± 20        | 80 ± 12         | 53 ± 8          | <9            |
| Ga-72  | <4            | 3.7 ± 0.7       | 4.3 ± 0.7       | <4              | <4            |
| As-76  | 21 ± 2        | 13.0 ± 1.4      | 13.8 ± 1.4      | 12.9 ± 1.3      | 13.4 ± 1.4    |
| Se-75  | 1.7 ± 0.5     | 2.2 ± 0.7       | 4.9 ± 1.2       | 3.9 ± 1.0       | 3.6 ± 0.9     |
| Br-82  | 1.51 ± 0.18   | 0.63 ± 0.09     | 0.37 ± 0.13     | 1.04 ± 0.16     | 0.7 ± 0.4     |
| Rb-86  | 48 ± 4        | 45 ± 5          | 49 ± 4          | 42 ± 4          | 35 ± 3        |
| Sr-87  | <400          | <500            | <300            | <400            | <400          |
| Zr-95  | <200          | <200            | <160            | <170            | <180          |
| Mo-99  | <13           | 34 ± 6          | 19 ± 3          | 8.5 ± 1.3       | <12           |
| Ag-110 | <4            | <4              | <3              | <3              | <3            |
| In-116 | <0.20         | <0.3            | <0.20           | <0.16           | <0.19         |
| Sb-122 | 2.23 ± 0.11   | 1.42 ± 0.08     | 1.50 ± 0.08     | 1.35 ± 0.08     | 1.49 ± 0.08   |
| I-128  | <30           | <30             | <19             | <20             | <30           |
| Cs-134 | 2.9 ± 0.3     | 2.4 ± 0.3       | 2.52 ± 0.20     | 2.07 ± 0.17     | 2.11 ± 0.17   |
| Ba-131 | 90 ± 30       | <400            | <300            | 140 ± 40        | 70 ± 30       |
| Ba-139 | <5000         | <7000           | <4000           | <5000           | <5000         |
| La-140 | 18.0 ± 1.0    | 11.4 ± 0.6      | 12.3 ± 0.6      | 11.2 ± 0.5      | 13.1 ± 0.7    |
| Ce-141 | 28.0 ± 1.5    | 22.4 ± 1.4      | 23.3 ± 1.3      | 19.3 ± 1.2      | 18.7 ± 1.2    |
| Nd-147 | <16           | <20             | <15             | 16 ± 4          | <13           |
| Sm-153 | <0.19         | 2.51 ± 0.12     | 2.10 ± 0.10     | 2.29 ± 0.11     | <0.15         |
| Eu-152 | 0.61 ± 0.13   | 0.44 ± 0.15     | 0.51 ± 0.09     | 0.47 ± 0.10     | 0.41 ± 0.10   |
| Tb-160 | 0.45 ± 0.05   | 0.48 ± 0.07     | 0.39 ± 0.04     | 0.31 ± 0.04     | 0.31 ± 0.04   |
| Dy-165 | 3.5 ± 0.4     | 2.9 ± 0.5       | 3.4 ± 0.4       | 2.2 ± 0.3       | 2.1 ± 0.4     |
| Yb-175 | 3.5 ± 0.5     | 1.19 ± 0.07     | 1.18 ± 0.09     | 1.10 ± 0.08     | 1.41 ± 0.09   |
| Lu-177 | 0.216 ± 0.018 | 0.17 ± 0.02     | 0.192 ± 0.017   | 0.174 ± 0.016   | 0.162 ± 0.015 |
| Hf-181 | 1.16 ± 0.12   | 0.75 ± 0.09     | 1.01 ± 0.08     | 0.72 ± 0.12     | 0.81 ± 0.11   |
| Ta-182 | 0.24 ± 0.05   | <0.8            | 0.27 ± 0.06     | <0.5            | <0.5          |
| W-187  | 2.5 ± 0.7     | 0.52 ± 0.14     | 0.73 ± 0.12     | 0.64 ± 0.11     | 0.97 ± 0.18   |
| Au-198 | <0.003        | 0.0085 ± 0.0013 | 0.0069 ± 0.0010 | 0.0061 ± 0.0010 | <0.002        |
| Hg-203 | <0.6          | <0.8            | <0.6            | 0.6 ± 0.3       | <0.5          |
| Th-233 | 3.76 ± 0.17   | 3.27 ± 0.17     | 3.55 ± 0.16     | 2.76 ± 0.13     | 2.95 ± 0.14   |
| U-235  | 5.4 ± 0.2     | 4.61 ± 0.19     | 6.1 ± 0.2       | 4.34 ± 0.16     | 4.47 ± 0.17   |

|        | 988036          | 988037          | 988038          | 988039          | 988040         |
|--------|-----------------|-----------------|-----------------|-----------------|----------------|
| Na-24  | 151 ± 8         | 158 ± 9         | 140 ± 6         | 154 ± 9         | 132 ± 7        |
| Mg-27  | 3700 ± 600      | 3800 ± 600      | 2500 ± 400      | 2800 ± 400      | 2700 ± 600     |
| Al-28  | 16200 ± 600     | 17000 ± 700     | 12000 ± 500     | 9800 ± 400      | 11700 ± 600    |
| Cl-38  | <130            | <110            | <100            | <100            | <150           |
| K-42   | 8400 ± 500      | 8300 ± 500      | 6600 ± 400      | 8200 ± 500      | 5800 ± 400     |
| Ca-49  | 211000 ± 9000   | 227000 ± 10000  | 251000 ± 18000  | 228000 ± 9000   | 249000 ± 11000 |
| Sc-46  | 3.49 ± 0.18     | 3.17 ± 0.17     | 2.71 ± 0.15     | 2.36 ± 0.13     | 2.15 ± 0.13    |
| Ti-51  | 700 ± 200       | 700 ± 200       | <5000           | <5000           | <8000          |
| V-52   | 115 ± 5         | 130 ± 6         | 96 ± 4          | 77 ± 4          | 80 ± 5         |
| Cr-51  | 20.0 ± 1.4      | 20.4 ± 1.4      | 15.0 ± 1.1      | 14.9 ± 1.1      | 22.7 ± 1.7     |
| Mn-56  | 670 ± 30        | 630 ± 30        | 610 ± 20        | 530 ± 20        | 840 ± 30       |
| Fe-59  | 10300 ± 500     | 10000 ± 600     | 10400 ± 500     | 7800 ± 400      | 29100 ± 1500   |
| Co-60  | 8.1 ± 0.5       | 6.3 ± 0.4       | 5.3 ± 0.3       | 4.8 ± 0.4       | 7.3 ± 0.4      |
| Cu-66  | <300            | <300            | <200            | <200            | <300           |
| Zn-65  | 98 ± 13         | 41 ± 8          | 30 ± 4          | <8              | 89 ± 12        |
| Ga-72  | <4              | 4.1 ± 0.8       | <3              | 2.3 ± 0.6       | <4             |
| As-76  | 10.8 ± 1.1      | 9.7 ± 1.1       | 8.7 ± 0.9       | 9.2 ± 0.9       | 7.5 ± 0.8      |
| Se-75  | 2.7 ± 0.7       | 3.7 ± 1.0       | 2.3 ± 0.6       | 1.5 ± 0.4       | 1.0 ± 0.5      |
| Br-82  | 0.61 ± 0.12     | 0.80 ± 0.11     | 0.73 ± 0.10     | 0.74 ± 0.15     | 0.77 ± 0.13    |
| Rb-86  | 43 ± 4          | 34 ± 3          | 32 ± 3          | 25 ± 3          | 24 ± 5         |
| Sr-87  | <400            | <400            | <400            | <400            | <500           |
| Zr-95  | <160            | <160            | <140            | <150            | <190           |
| Mo-99  | 29 ± 5          | 13 ± 2          | 4.7 ± 1.1       | 7.8 ± 1.1       | 18 ± 5         |
| Ag-110 | <3              | <3              | <3              | <2              | <4             |
| In-116 | <0.3            | <0.2            | <0.16           | <0.18           | <0.3           |
| Sb-122 | 1.33 ± 0.07     | 1.16 ± 0.06     | 0.94 ± 0.06     | 0.96 ± 0.05     | 0.88 ± 0.05    |
| I-128  | <30             | <20             | <20             | <30             | <30            |
| Cs-134 | 2.02 ± 0.16     | 1.96 ± 0.18     | 1.60 ± 0.12     | 1.55 ± 0.12     | 1.36 ± 0.17    |
| Ba-131 | <300            | <300            | <200            | 900 ± 300       | <400           |
| Ba-139 | <6000           | <5000           | <5000           | <5000           | <8000          |
| La-140 | 9.8 ± 0.6       | 9.1 ± 0.4       | 9.3 ± 0.5       | 10.3 ± 0.5      | 8.3 ± 0.5      |
| Ce-141 | 19.0 ± 1.2      | 17.6 ± 1.1      | 16.0 ± 1.0      | 14.6 ± 0.9      | 14.9 ± 1.1     |
| Nd-147 | <17             | <14             | <11             | <11             | <20            |
| Sm-153 | 2.22 ± 0.10     | 1.47 ± 0.07     | 1.75 ± 0.08     | 1.85 ± 0.09     | 1.71 ± 0.08    |
| Eu-152 | 0.47 ± 0.03     | 0.41 ± 0.10     | 0.33 ± 0.10     | 0.35 ± 0.10     | 0.32 ± 0.13    |
| Tb-160 | 0.26 ± 0.04     | 0.23 ± 0.04     | 0.28 ± 0.03     | 0.26 ± 0.03     | 0.24 ± 0.04    |
| Dy-165 | 1.6 ± 0.3       | 2.9 ± 0.5       | 1.7 ± 0.3       | 1.9 ± 0.4       | 1.5 ± 0.4      |
| Yb-175 | 0.96 ± 0.06     | 0.93 ± 0.09     | 0.93 ± 0.06     | 1.05 ± 0.06     | 0.83 ± 0.06    |
| Lu-177 | 0.150 ± 0.018   | 0.144 ± 0.017   | 0.129 ± 0.014   | 0.141 ± 0.013   | 0.122 ± 0.016  |
| Hf-181 | 0.82 ± 0.08     | 0.80 ± 0.07     | 0.60 ± 0.06     | 0.53 ± 0.05     | 0.56 ± 0.07    |
| Ta-182 | <0.6            | <0.6            | 0.27 ± 0.07     | 0.18 ± 0.04     | 0.9 ± 0.5      |
| W-187  | 0.62 ± 0.13     | 0.59 ± 0.12     | 0.84 ± 0.13     | 0.54 ± 0.16     | 1.3 ± 0.3      |
| Au-198 | 0.0053 ± 0.0009 | 0.0063 ± 0.0009 | 0.0059 ± 0.0009 | 0.0040 ± 0.0007 | <0.003         |
| Hg-203 | <0.6            | <0.6            | <0.5            | <0.4            | <0.7           |
| Th-233 | 3.00 ± 0.14     | 2.88 ± 0.13     | 2.21 ± 0.10     | 2.22 ± 0.11     | 2.09 ± 0.13    |
| U-235  | 4.19 ± 0.17     | 4.47 ± 0.18     | 3.49 ± 0.14     | 3.39 ± 0.14     | 3.22 ± 0.14    |

|        | 988041          | 988042         | 988043         | 988044          | 988045        |
|--------|-----------------|----------------|----------------|-----------------|---------------|
| Na-24  | 146 ± 7         | 88 ± 4         | 174 ± 10       | 109 ± 5         | 540 ± 30      |
| Mg-27  | 4300 ± 600      | <1600          | 1500 ± 400     | 2600 ± 500      | 5900 ± 400    |
| Al-28  | 14900 ± 600     | 2700 ± 200     | 11900 ± 500    | 6300 ± 400      | 75000 ± 2000  |
| Cl-38  | <110            | <120           | <130           | <150            | <60           |
| K-42   | 7700 ± 500      | 1220 ± 100     | 7800 ± 500     | 3800 ± 300      | 47000 ± 3000  |
| Ca-49  | 263000 ± 11000  | 387000 ± 15000 | 260000 ± 11000 | 344000 ± 14000  | 17900 ± 1100  |
| Sc-46  | 3.04 ± 0.16     | 0.66 ± 0.04    | 2.46 ± 0.13    | 1.46 ± 0.08     | 10.0 ± 0.5    |
| Ti-51  | 1500 ± 300      | <5000          | <6000          | <7000           | 3700 ± 500    |
| V-52   | 100 ± 5         | 15.4 ± 1.8     | 69 ± 4         | 44 ± 8          | 347 ± 13      |
| Cr-51  | 19.1 ± 1.3      | 3.2 ± 0.4      | 14.4 ± 1.1     | 9.3 ± 0.8       | 102 ± 6       |
| Mn-56  | 730 ± 30        | 660 ± 30       | 520 ± 20       | 1220 ± 50       | 189 ± 8       |
| Fe-59  | 12500 ± 700     | 8900 ± 500     | 8100 ± 500     | 6000 ± 300      | 50000 ± 3000  |
| Co-60  | 6.3 ± 0.4       | 1.40 ± 0.11    | 4.2 ± 0.5      | 3.3 ± 0.2       | 8.9 ± 0.5     |
| Cu-66  | <300            | <200           | <300           | <300            | <200          |
| Zn-65  | 24 ± 5          | 22 ± 3         | <10            | 54 ± 7          | <15           |
| Ga-72  | 3.6 ± 0.6       | <2             | 3.2 ± 1.0      | <3              | 18.2 ± 1.5    |
| As-76  | 9.1 ± 1.0       | 4.4 ± 0.5      | 11.4 ± 1.2     | 6.4 ± 0.7       | 45 ± 5        |
| Se-75  | 1.9 ± 0.6       | 1.2 ± 0.3      | 1.4 ± 0.5      | 1.3 ± 0.4       | 13 ± 3        |
| Br-82  | 0.86 ± 0.11     | 0.60 ± 0.07    | 0.88 ± 0.13    | 0.85 ± 0.10     | 3.1 ± 0.4     |
| Rb-86  | 28 ± 3          | <7             | 27 ± 3         | 13 ± 2          | 187 ± 10      |
| Sr-87  | <400            | 430 ± 110      | 620 ± 150      | <400            | <200          |
| Zr-95  | <140            | <100           | <190           | <100            | 210 ± 50      |
| Mo-99  | 12 ± 2          | 2.6 ± 0.7      | 9.6 ± 1.5      | 18 ± 3          | 74 ± 5        |
| Ag-110 | <3              | <1.9           | <3             | <2.0            | <4            |
| In-116 | <0.20           | <0.16          | <0.2           | <0.2            | <0.18         |
| Sb-122 | 1.11 ± 0.06     | 0.31 ± 0.02    | 1.23 ± 0.07    | 0.67 ± 0.04     | 8.5 ± 0.4     |
| I-128  | <20             | <30            | <40            | <30             | <13           |
| Cs-134 | 1.92 ± 0.14     | 0.32 ± 0.09    | 1.50 ± 0.20    | 0.89 ± 0.09     | 12.4 ± 0.7    |
| Ba-131 | 90 ± 30         | 300 ± 200      | 130 ± 40       | 68 ± 16         | 510 ± 60      |
| Ba-139 | 120 ± 40        | <5000          | <7000          | <7000           | <3000         |
| La-140 | 9.7 ± 0.4       | 3.75 ± 0.19    | 12.6 ± 0.6     | 6.1 ± 0.4       | 27.4 ± 1.4    |
| Ce-141 | 17.8 ± 1.0      | 5.7 ± 0.5      | 16.9 ± 1.2     | 11.4 ± 0.7      | 56 ± 3        |
| Nd-147 | <12             | <7             | <14            | <11             | <19           |
| Sm-153 | 1.61 ± 0.08     | 0.56 ± 0.03    | 2.21 ± 0.10    | 1.43 ± 0.07     | 2.66 ± 0.12   |
| Eu-152 | 0.39 ± 0.11     | 0.145 ± 0.014  | 0.33 ± 0.11    | 0.26 ± 0.11     | 0.59 ± 0.06   |
| Tb-160 | 0.32 ± 0.05     | 0.09 ± 0.04    | 0.23 ± 0.05    | 0.18 ± 0.03     | 0.41 ± 0.12   |
| Dy-165 | 3.2 ± 0.5       | <7             | 2.7 ± 0.5      | <8              | 3.6 ± 0.4     |
| Yb-175 | 0.92 ± 0.09     | 0.37 ± 0.03    | 1.17 ± 0.07    | 0.61 ± 0.05     | 1.6 ± 0.2     |
| Lu-177 | 0.138 ± 0.012   | 0.050 ± 0.008  | 0.162 ± 0.018  | 0.102 ± 0.013   | 0.28 ± 0.02   |
| Hf-181 | 0.76 ± 0.06     | 2.4 ± 0.2      | 0.53 ± 0.07    | 0.44 ± 0.05     | 4.2 ± 0.5     |
| Ta-182 | <0.5            | <0.3           | 0.17 ± 0.05    | <0.4            | 1.13 ± 0.09   |
| W-187  | 0.75 ± 0.17     | 0.26 ± 0.07    | 0.65 ± 0.16    | 0.29 ± 0.06     | 3.4 ± 0.5     |
| Au-198 | 0.0043 ± 0.0008 | <0.0015        | <0.002         | 0.0023 ± 0.0005 | 0.056 ± 0.005 |
| Hg-203 | <0.5            | <0.4           | <0.6           | 0.32 ± 0.16     | 1.7 ± 0.4     |
| Th-233 | 2.98 ± 0.13     | 0.39 ± 0.04    | 2.5 ± 0.1      | 1.75 ± 0.09     | 18.9 ± 0.7    |
| U-235  | 3.90 ± 0.15     | 1.21 ± 0.06    | 4.5 ± 0.1      | 2.14 ± 0.09     | 13.8 ± 0.5    |

## Appendix 10

Analytical results of  $\delta^{13}\text{C}$  and  $\delta^{18}\text{O}$   
in carbonate samples from the  
Qidong Section, Hunan.

| Sample | $\delta^{13}\text{C}$ | $\delta^{18}\text{O}$ |
|--------|-----------------------|-----------------------|
| QD-1   | -0.14                 | -7.56                 |
| QD-2   | -1.26                 | -8.01                 |
| QD-3   | 0.1                   | -8.98                 |
| QD-4   | 0.2                   | -7.27                 |
| QD-6   | -1.5                  | -7.46                 |
| QD-7   | 0.44                  | -7.74                 |
| QD-31  | 0.34                  | -7.65                 |
| QD-32  | -1.7                  | -7.56                 |
| QD-8   | -0.27                 | -8.52                 |
| QD-33  | -1.07                 | -10.71                |
| QD-37  | -0.45                 | -9.50                 |
| QD-36  | -0.76                 | -8.80                 |
| QD-35  | -0.81                 | -9.26                 |
| QD-34  | -0.95                 | -9.03                 |
| QD-38  | -0.73                 | -9.35                 |
| QD-39  | -0.98                 | -10.05                |
| QD-9a  | -1.97                 | -9.91                 |
| QD-9b  | -1.11                 | -10.17                |
| QD-40  | 0.18                  | -7.87                 |
| QD-10  | 0.78                  | -7.16                 |
| QD-41  | 0.76                  | -7.06                 |
| QD-42  | 0.23                  | -8.19                 |
| QD-11  | 0.52                  | -8.70                 |
| QD-43  | 0.16                  | -8.75                 |
| QD-44  | 0.05                  | -8.64                 |
| QD-45  | 0.04                  | -9.12                 |
| QD-12  | 0.89                  | -7.98                 |
| QD-13  | 0.78                  | -9.32                 |
| QD-14  | 0.14                  | -10.66                |

$\delta^{13}\text{C}$  and  $\delta^{18}\text{O}$  are in per mil relative  
to PDB standard.



| Sample | $\delta^{13}\text{C}$ | $\delta^{18}\text{O}$ |
|--------|-----------------------|-----------------------|
| QD-15  | 0.01                  | -8.54                 |
| QD-16  | 0.23                  | -8.31                 |
| QD-17  | 0.12                  | -8.00                 |
| QD-18  | 0.23                  | -9.37                 |
| QD-46  | 0.06                  | -8.91                 |
| QD-47  | 0.17                  | -8.79                 |

$\delta^{13}\text{C}$  and  $\delta^{18}\text{O}$  are in per mil relative to PDB standard.

## Appendix 11

NAA results of some elemental abundances in samples from the Qidong Section, Hunan.

| Sample | Ir (ppt) | Fe (%) | Co (ppm) | Cr (ppm) | As (ppm) | V (ppm) | Zn (ppm) | Ca (%) | Al (%) |
|--------|----------|--------|----------|----------|----------|---------|----------|--------|--------|
| QD-1   | 11.1     | 1.36   | 4.05     | 12.2     | 6.26     | 9.6     | 20       | 25.2   | 0.99   |
| QD-2   | 9.1      | 0.86   | 3.16     | 14.0     | 4.92     | 13.6    | 22       | 29.7   | 1.44   |
| QD-3   | 15.3     | 0.79   | 5.45     | 17.7     | 5.66     | 16.2    | 7.3      | 24.6   | 1.43   |
| QD-4   | 11.2     | 0.64   | 3.34     | 6.7      | 4.16     | 5.6     | 15       | 26.7   | 0.45   |
| QD-5   | 20.0     | 1.01   | 4.32     | 20.6     | 5.72     | 19.9    | 27       | 27.9   | 1.86   |
| QD-6   | 16.5     | 1.13   | 3.85     | 14.2     | 5.80     | 18.5    | 42       | 25.2   | 1.33   |
| QD-7   | 3.2      | 1.84   | 4.16     | 9.11     | 5.21     | 12.8    | 37       | 35.7   | 0.71   |
| QD-8   | 9.5      | 1.09   | 2.36     | 10.4     | 1.41     | 13.0    | 14       | 36.0   | 0.66   |
| QD-9a  | 31.0     | 2.80   | 16.2     | 105.1    | 10.9     | 99.0    | 74       | 11.8   | 8.80   |
| QD-9b  | 22.9     | 2.55   | 7.97     | 92.7     | 9.60     | 119.3   | 16       | 5.72   | 11.21  |
| QD-10  | 8.4      | 0.89   | 0.70     | 4.71     | 0.47     | 5.8     | 28       | 39.1   | 0.27   |
| QD-11  | 6.2      | 0.01   | 0.14     | 1.6      | 5.38     | 10.9    | 6.7      | 37.4   | 0.39   |
| QD-12  | 8.6      | 0.49   | 0.61     | 11.6     | 1.38     | 19.2    | 27       | 35.9   | 1.29   |
| QD-13  | 10.6     | 0.72   | 0.81     | 4.72     | 20.7     | 11.1    | 28       | 39.1   | 0.41   |
| QD-14  | 13.9     | 0.59   | 1.12     | 16.5     | 3.88     | 13.5    | 32       | 35.5   | 1.30   |
| QD-15  | 22.2     | 1.05   | 1.75     | 19.7     | 4.01     | 24.6    | 22       | 31.5   | 1.67   |
| QD-16  | 13.9     | 0.47   | 0.71     | 12.2     | 2.33     | 15.5    | 21       | 36.9   | 0.99   |
| QD-17  | 9.0      | 0.25   | 1.00     | 5.79     | 0.57     | 5.1     | 22       | 37.2   | 0.49   |
| QD-18  | 12.1     | 0.44   | 0.86     | 11.0     | 0.85     | 11.0    | 37       | 37.0   | 0.80   |